UNIVERSITAT POLITÈCNICA DE CATALUNYA BARCELONATECH

Competitive power control of distributed power plants

Antonio Mir Cantarellas

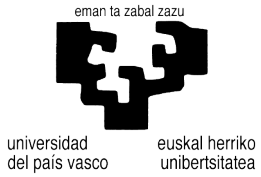

PhD Thesis

Competitive Power Control of Distributed Power Plants

Antonio Mir Cantarellas

Barcelona, January 2018

Competitive Power Control of Distributed Power Plants

Antonio Mir Cantarellas

Dissertation submitted to the Doctorate Office of the Universitat Politècnica de Catalunya in partial fulfillment of the requirements for the degree of Doctor of Philosophy by the

UNIVERSIDAD DE MALAGA
UNIVERSIDAD DE SEVILLA
UNIVERSIDAD DEL PAÍS VASCO/EUSKAL ERRIKO UNIBERTSITATEA
UNIVERSITAT POLITÈCNICA DE CATALUNYA

Joint Doctoral Programme in Electric Energy Systems

Barcelona, January 2018

Acknowledgements

The research work carried out along this Thesis could only be possible thanks to the deep team-work collaboration along many parters and institutions. The successfully achievement of the principal goals of this Thesis was the result of many efforts of principal actors to whom I would like to express my appreciation.

First, I would like to mention the profound gratitude I have to Professor Pedro Rodriguez, who strongly believed in my capacities towards arriving safe home to port. Pedro, thank you very much for offering me the possibility of performing a first level industrial research work by your side. I can only say that it was an honour to be there. Thank you also for providing me an indefatigable guidance and support, as for me you were always the lighthouse throwing light to the tortuous research journey. It was a extremely enriching experience to play an active role in your team, and I take the best with me, which is to have the rigorous capacity of developing my own research thoughts and ideas against a blank piece of paper.

Of course, the work performed, and learning experience achieved, could only be possible thanks to the funding institutions which supported me during these years. Special mention should be provided to Abengoa Research and the SEER research group, who offered me the capability of developing my own research work and involving myself in cutting edge industrial projects hand by hand with world class researchers and collaboration partners.

Additionally I would like to thank all the reserachers who shared a valuable altruistic time with me in holdind countless technical discussions. Specially to Alvaro Luna, Iñaki Candela, Joan Rocabert, Endika Bilbao, and Salvador Valenzuela.

Special mention should be provided to Jorge Martinez and Daniel Remon, with whom I not only worked side by side, but you also widened my mind in many professional and personal aspects. The only thing I can say is that I am proud to have been by your side.

At last, but not least, I would like to thank to my beloved girlfriend and my parents for being always there. You are the strongest pillars of my live, who give me the necessary strength to carry on with the main challenges I face. Thank you also for all the good moments full of joy we shared toghether, as they undoubtedly contributed in taking things easier. I am pleased to say that all I have achieved is because of you. Thus all my merits are also yourse.

Antoni Mir Cantarellas
Sevilla, Spain
January, 2018

Abstract

Nowadays, the electrical energy sector is currently found in a dramatic changing paradigm, which moves towards an increasing trend in generating power at distribution levels, where electricity is typically consumed, by means of non-conventional/renewable based generation units, such as PV, wind, combined heat and power, etc. These new generation technologies, termed as distributed generation, not only offers a non-pollutant, cheap and efficient source of energy to cover increasing demand, but also enhance the reliability of supply to critical loads and reduce the need for additional grid reinforcements. Aside of the technical benefits provided, distributed generation will massively integrate renewable energy resources, with new type of loads and end-user actors, such as prosumers, demand responsive loads, or electric vehicles. Where these actors will actively participate in energy and auxiliary service markets, depending on their available or constrained energy needs.

However, the main limiting factor to achieve larger shares of renewable based distributed generation on the current power system scenario comes motivated due to the unpredictable and highly stochastic nature of distributed energy resources. Due to the large shares of renewable generation already achieved and the negative impact they have on current power systems, most grid codes currently in place force distributed power plants to provide anvanced grid interaction control capabilities, very similar to the ones provided by conventional generation. Therefore, under this futuristic distributed power system scenario, there is a clear need for addressing the main operation and control challenges that these new generation technologies will pose on conventional power systems, and identify the main opportunities that could arise from their suitable system integration. For this reason, the work presented in this Thesis deals with designing and implementing advanced hierarchical control solutions to renewable-based power plants with the purpose of achieving advanced grid conection performance while reaching maximum economic benefits from its optimum real-time operation.

Initially, an extensive analysis on the main renewable-based power plant hierarchical control solutions currently on the shelf, is performed. This study not only covered the

specific case of renewable-based power plants, but also advanced microgrid and smart grid control solutions. The main hierarchical control structures were initially analyzed, from where it was observed that many of them follow similar master/slave approaches, where a centralized controller ensures an acceptable power supply control through the grid point of connection, while providing suitable power dispatch references to the local controllers of generation units. In addition, a revision on energy management systems solutions was performed when being applied in such distributed network structures, where most implementations rely on complex optimization algorithms with the objective of minimizing the operation costs of microgrids. However, as most of these approaches require large computation efforts, they do not arise as suitable candidates for performing real-time power dispatch capabilities.

Once the main renewable-based power plant hierarchical solutions were analized, a novel Hierarchical Distributed Control Structure (HDCS) is proposed for increased management of renewable-based active distributed plants. This hierarchical control structure comprises all possible functional levels from the higher long-term economic scheduling layer, to the instantaneous supervisory control of the resource, emphasizing the entire operation and control functionalities needed for increasing the integration of active distributed power plants. In order to achieve real-time control capabilities in active distribution systems, the present chapter introduced a novel power sharing control strategy, based on the competitive operation of multiple active participating agents (distributed generators, demand response and energy storage systems) through the implementation of market rules. Such control capabilities are satisfied by applying a price control signal over the entire grid control architecture, being the final-end participating agent, the responsible entity in charge of deciding its own generation/demand involvement based on its marginal or affordable electricity costs. In addition, it reduces the information volume to be transmitted and processing requirements, as the higher control levels do not need to have knowledge on the detailed distribution system topology and contributing actors.

In order to have a meaningful evaluation of the proposed competitive control capabilities, a wave power plant application has been selected, which constitutes a challenging scenario for the controller itself to achieve advanced real-time control capabilities in such an oscillating renewable energy resource. Then, the proposed plant controller is intendeded to control the real-time production of the wave power plant in order to meet the flat and stable power generation schedules agreed in day-ahead or intra-day markets.

In order to suitably characterize the wave energy resource profile resulting from maximum energy absorption, this Thesis introduce a novel adaptive vector controller, which maximizes the energy extraction from the resource regardless of the dominant irregular wave frequency characteristics.

As a conclusion, it can be mentioned that the proposed competitive controller results on a suitable alternative to the already existing energy management systems in distributed systems, as it solve the major drawbacks found in ensuring a real time optimum economic control of participating agents. For the specific wave power plant application considered, the

competitive control does not only ensures real-time optimum resource allocation for satisfying a given production objective, but also provides optimum long term operation of the system.

As a result, overall plant costs reductions can be achieved under the competitive operation, since the plant scheduled energy is satisfied by making use of the generation units with cheaper cumulative operation costs. This means that the generation units incurring in frequent and costly operation and maintenance duties will be minimally used, only contributing in specific periods where the scheduled power cannot be satisfied by the cheapest ones.

Finally, the wave energy resource characterization has been considered in the competitive wave power plant implementation, giving rise to the maximum power supply capacity from individual resource generation units. From the real time implementation of the competitive power controller in the selected wave power plant application, it is worth noting that the main competitive controllers and associated costs are introduced in detail within the wave power plant architecture. Besides, the plant controller is suitablly tuned to reach the required grid connection performance dynamics. Finally, two sets of simulations are performed in order to evaluate the competitive power plant performance under steady-state and real-time operating conditions.

Contents

List of Figures

Chapter
1.

1 Introduction

1.1 Introduction

Up to date, the electrical energy sector has been characterized by its ever increasing worldwide electricity demand. As specified in the International Energy Outlook 2017 [1], the electricity generation, needed to cope with such demand from 2015 to 2040, is expected to increase an average of 2.9%/year for both OECD and non-OECD countries. Therefore, the future growth in global electricity demand will call for an increased expansion of generation and transmission capacities.

Nowadays fossil fuels continue dominating the energy generation mix, contributing with the largest share of global energy production. However, as it can be observed in Fig. 1.1 there is a clear trend in achieving increased diversification by 2040, experiencing reduced penetration levels of conventional energy resources (coal, oil and nuclear), while the share of renewables (bioenergy, wind, solar PV, etc.) and natural gas becomes more and more relevant. This energy resource transition is due to that, the large scale exploitation of fossil fuels experienced so far, has not only led to harmful environmental impacts and climate change, but it has also contributed in the depletion of finite available resources, and as a consequence, the increase in electrical energy prices. In contrast, a major energy mix diversification is sought in favor of renewables, motivated from the inexhaustible and environmentally friendly nature of these energy resources. In addition, as the renewable generation technologies reach acceptable maturity levels and its installation costs drop down, this type of generation becomes highly attractive due to its low or near zero variable operation costs, leading its massive integration in the long term run to reduce electricity prices. Therefore, as depicted in

Fig. 1.2, an ambitious move towards increased installed capacity and higher participation shares of renewables will become a reality in a near-term future, where wind and solar PV are the ones appearing with a leadership position in terms of future penetration of renewable energy sources (RES) [1, 2].

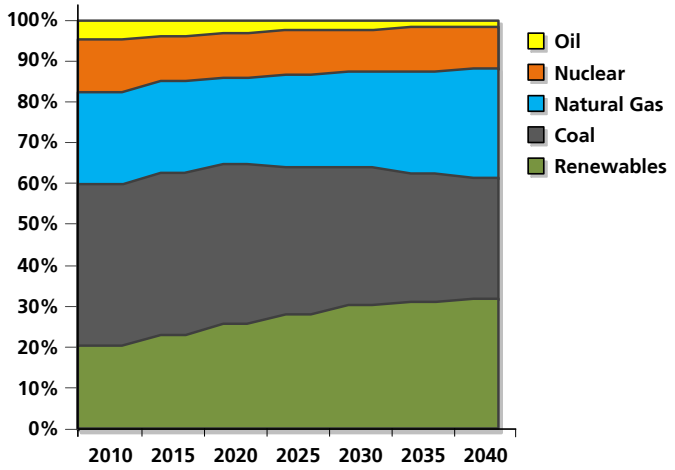

Fig. 1.1. Overall energy generation mix evolution from 2010 to 2040 [1]

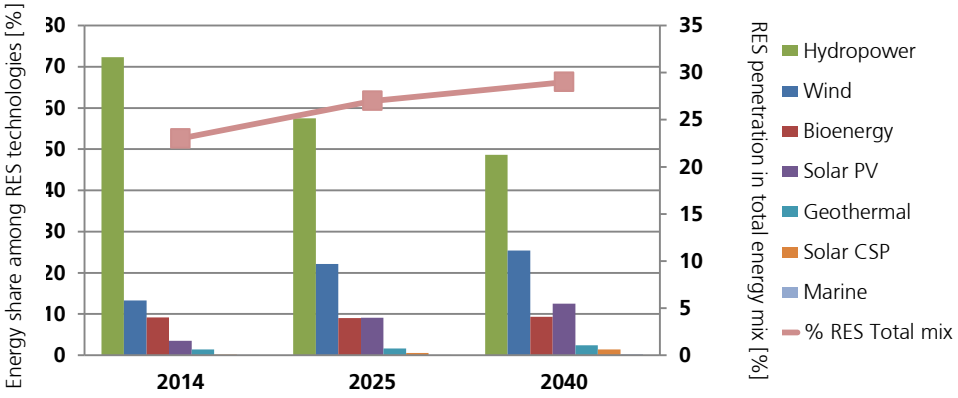

Fig. 1.2. Incremental growth on world-wide renewable-based electricity generation [2]

Regarding the future evolution of transmission and distribution (T&D) networks, it is worth noting that a great expansion will be achieved, motivated by the need to improve the quality of supply to existing consumers, and to provide interconnection access to new and wide ranging end-user types. Robust T&D networks, together with higher generation and demand control capabilities, provide increased system flexibility, which is essential for allocating the large penetration expected of stochastic renewable generation. In this regard, it

is expected that future T&D grids will increasingly integrate new smart grid and micro grid developments, which are characterized by its large implementation of real time control and communication technologies, while meeting generation and demand locally. Such intelligent systems will provide optimum system operation, decrease of distribution losses and integrate new type of loads and end-user actors, such as prosumers, demand responsive loads, or electric vehicles (EV). Where these actors will actively participate in energy and auxiliary service markets, depending on their available or constrained energy needs [3].

Finally, in terms of global integration of electrical transmission systems, there is an increasing trend in unifying large interconnection systems able to cover extensive control areas [3].

This chapter presents the operation and control mechanisms typically found in conventional power systems, which constitute the pillars over which the current power industry has been construted. The main purpose of this section is to bring to light the new operation and control challenges that large penetration levels of RES-based generation will pose on existing power systems, and emphasize the main research efforts that should be addressed in order to gradually move towards the power system of the future. Being this new scenario characterized by the massive integration of RES generation along with energy storage systems and demand side management at the final end-user level.

1.2 Conventional power system operation and control

One of the major features characterizing the current energy sector is that up to date, electrical energy cannot be stored in large quantities, due to the unavailability of commercial large scale storage technologies, and the vast costs/poor performance associated to lower scale implementations. Therefore, the electrical energy is generated as it is consumed, making use of an immense and very complex dynamic power system to transmit it. In order to ensure a stable and safe operation of the system, a dynamic equilibrium point between generation and demand must be ensured at any time, as in the event of any maintained mismatch, the associated power disturbance may be propagated almost instantaneously over the entire system, leading to a final collapse if not adequately resolved.

Another differential aspect of electrical energy systems is that the delivery route over which the power is being transmitted or distributed cannot be chosen at will, or as a result of any buyer/seller agreement. Instead, electricity flows respond to its physical nature, being restricted by the Kirchhoff's law and the minimum impedance paths, existing from generation to consumption nodes. Moreover, any change on the physical nature of network facilities may have a direct impact on energy flow reconfigurations, giving rise to possible undesired stressing conditions on other system facilities (e.g. congestions, overloads). All these system constraints, hinders even more the complicated task of meeting a real-time balance between generation and demand to safely operate the grid.

Therefore, both of the above mentioned peculiarities differentiating the electricity product from any other commodity have a crucial relevance in the manner in which the power systems are operated and controlled [4, 5]

1.2.1 Power system operation and control

Electric power systems have been considerably evolving during the past, from their initial simplistic electricifications, to the immense and very sophisticated electrical systems currently in place. The actual size of power systems is a result of the enormous interconnected actors making use of electricity, since energy is delivered from site-specific generation resources to practically any inhabited places in the world. Therefore, the operation and control duties required under these power system scenarios becomes highly complex, as a dynamic balance between total generation and demand must be satisfied at any time. In order to achieve that, electrical power systems have been traditionally operated under the rule of a centralized controller [6, 5], being in charge of ensuring the supply of electricity to satisfy consumer requirements, as well as guaranteeing power quality and stability of this supply. In this regard, the controller provides specific commands to each generation power plant participating in the control of the power system, where these controller commands are determined attending to optimality reasons (minimum operation costs) or following a market process. Many of the power control applications currently being considered are implemented in System Operators' control centers, where countless measurement signals are aggregated to continuously react to any changing system operating conditions. Furthermore, these system management applications cover several time domains, from months, days or hours in advance to real-time operation, since the degree of uncertainty narrows when approaching to real-time.

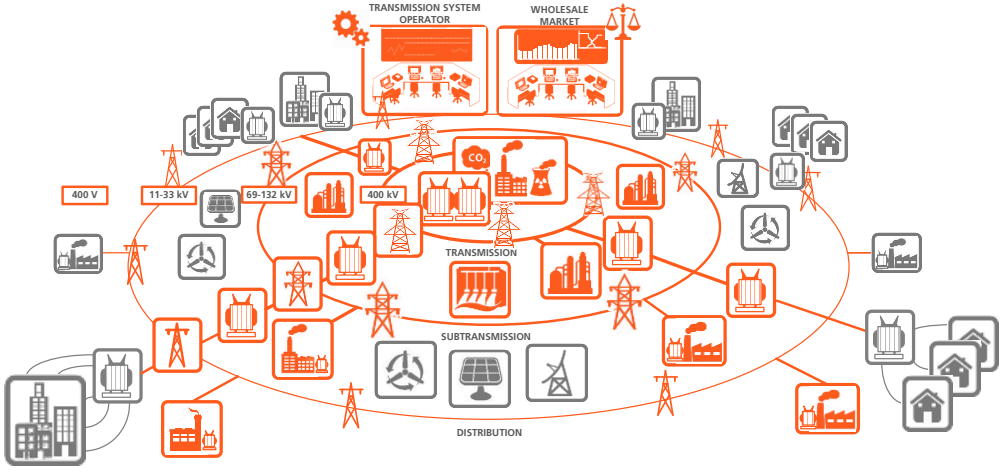

Fig. 1.3. Conventional power system structure and current scenario

In terms of power system structure, conventional power systems, as the one depicted in Fig. 1.3, have appeared with very similar configurations worldwide. In this regard, electrical power systems are typically characterized by their unidirectional power flows, whose power is transferred from the large generation units to the final-end load centers, where the energy is consumed.

In such systems, the large scale power plants are located far away from load centers due to their resource-specific requirements. Thus, the energy generated need to be transmitted over long distances through the typically meshed high voltage (HV) transmission network, until reaching load center neighboring nodes. At this point, the energy is delivered to the final-end consumption loads through the medium and low voltage (MV and LV) distribution grid, whose grid structure may vary from urban to rural, but it is typically operated radially. At the back-end of the system, loads connect where they most suitably fit to satisfy their energy consumption needs. Then, many large industrial loads may be found connected to the subtransmission system, where most commercial and residential consumers respectively interconnect to primary and secondary distribution system feeders. Therefore, it can be stated that conventional power systems are organized around, generation, transmission, distribution and consumption - often called supply - facilities, while also accounting for protection and control systems [5].

Generation

Generation power plants constitute the power system actors in charge of meeting the time-scheduled energy needs of end-user consumption loads. The technological aspects of such generating facilities cover a wide range of applications, since electrical energy is produced from many different forms of primary energy resources. Then, the dominating technologies traditionally used in bulk power generation are mainly divided in hydroelectric, thermal and nuclear power plants. However, the technological advancements recently achieved in renewable energy systems, drive this type of generation into the actual energy generation mix.

The existence of a highly diversified energy generation portfolio arises as a common goal in many modern power systems, as it provides a set of sound techno/economical benefits for supplying demand. In this regard, this generation portfolio adapts to the daily load curve, by considering a merit order among the participating generation units, which result from their operation costs involved together with their dynamic response characteristics. For instance, nuclear power plants account for very large investments, while the operation costs keep comparatively low due to the energy conversion efficiency and fuel price. In addition the large plant size (in the range of few GWs) and the technical difficulties found in regulating the nuclear energy resource, make this type of generation particulary suitable for covering the base loads. Opposing to nuclear generation, combined cycle gas turbines (CCGTs) arise as an attractive generation technology for covering consumption peaks, since they have the highest operating, but minimal investment costs with a high degree of modularity. A similar

role applies to hydroelectric power plants, whose resource inventories need to be suitably managed (large opportunity costs), as it depends on random rainfalls and its use may have collateral consequences on the water supply to neighbouring communities. In addition its connection /disconnection flexibility makes perfect to suit this purpose. Finally, conventional steam plants fit in between, and they are suitable to cover the steady load fluctuations from base to peak. This is due to the moderate fuel cost and efficiencies, combined with existing limitations on its thermal inertia, which hinders the continuous start/stop events usually found in peaking units.

Finally, as previously mentioned, most large scale power plants are dispersed over wide geographical areas, being usually located far away from load centers due to many reasons, such as site specific availability of generation resources or cooling water, larger size deployments to benefit from economies of scale, and pollution or social reaction impacts. All this makes transmission networs a must to deliver energy form generation plants to final energy consumers. However, an increasing trend is arisig to shape the power system of the future, where large penetration of distributed generation and storage systems will appear interconnected closer to consumption centers. This will result in a more efficient utilization of available generation resources, since energy will be consumed locally, avoiding any need for transmission and related losses, while releasing transmission congestions and system constraints.

Transmission

The purpose of the transmission networks is to transmit power from large scale scattered power plants to neighbouring nodes close to load centers, typically located near population areas or industrial facilities, while keeping strong interconnections with other power system areas in synchronism. The suitable transmission of bulk power makes use of high voltage network facilities in order to minimize the joule-effect losses over the existing large transmission distances. Therefore the transmission network arises as the power system backbone, interconnecting all main power centers through a meshed topology, which plays a key role in maintaining the dynamic balance between generation and demand. Thus in the unlikely event of missoperation or sudden failure of a given generation or transmission facility, the transmission network can easily reconfigure to cover the expected demand from other means of generation. In order to do so, the transmission network is equipped with advanced and reliable measurement, protection and control devices, to guarantee a stable and safe delivery of electrical energy to a given system area regardless of any existing shortcircuit, overload, dispatch error or equipment failure.

Transmission systems have also appeared as a key infrastructure in the latests liberalized and competitive regulatory frameworks, as it constitute the meeting point to all market actors, which facilitates the power delivery from seller to buyer energy transactions.

Under this scenario, one of the main components are power lines and cables, which carry power flows over the transmission network depending on Kirchhoff laws and related

equivalent impedance. However, the advancement of Flexible AC transmission system (FACTS) equipment, based on power electronic devices, provides a new controllability degree in transmission networks, as by virtually modifying the equivalent line parameters they may extend power capacity or drive power flows towards lighter loaded transmission lines.

Finally, substations constitute the remaining relevant power transmission components that should also be considered. Their main role is to serve as grid connection nodes between transmission lines, while providing interconnection acces for generation power plants and load centers. Besides that, they also serve as power transformation nodes, where measurement, protection, interruption and dispatch take place.

Distribution

Lower voltage distribution networks expand downstream from transmission substation nodes to interconnect smaller industrial, commercial and residential loads to the power system. This power delivery network structure has a radial configuration and entails several remarked differences from the transmission grid standpoint. From one side, the so called subtransmission system appears at the upper or regional distribution grid level interfacing with transmission, where this network operates at slightly lower voltage ranges (typically 132, 66 or 45kV), and with a poorly meshed or looped grid configuration. At the same time, subtransmission substations further step down voltages (20, 15 or 6.6kV) to supply electrical power to the pure distribution network, being the responsible grid infrastructure to radially deliver energy to the final end users through the main distribution feeders. Finally, distribution feeders expand downstream towards the lowest consumption substations, where residential loads connect. Accordingly, this back-end substation drop down the voltage to the final end-user level (380, 220, 127, or 110V), in order to host the interconnection of lowest power loads. Therefore, under this grid infrastructure, consumption loads interconnect at the distribution level best suited to satisfy their power and voltage requirements.

In the case of rural areas, distribution networks expand radially over long distances using mainly LV overhead lines, due to the lower power density and reliability levels required for serving such loads. However, one of the key problems is that the stability of distribution network weakens as distance from the main substation transformer increases. Then the frequency and voltage grid variables are subject to larger deviations.

On the contrary, urban distribution grids typically run over meshed underground cables, even their operation is still radially, but this offers greater reliability and shorter cable distances to serve higher power demanding loads centers.

Distribution networks protection is handled by substation circuit breakers, which isolate a given faulted line and enable alternative grid reconfigurations, to still deliver the required power to affected consumers. However there is a lack of real-time control capabilities from local demand and generation units, which limits the distribution grid reliability to pure protection actions.

Demand

As it is well understood, electrical power systems must be designed and operated to provide the required daily consumption levels in real-time. This means that peak loads must be withstood, while covering the power demand over time. Therefore, the suitable operation of the system can be ensured only if participating demand is properly characterized. This characterization is usually done by studying in detail the particular shape of the aggregated load curve. As electricity consumers usually follow repetitive habits, load curve shapes and deviations can be suitably estimated over several time frames, such as daily, weekly, monthly, yearly or multiyearly. So the generation and transmission dispatch can be scheduled in advance to cover the forecasted load curve. In this regard, demand prediction has a key role in anticipating to any transmission system restrictions and power system problems that may arise from the operation of the system and it should be suitably determined in the short, medium and long term basis. The load curve forecast is usually determined from historical data, being subject to light readjustments depending mainly on economic growth, temperature, working days activity, and punctual special events.

In addition, the demand shape have direct implications on the economic activity derived from system operation, as flattered demand profiles can be easily supplied by cheaper base load generation units, while spiker ones need to be covered by expensive peaking generators.

Power System Control

Regarding the control of electrical power systems, they have been traditionally operated under the rule of a centralized controller [6, 5]. This controller has been in charge of ensuring the supply of electricity to satisfy consumer requirements, as well as guaranteeing power quality and stability of this supply. In order to achieve that, the controller provides specific commands to each generation power plant participating in the control of the power system, where these controller commands are determined attending to optimality reasons (minimum operation costs) or following a market process.

As depicted in Fig. 1.4, this control structure involves several control levels in order to suitably cope with the major power system operation requirements. At the bottom of the hierarchical structure, it can be observed that individual system elements are directly controlled by dedicated local controllers, such as in the case of excitation systems, prime mover mechanisms, transformer stations or power electronic converters. All these local controllers are coordinated at a higher hierarchical level by the power plant controller or the alike. Then, power plants should respond as single entity units to any operative requirements set by system operators of higher hierarchical levels. Accordingly, the plant controllers are closely supervised by system operation controllers at system control centers, which are the responsible entities in charge of ensuring a safe and reliable operation of the power system. Finally, the system control duties required are determined by pool master controllers, which are the ones setting the power generation and demand schedules of the participating power plants and load centers, according to economic optimality reasons or market processes.

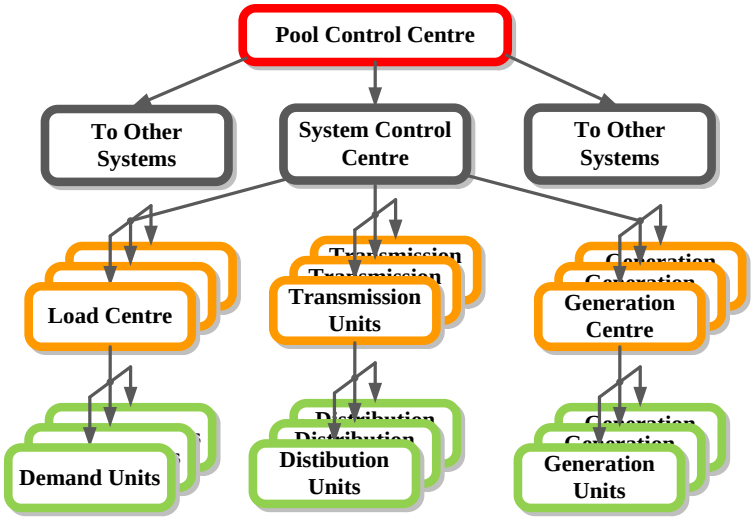

Fig. 1.4. Hierarchical control structure of conventional power systems [6]

All this hierarchical structure lays down over large power systems, covering all the above mentioned generation, transmission/distribution and demand domains. Is for this reason that extensive measurement deployment and telemetry is needed in each level, to monitor the performance of all system related elements, but also as a feedback to define suitable control actions in each of the controllers involved. Of course, as the hierarchical levels increase from bottom to top, the degree of detail of processed information decreases, being the power system controller mainly aware of the overall system performance, along with considered gross participating actors. Besides, all these hierarchical control centers are provided with Supervisory Control and Data Acquisition (SCADA) systems, which allow human operators to monitor the related system performance and consequently react with appropriately control actions under normal, emergency or restoration system conditions.

Under the most traditional monopolistic regulation approaches, the electric utilities arise as the single entity in charge of controlling the power system in an optimum techno-economical manner. Where, in most modern unbundled and liberalized energy regulation scenarios a competitive market mechanism coexists with an independent system operator. In this manner the optimum energy price can be found from the participation of multiple generation and load actors, while considering the technical electrical system restrictions [4].

The wholesale electricity market and the transmission system operator appear depicted in Fig. 1.3 as the power system control actors commonly found in modern power systems. In this regard, the major power system management has been typically performed at the transmission level between generation and consumption representatives, since the distribution system is operated radially and its main control issues only entail automatic feeder reconfigurations or sudden protection trips.

However, this control approach is gradually becoming obsolete and it is facing new conceptual redesigns (i.e. the REV initiative from the state of NY [7, 8]), as the ever increasing penetration of renewable energy sources (RES), mainly at distribution level, is posing new operation and control challenges to existing power systems and system operators (SO). In this regard, a considerable barrier to the large-scale integration of RES-based distributed generation (DG) is that the SO cannot perform its traditional real-time control duties over the power and grid services provision, due to the overwhelming amount of information that should be handled and processed in real-time from thousands of different DGs [3].

In addition, the progressive change from deterministic to highly stochastic generation profiles experienced in distribution networks, will imply considerable challenges in the balancing of generation and consumption, making it necessary from distribution systems to perform not only their traditional network reconfiguration tasks, but also a detailed real-time control of the local on-line generation and demand [3, 9].

Up to date any disturbances introduced by RES-based generation systems were directly neglected from the SO, as the stability and reliability of distribution system was not affected due to its low penetration levels. However, this assumption cannot be considered any more, as the increasing implementation of RES-based distributed power plants and energy storage systems will raise new efficiency, reliability and security problems in the manner in which the distribution system has been operated and controlled up to date [9].

Therefore, there is a clear need in designing and operating highly controllable and manageable active distribution systems, whose main actors could achieve increased benefits from the direct participation in smaller electricity markets (e.g. retail markets), while contributing to improve the distribution system performance. At the same time, those participating actors need to provide advanced control capabilities in order to transform their traditionally stochastic power profiles into fully deterministic ones. Thus the uncertainty in matching generation and demand at low distribution levels can be minimized.

1.2.2 Conventional market system description

A considerable move towards deregulation of electricity markets has been increasingly experienced during the last years in order to facilitate the trade of electricity among a large number of market actors. Although, this massive liberalization has not been universally established, it is unquestionably the predominant regulatory scheme widely implemented so far, being the generation activity primarily involved. However, the particular nature of the electrictricity product, and the different power system topologies implemented worldwide, have raised many variants of wholesale market designs [3, 4].

The goal of the electricity markets is to offer a neutral trading platform where all market actors can participate at equal terms, to provide ease of access and reduced transactional costs, and to determine an equitable price reference for the entire power market. As it is well understood, the promotion of free market competitition leads to an optimum socioeconomic

welfare, because it makes pressure to participating actors to behave more efficiently. This competitive scenario is not only expected to drive supplier costs down, but also provide consumers a sound economic perception on the costs incurred to satisfy their energy needs.

One of the main characteristics that can be found in deregulated and competitive electricity markets is that all market actors have a wide range of purchasing and selling alternatives depending on their electricity usage and trade capacity for electricity services. Such actors are capable of participating in time scheduled markets and reach spot prices, which varies along the trading day depending on supply and demand rules.

Besides the characteristics defining energy transactions, electrical markets are directly related to the physical exchange of energy between producers and consumers. In this regard, it is worth noting that the stability and security of the transmission and distribution systems will be severely influenced by the final outcome of the trading actions. This is the reason why system operators should be closely involved in this process, in order to solve any system operation restrictions or reliability issues that may arise, and readjust the final generation and demand schedules to be followed by market participating actors. Therefore, a concatenation of successive market processes take place over different time scales, where energy is firstly traded among generation and demand actors, and then SOs call for ancillary services, needed to cover any readjustment from unexpected real-time generation or demand deviations.

The overall time-table where wholesale markets apply, account for long term (years or months before delivery time), short term (day to minutes before delivery time), real-time (at the delivery time), and post delivery time. According to this, the different markets involved can be classified in long term markets, day-ahead markets, and intraday/balancing markets (in the EU), or real-time markets (in the US). For the sake of simplicity long term markets have been avoided in the daily market process described hereinafter, as they are mainly involved in bilateral contracts devoted to reduce finantial risks of future energy transactions. Therefore, it can be stated that the daily market sequence starts the day before (D-1) the energy supply takes place (Fig. 1.5).

Aside of the early settled bilateral energy transactions, the day-ahead market (DAM) collects all the generation and demand bids provided from participating actors, and sets an hourly energy price and preliminary generation and demand schedules, attending to purely economic demand/offer rules. If nodal transmission constraints are not considered within the market clearing process (which is the case for the EU), the SO receives the overall generation and demand program (from bilateral and DAM transactions), and validates that the energy trades among individuals can be physically carried out. Then, in the presence of any transmission system restriction, the SO is responsible of solving it, by readjusting the preliminary schedules at minimum costs.

Once the feasible day-ahead schedules have been set, the daily market sequence moves forward in time, and call for additional market or SO mechanisms, to cover any energy deviations that may arise, as time get closer to real-time. For example, this is the case of intra-day markets, where generation and demand actors readjust their schedules as the

uncertainty level gets reduced. In addition, SO offer balancing markets in order to set the level of involvement, mainly of generation units, to increase/decrease their generation in the case of any real-time energy mismatch.

Finally, when the gate closure time arrives, there is no more room for transactional readjustments, and consequently any market process get closed. At this time, the real-time control of the power system is entirely conducted by the SO. Therefore, the resulting production schedule is definitive at this stage, and the generation units involved are commited to follow such programmes. Any possible deviations from the bidding actors in their physical power exchange must be corrected by the SO in order to ensure the energy balance between production and consumption. In this regard, in the situations where the power production is higher than the settled bids, other producers will have to decrease their power production accordingly, or consumption levels should increase, so energy balance is always ensured within the control area. On the other hand, if there is a deficit of power production from the scheduled energy bid, other producers should increase their power production or reduce the consumption levels. This extra delivered power has an increased price than the market clearing price (MCP), which will be paid by such generators responsible producing the energy imbalance.

Then, after the delivery time, the SO appear in charge of setting economic penalties to generation units that deviated from their bounded schedules. The SO has a record of real-time production profiles, and through this mechanism, they force the energy deviation responsible actors to pay their share of the total costs needed for re-establishing the energy balance of the control area.

The settlement of such penalty fees motivate energy producers to avoid incurring in large energy deviation from the scheduled bids. An increased problem will be found in this aspect when large integration of renewable generation takes place, as the SOs will require more regulating power capacity for performing power balancing services.

1.3 The distributed power system paradigm: the future of power generation, distribution and consumption

Nowadays, the electrical energy is being generated by large scale conventional power plants (mainly fossil fuel, nuclear or hydro), whose electricity is radially transmitted over long distances, due to the logistic and geographical site-dependence of such generation units. However, the strong dependence of conventional power plants on progressive depletion of fuel resources, their negative impact on environmental pollution, and the lack of system efficiency from large transportation distances, results on a long term unsustainable power generation scenario [9].

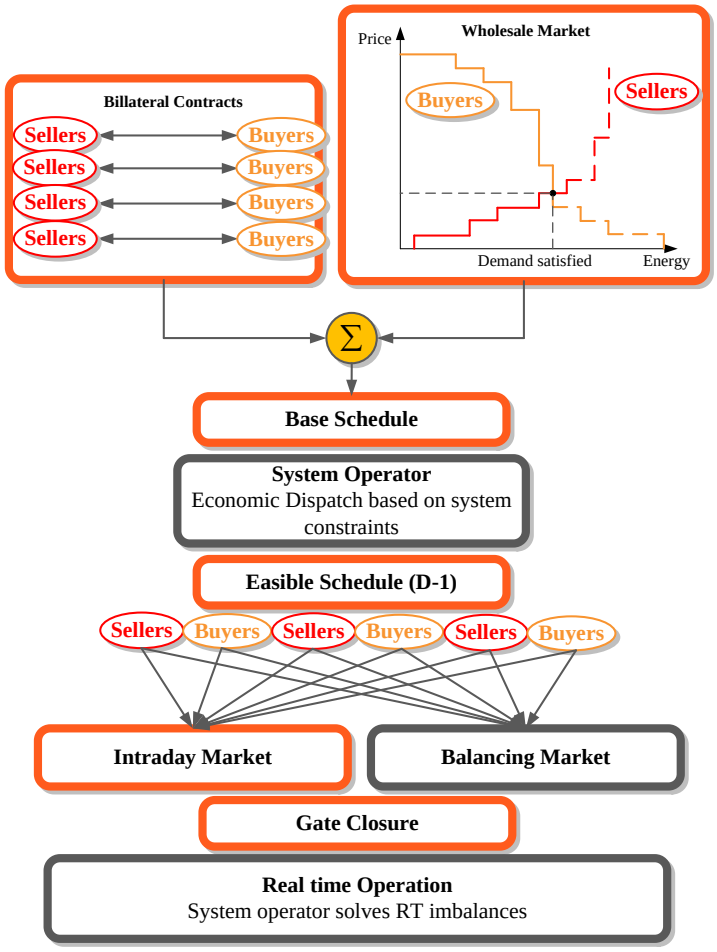

Fig. 1.5. Typical daily wholesale market sequence followed in the EU [4]

Such problems could be overcome thanks to the increasing trend in generating power at distribution levels, where electricity is typically consumed, by means of non-conventional/renewable based generation units, such as PV, wind, combined heat and power (CHP), etc. These new generation technologies, termed as distributed generation (DG), not only offers a non-pollutant, cheap and efficient source of energy to cover increasing demand, but also enhance the reliability of supply to critical loads and reduce the need for additional grid reinforcements. Aside of the technical benefits provided, DG will integrate new type of loads and end-user actors, such as prosumers, demand responsive loads, or electric vehicles (EV). Where these actors will actively participate in energy and auxiliary service markets, depending on their available or constrained energy needs [3].

However, the main limiting factor to achieve larger shares of renewable based DG on the current power system scenario, comes motivated due to the unpredictable and highly stochastic nature of distributed energy resources (DER). Therefore, under this futuristic distributed power system scenario, there is a clear need for addressing the main operation and control challenges that these new generation technologies will pose on conventional power systems, and identify the main opportunities that could arise from their suitable system integration.

1.3.1 Distributed generation: technical and operational scenario

Traditionally, the control of the electrical power system was designed to manage a few large generation units, so a reliable and safe operation could be achieved by closely monitoring and controlling the real-time performance of such units [5, 6]. Nevertheless, the ever increasing penetration of DERs, mainly at distribution level, is posing new operation and control challenges to existing power systems and SOs, as considering the same degree of information and communication from thousands of DGs, would result in an overwhelming amount of information that should be processed in real-time. In this regard, a considerable barrier to increase DG integration is that the SOs cannot perform real-time control over the power and grid services provision, due to the excessive information and communication technologies required [3].

Instead, this real-time control could be performed by aggregators (i.e. active distribution systems), such as distributed power plants, energy districts or microgrids, which would handle the communication and control activities required among DGs, while providing the SO with a compounded amount of net generation or demand capacity. Therefore, the aggregator would be not only in charge of performing real time control and coordination between DGs, but they would also enable direct participation with smaller retail electricity markets.

In addition, the gradual change from deterministic to high stochastic generation profiles, along with the appearance of bidirectional power flows in distribution networks, will imply considerable challenges in the balancing of generation and consumption, making it necessary to consider the figure of distribution system operators (DSOs). In this regard, DSOs would be in charge of performing the traditional distribution network reconfiguration duties, but also a detailed real-time control of the local on-line generation and demand [3, 9].

This progressive evolution to highly distributed power systems is a hot topic today, being driven by several regulatory frameworks, such as the REV initiative from the state of NY [7, 8], which settles the path towards the power system of the future, where massive participation of end-user demand and DG actors will play a crucial role in meeting the overall energy needs.

Such previously outlined power system scenario, is represented in Fig. 1.6, where DSOs and retail marets coexist, in a similar manner as TSOs and wholesale markets, but applied to smaller restricted areas.

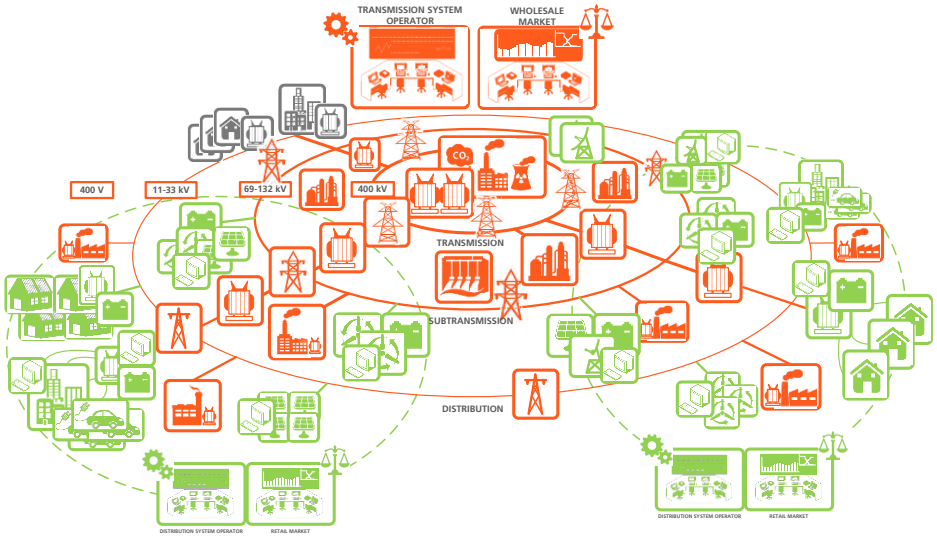

Fig. 1.6. Future power system scenario with high penetration of DG [4]

As it can be observed in Fig. 1.6, it is worth noting that while conventional plants are constituted by a few large synchronous generation units, RES based active distribution systems are usually formed by large amounts of small scale power electronic units, normally dispersed over a wide geographical area. Considering the large number of power generation/demand units involved and its inherent stochastic behavior, such distributed energy systems require more complex control solutions in order to ensure grid code compliance, while contributing to the safe and reliable operation of the system. In this regard SOs are likely to force active distribution networs to behave as conventional power plants, thus providing increased control capabilities and grid services in case it is needed. These services include conventional generation control, frequency regulation, reserves capacity provision, reactive power supply, voltage control, island operation and black-start capabilities. Thus, in order to provide such advanced power supply and grid service functionalities in a coordinated manner, a supervisory control and data acquisition (SCADA) system need to be fully integrated [3, 10, 11].

SCADA systems appeared as a suitable solution for providing real-time visibility of the plant operation, as well as centralized/decentralized power plant control capabilities. The implementation of efficient and cost-effective SCADA technologies at larger scales will result as one of the main drivers for the success of future microgrids and active distribution system deployments, as they can provide communication and operation control capabilities in the network management. SCADA system functionalities range from data acquisition, data and alarm processing, remote control, graphical human-machine interface (HMI), etc.

Where, distributed control systems (DCS) appear as the last trend in SCADA systems for communication and control purposes [9].

Finally, a common characteristic of DGs is that they are usually interfaced through power electronic converters, whose power supply dynamics considerably differ from the synchronous characteristic behavior of conventional power systems. Although power electronics generation initially appeared hindering the stability of the system, due to the poor controllability of power generation (MPPT), lack of inertia and odd transient dynamics, they currently appear as fully controllable generation units, offering many system integration features similar to the ones provided by synchronous generators. This evolution results from the active research efforts conducted over the last decade, where the advanced control of power electronic converters was a key topic in moving forward towards increased RES penetration levels [12].

Among many grid code specifications currently in place, DG should remain working normally, providing controllable active and reactive power injection, within a given operational window around the rated values of voltage and frequency. Besides of ensuring normal operation when grid voltage and frequency remain within the limits, DGs should actively contribute with voltage and frequency regulation in order to improve the steady state and transient dynamics of the grid. Thus, DGs are required to support the voltage and frequency of the grid through reactive and active power supply respectively. Ultimately, current grid codes additionally set specific low voltage ride through (LVRT) requirements to the DGs dynamic performance in case of grid faults, so the massive disconnection of DG can be avoided.

Despite of the specific requirements mentioned above, the massive penetration of renewables based DGs expected in a near future, are forcing the TSO to impose more stringent grid connection codes. So grid connected DGs, based on power electronic converters, will allow a similar behavior as conventional synchronous generation units in terms of grid regulation, robustness and transient response capabilities. In this regard, the main requirements likely to be adopted by future grid codes consist among others on inertia emulation, power oscillations damping, islanding operation, black start, etc. Therefore, it can be stated that power electronics based DG are technologically ready to be seamlessly integrated to the grid, and they should no more be considered as power system disturbant generation units.

1.3.2 Distributed generation actors and market scenario

Nowadays, there is a clear trend towards integrating a more automated control and operation of electrical systems through future electrical market scenarios, where most actors participate motivated by economic interests, similar as stocks market do. In this regard, market actors could decide whether to invest or not in providing raw power or increased system flexibility by observing the evolution of energy and auxiliary service markets. Hence,

electricity markets arise as the entities optimizing future power systems and individual actor businesses, while minimizing central planning and control issues.

Such future market models are likely to embrace wider additional markets, resulting from the emerging opportunities provided by increased penetration of DG, active demand management or energy storage systems [3]. Among them, retail markets will be of vital importance along with the fully liberalization of the retail activity for both energy producers and consumers, which would enable to buy and sell energy products and grid services locally, limiting the need of undertaking wholesale transactions [4].

At some point in the future the power system will fully integrate RES based DGs, and enable such systems for direct participation with energy and ancillary service markets, where prices for energy and ancillary service provision will change hourly (or faster) depending on real-time performance and capacity allocated in the system. As the electric power system become stressed prices tend to rise. Therefore, broadcasting market prices would enable RES generation units, to respond and reduce reliability concerns, where price signals would be the dominant means of achieving a desired response. Generation units that could not respond, due to their own economic or physical constraints by reducing their service offers to the market, would continue operating as locally commanded units unless the system operator interrupts for security reasons. However, those able to provide several services and to respond to fast price variations would receive increased economic benefits.

Besides of scheduled energy provision, RES based generation systems can provide additional services related with the stability and power quality of distribution systems. This requires new possibilities and regulation of distribution systems to ensure active participation of RES and DG in the deregulated electricity market [3].

1.4 Goal and objectives of the Thesis

As early mentioned, a progressive transition is currently being experienced in electrical power systems; where stable passive distribution networks with unidirectional power flows, evolve into active distribution grids with bi-directional power transportation [9]. In this regard, present electrical distribution systems calls for considerable changes related with the operation and control of such networks, moving towards a system enabling a higher degree of DG, real-time control and active market participation. Therefore, increasing research efforts should be focused on new modular, adaptable and scalable active distribution systems and control solutions, able to cope with rising technological and economical demands [3, 9].

Up to date any disturbances introduced by RES-based generation systems were directly neglected from the SO, as the stability and reliability of distribution system was not affected due to its low penetration levels. However, this assumption cannot be considered any more, as the increasing implementation of RES-based distributed power plants and energy storage systems will raise new efficiency, reliability and security problems in the manner in which the distribution system has been operated and controlled up to date [4].

Therefore, with the purpose of successfully determining a clear scope and the main contributions of this PhD Thesis, the research hypothesis, principal goal and objectives to be achieved during the research process will be clearly identified below.

Hypothesis: Due to the high penetration of poorly controlled distributed generation systems, being most of them operating at maximum power production, there is a clear need in designing and operating highly controllable and manageable distributed power plants, which could achieve increased benefits from the energy and ancillary service markets, while considerably improving power system performance.

For this reason, the **principal goal** of this Thesis addresses the main challenges associated with the hierarchical control design and implementation of large scale Distributed Power Plants (DPPs), with the purpose of achieving advanced grid conection performance while reaching maximum economic benefits from its optimum real-time operation

In order to suitably highlight the full potential of the proposed control solution, this Thesis presents a generic control system, valid for any type of active distributed power plants, such as wind, PV and wave power plants, but also for hybrid power plants or microgrids, where different renewable and conventional generation technologies coexist. Thus, the main implementation adjustments among the different application scenarios, relate to the real-time power profile characterization of each generation technology, and to the corresponding plant specific configuration.

However, the validation of the proposed real-time controller will be evaluated in a wave power plant application, which comes motivated due to the tremendous potential of wave energy, but also for the challenge it constitute to achieve advanced real-time control capabilities in such an oscillating renewable energy resource. Then, the proposed plant controller is intended to control the real-time production of the wave power plant in order to meet the flat and stable power generation schedules agreed in day-ahead or intra-day markets. Furthermore, an increasing concern is recently being experienced in the wave energy sector, regarding the seamless grid integration of such highly oscillating power plants, due to the near-commercial deployments already achieved of several wave energy converter technologies.

Therefore with the purpose of achieving the before mentioned goal of the PhD Thesis, the following objectives were clearly settled and successfully achieved;

1. Design of the power processor and control of Wave Energy Converters (WECs)
2. WPP topologies analysis and electrical distribution system design
3. Control of a large scale Wave Power Plant (WPP) for achieving high performance grid integration

The first objective of this project (design of the power processor and control of the WECs) was based on the modelling and control of a single wave energy generation unit. A wave to grid model of a WEC was developed, in which special attention was paid on the control strategy implemented for obtaining maximum power extraction from the sea. With the purpose of validating the wave to wire model and its control, the proposed electrical

system was tested on a smaller scale laboratory setup. In addition, the entire WEC model was also implemented in simulation to later implement the plant controller, and determine the entire WPP system behaviour.

The second objective of the project (WPP topologies analysis and electrical distribution system design) was dealing with analysing several WPP topologies and designing the distribution system of the wave farm in order to obtain a suitable grid connection of the plant, while ensuring an efficient, reliable and safe operation. In addition the performance of the multiple interconnected wave energy converter units was assessed in order to overcome any of the possible power quality and stability problems due to a detrimental effect from the interconnection of several WECs. The evaluation and analysis of the proposed configuration system was developed on a time domain simulation model, which considered the entire WPP layout proposed in this section.

Finally, the last objective (Control of large scale WPPs for achieving high performance grid integration), which constituted the main contribution of the project, was based on proposing an innovative and original wave farm control strategy with the purpose of achieving a seamless grid integration and SO compliant power plant performance. In this case, a hierarchical power plant control structure was designed, along with the real-time power sharing controller, where the resulting plant performance and system behaviour was analyzed in a real-time domain simulation.

1.5 Contributions of the Thesis

In order to assess the real outcome of this PhD dissertation, the present section introduces the main contributions of the thesis, which are briefly summarized as follows:

Adaptive vector control for maximum power extraction of wave energy converters

The main contribution of this section is found in the adaptive controller proposed, which maximizes the energy extraction from the resource regardless of the dominant irregular wave frequency characteristics. This adaptive performance is achieved from a signal monitoring and synchronization system, whose implementation in the wave energy sector has never been considered up to date. In addition, a novel vectorial approach has been introduced for determining the PTO forces acting on the wave energy conversion system, which maximizes the instantaneous or average power extraction from the resource.

Hierarchical control structure of distribution power plants

This Thesis proposes a novel Hierarchical Distributed Control Structure (HDCS) for increased management of renewable-based active distributed plants. This hierarchical control structure comprises all possible functional levels from the higher long-term economic scheduling layer, to the instantaneous supervisory control of the resource, emphasizing the

entire operation and control functionalities needed for increasing the integration of active distributed power plants.

In addition, thanks to the modularity of the proposed solution, such HDCS can be applied to a large variety of distributed power applications, ranging from: (a) subtransmission or distribution networks, with distributed generators and controllable loads, (b) power plants, with multiple generating units or (c) buildings or campuses, with controllable loads and power generation units.

Competitive power control of distributed power plants

In order to achieve real-time control capabilities along the distributed hierarchical control structure, this Thesis introduces a novel power sharing control strategy, based on the competitive operation of multiple generation units through the implementation of real-time market rules. The principal feature of the competitive power controller deals with ensuring real-time control of the plant generation at minimum operation costs, through optimal allocation of available resources. Such advanced plant control capabilities are achieved by propagating a virtual price signal over the entire hierarchical structure, being the final-end generation unit the responsible entity for deciding its generation involvement, based on the price signal received and its own marginal costs. The main advantage of the proposed competitive controller is based on the achievement of real-time optimum power dispatch capabilities, even in large distributed systems handling overwhelming amounts of information, or where such information is not available at all. In addition, it can provide multi-objective real-time control capabilities, achieving a controllable supply of active, reactive and ancillary service provision.

Again, the proposed competitive power control solution can be also applied to generalized active distribution system, integrating an heterogeneous set of DG, demand response and energy storage technologies.

1.6 Outline of the Thesis

This PhD dissertation is organized around 6 main chapters, where the content is suitably structured as follows.

The first chapter introduces the reader into the actual power system scenario and dominant market structures implemented worldwide, which constitutes the pillars over which the current power industry has been construted. The main purpose of this chapter is to bring to light the new operation and control challenges that large penetration levels of RES-based DG will pose on existing power systems, and emphasize the main research efforts that should be addressed in order to gradually move towards the power system of the future. Thus, this chapter sets the real motivations driving the interest of this Thesis, where the lack of controllability found in distributed power systems, and particularly in distributed power plants arise as the key topic to be resolved. Finally, the main hypothesis, goal and objectives

of the Thesis are introduced, along with the main outcome contributions derived from the research process.

The second chapter presents the current state of the art on hierarchical control of structures found in distributed power plants, paying special attention to wind and PV applications, which appear as the dominant RES-based DG deployments. Furthermore the hierarchical control solutions found in more advanced active distribution grids, such as smart-grids, virtual power plants and microgrids have been also revised, due to the intelligent control requirements needed in such systems to integrate DG, energy storage and demand response.

The proposed hierarchical control structure and real-time control solution developed in this PhD Thesis appears thoroughly described in Chapter 3. The objective of this chapter is to presents the concept and operation characteristics of the proposed competitive control in active distribution systems, along with its main capabilities, limitations and preferred applications. In this regard, a hierarchical control structure is initially introduced with the purpose of laying down the control layers considered, for achieving increased management in renewable-based active distribution systems. Then, the competitive power control concept is presented, with its main control capabilities, including a cost of operation breakdown for generic RES based distributed systems. Finally, the competitive power control results are analyzed in a very simplistic simulation model, which considers a generic active distribution grid integrating DG, energy storage and demand responsive loads.

The detailed modelling and control of a single wave energy generation unit is presented in Chapter 4. A wave to grid model of a WEC is provided, in which special attention is paid on the control strategy implemented for obtaining maximum power extraction from the sea. With the purpose of validating the wave to wire model and its control, the proposed system was tested on a smaller scale laboratory setup, and the obtained results are described in detail. In addition, the results of the simulated time-domain model of the WEC are validated. This resource characterization is of vital importance, as it will reproduce the expected real-time power oscillating performance, which will be used in a later stage for the competitive controller as the instanateous maximum resource capacity

The detailed implementation of the competitive power control in distributed power plants is provided in Chapter 5, making special emphasis on the selected wave power plant scenario. Once the wave energy resource characterization and control have been validated, the competitive controller is implemented along with the detailed operation and maintenance cost models. Finally, the power plant performance and final incurred costs are analyzed through the entire operational lifetime of the plant. In order to have a meaningful evaluation of the long-term benefits provided by the competitive control strategy, the competitive simulation is compared with the conventional (1/n) power sharing strategy, in which the plant power setpoint is equally shared over the n available resources.

Finally, Chapter 6 provides the main conclusions from the achievements obtained, and draws the main lines towards future research challenges that may arise.

1.7 Publications

Patents:

[1] **Antoni M. Cantarellas**, Daniel Remon, Pedro Rodriguez, “Estructura y método de control para un sistema de potencia eléctrico distribuido, y sistema de potencia eléctrico distribuido,” WO2017114991 A1, Jul 6, 2017.

[2] **Antoni M. Cantarellas**, Daniel Remon, Pedro Rodriguez, “Convertidor de energía undimotriz y método”, P201431323, 2014

List of Journal Publications:

[1] **A. Cantarellas**, D. Remon, W. Zhang and P. Rodriguez, "Adaptive vector control based wave-to-wire model of wave energy converters," in *IET Power Electronics*, vol. 10, no. 10, pp. 1111-1119, 8 18 2017.

[2] D. Remon, **A. M. Cantarellas**, J. M. Mauricio and P. Rodriguez, "Power system stability analysis under increasing penetration of photovoltaic power plants with synchronous power controllers," in *IET Renewable Power Generation*, vol. 11, no. 6, pp. 733-741, 5 10 2017.

[3] **A. M. Cantarellas**, D. Remon and P. Rodriguez, "Adaptive Vector Control of Wave Energy Converters," in *IEEE Transactions on Industry Applications*, vol. 53, no. 3, pp. 2382-2391, May-June 2017.

[4] E. Rakhshani, D. Remon, **A. M. Cantarellas**, J. M. Garcia and P. Rodriguez, "Virtual Synchronous Power Strategy for Multiple HVDC Interconnections of Multi-Area AGC Power Systems," in *IEEE Transactions on Power Systems*, vol. 32, no. 3, pp. 1665-1677, May 2017

[5] W. Zhang, **A. M. Cantarellas**, J. Rocabert, A. Luna and P. Rodriguez, "Synchronous Power Controller With Flexible Droop Characteristics for Renewable Power Generation Systems," in *IEEE Transactions on Sustainable Energy*, vol. 7, no. 4, pp. 1572-1582, Oct. 2016.

[6] D. Remon, **A. M. Cantarellas** and P. Rodriguez, "Equivalent Model of Large-Scale Synchronous Photovoltaic Power Plants," in *IEEE Transactions on Industry Applications*, vol. 52, no. 6, pp. 5029-5040, Nov.-Dec. 2016.

[7] E. Rakhshani, D. Remon, **A. Mir Cantarellas** and P. Rodriguez, "Analysis of derivative control based virtual inertia in multi-area high-voltage direct current interconnected power systems," in *IET Generation, Transmission & Distribution*, vol. 10, no. 6, pp. 1458-1469, 4 21 2016.

List of Conference Publications:

[1] **A. M. Cantarellas**, D. Remon, J. M. Garcia and P. Rodriguez, "Competitive control of wave power plants through price-signal optimum allocation of available resources," 2017 IEEE Energy Conversion Congress and Exposition (ECCE), Cincinnati, OH, 2017, pp. 5579-5586.

[2] D. Remon, **A. M. Cantarellas**, J. Martinez-Garcia, J. M. Escaño and P. Rodriguez, "Hybrid solar plant with synchronous power controllers contribution to power system stability," 2017 IEEE Energy Conversion Congress and Exposition (ECCE), Cincinnati, OH, 2017, pp. 4069-4076.

[3] D. Remon, **A. M. Cantarellas**, Weiyi Zhang, I. Candela and P. Rodriguez, "Enhancement of the stability of a distribution system through synchronous PV," 2016 IEEE Power and Energy Society General Meeting (PESGM), Boston, MA, 2016, pp. 1-5.

[4] **A. M. Cantarellas**, D. Remon, C. Koch-Ciobotaru and P. Rodriguez, "Adaptive power control of wave energy converters for maximum power absorption under irregular sea-state conditions," 2015 IEEE Energy Conversion Congress and Exposition (ECCE), Montreal, QC, 2015, pp. 6655-6659.

[5] D. Remon, **A. M. Cantarellas**, M. A. A. Elsaharty, C. Koch-Ciobotaru and P. Rodriguez, "Equivalent model of a synchronous PV power plant," 2015 IEEE Energy Conversion Congress and Exposition (ECCE), Montreal, QC, 2015, pp. 47-53.

[6] D. Remon, **A. M. Cantarellas**, J. D. Nieto, Weiyi Zhang and P. Rodriguez, "Aggregated model of a distributed PV plant using the synchronous power controller," 2015 IEEE 24th International Symposium on Industrial Electronics (ISIE), Buzios, 2015, pp. 654-659.

[7] J. D. Nieto, D. Remon, **A. M. Cantarellas**, C. Koch-Ciobotaru and P. Rodriguez, "Overview of intelligent substation automation in distribution systems," 2015 IEEE 24th International Symposium on Industrial Electronics (ISIE), Buzios, 2015, pp. 922-927.

[8] W. Zhang, **A. M. Cantarellas**, D. Remon, A. Luna and P. Rodriguez, "A proportional resonant controller tuning method for grid connected power converters

with LCL+trap filter," 2014 International Conference on Renewable Energy Research and Application (ICRERA), Milwaukee, WI, 2014, pp. 445-450.

[9] **A. M. Cantarellas**, E. Rakhshani, D. Remon and P. Rodriguez, "Grid connection control of VSC-based high power converters for wave energy applications," IECON 2013 - 39th Annual Conference of the IEEE Industrial Electronics Society, Vienna, 2013, pp. 5092-5097

[10] K. N. Md Hasan, **A. M. Cantarellas**, A. Luna, J. I. Candela and P. Rodriguez, "Grid harmonic detection and system resonances indentification in wave power plant applications," IECON 2013 - 39th Annual Conference of the IEEE Industrial Electronics Society, Vienna, 2013, pp. 1644-1649.

[11] **A. M. Cantarellas**, E. Rakhshani, D. Remon and P. Rodriguez, "Design of the LCL+trap filter for the two-level VSC installed in a large-scale wave power plant," 2013 IEEE Energy Conversion Congress and Exposition, Denver, CO, 2013, pp. 707-712.

Chapter 2.

2 State of the Art

2.1 Introduction

This section analyzes the main hierarchical control structures on the shelf, regarding control of RES based active distribution networks, covering the main solutions applied in distributed power plants, virtual power plants (VPPs), smart-grids and micro-grid applications. Afterwards, a review on energy management systems and real-time controllers is performed, in order to have a clear scope on the main control philosophies currently in place in such advanced distributed grid configurations. Finally, a deep description will be provided, along with the main control capabilities and limitations, of the transactive energy concept, which constitutes one of the latest hot research topic in this field.

2.2 Hierarchical control of RES based active distribution networks

Hierarchical control structures of RES based power plants

While conventional plants are constituted by a few large synchronous generation units, RES based power plants are usually formed by larger amounts of smaller scale power electronic converters, normally dispersed over wide geographical areas. Considering the large number of DG involved and its inherent stochastic behavior, RES based power plants require more complex control solutions in order to meet stable power supply schedules, while ensuring advanced grid code compliance. Non-hydro renewable power plants have

been traditionally controlled under the "feed-and-forget" philosophy, which consists on providing maximum available power supply, receiving SO control restrictions only in case of system security and reliability problems. However, with the large penetration levels of RES based DG already achieved, SOs require that these plants provide increased control capabilities and grid services similarly as conventional power plants do. Among others, these services cover conventional generation control, frequency regulation, reserves capacity provision, reactive power supply, voltage control, island operation and black-start capabilities. In order to provide such power supply and grid service functionalities when required, the implementation of a hierarchical control system becomes a must [3, 10, 11, 13].

Supervisory Control and Data Acquisition (SCADA) systems initially appeared as suitable centralized control platforms, allowing the plant operator to have real-time visibility and direct control capabilities on a few individual DG units. However, as power electronic based DG integrate more advanced embedded control features, and distributed power plants rapidly grow towards large scale deployments (hundreds of DG), this centralized control structure becomes obsolete, rising a growing demand on distributed control systems (DCS), which could manage the entire generation asset in a more automated and coordinated manner. Therefore the instantaneous performance from hundreds of DGs does not purely depend on the plant operator skills, and control actions can be automatically taken in real-time to prevent any suddent unexpected harmful situation [9].

In contrast with centralized control systems (CCS), DCS integrate a more complex control architecture, where several hierarchical controllers coexist, with devoted specific control functions and responsabilities among the different control levels. For instance many RES-based DCS deploy remote locally emedded controllers within DG units, allowing them to behave as autonomously as possible, and receiving only coordination actions from superior controllers when needed. This is the case of most currently implemented Wind or PV power plant control systems, where a central SCADA system at the plant level coordinates the steady state performance of multiple DG controllers in order to achieve a desired plant operation performance.

The vast majority of locally implemented control algorithms are executed by remote terminal units (RTUs) and/or programmable logic controllers (PLCs), allowing the field equipment to operate automatically, without receiving real-time information from the master station. In addition, RTUs and PLCs are in charge of performing data acquisition of field variables for monitoring and closed loop control purposes at higher control levels. Such information is compiled and processed through the SCADA system, which through a human-machine interface (HMI), allows the operator to perform suitable online supervision and basic control actions. Control system data can also be stored in databases, which will allow the plant operator to perform deeper evaluation analysis on specific plant performance. Further detailed information regarding actual SCADA and DCS control structures and capabilities can be found in [11] and [9] when applied to wind power plants and microgrids respectively.

With respect to the main hierarchical control structures found in the literature, wind and PV power plants collect the main advancements developed so far in this field, as they have proved higher maturity levels than any other types of RES. A hierarchical wind power plant control structure was introduced in [14] (Fig. 2.1), which is based on two main control levels. There is a central wind farm control layer in charge of managing the entire production of the plant and sending dispatching signals to each individual turbine; and another local wind turbine control level ensuring that the power reference received from the central controller is finally provided. This two-level based hierarchical control structure arise as one of the most commonly found solution in the industry, where one controller supervises and controls the suitable operation of the plant.

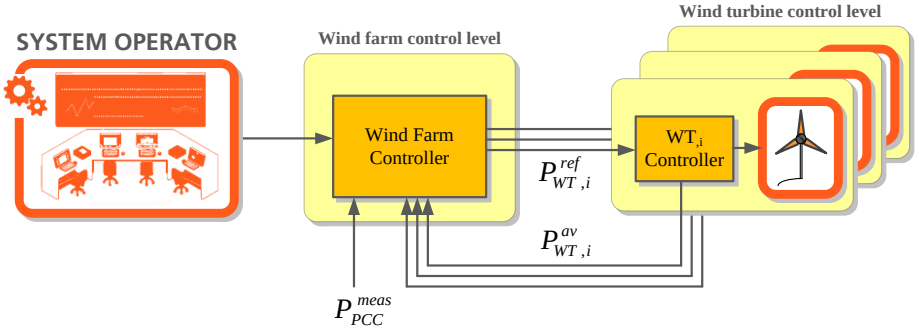

Fig. 2.1. Overall wind power plant control system [14]

Another more advanced hierarchical control structure has been proposed in [3, 15] for wind power plant applications, but also being extensible to generalized active distribution networks. In these references, a wind power plant system controller (WPP-SC) is considered as the central master control unit, serving as the interface between the SO and the local wind turbine generators. Therefore, the WPP-SC appear in charge of performing suitable power dispatch and scheduling duties among wind turbines (WTs), in order to ensure optimum wind power plant operation and control.

As it can be observed in Fig. 2.2 (a), the proposed power plant configuration is composed of several wind turbine units grouped together forming clusters, with a dedicated energy management system (EMS) responsible of coordinating their real-time performance. Thus, [3, 15] introduce an additional hierarchical control level between the WPP-SC and the individual WT controllers. This can be observed in Fig. 2.2 (b), where the functional control hierarchy of the wind power plant is divided in 3 main layers:

- The system block (SB) represent the functionalities found in the WPP-SC software, which entails allocation and coordination of all WTunits;
- The group block (GB) coordinates the operation of object blocks that have some kinds of predefined functions and interconnections. Constitutes the cluster control functionalities.

- The object block (OB) represents the local control implemented within each individual wind turbine unit.

(a)

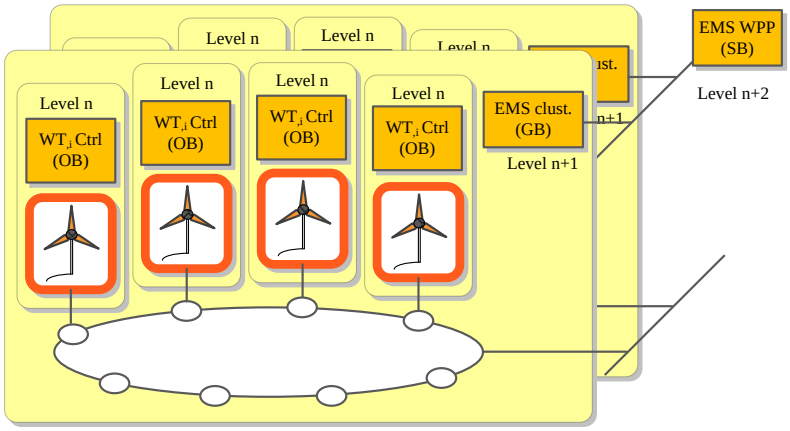

(b)

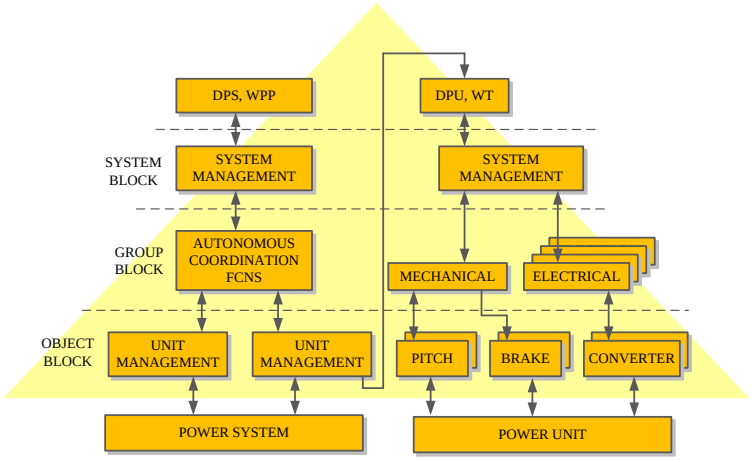

Fig. 2.2. (a) Wind power plant structure, (b) Wind power plant functional control hierarchy [3][11]

Regarding the hierarchical control solutions proposed by the industry, the two main approaches previously defined have a clear dominant position. However, an increasing trend is found in following the second approach (mainly in large scale applications), where a third cluster control level is placed between the plant controller and local WT controllers to provide a coordinated action between WT groups. For instance, this is the particular case of the wind park solution from Mita-Teknic [16], which appear depicted in Fig. 2.3.

. This wind farm control structure provides a central plant controller that dispatches the active and reactive power setpoints directly to the WT controllers or through a cluster controller, that enables increased power plant flexibility in case of large scale wind parks or

where there is more than a single grid interconnection point. Therefore, this solution allows to perform real-time control over a total of 2500WTs distributed through 50 clusters, by integrating selectively placed grid and weather measurements in the plant or cluster controllers. Besides active and reactive power control, this wind power plant offer advanced control features such as frequency and voltage control, power reserves control, LVRT detection, intelligent setpoint dispatcher, etc.

General control and SCADA system requirements for wind power plants are introduced in [17]. This reference provide a set of requirements regarding the control functionalities, monitoring and communication technologies suitable for achieving high performance grid integration of wind power plants.

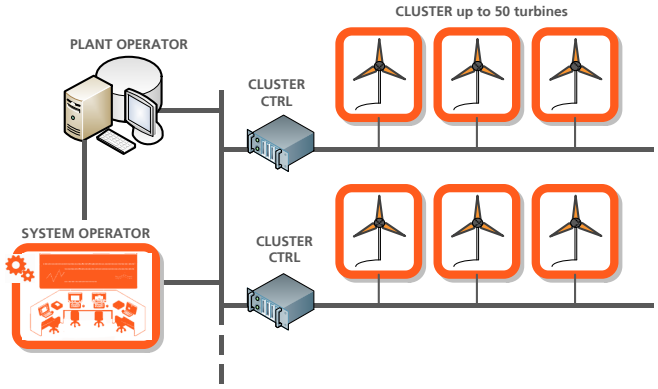

Fig. 2.3. (a) Wind power plant architecture [16]

Finally, in the case of electrical systems with large penetration of wind generation, [18, 19, 20] introduce the concept of grouping wind farms into wind farm clusters (later renamed as Virtual Power Plants). The goal of such concept is to allow SOs to manage wind energy in a similar manner as conventional generation systems, limiting their negative grid integration impacts associated with the variability of the resource, their distributed location and the wide range of generator technologies used. A so called “Wind Farm Cluster Management System (WCMS)” is introduced here as the highest control level in charge of coordinating the real time performance of a set of wind power plants. The proposed control structure allows wind farm clusters to provide advanced grid integration services, such as active and reactive power control, reserves provision, congestion management, gradient control, local voltage control at given busses, etc. The wind farm clustering layout is introduced in Fig. 2.4(a), where wind farms pending from the same interconnection node are considered as clusters. As it can be observed in Fig. 2.4(b), the WCMS is formed by two hierarchical levels: the superior level deals with typical SO control functionalities, and the remaining level (Wind farms dispatch center level) appear in charge of providing the optimum dispatching production setpoints to each of the power plants within the wind farm cluster.

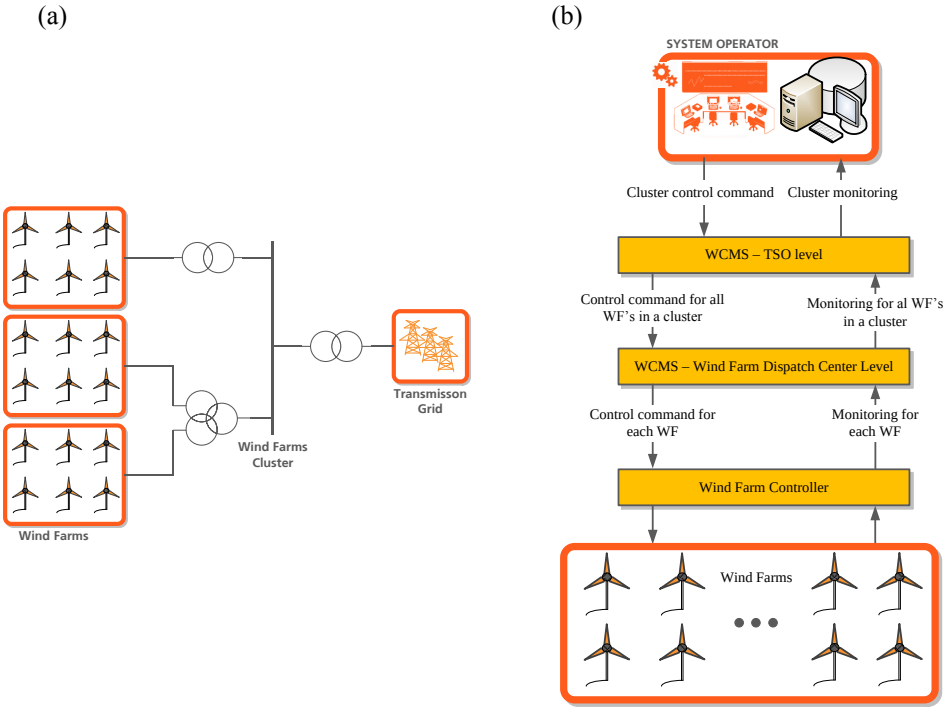

Fig. 2.4. (a) Wind power plant clustering concept, (b) Wind power plant clustering functional control hierarchy [18]

In line with the previously introduced control structure, it has been found that many generation companies (GENCOs) recently implement high level monitoring and control tools related with the entire asset management of generation plants, which appear distributed over a given electrical system. In this regard, it is possible to evaluate the wholistic performance of generation plants at a glance, and allows to take corrective or even preventive actions to ensure optimum operation and maintenance duties in a coordinated manner. This control solutions provide added value to the entire generation asset management, by mainly analyzing past, present and maybe future performance of individual power plants.

Regarding PV plant control systems, very few references have been found introducing any control strategies or SCADA system solutions purely specific to PV power plants [21, 22]. This is due to the simplistic control nature of such plants, which basically make use of similar control structures as in the wind energy sector. Alike, a centralized PV plant controller appears in charge of controlling the active and reactive power supply at the plant poit of common coupling (PCC), by providing suitable power dispatch references to the local PV controllers. As power electronic based PV units integrate more advanced embedded control features, such as frequency and voltage droops, LVRT, inertial response, etc., they are only required to inject the active and reactive power references received during normal

operation conditions, while these advanced local controllers instantaneously react in case of any sudden system disturbance.

Instead, increased research efforts have been found in hierarchical control structures of PV-based microgrids or hybrid PV power plants (PV-diesel, PV-ESS, PV-wind), as higher interoperability levels among DGs of different nature call for more advanced control solutions. As previously introduced, details on these control structures will be provided in following sections.

Finally, in the field of hydro power plants, [23] presents an overview and analysis of the new trends towards a more distributed control, protection and supervisory management system strategies, implemented in hydro power plants. Automation systems in hydro power plants are characterized by the presence of three hierarchical levels: command and supervision, interface and data acquisition and process layers. The interface and data acquisition system comprises the data acquisition and control units (DACUs), which main responsibility lies on providing sufficient intelligence to the control commands and on transferring all the information required from the command and supervisory to the process level. The process level hosts several specific intelligent electronic devices (IEDs) for ensuring a suitable hydro power plant automated system

Other references can be found in the management of hydro power plants, as [24], where a hierarchical power plant control structure has been proposed based on the enterprise level, supervision and control level, and a final process level.

Hierarchical control structures in RES based active distribution networks

As suitably defined in [9], active distribution networks represent a recent evolution of distribution grids, where massive integration of DG units and demand response take place to contribute towards meeting the energy needs of the future. Therefore, such distribution grids call for advanced hierarchical control solutions to ensure a safe and reliable system operation, but also to limit any undesired effect of such highly stochastic and unpredictable energy actors. Particular embodiments of active distribution grids appear in the form of smart-grids, micro-grids, Virtual Power Plants (VPPs), or even Hybrid Power Plants (HPPs), which constitute the applications of interest of this section.

From the literature review it has been found that hierarchical control structures have a stronger presence in smart-grids, virtual power plants and microgrid advanced network applications, mainly due to the large amount of distributed and intelligent control required in such systems. These network configurations are constituted of large amounts of smaller generation systems, usually in the form of RES based DGs widespread over large geographical areas, which should interact with the main distribution system as a single controllable, manageable and tradable entity. In contrast with RES based power plants, which mainly consider the management of power generation units, such advanced network systems also consider local loads which could be directly feed when operating islanded from the main

grid. Therefore, smart-grid and other applications use to perform DSO functionalities when being disconnected from the distribution system network.

In the field of smart-grids, many references appeared proposing novel hierarchical control structures, but for the sake of simplicity, this SOA document focus on [25], which proposes a very complete standardized control solution, similar to the ones provided in the automation process industry. In this reference the CEN-CENELEC-ETSI Smart Grid Coordination Group is setting the Smart Grid Architecture Model (SGAM) Framework, which can be applied as a mapping methodology, to document smart grid use cases from a technical, business, and security point of view.

Management of electrical power networks generally consider a combination of different working fields, from the purely related to physical energy conversion processes, up to the ones associated to higher functional control structures (refer to IEC 62357-1 [26] and IEC 62264 [27]). If this is applied to the Smart grid concept, it leads to the apparition of the SGAM framework, which is depicted in Fig. 2.5, and represents the hierarchical control levels of power system management that take place within the different power system domains. The domains represent the entire electric energy conversion chain (bulk generation, transmission, distribution, DER and customer premises), while the SGAM zones represent the hierarchical levels needed for performing power system management duties [26]. This hierarchical model has aroused as an extension of the already existing Purdue Reference Model for computer integrated manufacturing (adopted by IEC 62264-1), translating the hierarchical layers of the manufacturing process automation industry in the power system management field.

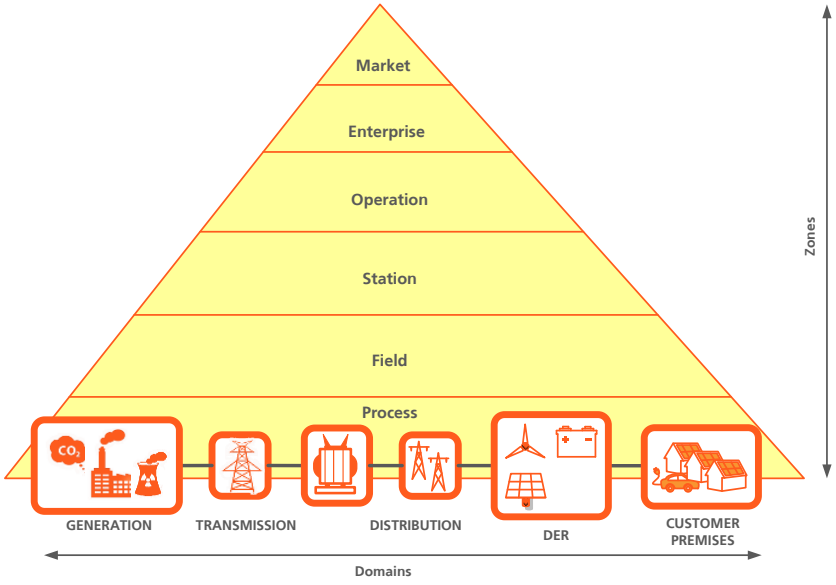

Fig. 2.5. Smart Grid Architecture Model (SGAM) Framework [25]

The hierarchical zones are composed by: the process level, which considers any transformation of energy and the equipment involved (e.g. generators, transformers, circuit breakers, sensors and actuators, etc.); the field level, which considers the required equipment for performing monitoring, control and protection of power system processes (intelligent electronic devices-IEDs, protection relays, etc.); the station level, which represents the aggregation of field level equipment (data aggregators, functional aggregation of field devices, local SCADA systems, supervisory plant systems, etc.); the operation level, represents power system control functionalities at each of the different levels (DMS, EMS, microgrid management systems, VPP management systems, etc.); enterprise level, which includes pure economical and organizational management functionalities for enterprises (asset management, personnel workforce management, billing and trading services management); and the market level, which considers the market operation for electricity trading over the entire power system energy conversion chain.

In the field of microgrids and virtual power plants (VPPs), [28] presents a hierarchical control structure, initially implemented in a smart microgrid, for finally aggregating several of these microgrids to constitute a VPP. The microgrid hierarchical control system is based on a 2-level structure, similar to the ones early introduced for wind and PV power plants. The primary control level focus on providing local control functionalities to the DG units. This control level is characterized by its autonomous operation and fast response times, as it arise as the responsible for ensuring local system stability and reliability. The secondary control works with a larger time step and appear in charge of performing higher level control functionalities, such as power exchange management between the microgrid and the utility network, optimum resource allocation, voltage optimization and frequency regulation, etc.

After introducing the concept of VPPs, as the aggregation of multiple individual RES based smart-microgrid systems, an additional control layer is required, which will perform functionalities very similar to the ones introduced by aggregators. Then, this tertiary control level deals with electrical market participation duties, while providing suitable power dispatch references for each of the microgrid structures, for finally reaching the required production specifications scheduled or dictated by DSOs.

Another reference which goes one step further in microgrid hierarchical control structures is found in [29, 30], in which the international standard for enterprise-control system integration IEC/ISO 62264 was applied to microgrid and VPPs. The hierarchical control proposed here allows microgrids and VPPs to perform both active network management and direct electrical market participation. This hierarchical control system is introduced in Fig. 2.6, where the left side hierarchical system describes the levels found in the IEC62264 and the right-side hierarchical system represents the equivalent microgrid levels. As it can be observed from this figure, the hierarchical system is divided in 4 main layers, which are described as follows:

- The zero level represents the inner DG control loop required for achieving the desired output current and voltage of the power converter units.

- The level one appear as the responsible of generating the reference for the inner control loop. This control layer implements droop control and active load sharing functionalities for determining such inner control loop references from the actial behavior of the grid connection frequency and voltage.
- The level two represents the secondary control of the system, which performs supervisory and monitoring duties for compensating larger voltage and frequency deviations and regulating the operational setpoints of the microgrid. This secondary control can be performed following centralized or decentralized control philosophies.
- The level three, includes the functionalities inherent of the tertiary control level, wich technically and economically manages the optimum power flow exchange between the microgrid and the main grid.

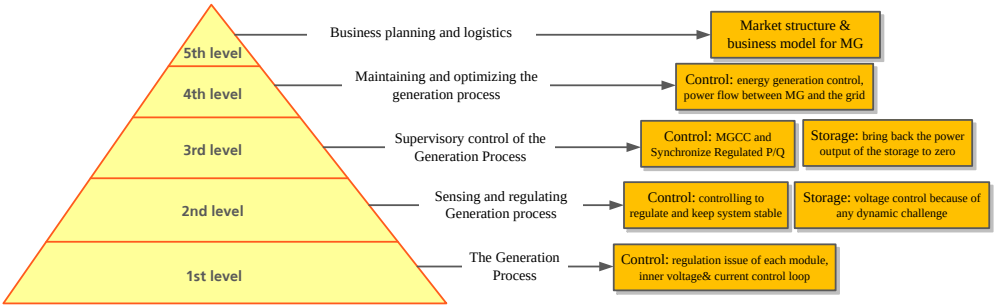

Fig. 2.6. IEC/ISA 62264std. levels applied in microgrid applications

2.3 Energy management systems and real-time controllers in active distributed systems

Real-time power control strategies of RES based power plants

This section introduces the principal real-time controllers and power dispatch strategies most commonly found in RES based power plants. As previously outlined, such real-time power generation strategies arise as a growing need, since DGs are progressively required to provide advanced plant control capabilities (similar to conventional generation) to ensure suitable market participation schedules or SO production requests.

Regarding the plant control structures appearing in the industry, a generalized control approach, as the one introduced in Fig. 2.7 [14, 31], has been typically implemented, where a given plant production objective is satisfied by placing suitable measurement units that describe the actual state of the system. Based the production references and the online measurements received, the power plant controller along with the corresponding dispatcher, specify appropriate power generation setpoints to all the generation unis of the power plant.

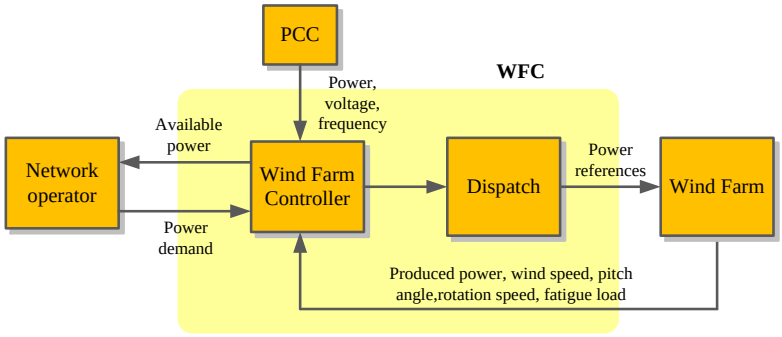

Fig. 2.7. Generalized control structure of RES based power plant controllers

As specified in most of the grid codes currently in place, the control structure implemented in Fig. 2.7 provides multi-objective control capabilities, since it is able to control the active and reactive power delivered at the plant point of common coupling (PCC). In addition, it has the possibility of integrating primary frequency and voltage controllers, which have a direct implication on the final active and reactive power supply, based on the actual state of grid frequency and voltage. The particular realization of such RES based power plant controller is depicted in Fig. 2.8. From this figure it can be observed that the plant controller receives the corresponding P and Q references (P_{PCC}^{ref} and Q_{PCC}^{ref}) to be provided at the PCC, and modifies them according to the frequency and voltage droop response (ΔP and ΔQ). Then the resulting references (P_{Plant}^{ref} and Q_{Plant}^{ref}) are provided to a PI plant controller, whose control purpose is to provide zero steady state error between the plant power reference and measurement. Finally, the PI plant control action (P_{RES}^{ref}) is provided to the plant power dispatcher, which will send appropriate power references to the locally implemented RES controllers in order to achieve the specified control objectives.

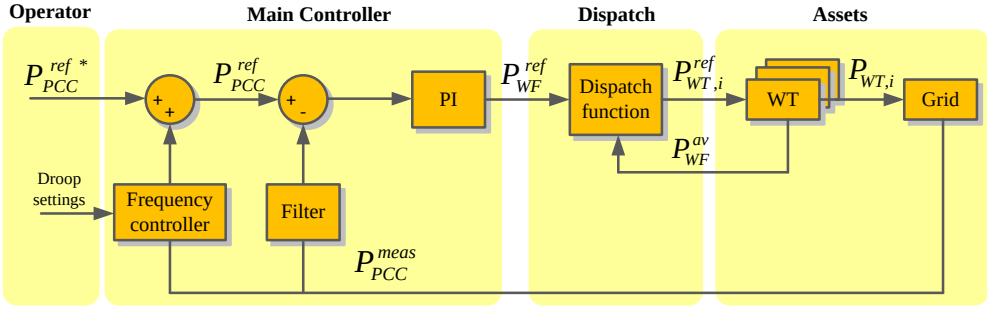

Fig. 2.8 Detailed control diagram of RES based power plant controllers

Finally, it is worth noting that real PV and wind farm applications have successfully implemented the plant control strategy introduced hereinabove, being the Atacama I PV plant and the Horns Rev wind farm clear examples of the suitability of this control solution.

Several power dispatch functions have been implemented so far, being the most popular based on the equal refenrece dispatch and proportional reference dispatch strategies, which have been respectively introduced in (2.1) and (2.2).

$$P_{RES,i}^{ref} = \frac{P_{RES}^{ref}}{n} \tag{2.1}$$

$$P_{RES,i}^{ref} = \frac{P_{RES,i}^{av}}{P_{plant}^{av}} P_{RES}^{ref} \tag{2.2}$$

Where

$$P_{plant}^{av} = \sum_{i=1}^{n} P_{RES,i}^{av} \tag{2.3}$$

The proportional reference dispatch s appears as the prefered solution, when compared with the equal reference dispatch, as the resulting power sharing takes into consideration the real-time loading conditions of each RES generation unit. This is determined thanks to the online calculation of $P_{RES,i}^{av}$, which represent the available power at any given instant based on the offline calculated MPPT lookup table as a function of wind speed.

Other plant control soutions have been proposed in [32, 33, 34, 35, 36, 37, 38, 39], based on fuzzy logic and more advanced optimization approaches, but most of them have been only tested in simulation or in smal-scale laboratory setups. In addition of ensuring the power production requests at the plant PCC, many of them consider the minimization of wind turbine startup/shutdown operations, fatigue loads, loading capabilities, or active power losses in the plant distribution network. Oposing to the clear benefits introduced in these optimum power dispatching approaches, the main concern lies on the execution times of the proposed algorithms, as they might be excesive for ensuring real time operation of very large RES based power plant applications.

Real-time power control strategies of RES based microgrids

One of the principal features found in most microgrid structures, is that they are constituted by participating actors of many diverse nature, such as DGs, demand loads and energy storage systems (ESS), all of them making use of electrical energy in a particular manner. Due to this heterogeneity, advanced control structures are typically required in microgrid applications, with the goal of ensuring an optimum techno-economic operation at

any time. From the literature review it has been found that microgrid control structures and associated energy management systems (EMs) are mainly divided in centralized and descentralized control approaches [40].

From one side, the centralized approach allows optimization control duties to be implemented in a central microgrid master controller (MMC), which further distributes the online operating setpoints to each of the underneath energy actors' controllers. This optimization problem is solved by gathering all the relevant knowledge on microgrid participating actors and network status (DGs, loads, and ESS cost functions, operational limitations, power supply/consumption performance, network parameters, etc.), along with predicted variables influencing the EMS, such as load forecast, wind/PV resource forecast, or energy spot price forecast. For a better understanding, a generalized centralized control structure is depicted in Fig. 2.9.

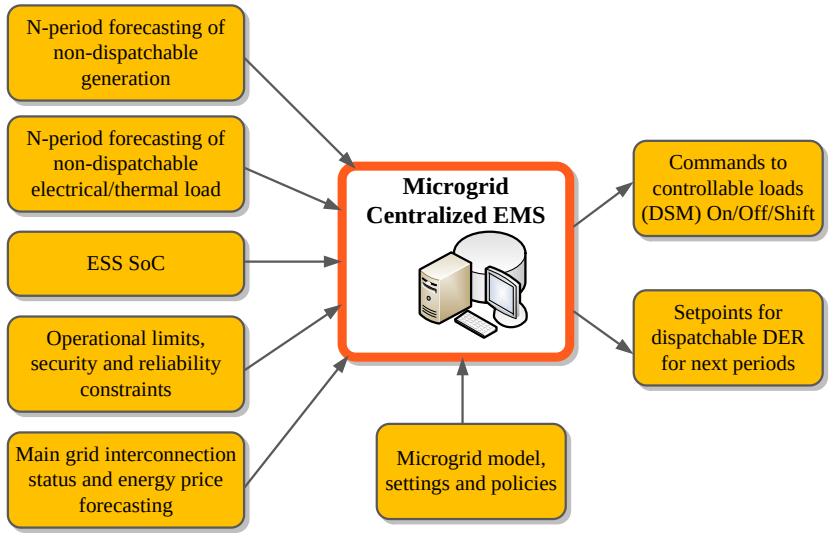

Fig. 2.9 Generalized control structure of centralized EMS in microgrids

From the central optimization algorithms implemented so far, it has been found that many of them apply offline optimization rules for determining the optimum economic schedules of dispatchable units at day-ahead basis [41, 42, 43, 44, 45, 46, 47]. Although these control techniques are well suited, in terms of cost and system performance, to achieve optimal operation in small scale microgrids with limited amounts of generation possibilities [40]; they underperform in typical real-time microgrid applications, as the optimization results are based on static system assumptions. These assumptions reduce the randomness and variability effect on forecasted and real-time performance of RES based generation, loads, and spot energy prices [48], which is not a realistic assumption in such scenarios. In [49] the optimum generation schedule has been calculated offline considering all the possible

microgrid scenarios, and a lookup table has been generated for determining the real-time refefrences to be provided to each generation unit. Although this control strategy provides suitable real-time dispatching references with microgrid changing conditions, it has a limited scope, as it is not feasible to embrace all possible grid operation events that may arise (e.g. system faults, grid reconfiguration events, etc.).

In order to tackle the beforementioned variability issues of offline optimization methods, a growing effort has been experienced to introduce uncertainties in day-ahead microgrid scheduling [50, 51, 52, 53, 54, 55]. Stochastic programming has been considered in most of these references in order to translate the energy management strategy into a deterministic problem, making use of Monte Carlo simulations to achieve a representative set of variable operating scenarios. However, these methods are computational expensive, due to the diversity of possible operating scenarios, and they still do not adjust to unpredictable real-time changing conditions [48].

In addition to all of this, a time dependence correlation need to be considered due to the highly presence of energy storage systems, as the optimum operation of microgrids will be highly impacted by the current the state of charge (SOC) conditions of such units.

In order to overcome all these limitations, many references have recently focused their concerns in developing suitable online energy management controllers, which optimizes the real-time operation of microgrids through minimization of long term costs, while also accounting for the uncertainties of the system [56, 57, 58]. These energy management systems intrinsically cover the variability of RES generation and demand performance, without need of statistically modeling their behavior, while also allowing the microgrid central controller to react to any online time-depending changes. Nevertheless, these optimization approaches neglect the real-time physical operational constraints (line congestions, voltage deviations, etc.) and associated losses of microgrid networks, as they mainly focuss on matching generation and demand on an aggregated basis. Therefore, the optimum power dispatch of these strategies may lead to unfeasible control actions, which would trouble the safe and reliable operation of the system [48]. In addition to this, DG and ESS operational constrains should also be taken into consideration, to avoid setting operational references beyond their limits. Solving these network constrained problems puts an additional degree of complexity to existing optimization algorithms, where [59, 60, 61, 62] apply heuristic optimization approaches based on Genetic Algorthms (GA), Particle Swarm Optimization (PSO), and Ant Colony Optimization (ACO) respectively, to solve such highly complex systems. In addition a relaxation of the optimization algorithm was achieved, by integrating inequatlity constraints in the form of penalty terms, within the objective cost function. In [48] a microgrid real time energy management system is proposed in order to minimize the long-term costs, while ensuring quality of supply to delivered loads, and minimizing the network losses. To achieve this, the operational network constraints of the individual actors and the entire system are integrated in the stochastic optimal power flow (SOPF) problem.

Besides the typical economic related optimization goals found in most mcirogrid central controllers (i.e. operating costs minimization or revenues maximization), additional performance objectives can be integrated in multi-objective optimization platforms. I this manner, it is possible to optimize the economic operation of microgrids, while also maximizing the usage of renewables, minimizing system losses, etc. [63] In order to solve this optimization problems, [61, 62] propose the implementation of pareto optimal methods by using PSO and ACO respectively. This multi-objective approach can also be applied as in [64, 65] by combining several objective functions into an aggregated wheighted cost function.

From the revision of centralized optimum control strategies found in microgrid applications, it can be concluded that many interesting approaches have been developed, considering a set of techno-economical objectives through the implementation of advanced optimization algorithms. However, the main concern in this point is that these algorithms are not computationally free, and may have difficulties in ensuring real-time control capabilities, due to the large execution times required. In addition, large amounts of information need to be transferred and processed in real-time, as these optimum central controllers have a strong dependence on microgrid participating actors and network status knowledge (DGs, loads, and ESS cost functions, operational limitations, power supply/consumption performance, network parameters, etc.). This fact weakens the robustness of these type of controllers, as in the unlikely event of a single communication failure or malfunction, the optimum energy dispatch references may be severely affected, leading to suboptimum microgrid operation. In addition, the rigid behaviour of centralized optimum approaches, makes it difficult to integrate newly implemented dispatchable units in a plug and play fashion. Therefore, any network extensions may require complex modifications on the central microgrid controller. Lastly, the participation of energy dispatch units from different owners may lead to conflictive situations if not suitably addressed, as they are forced to meet a global optimization objective, which neglects the particular interests of individual participating agents.

In contrast to centralized optimum control structures, the descentralized approach offers the possibility of overcoming most of the abovementioned drawbacks, as they solve the optimum energy management problem by providing a high degree of autonomy to the microgrid controllable units. Under this approach, the low level DER, demand responsive and ESS units, are the entities in charge of determining their level of involvement on the global energy dispatch. Thus, the power dispatch setpoints of such units respond to the optimization of local operation objectives (i.e. maximization of supply revenues, or minimization of operating costs), which highly depend on final end-user (owner) preferences. Although, some sort of hierarchical control structure can be found in these approaches, the final power dispatching decisions are made locally.

In most cases, the hierarchical control structure is mainly built around 2-levels, making use of a centralized microgrid controller (CMC) with many distributed or local controllers

(DCs) [66]. From Fig. 2.10(a), it can be observed that the CMC is the central controller in charge of coordinating the aggregated operation of the microgrid in a suitable techno-economical manner, while simultaneously providing acceptable interface conditions with the main grid. The DCs, instead, intend to satisfy optimum local control objectives by considering a deep knowledge on their individual current state and optimum energy use. In addition extensive communication pathways are settled between CMC-DCs and DCs-DCs, sharing ther individual operational experience in order to find a global optimum operating point. A particular realization of DCs appear depicted in Fig. 2.10(b).

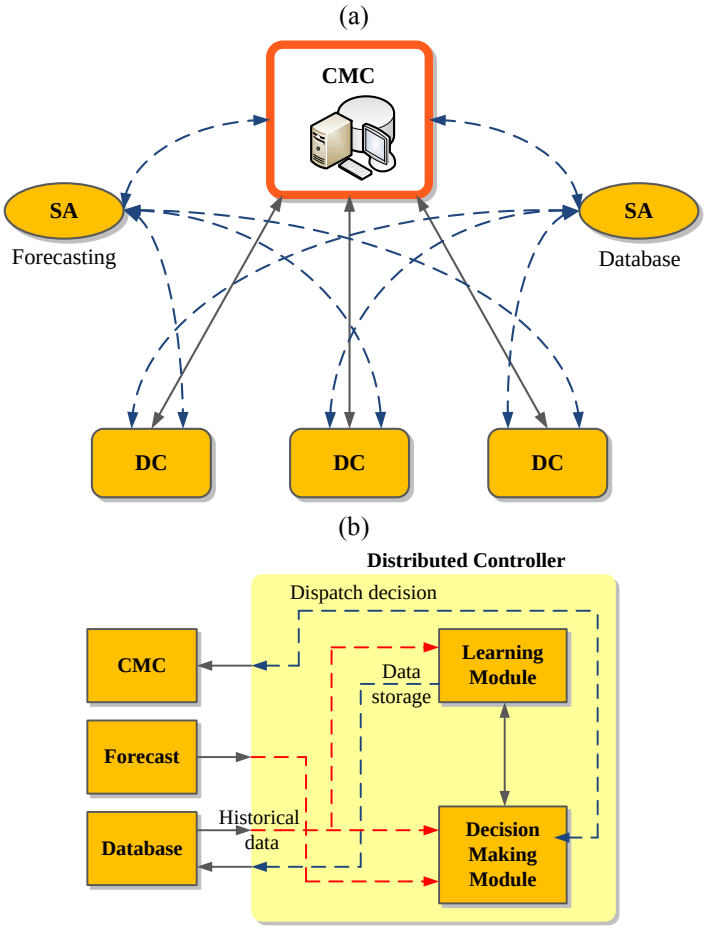

Fig. 2.10 (a) MAS hierarchical control philosophy, (b) Detailed control structure of distributed controllers

Under this operational framework, most of the descentralized microgrid control solutions have been addressed by multi-agent system (MAS) strategies [40]. Multi-agent systems are characterized by the implementation of intelligent DCs, intended to optimize local and global

microgrid objectives, through the massive coordination/collaboration of participating agents with embedded local information knowledge. Therefore, at each time step, individual DCs evaluate its current situation, determine its optimum operating point (based on local obectives), and shares its local knowledge with other participating agents, which if needed readjusts its operation setpoints based on collective negotiation. Of course, setting appropriate DC obligations, interactions and negotionation rules, along with a suitable information exchange among DCs, results in a challenging duty and may play a crucial role in achieving the desired optimum global objectives of microgrids [40, 67]. Examples on implemented MAS control strategies can be found in [68, 69, 70, 71, 72], without a clear sign of a preferred control embodiment resulting on a straightforward candidate solution.

2.4 Price signal based energy management systems – the transactive energy concept

Up to date, several methods have been proposed to control distributed power systems through the implementation of market rules. In this regard, the transactive energy approach appears as a hot research topic [73, 74], with the need for addressing not only economic, but also grid reliability control issues that could arise from the large penetration of flexible distributed generation, energy storage and consumer loads. The transactive energy concept was defined in [75] as "A set of economic and control mechanisms that allows the dynamic balance of supply and demand across the entire electrical infrastructure using value as a key operational parameter". A generalization and standardization of the transactive energy control approach was introduced in [76].

In this control strategy, large amounts of information need to be processed in each node of the grid, since the desired generation/demand profiles from multiple downstream consumers are aggregated in collecting nodes in a hierarchical manner. In addition, many generation/demand models should be considered for firmly reproducing the desired end-user needs. In addition, a two-way communication system is needed for the transactive control to achieve the required power system dispatching performance, which consists on a transactive feedback signal (TFS) and a transactive incentive signal (TIS).

The TFS is transmitted upwards from local loads and distributed generators in the grid control architecture, determining how much power demand is expected to be assumed by each transactive node. Automated energy management systems could be considered for controlling loads depending on user preferences and market prices, where these loads monitor the market price of electricity and convert the residents' comfort preferences to formal market demands. The transactive grid dispatching controller collects the overall aggregated information from local loads and generators, along with bulk power and renewable generation forecast to determine a price based transactive incentive signal (TIS). This control signal is transferred downwards through all hierarchical control nodes and

represents the cost of the power supply to any grid node considering possible system constraints. This price signal is usually determined through a market control mechanism, which clears the price where aggregated supply and demand intersect [75, 77, 78, 79]. As a result, the transactive energy dispatching concept has a considerably centralized structure, since the decisions on the individual production and demand schedules are determined by this central market based control structure, adding the additional operational costs in each grid node due to the technical constraints.

Other transactive control mechanisms could result from iterative TIS and TFS negotiations between neighboring nodes until an agreement is reached between the supply price and desired demand [75, 80]. However, the control algorithms implemented in order to update the TIS and TFS signals should drive the transactive system to convergence, otherwise oscillations may occur in this series of interactions leading the control system towards instability.

Finally, transactive control systems appear particularly suited for dispatching distributed generating units and controllable loads through the implementation of market trading mechanisms. Most of these trading mechanisms are periodically executed in fixed steps following minimum global electricity market timings. Besides existing dispatching strategies, the operation of electrical systems relies on real-time control systems for ensuring a reliable and safe operation. Therefore, it is necessary to develop strategies that address real-time control.

The transactive energy concept has been applied to provide energy dispatching management of electrical systems. However, the transactive energy concept could also be applied to the control of distributed demand resources for the provision of ancillary services, such as spinning and non-spinning resources [81]. However, no references have been found in applying the transactive control mechanism for the provision of reactive power.

Chapter 3.

3 Competitive Control of Active Distribution Grids

3.1 Introduction

Traditionally, the control of the electrical power system was designed to manage large centralized generation units, so their reliable and safe operation could be achieved by closely monitoring and controlling their real-time performance [82] [83]. Nevertheless, the ever increasing penetration of renewable energy sources (RES), mainly at distribution level, is posing new operation and control challenges to existing power systems and system operators (SOs), as considering the same degree of information and communication from thousands of distributed generators (DGs) would result in an overwhelming amount of information that should be processed in real-time by the SO. In this regard, a considerable barrier to the large-scale integration of RES-based DG is that the SO cannot perform real-time control over the power and grid services provision due to the excessive information and communication technologies required [84]. In addition, the gradually change from deterministic to highly stochastic generation profiles experienced in distribution networks, will imply considerable challenges in the balancing of generation and consumption, making it necessary from distribution system operators (DSO) to perform not only their traditional network reconfiguration duties, but also a detailed real-time control of the local on-line generation and demand [84], [85]. Up to date any disturbances introduced by RES-based generation systems were directly neglected from the DSO, as the stability and reliability of distribution system was not affected due to its low penetration levels. However,

this assumption cannot be considered any more, as the increasing implementation of RES-based distributed power plants and energy storage systems will raise new efficiency, reliability and security problems in the manner in which the distribution system has been operated and controlled up to date [85]. Therefore, there is a clear need in designing and operating highly manageable active distribution systems, where both controllable RES based plants, and demand responsive loads would become key actors in the real-time balancing of the generation and demand at distribution level. Furthermore, with the expected large penetration of energy storage systems (ESS) at such end-user level, increased benefits could be achieved from the direct participation in electricity markets, while contributing to improve the distribution system performance with ancillary services.

Regarding the control solutions already found in distribution system applications, the transactive control approach is currently gaining a considerable interest [86, 87, 88, 89, 90, 91], since it arises as a suitable energy management system achieving optimum balance of generation and demand through the implementation of market rules. However, there are some limitations in ensuring a suitable real-time control performance. Since the transactive market clearing mechanism needs to process all the aggregated generation and demand information received, and to execute the optimum economic dispatch for the next time horizon, it introduces an unavoidable time delay, which use to be in the range of 5 to 15 minutes, as generally considered in the literature [86, 88, 89]. The main problem arises when the RES-based generation or the demand variability, which occurs in the range of few seconds, takes place within this minimum time horizon. Then, the discrete transactive controller does not have any control capability over such a short term variations. As a result, the transactive control strategy appears as a suitable short-term energy scheduling solution, but it is unable to perform the required real-time generation/demand balancing duties due to the lack of real-time control capabilities.

In addition, the transactive energy approach requires detailed information on the participating aggregated generation and demand capabilities of the system, and consequently, the system under control need to be known, and accordingly modeled. Therefore, the complexity of large distributed energy systems with heterogeneous participating agents may pose additional time consuming challenges to the information processing and execution of the market clearing mechanism.

In order to achieve real-time control capabilities in active distribution systems, the present chapter introduces a novel power sharing control strategy, based on the competitive operation of multiple active participating agents (distributed generators, demand response and energy storage systems) through the implementation of market rules. This competitive power sharing strategy appears as an alternative to the transactive energy concept, as it proposes a method for real-time balancing of the scheduled generation and demand. Such control capabilities are satisfied by applying a price control signal over the entire grid control architecture, being the final-end participating agent, the responsible entity in charge of deciding its own generation/demand involvement based on its marginal or affordable

electricity costs. In addition, it reduces the information volume to be transmitted and processing requirements, as the higher control levels do not need to have knowledge on the detailed distribution system topology and contributing actors.

The main contribution of the proposed competitive controller is based on the real-time economic power balancing of active distribution grids, while being able to provide a reliable and safe operation of the grid through the active participation of distribution system end-users. In this manner, it is possible to combine the economic grid operation and grid controllers in a single competitive controller (Fig. 3.1), as it can provide multi-objective real-time control capabilities such as active and reactive power control, secondary and primary frequency and voltage control, reserves control, etc.

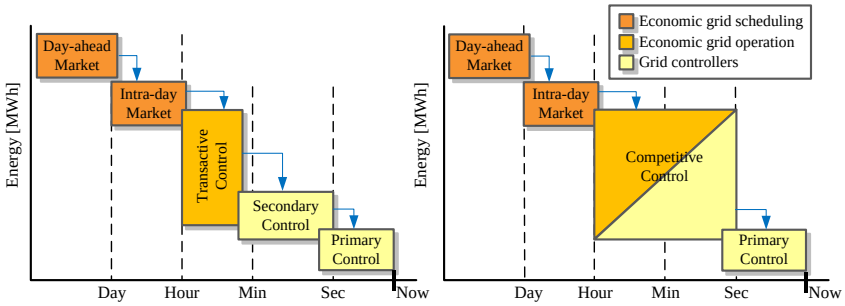

Fig. 3.1 The transactive and competitive marked-based controllers in the context of existing balancing market mechanisms and grid controllers

In the light thereof, the objective of this chapter is to presents the concept and operation characteristics of the proposed competitive control in active distribution systems, along with its main capabilities, limitations and preferred applications. In this regard, a hierarchical control structure will be initially introduced with the purpose of laying down the control layers considered, for achieving increased management in renewable-based active distribution systems. And finally, the competitive power control concept will be presented, with its main control capabilities, including a cost of operation breakdown for generic RES based distributed systems.

As an outcome of this work, it is worth noting that a patent has been issued to the Spanish patent office to present the proposed competitive power controller [92].

3.2 Hierarchical Control Structure of Competitive Active Distribution Systems

The competitive power controller, which is described in detail throughout this chapter, presents a modular structure, so it can be applied to a large variety of distributed power applications to achieve real-time balance between supply and demand, while ensuring minimum operation costs. These applications can range from: (a) subtransmission or distribution networks, with distributed generators and controllable loads, (b) power plants,

with multiple generating units or (c) buildings or campuses, with controllable loads and power generation units [92].

The competitive power controller lays on a hierarchical control structure that comprises all possible functional levels, ranging from the higher long-term economic scheduling layer, to the instantaneous supervisory control of the generation/demand resources. A descriptive schematic of such control structure is shown in Fig. 3.2 and Fig. 3.3, over which the main hierarchical control levels can be identified. From Fig. 3.2 it can be observed that two sets of control levels have been proposed, the ones related to the management and control of active distribution systems, and the ones related to the final end-user generation or demand facility. From one side, the generic control levels focus on providing a safe and reliable control of distribution grids, while ensuring a generation and demand balance at minimum operation costs. On the other side, the specific levels perform the real-time operation of the available resources at the end user facilities, optimizing their local generation/demand power profiles in order to satisfy their individual electricity needs.

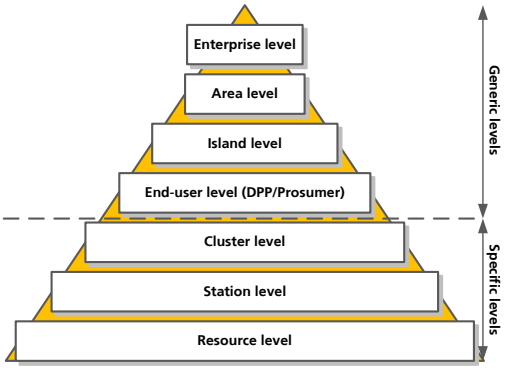

Fig. 3.2. Proposed hierarchical control levels for active distribution systems (specific DPP application)

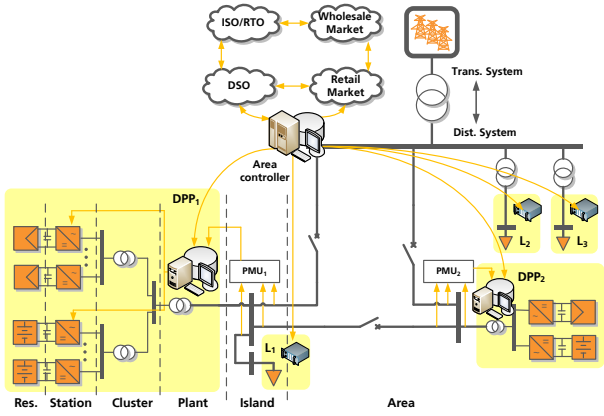

Fig. 3.3. Hierarchical network structure in active distribution grids (specific DPP application)

Due to the large diversity of future distribution systems and end-user actors, integrating generation and demand facilities with controllable and inelastic power profiles along with energy storage applications, special emphasis has been made to the specific hierarchical control levels of controllable Distributed Power Plants (DPP), which is the main end-user application that will be analyzed in the proposed competitive power control strategy.

Therefore, the specific control levels presented in the proposed hierarchical control structure of Fig. 3.2 and Fig. 3.3 correspond to the particular levels identified in renewables-based active DPPs. In the case of alternative end-user actors, the specific control levels of Fig. 3.2 and Fig. 3.3 should be suitably adapted to cover the particular control levels of such responsive generation/demand facilities, which can be found in residential, commercial or industrial applications.

The main purpose and principal functionalities of each of the hierarchical control levels presented in Fig. 3.2 and Fig. 3.3 are introduced as follows.

Enterprise control level

The principal objective of the enterprise level is to enable direct participation with the electrical markets, third party entities and SOs. This enterprise level performs as a pure management entity, able to perform as an aggregator, collecting the power capacity forecast of the entire generation/demand assets of a distributed network, and perform the optimum trade of energy and grid services with the wholesale or retail electricity markets and third party customers. The purpose of this level is to perform the trade of energy and services as a single entity, so increased benefits can be achieved than if each end-user performs the trading by itself. Besides of analyzing the future resource capacity available, the enterprise level could also perform predictive analyses of the markets and possible grid performance, so it will allow the enterprise to achieve maximum economic benefit from its trades by applying an advanced optimization control.

The exploitation of markets, grid and resource data analytics, optimization control solutions and advanced computing technologies, plays a crucial role and will allow the enterprise to continuously take the most convenient decisions related to the markets trading with the purpose of maximizing the overall economic benefit.

After receiving the market clearing result from the energy and auxiliary service bids provided, this control level performs the economic power scheduling corresponding to each participating agent, so the aggregated generation/demand traded at the wholesale level can be met.

This control level is characterized by its slow time execution requirements, which are usually imposed by the specific electricity markets. Therefore, it can range from hourly day-ahead to 10-5 minutes close to real-time schedules.

Area control level

An area could be understood as an active distribution grid where several distributed power plants and controllable loads are interconnected (Fig. 3.3). The main goal of the area

level is to perform the operational power balance between generation and demand within a specific control area while considering the real-time distribution network restrictions. This control level, thus compensate with available responsive generation/demand capacity any possible real-time deviations experienced in the overall power scheduled of the enterprise control level. Such deviations could appear due to a sudden unpredicted change in the generation or demand profiles, or due to unplanned distribution system restrictions or system failure events. In this manner, the overall area would continue operating according to the scheduled power, and the enterprise would avoid incurring in any penalties imposed by the SO.

With the access to real-time performance of the area, this control level could provide secondary frequency control capabilities, and even ensure a suitable system performance in stand-alone operation from the main grid. Therefore, this control layer provides functionalities very similar to the ones of the secondary control performed by the TSO, but applied to the active distribution grid.

The area performance awareness plays a crucial role in this layer, as it requires the placement of specific sensors deployed on distribution networks to monitor the conditions of the grid. So real-time analytics can be performed to assess the state of the grid in real time and then respond more efficiently to any issues that may arise. This area control level should also perform continuous optimum power flow analyses, in order to determine any technical restrictions of the distribution system performance, and to achieve increased distribution system efficiency through the implementation of optimum re-dispatching programs.

Depending on the ownership details of the active distribution network, many of the tasks involved in this control layer could be covered by an independent distribution system operator, so there is not any conflict of interest between the multiple active participating agents and the entity in charge of ensuring a reliable and safe operation of the system. In contrast, if the distributed generation/responsive loads and the grid infrastructure belongs to a single entity, such as in the case of many microgrids or distributed power plants, such entity is the responsible of ensuring a reliable and safe operation of the system.

The time execution requirements of this control levels are the same as the ones of the secondary control, ranging from tens of minutes to seconds.

Island control level

The main role of this control level is to ensure security of supply from a single power plant to the closest loads, and allow stand-alone operation in case of a major system disturbance. This control level can also contribute to provide progresive system restoration, since distributed power plants with black start capabilities can form an island with its local loads, prior being resynchronized and interconnected with the main restablished grid. Therefore, this control level is only enabled in case of abnormal system operating conditions.

Under islanding system conditions (stand-alone operation), this control level can provide primary frequency and voltage control at the island level in order to ensure security of supply to a group of loads or suitable system restoration in case of major system collapse.

Besides, advanced active distributed plants could also provide quality of supply services to its closest loads, by implementing additional power quality functionalities such as harmonic active filtering and reactive power compensation. Therefore, this control level plays a major role in case that critical load centers require security and quality of supply.

As in the case of the area level, collecting and analyzing real-time information from the actual performance of the local distribution system (distributed power plant with local loads) is of major importance, as according to the state of the grid the controllable generation/demand facilities could react more efficiently to any issues that may arise.

Finally, it is worth mentioning that the islanding controllers should be coordinated with the area controller, as once the main grid has been restored, they should re-synchronize and interconnect progressively in order to ensure a safe and reliable distribution system restoration process. This issue entails also the progressive reconnection/disconnection of loads based on current system performance.

The island level has faster execution time requirements than the area control level. Particularly, in the range of tens of seconds to tens of miliseconds.

End-user control level (Distributed Power Plants)

The main goal of this control level is to perform the operational and control management of the end-user facility. This control level is the responsible entity for on-site controlling that such facility meets the desired performance, while locally optimizing its real-time power dispatch to ensure minimum operation costs through optimal allocation of available resources.

Thanks to the implementation of an end-user facility supervisory control and data acquisition (SCADA) system, along with advanced data analytics it is possible to monitor the real-time performance of the system, and allows the operator to take instantaneous decisions affecting the final generation or demand being supplied. In addition, it allows the end-user to analyze the impact of the generation/demand strategies implemented and to make possible changes to maximize its individual profitability.

Furthermore, the implementation of predictive analyses on end-user systems behaviour is gaining a considerable interest, as it allows the operator to take better online decisions and to achieve optimum management of the facility for reaching maximum economic revenues. Such predictive analyses can cover diverse aspects such as possible inminent internal system failures, future maintenance duties or available generation/demand resource capacity forecasts (weather and demand prediction).

Finally, the implementation of automated plant coordination and control systems is critical, allowing the facility to be suitably managed regardless of the operator specific knowledge or experience in the field.

Cluster control level

As it can be observed in Fig. 3.2, the cluster level is the first of the specific set of control levels, which are proposed for a distributed power plant control structure.

A cluster can be understood as a group of distributed generation units with similar performance dynamics, which are interconnected toghether sharing a common power distribution path (Fig. 3.3).

The main objective of this control level entails controlling the power plant in a more flexible and coordinated manner, as in case of any internal distribution system failure, the affected cluster could be isolated, while the plant would continue operating. It is also responsible of ensuring security of supply to critical internal loads (house load operation) in case of a sudden grid loss, and to provide suitable system restoration after a black start process. Therefore, this control level could also provide primary frequency and voltage control capabilities at the cluster level for such cases, where an internal island is created within the plant.

Finally, this control level is also responsible of extending the suitable power sharing references to the underneath power stations, while considering any operating restrictions that may arise. So the cluster's production can be met according to the plant specifications.

Station control level

A station is representative of any individual generation unit capable of supplying AC power to the grid. Therefore in the case of RES based power plants interfaced with power electronics, the station correspond to the voltage source inverter used for integrating such generation units to the grid. Conversely, in the cases where the power plant implement conventional turbine driven synchronous generators instead of power converters (e.g. the case of CSP) the station is representative of the AC generator used.

The main goal of this layer is to control the active and reactive power delivery to the system according to a given specified references and dynamic requirements. Therefore, this control level performs a supervisory control of the local AC power generation unit. In addition, this control can also integrate the local primary frequency and voltage control at the generation unit level.

Similarly as in the case of the cluster level, the station control also extends the active power sharing references to the corresponding resource controllers interfaced by such station, while considering any station operating restrictions that may arise. Besides the active power control, the station control layer can also perform the local supervisory control on the reactive power and advanced grid services provided.

Resource control level

The main purpose of this level is to control the active power supply from a given resource generation unit by acting on the energy extraction mechanism. Therefore, the resource control level appears in charge of providing to the local embedded controller the active power references to be supplied by the individual resource units. In this manner a global resource power production can be satisfied by individually considering at each resource controller, the required references provided from the corresponding station controller. As a result, this control level performs the supervisory control of the local resource controller,

sending the required active power references in the different modes of operation to the resource embedded controller.

The proposed hierarchical control structure presented in this section appears as a generic solution for any kind of distributed power plant (solar, wind, wave, etc.), since the main differences found among plants is in the manner in which the final resource is controlled.

In addition, the overall hierarchical structure can be adapted to cover the specific control levels of other end-user facilities such as responsive loads in buildings or campuses. In this regard, the power plant, cluster, station and resource levels would be replaced by the particular building or campus energy management system hierarchical control structure.

The successful implementation of the previously proposed hierarchical control structure provides a set of technical and economical benefits, which could release the full potential for achieving a large scale seamless grid integration of renewable energy sources. These advantages appear summarized as follows:

- The proposed hierarchical control structure allows a direct participation of distributed power plants and responsive loads with electricity markets, in order to achieve maximum economic benefits from the particular end-user power generation and demand needs. The aggregator arise as a key actor, representing the market participation of the entire generation and demand conglomerate.
- Several control layers such as the area and island levels enable the provision of advanced grid support services from distributed generation/demand units, needed by distribution system operators (DSOs) in order to ensure a safe and reliable operation of distribution systems.
- The end-user facilities become highly controllable thanks to the advanced monitoring, control and data analytic capabilities provided, allowing the final end-user to reach maximum economic benefits from the optimum operation of its local facility.

3.3 Competitive power control of active distribution grids

The proposed competitive power sharing control strategy is presented in detail throughout this section, focusing on the competitive power concept itself, on the distributed control system capabilities provided, and on its possible limitations, when being applied to a generic active distribution network.

3.3.1 The Competitive Power Control Concept

The objective of the proposed competitive controller is to achieve real-time control over the power being supplied or consumed within an active distribution grid. So the power exchange schedules set, from the market clearing mechanisms or grid operators, between the active distribution network and main grid can be met in real-time, regardless of the large variability introduced by the stochastic renewable generation or inelastic demand units. In this regard, the principal feature of the competitive controller is that it ensures real-time

balance between generation and demand, to meet the power exchange schedules at minimum operation costs through the optimum allocation of available resources. Such advanced control capabilities can be achieved by applying a price signal (virtual or not) as a stimulus control signal over the entire hierarchical structure, being the distributed energy resources of the final end-users (generation/demand units) the responsible entities for deciding its generation/demand involvement based on the price signal received and its own marginal costs.

As it can be observed in Fig. 3.4, a large range of generic active distribution grids, with many end-users and final generation/demand resource types, can be fitted in the hierarchical control structure introduced in the previous section. In such grid structures, there is front-end controller, responsible for controlling the power exchange at the interconnection point with the main grid, and many intermediate controllers representing each of the intermediate hierarchical structures (e. g. a controller corresponding to each island, end-user and its individual inner specific levels associated).

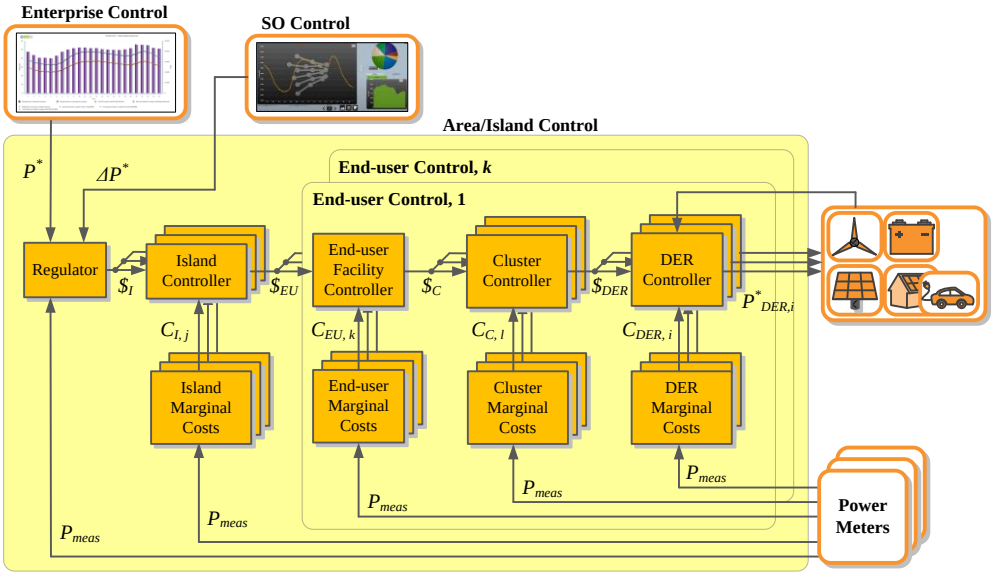

Fig. 3.4 Generic competitive power control implementation in active distribution grids

From this structure presented in Fig. 3.4, the area controller appears as the front-end regulator in charge of generating a real-time price signal, resulting from the degree of fulfillment of a given production objective set over the active distribution grid. This production objetive could be of diverse nature, such as to control the active or reactive power exchange between the active distribution grid and the main grid, to perform the secondary frequency control over the active distribution grid, to perform optimum allocation of reserves, etc. Additionally, the proposed controller can provide simultaneous real-time multi-objective control capabilities, by just replicating the control structure introduced in Fig. 3.4

for each of the control objectives considered. However, for the sake of simplicity, the active power exchange between the active distribution grid (area) and main grid will be considered in this section as the single control objective.

In this regard, the front-end regulator provides a real-time price signal, serving from the scheduled power setpoint and the measured active power exchange between the area and the main grid. This price signal is representative of the price that the area controller would be willing to pay to the controllers of the level below, in order to provide the required production setpoint at the point of interconnection of the area. This price signal, is expressed in price per unit of energy (e. g. in $/MWh). Once the price signal has been generated, it is transmitted as a control signal to the controllers of the next level, where it is modified considering the individual marginal costs associated with the corresponding controllers.

In the next level, each island controller represents a portion of the active distribution grid where a group of different end-user facilities are closely interconnected and sharing a common distribution path. Therefore, each island controller receives the generated price signal ($\$_I$) and modifies it, according to its internal distribution marginal costs, associated to the power delivery/demand of each end-user facility. These costs are calculated in the corresponding Island Marginal Costs block (from Fig. 3.4) and consider among others, the costs of power losses, the grid maintenance costs, and the costs due to sudden system restrictions (e.g. congestion costs) found in the distribution system equipment involved. Now, the resulting island prices ($\$_{EU}$) are representative of the price that each island would be willing to pay to each end-user connected to it for generating the desired amount of power at the island point of connection. This cost modification will have a direct impact on the final power being supplied or consumed by each end-user, as according to their electrical location and particular real-time distribution losses or system restrictions, the price signal received by each end-user will be different. Hence, encouraging or discouraging the generation/demand involvement of given end-user facilities based on their electrical location and real-time grid conditions. This produces a similar effect as the nodal pricing mechanism implemented in many US utilities such as PJM, CAISO or ERCOT [93, 94, 95, 96], where a different electricity price is considered in each distribution node, based on the cost associated for supplying power to that particular node.

Similarly, the island price signals ($\$_{EU}$) are provided as a control signal to each of the corresponding end-user facilities connected to it, where it is modified considering the particular operation and maintenance costs associated to the management of that facility. Such costs are determined in the End-user Marginal Costs block from Fig. 3.4. Then, the resulting end-user price signal ($\$_C$) is representative of the price that each end-user would be willing to pay to each internal generation/demand units for generating/consuming at the end-user facility point of connection.

Depending on the type of end-user facility and its specific control architecture, there may be several control layers between the end-user facility and the final resource controller. In many cases where such final resources appear in the form of distributed generation or

demand units (DER units), it might be necessary to consider the costs of internal distribution losses and real-time restrictions, as the length and complexity of such internal end-user electrical layout may be quite extensive. Therefore, replicating the control philosophy introduced in the island level, the cluster controller can be understood as a portion of the internal end-user facility grid where a group of different DER units are closely interconnected and sharing a common distribution path. In this regard, each cluster controller receives the end-user facility price ($\$_C$) and modifies it considering the particular costs associated to the distribution cluster layout. These costs are calculated in the corresponding Cluster Marginal Costs block (from Fig. 3.4) and consider among others, the costs of internal distribution losses, the maintenance costs of internal layout equipment, and the costs due to sudden system restrictions (e.g. congestion costs). The resulting cluster price signal ($\$_{DER}$) is representative of the price that the cluster controller would be willing to pay to each DER unit connected to it for generating/consuming at the cluster point of connection.

Finally, the cluster price signal ($\$_{DER}$) is provided to the final DER controller, where the final DER power reference to be generated or consumed will be specified. Since the DER units can represent up to 3 main types of generation or demand technologies, each of them will determine its DER power references in a different manner:

- Distributed generation units: the price signal received by the final-end DER controller ($\$_{DER}$) is compared in real-time with the marginal production costs (C_{gen}) of the DER unit, and if the error is positive, it linearly increases the power production reference, until it reaches the maximum power operation point. In the same manner, if the error is negative the DER controller linearly decreases the power production reference until zero power is being generated, and if it zero it maintains the power reference unchanged. Therefore the power reference setpoint could be generated as in (3.1) and (3.2), providing a rate of change proportional to the error between the price signal received and the generation costs.

$$P_{gen,i} = \int \left(\$_{DER,i} - C_{gen,i}\right) dt \tag{3.1}$$

$$P^*_{DER,i} = \begin{cases} P_{max} & if\ P_{gen,i} > P_{max} \\ P_{gen,i} & if\ 0 > P_{gen,i} > P_{max} \\ 0 & if\ P_{gen,i} < 0 \end{cases} \tag{3.2}$$

From the sign criteria considered, a positive power reference refers to an amount of power being generated. Then, the final power reference provided to the DER unit $\left(P^*_{DER,i}\right)$ has a positive value between zero and the resource maximum available power.

The marginal production costs are calculated in the DER Costs block from Fig. 3.4, and mainly consider the costs due to the specific DER maintenance duties, energy conversion efficiency and resource cost, which in case of non-storable renewables is zero.

- Distributed load units: the price signal received by the final-end DER controller ($\$_{DER}$) is compared in real-time with the marginal cost that each load is willing to pay for consuming from the grid (C_{load}), and if the error is positive, it linearly decreases the power demand reference until the zero demand is achieved. Conversely, if the error is negative the demand reference linearly increases until the maximum power demand, and if the error is zero, the demand reference keep unchanged. Therefore the power reference setpoint could be generated as in (3.3) and (3.4) providing a rate of change proportional to the error between the price signal received and the consumption costs.

$$P_{load,i} = \int (\$_{DER,i} - C_{load,i}) dt \tag{3.3}$$

$$P^*_{DER,i} = \begin{cases} 0 & if\ P_{load,i} > 0 \\ P_{load,i} & if\ 0 > P_{load,i} > -P_{max} \\ -P_{max} & if\ P_{load,i} < -P_{max} \end{cases} \tag{3.4}$$

In this case, a negative power reference refers to an amount of power being consumed. Then, the final power reference provided to the DER unit $\left(P^*_{DER,i}\right)$ has a negative value between zero and the maximum power consumption $(-P_{max})$.

The price that the distributed load is willing to pay is determined in the DER Costs block from Fig. 3.4, according to some predefined comfort or energy dependency requirements, which are set from the final-user preferences. In this manner, the final-user could specify the time window over which a given energy should be demanded, and the maximum price that it is willing to be paid for such energy.

- Distributed energy storage unit: in the specific case of storage-based DER units, the price signal received ($\$_{DER}$) could be compared with the two previously considered costs signals (C_{gen}) and (C_{load}), which respectively represent the marginal generation costs (generation cost), and the marginal costs that the DER unit is willing to pay for consuming energy from the grid (consumption cost). Again, such costs are provided by the DER Costs block from Fig. 3.4. In this case the power generation and consumption rules are combined together as introduced in (3.5), (3.6) and (3.7).

$$P_{gen,i} = \int (\$_{DER,i} - C_{gen,i}) dt \Rightarrow P^{ESS}_{gen,i} = \begin{cases} P_{max} & if\ P_{gen,i} > P_{max} \\ P_{gen,i} & if\ 0 > P_{gen,i} > P_{max} \\ 0 & if\ P_{gen,i} < 0 \end{cases} \tag{3.5}$$

$$P_{load,i} = \int \left(\$_{DER,i} - C_{load,i}\right)dt \Rightarrow P_{load,i}^{ESS} = \begin{cases} 0 & if\ P_{load,i} > 0 \\ P_{load,i} & if\ 0 > P_{load,i} > -P_{max} \\ -P_{max} & if\ P_{load,i} < -P_{max} \end{cases} \quad (3.6)$$

$$P_{DER,i}^{*} = P_{gen,i}^{ESS} + P_{load,i}^{ESS} \quad (3.7)$$

Where the power reference that can be provided or absorbed from the grid can take any value between the maximum and minimum available energy storage power limits (P_{max} and $-P_{max}$).

From the above equations in (3.5), (3.6) and (3.7), it can be stated that a positive increment of power will be experienced for the case in which the error between the price signal received and the generation cost is higher than the error between the price signal and the consumption cost, and vice versa. This assumption can be better highlighted in (3.8) and (3.9). Finally it must be emphasized that the generation marginal costs $\left(C_{gen,i}\right)$ should always be greater than the price willing to be paid for consuming energy from the grid $\left(C_{load,i}\right)$, as otherwise there is not any economic benefit in supplying power to the grid from a energy storage system.

$$\Delta P_{DER,i}^{*} > 0 = if\ \left(\$_{DER,i} - C_{gen,i}\right) > \left(\$_{DER,i} - C_{load,i}\right) \quad (3.8)$$

$$\Delta P_{DER,i}^{*} < 0 = if\ \left(\$_{DER,i} - C_{gen,i}\right) < \left(\$_{DER,i} - C_{load,i}\right) \quad (3.9)$$

As the proposed competitive control strategy is based on receiving common price control signals among the controllers of the same hierarchical level, there is a direct competition between them in order to achieve the desired production objective. Therefore for a given price signal, the generation units with lower overall marginal costs will start producing earlier, being progressively introduced the generation units with higher costs as the price signal increases. Similarly, the generation units with higher costs will stop producing earlier for a price signal decrease, remaining only the generation units required for ensuring minimum operation costs.

In the case of the price responsive loads the contrary effect applies as, the loads with higher demand requirements will start consuming first (inelastic loads), at higher price signal rates, while the other more flexible loads will progressively increase their consumption as the price signal decreases. Inversely, for a price signal increase, the loads with lower energy requirements (flexible loads) will stop consuming first, remaining only the demand with more inelastic profiles.

As a result the proposed competitive control system dynamically achieves a real-time optimum equilibrium between supply and demand at minimum electricity price. This

beahviour is introduced in [97], where the market equilibrium conditions were described under short-term (hourly day-ahead or intra-day) perfectly competitive markets.

In a perfect competitive market, the marginal costs and demand curves provided by each generation unit and loads describe the optimum amount of energy they are willing to produce/consume and its associated costs, ensuring in aggregate that the most crucial demand is met at minimum costs by making use of the most efficient generation units. This feature is represented in Fig. 3.5, where the equilibrium is found in the intersection point between the aggregated generation and demand curves.

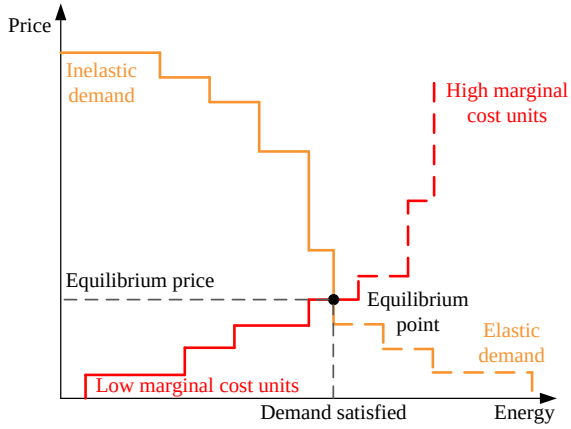

Fig. 3.5 Generation and demand equilibrium in perfect competitive electricity markets [97]

From this figure, the generation units with real-time marginal costs cheaper than the dynamic equilibrium point (low marginal cost units), will be instantaneously dispatched to satisfy the real-time demand, while the generators with higher costs (high marginal cost units) will remain producing zero energy. Similarly, with the demand scope in mind, the most critical consumers (inelastic demand) whose real-time marginal utility price (price worthy to be paid to satisfy the demand) is higher than the dynamic equilibrium price will have their energy requirements satisfied, whereas the remaining loads with utility prices below the dynamic equilibrium point will not participate and consume zero energy (elastic demand).

Therefore, one of the contributions of the proposed control system is that it achieves a real-time competitive power control of active distribution grids (generation and demand) through the implementation of market rules, ensuring a real-time optimum dispatch of available resources and participating agents. In this regard, each time an unbalance between generation and demand occurs, the controller dynamically finds an alternative equilibrium point, setting a new equilibrium price, which gives rise to the corresponding energy dispatch for each of the generation and demand units involved. Being the final DER resources the ones deciding the level of involvement based on the real-time price signal received (stimulus control signal) and on their marginal costs, which are calculated in real-time and depend on their actual and cumulative DER resource performance. In the same manner, each time a

DER resource update its marginal costs, a new equilibrium control price is found, which gives rise to an updated energy redispatch reflecting the marginal cost increment or decrement of such generation/demand unit.

Finally, it is worth noting that proposed competitive power control structure, presented in this section appears as a generic solution for any kind of active distribution grids, integrating an extensive range of different generation, demand and storage technologies, with many different marginal costs and dynamic performance capabilities.

Moreover, the overall hierarchical structure and control solution can be adapted to cover dedicated specific smaller parts of the active distribution grid such as distributed power plants, or responsive demand buildings or campuses. The critical issues that need to be previously defined are the control objectives to be controlled and the specific control structure of such end-user facilities.

3.3.2 Generic marginal costs characterization in RES-based active distribution grids

This section introduces a generic characterization of the main marginal costs that could be considered over the entire competitive hierarchical control structure, when applied to active distribution grids. However, this is not an exhaustive costs representation, as the final costs considered strongly depend on the specific competitive power control application and on its morphology, in terms of system layout configuration and type of end-user facilities involved.

All the marginal costs considered are calculated in real time and depend on the actual and past performance of the electrical network elements. For this reason, all the costs calculation blocks found in the competitive control structure from Fig. 3.4 make use of the real-time measurements from selectively placed power meters. These power measurements are processed in the corresponding cost calculation blocks, where the finally associated operation costs are determined and further provided to the corresponding competitive controllers.

Island marginal costs

The island performance costs consist on the costs incurred from the usage and degradation of the network assets, such as cables, transformers, etc., belonging to a portion of the active distribution grid where a group of different end-user facilities are closely interconnected and sharing a common distribution path. Such costs are shared proportionally depending on the usage level among the end user facilities involved.

Moreover, the costs due to losses in such common distribution path are also accounted, since depending on the electrical location of the end-user facility they will have to generate larger amounts of power for satisfying a given power exchange setpoint at the island (reference) point of interconnection.

Finally, the cost due to sudden system restrictions (e. g. congested lines) can be also calculated and considered for the applying nodes. The congestion costs account for the marginal costs incurred due to the need of generating with other more expensive but advantageously located facilities.

Therefore, the island marginal costs calculator provide the necessary cost considerations to the island competitive controller, which determine, along with the price signal received from the reference node (island point of interconnection), the real-time locational marginal price that applies to the different nodes of the active distribnution network.

Similarly as performed in the Locational Marginal Price (LMP) calculations from several US Independent System Operators (ISOs), such as the CAISO [96, 97], a nodal cost $(C_{I,j})$ can be determined for each of the nodes associated to an island controller by considering the three main costs related to such node *"j"* (3.10).

$$C_{I,j}[\$/MWh] = C_{I,j}^{O\&Mgrid}[\$/MWh] + C_{I,j}^{loss}[\$/MWh] + C_{I,j}^{cong}[\$/MWh] \quad (3.10)$$

Where $C_{I,j}$ represent the total costs associated to a node *j* within the island, $C_{I,j}^{O\&Mgrid}$ represent the grid operation and maintenance cost associated to the usage of the network equipment interfacing that particular node, $C_{I,j}^{loss}$ account for the marginal cost of losses from the reference bus, to the particular *j* node, and $C_{I,j}^{cong}$ represent the marginal costs of congestion related to the bus *j*.

End-user facility marginal costs

The end-user facility costs relate to the costs incurred from the general real-time management of the end-user facility. Such costs consider among others, the investment costs, operation and maintenance costs and resource costs of the facility. Additional specific costs could be considered depending on the end-user facility type. Due to the large variety of possible end-user facility types, this section distinguish between generation and demand end-user facilities.

In the case of generating end-user facilities, the generic facility costs can be separated in 2 components, a fixed one which depends on the fix costs incurred over the life span of the end-user facility, and which not depend on the energy being produced or consumed (capital costs, labour costs, long-term leasing of services/facility/equipment, etc.), and the variable term which depends on the energy produced/consumed (operation and maintenance costs, fuel/resource costs, etc.). However, only the variable term is considered for determining the marginal costs in the facility end-user costs calculation block from Fig. 3.4. This is due to that only marginal costs are considered for the profit maximization of generation facilities (supply curve characteristics) when participating in perfectly competitive electricity markets [97].

In addition, the costs of internal electrical losses of the common distribution equipment of the end-user facility can be also accounted in this section.

Therefore, the end-user facility marginal cost $\left(C_{EU,k}\right)$ is introduced in (3.11), where $\sum_{t=0}^{t} C_{EU,k}^{O\&M}(t)$ are the cumulative operation and maintenance costs, $\int\left(P_{EU,k}^{meas}\right)dt$ the energy generated/consumed at the end-user point of interconnection, and $C_{EU,k}^{loss}$ the losses costs of common end-user facility equipment.

$$C_{EU,k}[\$/MWh] = \frac{\left(\sum_{t=0}^{t} C_{EU,k}^{O\&M}(t)\right)[\$]}{\int\left(P_{EU,k}^{meas}\right)dt\ [MWh]} + C_{EU,k}^{loss}[\$/MWh] \tag{3.11}$$

In the case of demand end-user facilities, the end-user facility marginal cost $\left(C_{EU,k}\right)$ will consider the marginal utility cost (consumer degree of satisfaction or profit) set by the daily consumer preferences and specific energy requirements. The marginal utility cost is considered by consumers for determining the optimum power willing to be consumed at each market price. Thus for generating the individual end-user demand curve.

For both generation and demand end-user types, it is worth noting that depending on the development level of the hierarchical control structure, the overall generation or utility marginal costs can be further broken down and distributed to the corresponding lower control levels of the end-user facility. In this manner it will be possible to further optimize the internal power dispatch of the end-user facility, by distributing the corresponding marginal costs to each of the individual generation/demand DER resources.

Cluster marginal costs

The cluster marginal costs account for the costs incurred from the usage and degradation of the inner end-user network assets, such as cables, transformers,etc, belonging to a portion of the internal end-user facility grid, where a group of different DER units are closely interconnected and sharing a common distribution path (cluster). Similarly as in the case of the island marginal costs, a nodal cost $C_{C,l}$ can be determined for each internal bus *l* of a cluster (3.12), by considering the costs of internal distribution losses, the maintenance costs of internal layout equipment, and the costs due to sudden system restrictions.

$$C_{C,l}[\$/MWh] = C_{C,l}^{O\&Mgrid}[\$/MWh] + C_{C,l}^{loss}[\$/MWh] + C_{C,l}^{cong}[\$/MWh] \tag{3.12}$$

Where $C_{C,l}$ represent the total costs associated to a node *l* within the cluster, $C_{C,l}^{O\&Mgrid}$ represent the operation and maintenance cost associated to the usage of the network equipment, $C_{C,l}^{loss}$ account for the marginal cost of losses from the reference bus, to the particular *l* node, and $C_{C,l}^{cong}$ represent the marginal costs of congestion related to an internal bus *l* of the cluster.

DER unit marginal costs

The DER costs account for the cost of generation or consumption related to the DER technology and fuel type used. These costs consider the operation and maintenance costs

costs, the fuel costs and the energy conversion chain costs related to the usage of a given DER unit.

As it was previously introduced, the marginal resource costs can be divided in generation and consumption costs. In this regard, the resource generation costs are closely related to the raw fuel costs, needed for generating a unit of energy (€/MWh). In the particular case of non-storable renewable generation units, their resource marginal costs is zero.

However, from the load resource standpoint, the marginal resource costs are set by the consumer behavior (energy consumption requirements) and its willingness to buy a given amount of energy at a given price for a given instant of time in the electricity markets. Hence, the resource costs considered are related to a demand curve provided by the demand unit, which sets the marginal economic value it has for the final end-consumer to increase or decrease its energy demand.

The final DER unit costs are introduced in (3.13), where $C_{DER,i}^{O\&M}$ represent the DER unit costs due to operation and maintenance duties, $C_{DER,i}^{eff}$ represent the costs due to efficiency losses due to the energy conversion mechanism, and $C_{DER,i}^{res}$ represent the cost of the DER generation or consumption resource.

$$C_{DER,i}[\$/MWh] = C_{DER,i}^{O\&M}[\$/MWh] + C_{DER,i}^{eff}[\$/MWh] + C_{DER,i}^{res}[\$/MWh] \quad (3.13)$$

3.3.3 Proof of concept of the competitive power controller applied in generatic active distribution networks

This section provides a meaningful evaluation of the competitive power concept and its working principles, through a simplidied example of the proposed controller in a generic active distribution grid application. From the active distribution grid considered, which is introduced in Fig. 3.6, it can be observed that it is a low voltage network combining a conglomerate of many DER of diverse nature. In such network, the generation is characterized by a controllable 60kW CHP microturbine, a 30kW PV unit operating at maximum power (MPPT), and a controllable 40kWh energy storage unit. From the demand standpoint, there are two residential inelastic loads of 40kW (L2) and 30kW (L3) respectively, and an elastic residential demand responsive unit of 60kW (L1).

The detailed competitive control diagram is presented in Fig. 3.7. From this figure it can be observed that there is a front-end regulator, whose main objective is to control the power exchange at the PCC between the active distribution grid and the main grid, and three controllable DER resources. For the sake of simplicity in the demonstration of the competitive controller operation principle, the controller implemented in this case is a very elemental example, which neglects the island, end-user and cluster control levels introduced in the previous sections (3.3.1 and 3.3.2), and solely consider the resource control level, which introduces a marginal cost at each of the controllable end-user resources.

The competitive power controller has been tested under two main study cases, which are correspondingly presented in the following sub-sections.

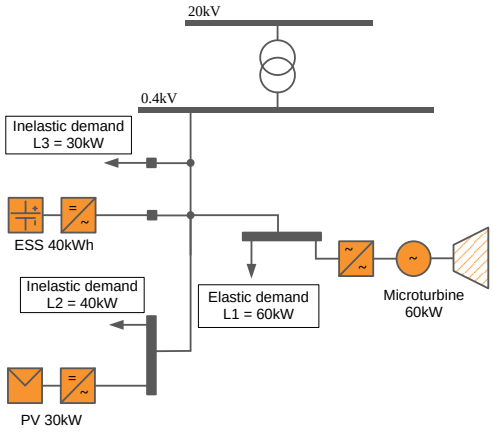

Fig. 3.6 Generic active distribution grid application for the competitive controller proof of concept

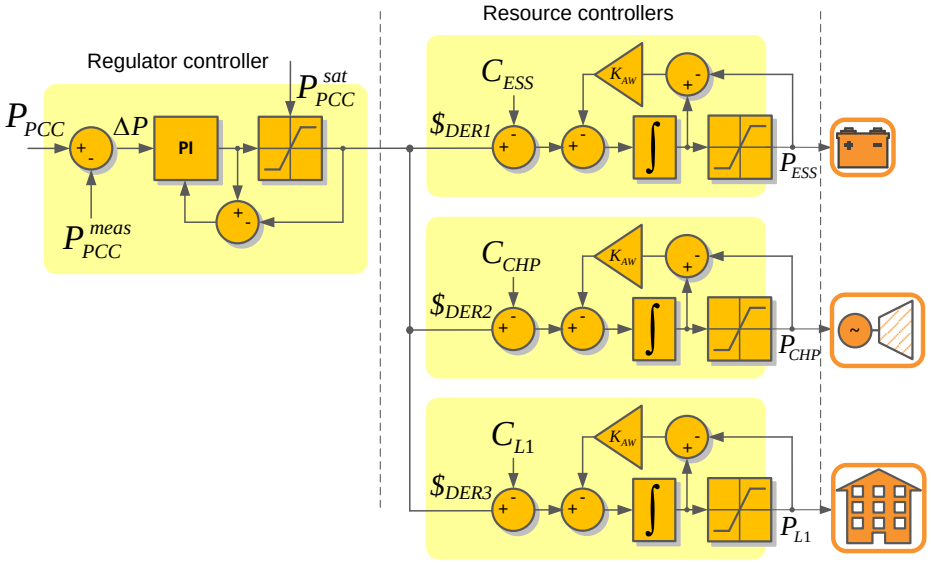

Fig. 3.7 Competitive power controller for the competitive controller proof of concept in a generic active distribution grid

It is worth noting that the generation and demand involvement rules of the energy storage, CHP microturbine and demand responsive load resource units have been implemented according to what it was already introduced in equations (3.1) to (3.7). However, in order to provide a better understanding, such equations will be recalled as follows by considering each of the specific costs mentioned in

Fig. 3.7.

- CHP microturbine generation unit: the price signal received by the final-end DER controller ($\$_{DER2}$) is compared in real-time with the marginal production costs (C_{gen}^{CHP}) of the generation unit, and its power production rate of change is proportional to the error between the controller price signal ($\$_{DER2}$) and the resource marginal costs (C_{gen}^{CHP}). In addition it includes the power production limits of the generation units which are set between 0 and 60kW.

$$P_{gen,CHP} = \int (\$_{DER1} - C_{gen}^{CHP})dt \tag{3.14}$$

$$P_{CHP}^{*} = \begin{cases} 60kW & if\ P_{gen,CHP} > 60kW \\ P_{gen,CHP} & if\ 0 > P_{gen,CHP} > 60kW \\ 0 & if\ P_{gen,CHP} < 0 \end{cases} \tag{3.15}$$

- L1 responsive demand unit: the price signal received by the final-end DER controller ($\$_{DER3}$) is compared in real-time with the marginal cost that the responsive load is willing to pay for consuming from the grid (C_{load}^{L1}), and its power consumption rate of change is proportional to the error between the controller price signal ($\$_{DER3}$) and the resource utility marginal costs (C_{load}^{L1}). In addition it includes the power limits of the demand unit which are set between 0 and P_{prof}^{L1}. Where P_{prof}^{L1} is the maximum instantaneous consumption profile of the resource, being the consumption sign criteria negative.

$$P_{load,L1} = \int (\$_{DER2} - C_{load}^{L1})dt \tag{3.16}$$

$$P_{L1}^{*} = \begin{cases} 0 & if\ P_{load,L1} > 0 \\ P_{load,L1} & if\ 0 > P_{load,L1} > P_{prof}^{L1} \\ P_{prof}^{L1} & if\ P_{load,i} < P_{prof}^{L1} \end{cases} \tag{3.17}$$

- Energy storage unit: in this specific case, the price signal received ($\$_{DER1}$) is compared with two costs signals (C_{gen}^{ESS}) and (C_{load}^{ESS}), which respectively represent the marginal generation costs, and the marginal costs that the DER unit is willing to pay for consuming energy from the grid. In this case the power generation and consumption rules are combined together

$$P_{gen,ESS} = \int (\$_{DER1} - C_{gen}^{ESS})dt \Rightarrow P_{gen}^{ESS} = \begin{cases} P_{max} & if\ P_{gen,ESS} > P_{max} \\ P_{gen,ESS} & if\ 0 > P_{gen,ESS} > P_{max} \\ 0 & if\ P_{gen,ESS} < 0 \end{cases} \tag{3.18}$$

$$P_{load,ESS} = \int (\$_{DER1} - C_{load}^{ESS})dt \Rightarrow P_{load}^{ESS} = \begin{cases} 0 & if\ P_{load,ESS} > 0 \\ P_{load,ESS} & if\ 0 > P_{load,ESS} > -P_{max} \\ -P_{max} & if\ P_{load,ESS} < -P_{max} \end{cases} \quad (3.19)$$

$$P_{ESS}^{*} = P_{gen,i}^{ESS} + P_{load,i}^{ESS} \quad (3.20)$$

These generation and demand involvement rules of the energy storage, CHP microturbine and demand responsive load resource units will be applied to both of the study cases considered.

Study case 1: Scheduled Power Exchange Control at the PCC

The main goal of this study case is to demonstrate that the competitive power controller is capable of controlling in real-time the power exchange at the PCC of the active distribution grid, according to the power schedules set from the day-ahed market clearing mechanisms or grid operators, executed beforehand.

In order to determine a suitable power schedule to be provided by the active distribution grid, several characteristic real-time generation and load profiles have been considered for each of the generation and demand units involved. Then, a power schedule has been calculated for each resource unit, based on the hourly average of the real-time power profiles, while the final power exchange schedule at the PCC results from the aggregation of such hourly resource power schedules.

Fig. 3.8(a) presents the resulting power schedule at the PCC of the active distribution grid, where the individual real-time (green lines) and hourly scheduled (blue lines) resource profiles are provided from Fig. 3.8(b) to Fig. 3.8(f).

From Fig. 3.8, it is worth noting that the generation/demand schedule of the energy storage system has not been considered to determine the final power schedule at the PCC, as its main duty will be to provide grid balancing capabilities within the active distribution grid. In addition, a power schedule has been proposed for the particular cases of the CHP microturbine and L1 demand responsive load. However the real-time power profile finally provided by these resources may differ from such schedules, as they will result from the competitive power controller applied. For the specific cases of the PV generation, L2 and L3 demand units, they will provide the real time power profiles respectively specified in Fig. 3.8(c), Fig. 3.8(e) and Fig. 3.8(f), as they are considered as uncontrollable inelastic resource units in the present study case.

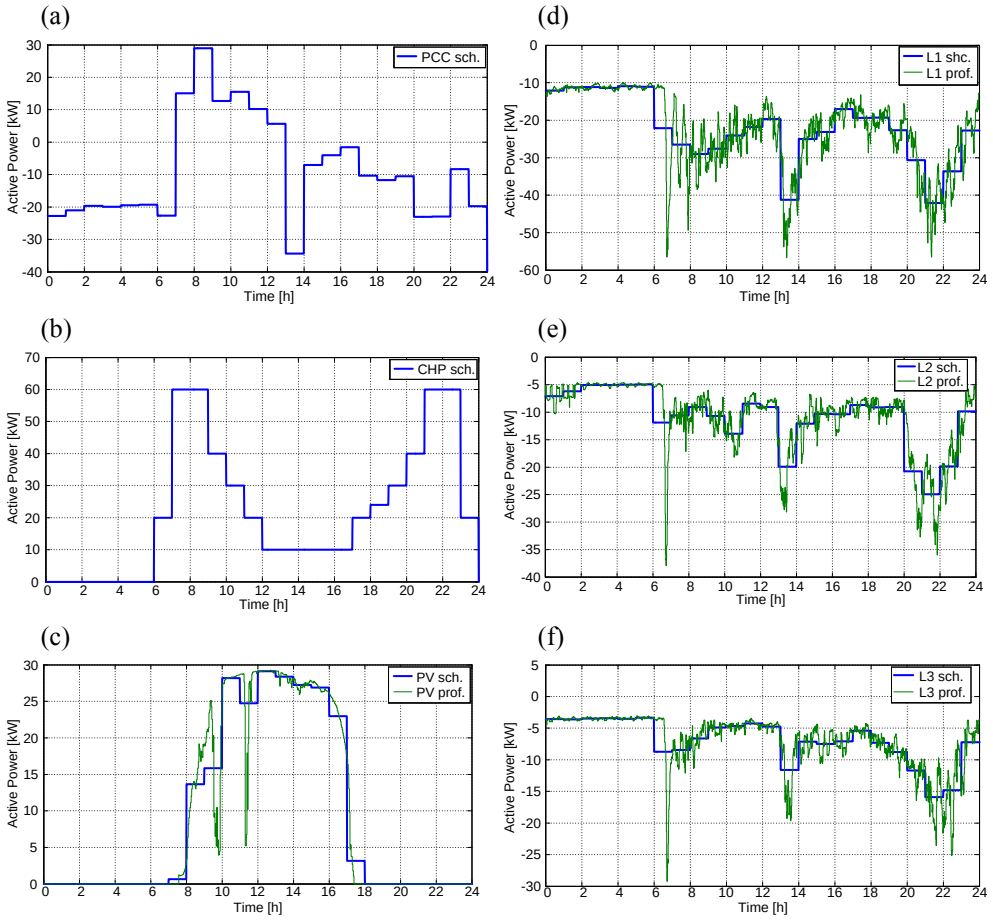

Fig. 3.8 (a)Scheduled and real-time power profiles at the PCC of the active distribution grid, (b) Scheduled power profile of the CHP microturbine, (c) Scheduled and real-time power profiles of the PV generation unit, (d) Scheduled and real-time power profiles of the L1 demand responsive unit, (e) Scheduled and real-time power profiles of the L2 inelastic demand unit, (f) Scheduled and real-time power profiles of the L3 inelastic demand unit

The stationary competitive power controller performance is introduced in Fig. 3.9, where the active distribution grid is trying to supply in real-time the proposed power exchange schedule (at the PCC) already specified in Fig. 3.8(a). From this figure it can be observed that the real-time power exchange at the PCC of the active distribution grid strictly follows the hourly grid production reference scheduled. Hence ensuring that the proposed competitive controller achieves real-time control over the power being supplied or consumed within an active distribution grid.

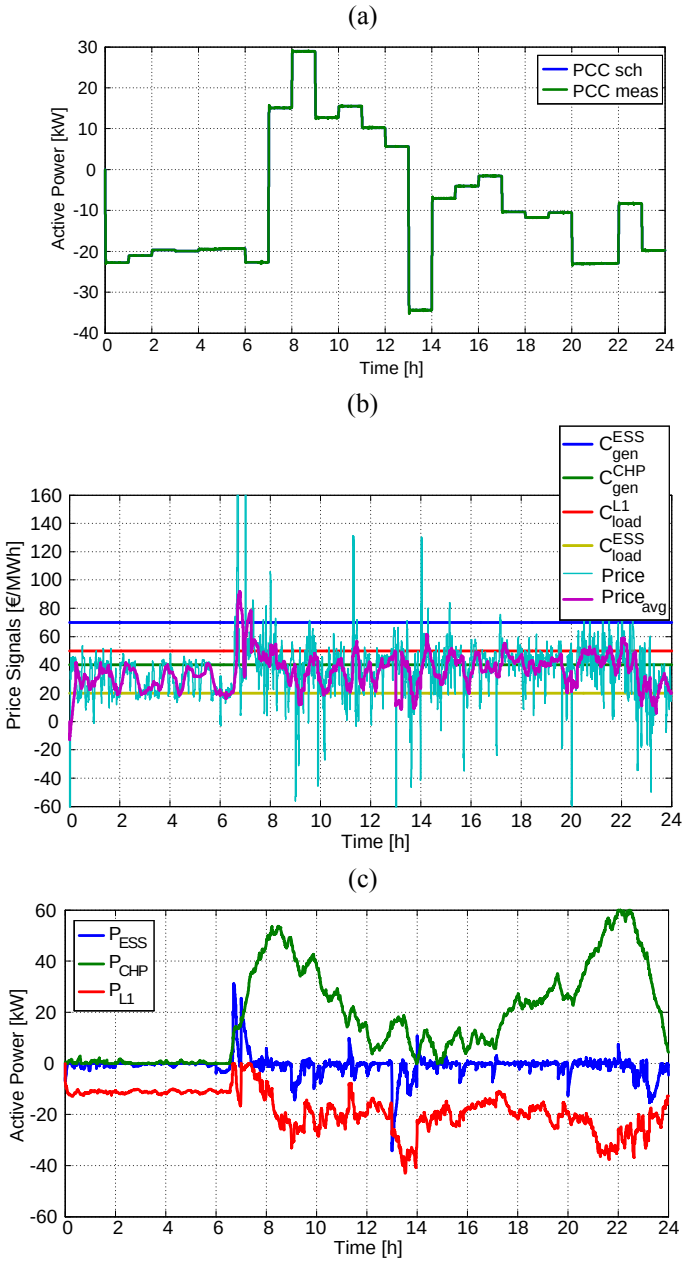

Fig. 3.9 Study case 1: (a) Stationary competitive controller response of the simulated active distribution grid during a representative day of operation; (b) Stationary comparison of the competitive controller price signal and the individual resource marginal costs; (c) Generation and demand involvement of the controllable DER units of the active distribution grid

In terms of the competitive power dispatch, it is worth noting from Fig. 3.9 (b) and Fig. 3.9(c), that the competitive controller sets real-time power production/consumption references to the individual resource units being controlled, based on the instantaneous difference between the controller price signal and marginal costs of the individual DER units.

Therefore, by considering the power generation and demand involvement rules of the resource controllers along with the price signals comparison from Fig. 3.9(b), it is possible to justify (in Table 3.1) that the competitive power controller achieves the desired PCC power exchange schedule at minimum operation costs. Hence, ensuring optimum allocation of the available resources.

Time interval	Price signals comparison	Power production/demand involvement
[0:00 to 6:00]	$Price_{avg} > C_{load}^{ESS} \Rightarrow \frac{dP_{load}^{ESS}}{dt} > 0$ $(Psaturated = 0)$	The PCC power is regulated through the L1 demand, as the average price signal is below the marginal utility price of L1
	$Price_{avg} < C_{gen}^{CHP} \Rightarrow \frac{dP_{gen}^{CHP}}{dt} < 0$ $(Psaturated = 0)$	
	$Price_{avg} < C_{load}^{L1} \Rightarrow \frac{dP_{load}^{L1}}{dt} < 0$	
	$Price_{avg} < C_{gen}^{ESS} \Rightarrow \frac{dP_{gen}^{ESS}}{dt} < 0$ $(Psaturated = 0)$	
[6:00 to 7:30]	$Price_{avg} > C_{load}^{ESS} \Rightarrow \frac{dP_{load}^{ESS}}{dt} > 0$ $(Psaturated = 0)$	There is a sudden price increase due to the morning peak demand, and all the resources contribute to the regulation. Due to the ramp rate limitation of the CHP the ESS and L1 load provide a faster regulation.
	$Price_{avg} > C_{gen}^{CHP} \Rightarrow \frac{dP_{gen}^{CHP}}{dt} > 0$	
	$Price_{avg} > C_{load}^{L1} \Rightarrow \frac{dP_{load}^{L1}}{dt} > 0$	
	$Price_{avg} > C_{gen}^{ESS} \Rightarrow \frac{dP_{gen}^{ESS}}{dt} > 0$	
[7:30 to 16:00]	$Price_{avg} > C_{load}^{ESS} \Rightarrow \frac{dP_{load}^{ESS}}{dt} > 0$ $(Psaturated = 0)$	The average price signal goes back to the range of the time interval [0:00 – 6:00], This is due to the inelastic PV generation contribution and off-peak load condition. Then, the CHP average power production decrease and L1 demand provides the required stationary
	$Price_{avg} \leq C_{gen}^{CHP} \Rightarrow \frac{dP_{gen}^{CHP}}{dt} < 0$	
	$Price_{avg} < C_{load}^{L1} \Rightarrow \frac{dP_{load}^{L1}}{dt} < 0$	

	$Price_{avg} < C_{gen}^{ESS} \Rightarrow \frac{dP_{gen}^{ESS}}{dt} < 0$ $(Psaturated = 0)$	regulation. Additionally, there is a sudden consumption peak scheduled at 13:00, which is almost entirely provided by the ESS and and L1.
[16:00 to 22:00]	$Price_{avg} > C_{load}^{ESS} \Rightarrow \frac{dP_{load}^{ESS}}{dt} > 0$ $(Psaturated = 0)$	There is an average price signal increase This is due to the PV power decrease. Now the average price signal stays between the L1 and ESS marginal utility prices (C_{load}^{L1}) and (C_{load}^{ESS}) respectively. Therefore, the desired power power exchange setpoint is satisfied mainly by the L1 demand response and the CHP generator.
	$Price_{avg} \geq C_{gen}^{CHP} \Rightarrow \frac{dP_{gen}^{CHP}}{dt} > 0$	
	$Price_{avg} < C_{load}^{L1} \Rightarrow \frac{dP_{load}^{L1}}{dt} < 0$	
	$Price_{avg} < C_{gen}^{ESS} \Rightarrow \frac{dP_{gen}^{ESS}}{dt} < 0$ $(Psaturated = 0)$	
[22:00 to 24:00]	$Price_{avg} < C_{load}^{ESS} \Rightarrow \frac{dP_{load}^{ESS}}{dt} < 0$	There is an average price decrease produced by a decrease in the inelastic load profiles. Due to the low average price achieved, the CHP generator progresivelly decreases its generation involvement, while the L1 demand response and ESS units increase its demand levels
	$Price_{avg} < C_{gen}^{CHP} \Rightarrow \frac{dP_{gen}^{CHP}}{dt} < 0$	
	$Price_{avg} < C_{load}^{L1} \Rightarrow \frac{dP_{load}^{L1}}{dt} < 0$	
	$Price_{avg} < C_{gen}^{ESS} \Rightarrow \frac{dP_{gen}^{ESS}}{dt} < 0$ $(Psaturated = 0)$	

Table 3.1 Study case 1: Stationary competitive dispatch justification of the results obtained from Fig. 3.9(b) and (c)

In order to provide a better understanding regarding the overall competitive power dispatch performance, Fig. 3.10 shows the power supply and demand profiles for each of the DER resource units conforming the active distribution grid.

Besides of an optimum stationary state performance, the competitive power controller provides suitable real-time control capabilities to the active distribution grid under control. As early mentioned, this is one of the principal contributions of such controller, as it allows to simultaneously provide grid control and economic dispatch duties.

Finally, the real-time performance of the L1 demand responsive load is introduced in Fig. 3.11, along with its maximum power consumption profile specified in Fig. 3.8(d). From this figure, it can be observed that L1 is considerably reducing its demand involvemente during the peak load periods, thus providing the desired demand response performance for achieving the active distribution grid control objective. At the off-peak periods, L1 approximately consumes the maximum load, as the electricity price during such periods is usually below the marginal utility set by the DER controller.

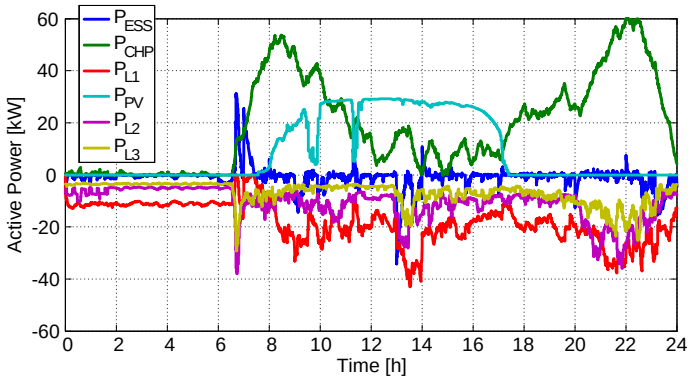

Fig. 3.10 Real-time power dispatch of the global DER energy resources conforming the active distribution grid

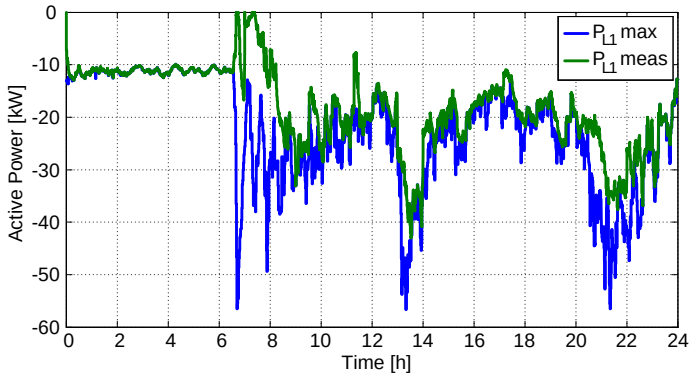

Fig. 3.11 Real-time performance of the L1 demand responsive load in comparison with its maximum load profile

In order to validate these real-time control capabilities, the real-time response of the competitive power controller is introduced in Fig. 3.12. From Fig. 3.12(a), it can be observed that the active power scheduled at the PCC is instantaneously met by the competitive controller, ensuring the required power levels within the desired controller dynamics.

Fig. 3.12(b) presents a comparison between the price control signal and the individual marginal costs considered in each DER resource unit. As it can be observed from this figure, the PI-based competitive front-end controller provides a price signal increase for the case in which the power reference is higher than the measurement, and a price signal decrease for the reverse case. Therefore the price signal increases as a consequence of a power deficit in the power being supplied by the active distribution grid, while a price signal decreases due to a power surplus.

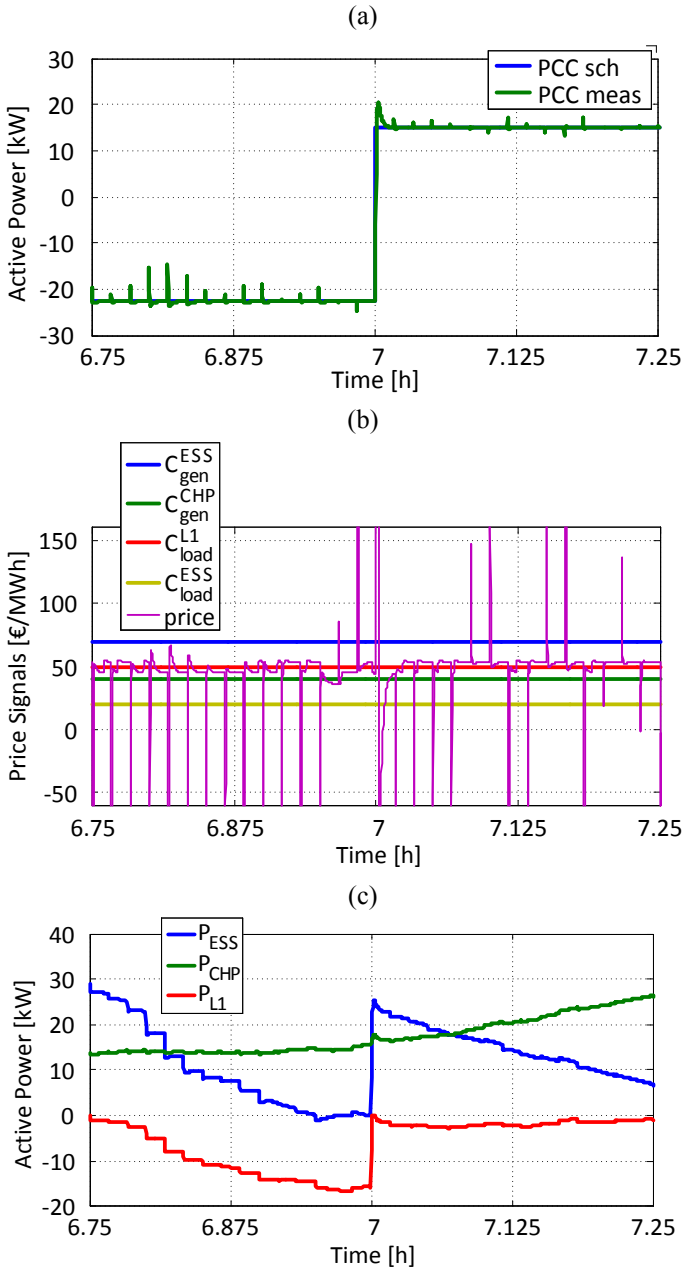

Fig. 3.12 (a) Real-time competitive controller response of the simulated active distribution grid during a representative short-time period; (b) Real-time comparison of the competitive controller price signal and the individual resource marginal costs; (c) Generation and demand involvement of the controllable DER units of the active distribution grid.

Under this price signal increase and decrease conditions, the individual controllable generation/demand units are being stimulated to modify its generation or demand power levels based on the involvement rules already introduced from (3.14)-(3.20) and on their marginal costs considered. As a result, Fig. 3.12(c) presents the real-time power dispatch of the controllable individuar DER generation and demand units, used to ensure that the real-time power exchange schedules are met at minimum operation costs, through the optimum allocation of available resources.

Study case 2: Stand-alone Control of Active Distribution Grids

This particular study case is very similar to the previous one, but considering in this case that the active distribution grid is isolated from the main grid. Therefore, all the load internally being demanded will be provided by the generation units of the active distribution grid.

In order to determine the optimum economic dispatch within the active distribution grid, the competitive power controller already introduced in

Fig. 3.7 will be implemented in simulation. However, in this specific case there is no need of determining a power exchange schedule to be provided at the PCC of the active distribution grid, as the power reference considered will be zero.

The stationary competitive power controller performance is introduced in Fig. 3.13. As it can be observed from Fig. 3.13(a), the competitive power controller ensures zero power supply at the PCC of the active distribution grid. This means that the competitive controller provides real-time balance between generation and demand, through the controllable generation and demand response units involved. In addition to this, the competitive controller instantaneously makes use of the cheaper DER units for achieving this purpose. This real-time optimum economic dispatch can be derived from Fig. 3.13(b) and Fig. 3.13(c), where the competitive price signal is compared with the individual marginal costs of the DER units, and the resulting power references are provided based on the DER involvement rules and marginal costs considered. The optimum economic dispatch justification of the competitive power controller is summarized in Table 3.2, which arises from the price signal/marginal costs comparison and the DER involvement rules considered.

In order to provide a better understanding regarding the overall competitive power dispatch performance, Fig. 3.14 shows the power supply and demand profiles for each of the DER resource units conforming the active distribution grid.

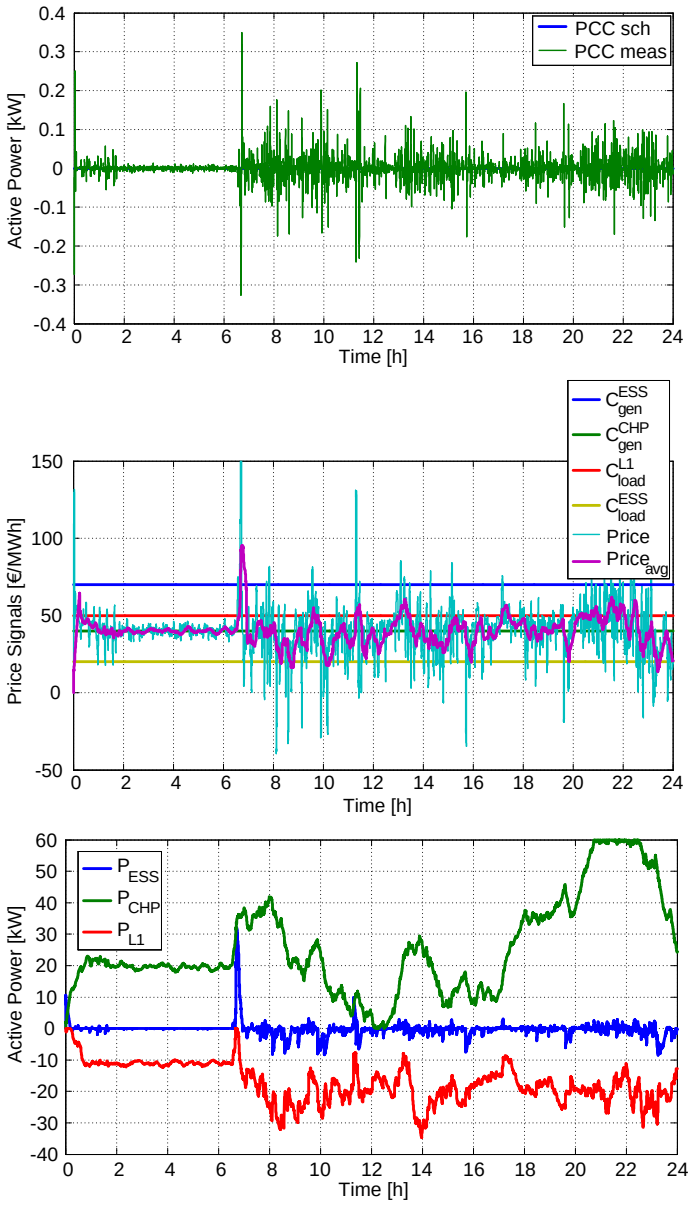

Fig. 3.13 Study case 2: (a) Stationary competitive controller response of the simulated active distribution grid during a representative day of operation; (b) Stationary comparison of the competitive controller price signal and the individual resource marginal costs; (c) Generation and demand involvement of the controllable DER units of the active distribution grid

Time interval	Price signals comparison	Power production/demand involvement
[0:00 to 6:00]	$Price_{avg} > C_{load}^{ESS} \Rightarrow \frac{dP_{load}^{ESS}}{dt} > 0$ $(Psaturated = 0)$	The generation/demand balance is ensured from the L1 demand response and the CHP generation unit. The CHP unit initially increases its generation as a result of a price peak, and later it keep the generation constant, as the steady state price singal equals the marginal CHP cost. The L1 responsive load consumes maximum power as the price signal is below its marginal utility cost.
	$Price_{avg} \geq C_{gen}^{CHP} \Rightarrow \frac{dP_{gen}^{CHP}}{dt} \geq 0$	
	$Price_{avg} < C_{load}^{L1} \Rightarrow \frac{dP_{load}^{L1}}{dt} < 0$	
	$Price_{avg} < C_{gen}^{ESS} \Rightarrow \frac{dP_{gen}^{ESS}}{dt} < 0$ $(Psaturated = 0)$	
[6:00 to 7:30]	$Price_{avg} > C_{load}^{ESS} \Rightarrow \frac{dP_{load}^{ESS}}{dt} > 0$ $(Psaturated = 0)$	There is a sudden price increase due to the morning peak demand, and all the resources contribute to the regulation. Due to the ramp rate limitation of the CHP the ESS and L1 load provide a faster regulation.
	$Price_{avg} > C_{gen}^{CHP} \Rightarrow \frac{dP_{gen}^{CHP}}{dt} > 0$	
	$Price_{avg} > C_{load}^{L1} \Rightarrow \frac{dP_{load}^{L1}}{dt} > 0$	
	$Price_{avg} > C_{gen}^{ESS} \Rightarrow \frac{dP_{gen}^{ESS}}{dt} > 0$	
[7:30 to 12:00]	$Price_{avg} > C_{load}^{ESS} \Rightarrow \frac{dP_{load}^{ESS}}{dt} > 0$ $(Psaturated = 0)$	The average price signal decrease and remains between the L1 and CHP marginal costs. This is due to the off-peak load condition and inelastic PV generation contribution. Then, the CHP average power production decrease and L1 demand provides the required stationary regulation.
	$Price_{avg} \leq C_{gen}^{CHP} \Rightarrow \frac{dP_{gen}^{CHP}}{dt} < 0$	
	$Price_{avg} < C_{load}^{L1} \Rightarrow \frac{dP_{load}^{L1}}{dt} < 0$	
	$Price_{avg} < C_{gen}^{ESS} \Rightarrow \frac{dP_{gen}^{ESS}}{dt} < 0$ $(Psaturated = 0)$	
[12:00 to 16:00]	$Price_{avg} > C_{load}^{ESS} \Rightarrow \frac{dP_{load}^{ESS}}{dt} > 0$ $(Psaturated = 0)$	There is an average price signal peak, corresponding to the peak load of L2 and L3. In this case the CHP generator and L1 load provide the required regulation during the peak-load condition.
	$Price_{avg} \geq C_{gen}^{CHP} \Rightarrow \frac{dP_{gen}^{CHP}}{dt} > 0$	
	$Price_{avg} < C_{load}^{L1} \Rightarrow \frac{dP_{load}^{L1}}{dt} < 0$	

	$Price_{avg} < C_{gen}^{ESS} \Rightarrow \frac{dP_{gen}^{ESS}}{dt} < 0$ $(Psaturated = 0)$	
[16:00 to 20:00]	$Price_{avg} > C_{load}^{ESS} \Rightarrow \frac{dP_{load}^{ESS}}{dt} 0$ $(Psaturated = 0)$	At the afternoon off-peak load, there is an slightly average price signal increase, which results in a CHP generation increase. This is mainly due to the PV generation decrease. The L1 responsive load is operating at almost its maximum power consumption, as the average price signal is below the marginal utility price of L1 (C_{load}^{L1}).
	$Price_{avg} \geq C_{gen}^{CHP} \Rightarrow \frac{dP_{gen}^{CHP}}{dt} \geq 0$	
	$Price_{avg} < C_{load}^{L1} \Rightarrow \frac{dP_{load}^{L1}}{dt} < 0$	
	$Price_{avg} < C_{gen}^{ESS} \Rightarrow \frac{dP_{gen}^{ESS}}{dt} < 0$ $(Psaturated = 0)$	
[20:00 to 22:00]	$Price_{avg} > C_{load}^{ESS} \Rightarrow \frac{dP_{load}^{ESS}}{dt} > 0$ $(Psaturated = 0)$	At the night peak-load condition, the CHP generation unit reaches its maximum power production, as the cheaper resource unit, while the L1 load provides the required regulation through its demand response to a price signal increase.
	$Price_{avg} \geq C_{gen}^{CHP} \Rightarrow \frac{dP_{gen}^{CHP}}{dt} \geq 0$	
	$Price_{avg} \geq C_{load}^{L1} \Rightarrow \frac{dP_{load}^{L1}}{dt} \geq 0$	
	$Price_{avg} < C_{gen}^{ESS} \Rightarrow \frac{dP_{gen}^{ESS}}{dt} < 0$ $(Psaturated = 0)$	
[22:00 to 24:00]	$Price_{avg} \leq C_{load}^{ESS} \Rightarrow \frac{dP_{load}^{ESS}}{dt} \leq 0$	Finally, the price signal decreases as a result of the inelastic power demand decrease. Consequently, the L1 demand increases towards its maximum desirable demand, and the CHP generation units decreases its generation involvement to adjust the generation to the new power demand levels. Finally, the ESS takes advantage of the very low price signals experienced and increases its charging levels when the price signal is below the charging marginal price (C_{load}^{ESS}).
	$Price_{avg} < C_{gen}^{CHP} \Rightarrow \frac{dP_{gen}^{CHP}}{dt} < 0$	
	$Price_{avg} < C_{load}^{L1} \Rightarrow \frac{dP_{load}^{L1}}{dt} < 0$	
	$Price_{avg} < C_{gen}^{ESS} \Rightarrow \frac{dP_{gen}^{ESS}}{dt} < 0$ $(Psaturated = 0)$	

Table 3.2 Study case 2: Stationary competitive dispatch justification of the results obtained from Fig. 3.13(b) and (c)

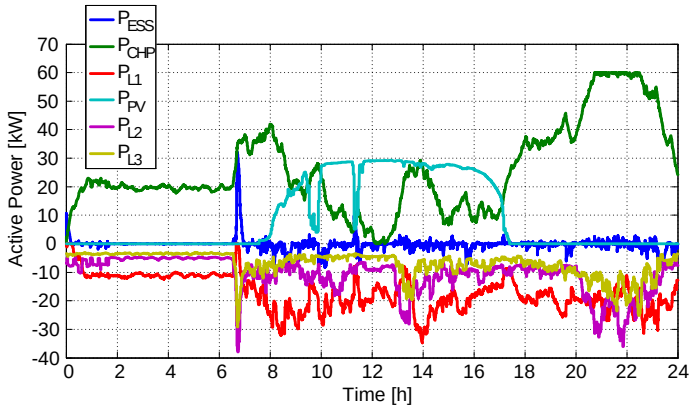

Fig. 3.14 Real-time power dispatch of the global DER energy resources conforming the active distribution grid

Finally, the real-time performance of the L1 demand responsive load is introduced in Fig. 3.15, along with its maximum power consumption profile specified in Fig. 3.8(d). From this figure, it can be observed that L1 is considerably reducing its demand involvemente during the peak load periods, thus providing the desired demand response performance for achieving the active distribution grid control objective. At the off-peak periods, L1 approximately consumes the maximum load, as the electricity price during such periods is usually below the marginal utility set by the DER controller.

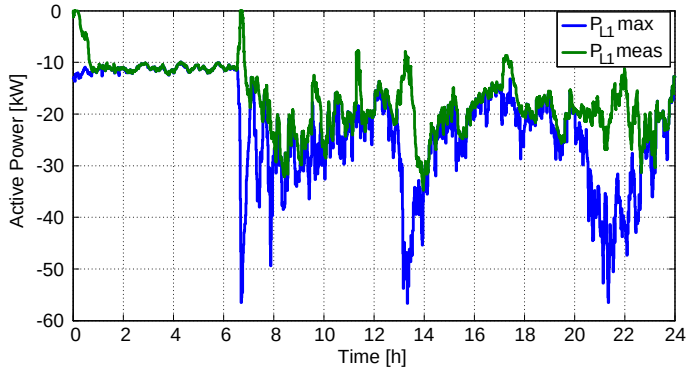

Fig. 3.15 Real-time performance of the L1 demand responsive load in comparison with its maximum load profile

In order to validate the real-time control capabilities under this study case, the real-time response of the competitive power controller is introduced in Fig. 3.16.

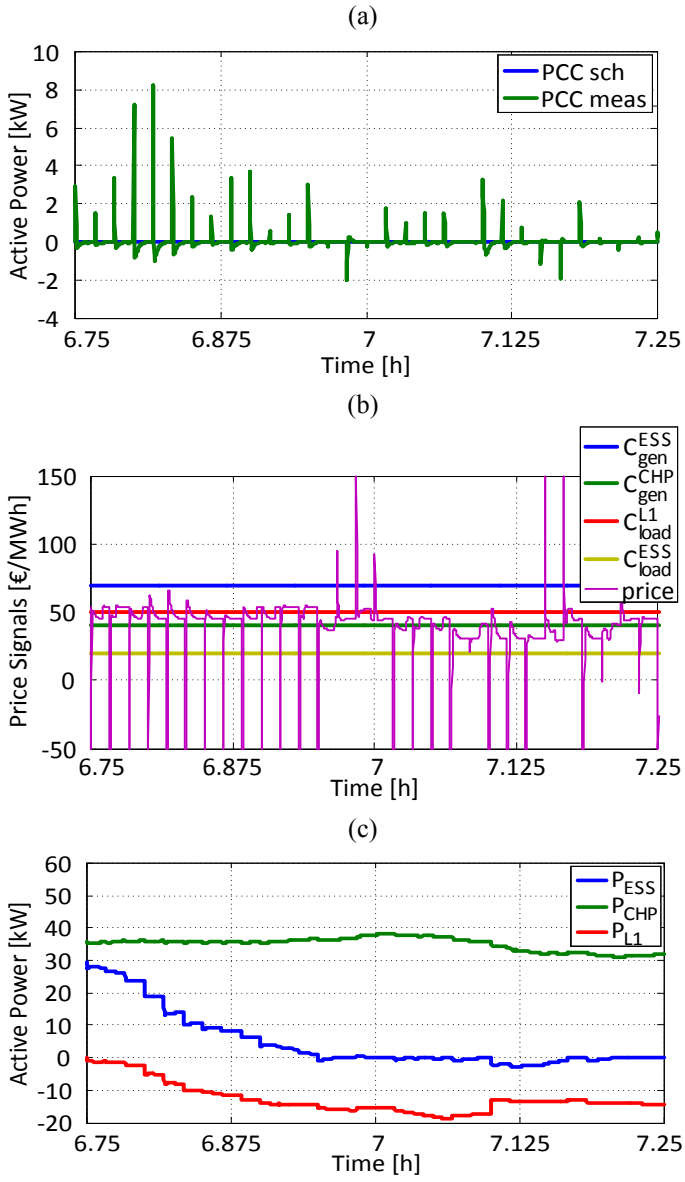

Fig. 3.16 (a) Real-time competitive controller response of the simulated active distribution grid during a representative short-time period; (b) Real-time comparison of the competitive controller price signal and the individual resource marginal costs; (c) Generation and demand involvement of the controllable DER units of the active distribution grid.

From Fig. 3.16(a), it can be observed that zero active power exchange at the PCC is instantaneously met by the competitive controller. Fig. 3.16(b) presents a comparison

between the price control signal and the individual marginal costs considered in each DER resource unit. As it can be observed from this figure, the PI-based competitive front-end controller provides a price signal increase for the case in which the power reference is higher than the measurement, and a price signal decrease for the reverse case. Therefore the price signal increases as a consequence of a power deficit in the power balance of the active distribution grid, while a price signal decreases due to a power surplus.

Under this price signal increase and decrease conditions, the individual controllable generation/demand units are being stimulated to modify its generation or demand power levels based on the involvement rules already introduced from (3.14)-(3.20) and on their marginal costs considered. As a result, Fig. 3.16(c) presents the real-time power dispatch of the controllable individuar DER generation and demand units, used to ensure that the real-time power exchange schedules are met at minimum operation costs, through the optimum allocation of available resources

Chapter 4.

4 Wave energy characterization and control for maximum power extraction

The first step needed for the suitable implementation of the competitive controller in the selected wave power plant application, correspond to the characterization of the wave energy resource for maximum power extraction. This resource characterization is of vital importance, as it will reproduce the expected real-time power oscillating performance, which will be used in a later stage for the competitive controller as the instanateous maximum resource capacity. Therefore, the present chapter introduces a novel wave energy converter control for maximum power extraction under real-time irregular wave conditions, which arises as one of the principal contributions of this thesis.

4.1 Introduction

Up to date, most of the research efforts conducted in the wave energy field have been focused on finding a well-accepted wave energy converter (WEC) concept with high power extraction efficiency and proven energy conversion technology, which would provide high sea performance capabilities (hydrodynamic efficiency and survivability) under realistic sea state conditions. However, many grid connection concerns, such as maximum power absorption and improved power quality, are currently gaining increased research interest, as several WEC concepts approach their near-commercial deployments [98, 99, 100, 101, 102, 103].

Besides the design and development of efficient primary energy capture mechanisms and technologies, the control applied to the WEC is of crucial relevance when pursuing

maximum energy extraction from the resource. Thence, depending on the implemented control strategy, the efficiency of the device can be severely affected [104, 105, 106, 107].

Moreover, one of the major concerns when performing maximum power extraction of the wave energy resource is the limitation of the instantaneous output power peak-to-average ratio, which has a direct impact on the mechanical and electrical system overrating and its costs. As the implemented controller approaches optimum energy extraction conditions, the wave energy converter operates at higher peak-to-average ratios [108], which imply that higher instantaneous power fluctuations are being processed by the energy conversion systems. In order to limit such power fluctuations, many WECs include additional energy storage solutions in the mechanical/electrical power take-off (PTO) system, resulting in larger overall system costs.

Regarding the control of the wave energy resource, it is worth noting that multiple control solutions have been proposed in the literature with no clear sign of a straightforward preferred control candidate, resulting in maximum power extraction under realistic sea state conditions. Linear damping, latching and reactive based controllers [104, 109] initially appeared as suitable candidates in the frequency-domain control of regular waves, leading in the case of the reactive control to maximum energy absorption from the resource. However, this approach reaches sub-optimum conditions when applied to irregular realistic waves, as the system is tuned at the sea state level rather than at the wave-to-wave level.

Other more advanced optimum and suboptimum time-domain approaches appeared in [110, 111, 112, 113] with the purpose of maximizing the instantaneous energy absorption. However, such control strategies usually require an accurate characterization of the incoming wave excitation force from far positioned measurement buoys, which are prone to introduce uncertainties or incorrect information depending on the distance to the wave energy converter and on their interactions, if any.

Therefore, the present chapter contributes to the wave energy sector by proposing a novel WEC control concept, which is able to achieve maximum power absorption of the resource thanks to its inherent adaptive behaviour. The adaptive vector control approach arises as a suitable and robust solution, as it determines the required control action, based on the self-velocity of the wave energy device and not based on the detailed knowledge from incoming waves. Thanks to the adaptive performance of the controller, the WEC is capable of achieving maximum power absorption regardless of the instantaneous performance of the resource, with no need of offline tuning parameters calculation depending on the incoming wave characteristics. Despite of achieving maximum energy resource extraction, the proposed vector controller goes one step further, as it contributes in reducing the peak-to-average ratio, which means that a reduction of the instantaneous power fluctuations can be achieved with no need of additional overrating and short term storage equipment and associated costs.

Finally, the overall wave to wire energy conversion system is introduced along this chapter in order to provide a general view of the particular WEC power processing scenario

considered in this thesis. The system configuration, which is depicted in Fig. 4.1, is built up around 4 heaving buoys, each of them connected to a hydraulic PTO.

Due to the fact that the goal of the project is not to contribute towards introducing a novel wave energy converter concept, the proposed system has been selected, because it is a realistic approach to the conventional heaving point absorber with a single degree of movement. This configuration arises as a well known and simple study case, as it does not consider any hydrodynamic interactions affecting different bodies of the structure.

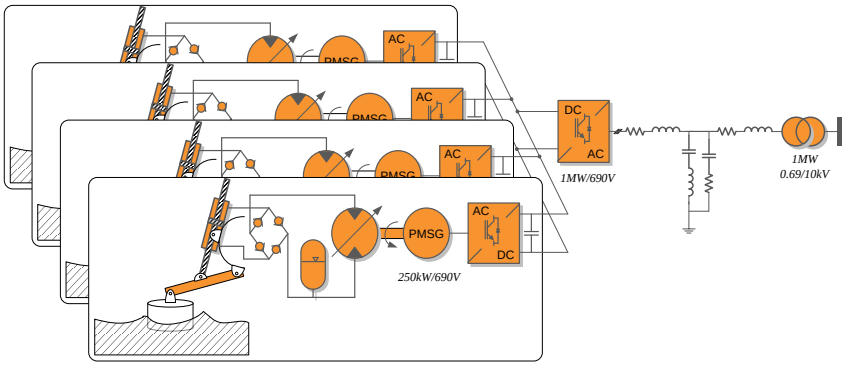

Fig. 4.1. Overall wave energy converter system configuration

A hydraulic PTO system has been considered in this particular implementation due to its inherent storage capacity, as it contributes to the reduction of the overall peak to average ratio. This hydraulic PTO system is comprised by a hydraulic cylinder with a set of hydraulic rectifying valves (i.e. to achieve unidirectional flow rate from the cylinder), a hydraulic accumulator, and a hydraulic motor. The main function of the accumulator is to smooth the flow rate fluctuations arriving to the hydraulic motor, and thus reducing the peak to average ratio.

Regarding the grid interconnection of wave energy converters, the selection of the generator, as well as the power electronic interface to be used plays a key role in achieving an efficient wave energy converter control, as well as in ensuring a high quality grid connection compliance [107, 114, 115]. As it was already discussed in the wind energy sector [116] and further derived for wave energy converters, the implementation of a permanent magnet synchronous generator along with a full-scale power electronic interface arise as the preferred grid interconnection solution, since they facilitate the interconnection of different frequency-voltage systems, thereby ensuring variable speed control of the generator, while providing acceptable grid voltage regulation and fault ride-through capabilities [107].

In the proposed wave energy converter configuration (Fig. 4.1), it is worth noting that the DC-link terminals of the PMSG drivers are interconnected together, and the overall wave energy converter power is processed through a single front end voltage source inverter (VSI). By implementing this interconnection design it is possible to achieve an aggregated effect in

the entire DC-link, since none of the power variations of the heaving buoys will pulsate in phase with the others. Therefore, this feature allows for an extra reduction of the final peak to average ratio obtained in the electrical point of interconnection.

4.2 Wave energy resource and hydrodynamic converter modeling

Real time modeling of the irregular wave energy resource

A straightforward manner of representing the stochastic behavior of irregular waves is based on considering the superposition effect of infinite sinusoidal waves of different frequencies, amplitudes and phase angles. Most of the approaches found in modeling the performance of realistic ocean waves serve from representative sea-state parameters to construct the energy spectrum characteristic of the sea. In this case, the Bretschneider spectrum has been considered with the particular sea-state parameters of the EMEC test site, where the most probable significant wave height (H_{wave}) and dominant wave period (T_{wave}) appear to be 1.47 m and 7.7 s respectively.

The Bretschneider wave energy spectrum has been obtained by following the equations introduced in (2.1)-(4.3) [117]. Where *f* represents each of the wave frequency components considered, and *S* stands for the wave energy spectrum magnitude, which is depicted in Fig. 4.2.

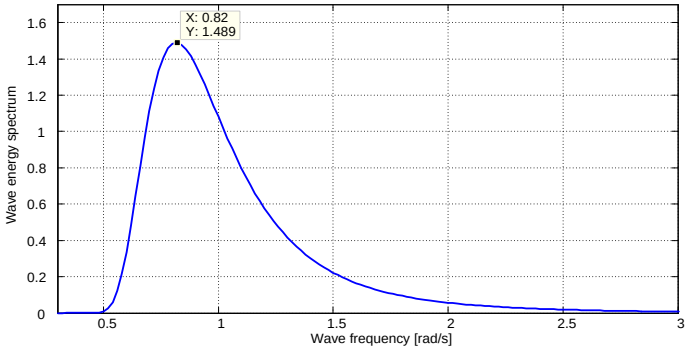

Fig. 4.2 Bretschneider wave energy spectrum corresponding to the characterization of irregular waves with $T_{wave} = 7.7s$ and $H_{wave} = 1.47m$

$$A = \frac{5}{16}\frac{H_{wave}^2}{T_{wave}^4} \tag{4.1}$$

$$B = \frac{5}{4}\frac{1}{T_{wave}^4} \tag{4.2}$$

$$S(f) = \frac{A}{f^5} e^{-\frac{B}{f^4}} \tag{4.3}$$

Once the energy spectrum has been characterized, the time domain excitation force can be depicted in Fig. 4.3, which directly results from equations (4.4) and (4.5).

Where $\tilde{F}_{exc}(\omega_i)$ are the excitation force coefficients calculated in frequency domain from a fluid dynamic software, which affects the wave energy converter under consideration; A_i are the wave amplitudes for each of the wave frequency components, which are obtained from the discretisation of the wave spectrum S; $\Delta\omega$ is the discretisation step of the spectrum and φ_i are the random phase angles for each of the frequency components considered.

$$A_i(\omega_i) = \sqrt{2S(\omega_i)\Delta\omega} \tag{4.4}$$

$$F_{exc}(t) = \sum_{i=1}^{N} A_i \Re\left(\tilde{F}_{exc}(\omega_i) e^{-j\omega_i t + j\varphi_i}\right) \tag{4.5}$$

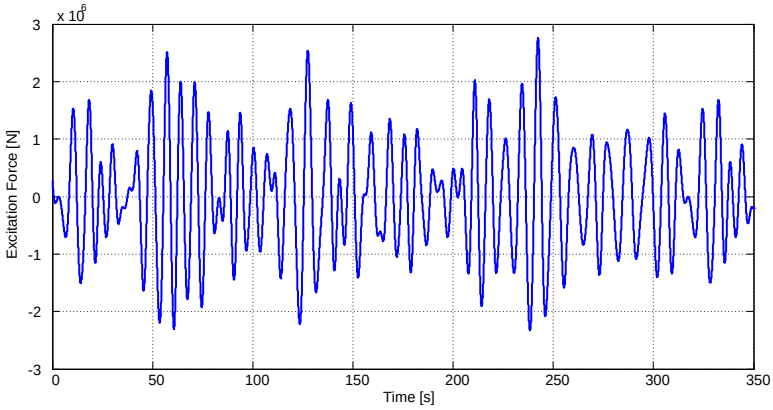

Fig. 4.3 Time domain excitation force corresponding to the characterization of irregular waves with $T_{wave} = 7.7s$ and $H_{wave} = 1.47m$

Wave energy converter modelling

Once the irregular wave energy field has been characterized, it is necessary to determine the equation of motion of the WEC, by performing a detailed evaluation of the forces acting upon the motion of the wave energy device [118].

Fig. 4.4 introduces the wave energy converter concept considered for this case, which is based on a simplified heaving point absorber with a single degree of freedom moving respect to a fixed bottom structure. A cylindrical point absorber has been considered here, since the

purpose of this chapter is to introduce and evaluate the proposed wave energy controller performance on a generic, simple and well known wave energy device.

The overall hydrodynamic forces acting in this particular wave energy system can be observed in Fig. 4.4, where f_{exc} represent the excitation force from incoming waves (determined in previous section); f_{PTO} represents the power take-off (PTO) force required for extracting energy from the system; f_{rad} accounts for the force of radiated waves; f_s represents the spring force due to the WEC buoyancy; and the *ma* stands from the resulting acceleration of the wave energy device mass.

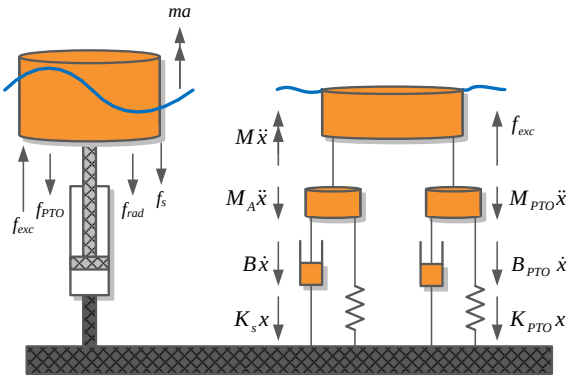

Fig. 4.4 Description of the WEC acting forces and justification of the frequency domain equation of motion [118]

The equations extending further the modeling of such terms are introduced in frequency domain from (4.6) to (4.9). The final equation of motion of the wave energy device is introduced in (4.10), which results from substituting (4.7), (4.8) and (4.9) into (4.6). From such equations $M_A(\omega)$, $B(\omega)$ and K_s respectively account for the radiation added mass, radiation force damping and buoyancy force coefficients, which have been accordingly determined from a computational fluid dynamic software, while the terms $B_{PTO}(\omega)$ and K_{PTO} represent the damping and spring PTO tuning control coefficients. For the sake of simplicity, an impedance term ($Z_{rad}(\omega)$ and $Z_{PTO}(\omega)$) has been introduced in equations (4.7) and (4.9), which describe how the wave energy converter opposes to its velocity. This impedance term will be referenced in later sections with the purpose of describing the PTO force conditions that should be satisfied in order to achieve maximum energy absorption from the resource.

$$F_{exc}(j\omega) - F_{rad}(j\omega) - F_s(j\omega) - F_{PTO}(j\omega) = -\omega M X(j\omega) \tag{4.6}$$

$$F_{rad}(j\omega) = Z_{rad}(\omega) j\omega X(j\omega) = \big(j\omega M_A(\omega) + B(\omega)\big) j\omega X(j\omega) \tag{4.7}$$

$$F_s(j\omega) = K_s X(j\omega) \tag{4.8}$$

$$F_{PTO}(j\omega) = Z_{PTO}(\omega)j\omega X(j\omega) = \left(B_{PTO}(\omega) + \frac{K_{PTO}(\omega)}{j\omega}\right)j\omega X(j\omega) \tag{4.9}$$

$$F_{exc}(j\omega) = \left[-\omega^2\left(M + M_A(\omega)\right)\right]X(j\omega) + j\omega B(\omega)X(j\omega) + K_s X(j\omega) + \left(B_{PTO}(\omega) + \frac{K_{PTO}(\omega)}{j\omega}\right)j\omega X(j\omega) \tag{4.10}$$

Where $X(j\omega)$ is the variable term representing the wave energy device position, being $j\omega X(j\omega)$ and $-\omega^2 X(j\omega)$ the variables representing the WEC velocity and acceleration respectively.

These modeling equations were firstly derived in frequency domain, as regular monochromatic incoming waves were considered. However, the frequency domain approach is no longer valid if real time modeling and control of wave energy converter is pursued for realistic irregular sea applications. Therefore, the time domain equation of motion is introduced in (4.11) from the Cummins' equation, resulting from the inverse Fourier transformation of equation (4.10). The relationship between the parameters from the frequency domain expression in (4.10) and the corresponding time domain expression in (4.11) are introduced in (4.12) and (4.13) [119].

$$[M + M_A]\ddot{x}(t) + \int_0^t K(t-\tau)\dot{x}(\tau)d\tau + K_s x(t) = f_{exc}(t) - f_{pto}(t) \tag{4.11}$$

$$K(t) = \frac{2}{\pi}\int_0^\infty B(\omega)\cos(\omega t)\,d\omega \tag{4.12}$$

$$M_A = \lim_{\omega\to\infty} M_A(\omega) = M_A(\infty) \tag{4.13}$$

Therefore, when merging (4.12) and (4.13) into (4.11), the following final expression is obtained in (4.14).

$$[M + M_A(\infty)]\ddot{x}(t) + \int_0^t K(t-\tau)\dot{x}(\tau)d\tau + K_s x(t) = f_{exc}(t) - f_{pto}(t) \tag{4.14}$$

Due to the fact that the entire real-time control system will be implemented in Matlab Simulink, it is necessary to develop the entire model in the Laplace form. In this regard, the highest complexity term to be modeled from the time domain equation of motion, is the convolution term representing the radiation damping. In this particular case, the damping radiation impulse response function has been introduced in (4.12) from the inverse Fourier transform of the damping hydrodynamic coefficient from (4.10) [108].

Once the radiation impulse response function representing the convolution term has been determined, then it is possible to use several identification methods in order to model the system, i.e in a transfer function or state space form [119]. In this particular case, the Prony approximation has been used as a parametric modeling technique in order to find the numerator and denominator coefficients of an IIR filter whose impulse response approximates the objective impulse response function from (4.12). As a result of the Prony approximation method, an 8th order system transfer function was obtained (4.15) to precisely represent the impulse response function dynamics. The comparison between the original radiation impulse response function (RIRF) and the Prony's method approximation is presented in Fig. 4.5 to validate the precision of the approximation.

$$H_{rad}(s) = \frac{\sum_{i=0}^{8} \alpha_i s^i}{\sum_{i=0}^{8} \beta_i s^i} \qquad (4.15)$$

$\alpha_8 = 6704$	$\alpha_7 = 2.812 \cdot 10^5$	$\beta_8 = 1$	$\beta_7 = 1.922$
$\alpha_6 = 6.352 \cdot 10^5$	$\alpha_5 = 4.675 \cdot 10^6$	$\beta_6 = 17.79$	$\beta_5 = 26.66$
$\alpha_4 = 7.163 \cdot 10^6$	$\alpha_3 = 1.777 \cdot 10^7$	$\beta_4 = 80.87$	$\beta_3 = 73.39$
$\alpha_2 = 1.393 \cdot 10^7$	$\alpha_1 = 1.119 \cdot 10^7$	$\beta_2 = 96.25$	$\beta_1 = 38.35$
$\alpha_0 = 5.613 \cdot 10^5$		$\beta_0 = 20.12$	

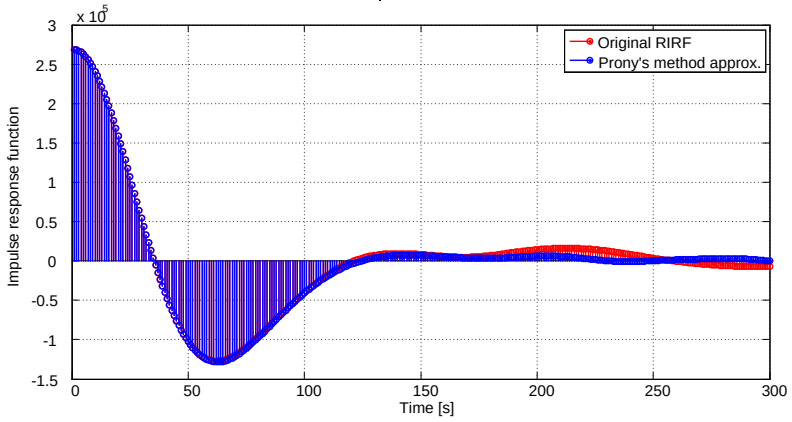

Fig. 4.5 RIRF approximation using the Prony's method

Once the radiation force transfer function has been determined, the Laplace representation of the time-domain equation from (4.14) can be easily derived in (4.16).

$$[M + A(\infty)]sV_{WEC}(s) + H_{rad}(s)V_{WEC}(s) + \frac{K_s}{s}V_{WEC}(s) + H_{PTO}(s)V_{WEC}(s) = F_{exc}(s) \quad (4.16)$$

Where the buoy velocity $V_{WEC}(s)$ appears as the state variable of the system and $H_{PTO}(s)$ represents the transfer function of the proposed adaptive vector controller.

4.3 Adaptive vector control for maximum power extraction of Wave Energy Converters

As it was outlined in previous research studies [108, 109, 120], the hydrodynamic wave energy converter model from (4.16) can be directly represented by an equivalent RLC electrical system (Fig. 4.6), where the mass term $\left(M + M_A(\infty)\right)$ and the imaginary term introduced from the radiation transfer function $\left(\Im\left(H_{rad}(s)\right)\right)$ represent the inductive term $\left(X_{L_{WEC}}\right)$ of the WEC impedance; the real component of the radiation force damping $\left(\Re\left(H_{rad}(s)\right)\right)$ represents the pure resistive term (R_{WEC}); and the spring term coefficient due to the WEC buoyancy (K_s) stand for the capacitive term of the wave energy converter impedance $\left(X_{C_{WEC}}\right)$. The voltage source $\left(U_{exc}(s)\right)$ represent the excitation force with all its frequency components; the voltage $\left(U_{PTO}(s)\right)$ represent the PTO force applied; and the current $\left(I(s)\right)$ represent the buoy velocity with all its frequency components.

From Fig. 4.6, it is remarked that maximum power absorption will be achieved for the case in which the wave energy conversion system appears at resonance with a given input frequency component $(X_{PTO} = -X_{WEC})$, as the totality of the power absorbed from the resource results in work-producing real power, and no power is extracted for energizing the wave energy converter structure. In addition to resonance conditions, maximum power extraction can only be achieved by applying a resistive PTO force equal to the intrinsic wave energy converter damping characteristic of the radiation force $\left(R_{PTO} = \Re\left(H_{rad}(s)\right)\right)$. Such optimal operating conditions are fulfilled by implementing the so called reactive or complex conjugate control, where the PTO provides a resistive force equal to the radiation damping term, and the imaginary PTO component is in charge of ensuring resonance operating conditions [108, 109, 120]. However, this control approach leads to sub-optimum conditions when applied to irregular realistic waves, as the system is tuned at the sea-state level rather than at the wave-to-wave level and maximum power absorption cannot be achieved in real-time.

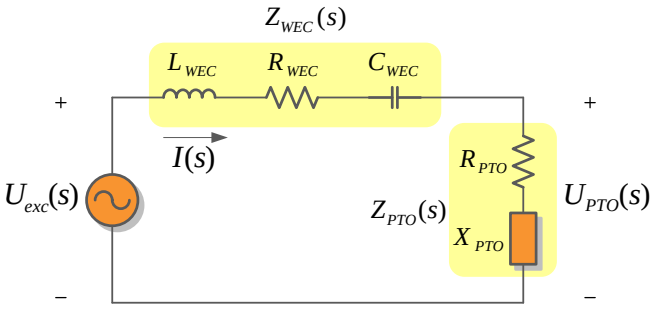

Fig. 4.6 Electrical representation of the considered wave energy converter

The main contribution of this section is found in the adaptive controller proposed, which maximizes the energy extraction from the resource regardless of the dominant irregular wave frequency characteristics. This adaptive performance is achieved from a signal monitoring and synchronization system, whose implementation in the wave energy sector has never been considered up to date. In addition, a novel vectorial approach has been introduced for determining the PTO forces acting on the wave energy conversion system, which maximizes the instantaneous or average power extraction from the resource. The proposed wave energy converter control strategy, which is presented in Fig. 4.7(a), is introduced in detail throughout this section.

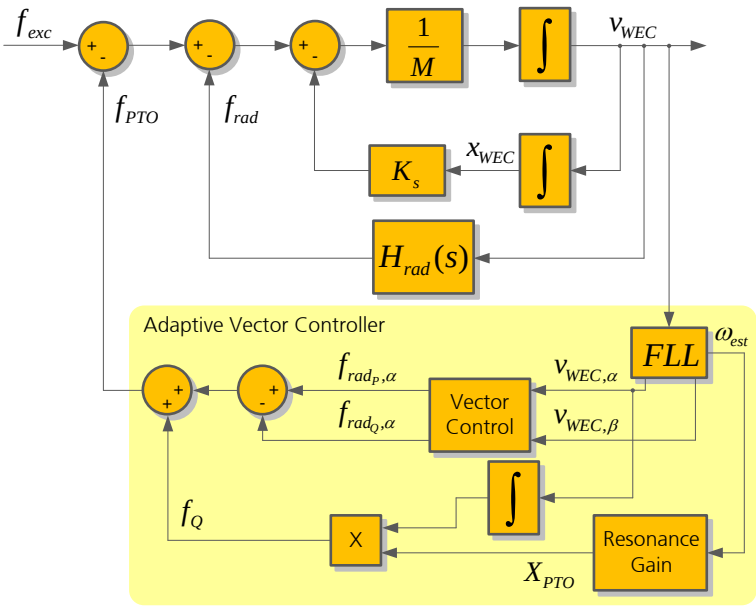

Fig. 4.7 Adaptive vector controller of wave energy converters for maximum power absorption

Signal monitoring and synchronization system (FLL)

Several other WEC control strategies also proposed the implementation of some sort of frequency detection techniques for the tuning of their controllers [121]. However, the novelty of the proposed controller is based on the application of an advanced synchronization method, namely, a Frequency Locked Loop (FLL) for detecting the waves' frequency. The FLL has been widely used in other fields, such as radio, telecommunications, computers, aerospace and other electrical and electronics systems [122, 123], but it was never applied to the wave energy field. The FLL is an effective alternative to other existing frequency estimation methods, as it provides singular features that allow improving even more the performance of the adaptive vector controller.

Thanks to its bandpass structure, the selectivity of the dominant frequency detection can be adjusted from the FLL tuning parameters in order to set the precision (or the optimality) of the frequency detection algorithm, going from the estimation of a more steadily sea-state dominant frequency component, to an instantaneous wave-to-wave frequency. In addition, the detection of multiple dominant frequency components could be achieved with the multiple SOGI FLL [124], leading to the implementation of a multi-frequency adaptive vector controller for enhanced power extraction capabilities.

The particular FLL structure implemented in the proposed controller appears in Fig. 4.8 as a dual purpose strategy: from one side, it is responsible of determining the instantaneous direct and quadrature components of the buoy velocity vector, which will be used later in the vector control system for determining the final PTO force. On the other side, the FLL provides the capability of instantaneously estimating the dominant frequency components of the WEC velocity. These are the frequency components to which the entire wave energy conversion system should resonate with in order to ensure optimal operation conditions.

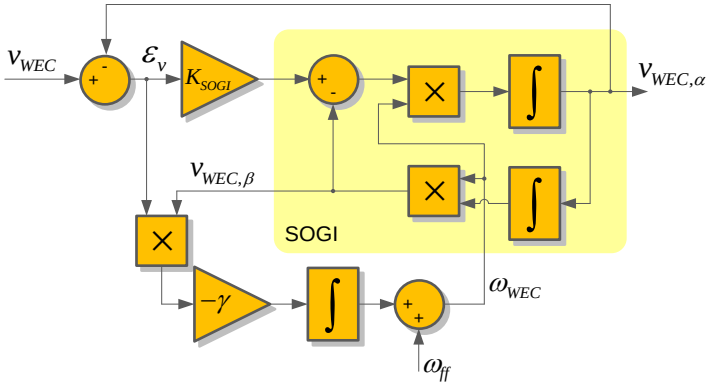

Fig. 4.8 Frequncy Locked Loop (FLL) structure implemented for monitoring the wave energy converter velocity [123]

As specified in [122, 123], the tuning parameters of the FLL are the gain of the SOGI (K_{SOGI}) and the FLL gain (γ), which determine the selectivity of this adaptive band pass filter and its tracking frequency dynamics. In this specific case a $K_{SOGI} = \sqrt{2}$ and $\gamma = 0.16$ have been considered as a trade-off for ensuring a high frequency selectivity, while providing accurate direct and quadrature components for the band pass frequencies comprised between 0.6 and 1rad/s.

(a)

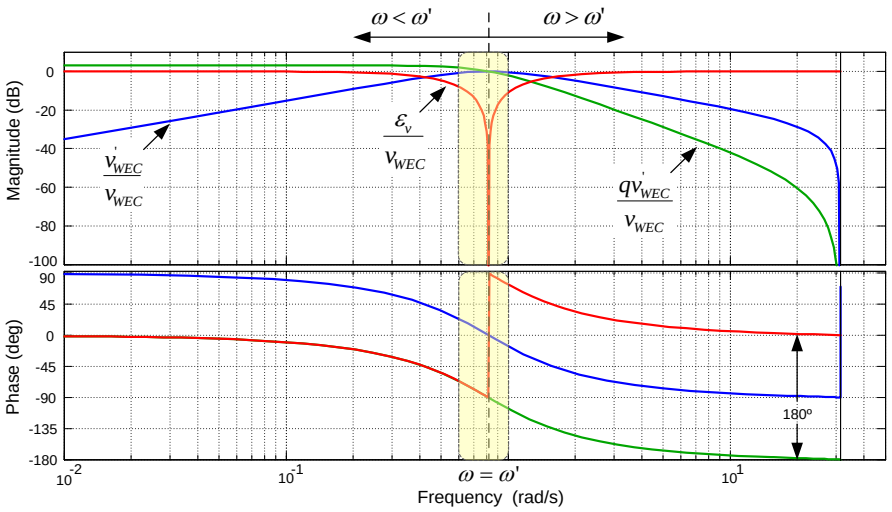

(b)

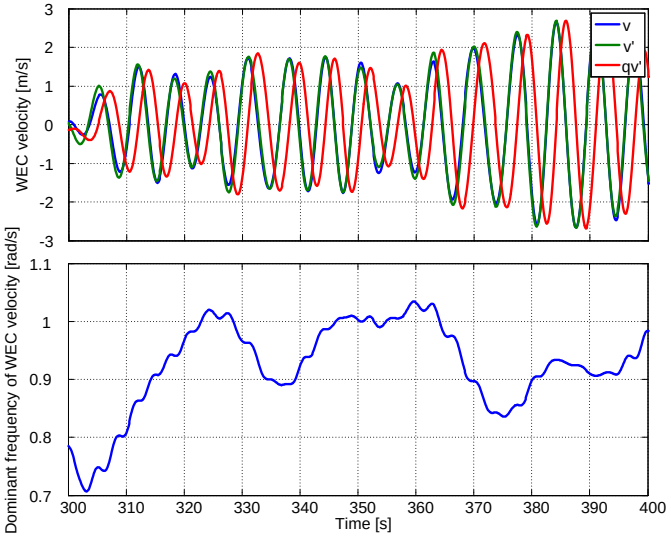

Fig. 4.9 (a) Bode diagrams ofthe direct, quadrature and error of SOGI based transfer functions; (b) Dynamic performance of the implemented SOGI frequency locked loop structure under real sea state conditions $T_1 = 7.7s$ and $H_{1/3} = 1.47m$

This frequency range corresponds to the wave periods between 9.1s and 6.3s respectively, which are used in further sections as the boundary wave energy resource periods for testing the suitability of the control concept under different resource conditions. The justification of the selected tuning parameters can be observed in the bode diagram of the implemented SOGI (Fig. 4.9(a)), while its dynamic detection of the velocity vector components and intrinsic frequency is introduced in Fig. 4.9(b). Thanks to the adaptive behaviour of the FLL, the proposed control structure has the ability of instantaneously estimating the frequency and the vector projections independently of any possible real-time modification in amplitude or frequency of the WEC velocity.

The feedforward term ω_{ff} introduced in Fig. 4.8 represents an initial approximation of the estimated wave frequency, which allows a faster detection of the estimated frequency after the system initialization. However, as there is not any fast dynamic detection requirement, the value of such feedforward term does not have any direct implication in the frequency detection results.

Vector control system

In order to have a meaningful evaluation of the proposed controller working principle, Fig. 4.10 introduces the vector representation of the control system, from which the radiation force $(\vec{f}_{rad})$ and WEC velocity $(\vec{v}_{WEC})$ vectors are clearly identified along with their orthogonal components. The vectorial approach introduced in this section is also found as a novel contribution in the wave energy field.

The radiation force vector and its components, which appear in Fig. 4.10, can be easily determined thanks to the FLL capability for extracting the direct and quadrature components of the buoy velocity vector, as they are obtained by multiplying the radiation force transfer function with the corresponding buoy velocity components (4.17) and (4.18).

$$f_{rad,\alpha} = H_{rad(s)} v_{WEC,\alpha} \tag{4.17}$$

$$f_{rad,\beta} = H_{rad(s)} v_{WEC,\beta} \tag{4.18}$$

The target of the proposed novel vectorial control is to achieve maximum instantaneous power extraction of the primary resource. For doing so, the controller determines the active and reactive power producing components $(\vec{f}_{rad_P})$ and $\left(\vec{f}_{rad_Q}\right)$ of the radiation force vector, which appear in-phase and in-quadrature with the buoy velocity vector.

As it can be observed in Fig. 4.10, the radiation force active power-producing term $(\vec{f}_{rad_P})$ results from the radiation force projection over the buoy velocity vector (i.e. the

radiation force component in-phase with the velocity vector), while the reactive power-producing term $\left(\vec{f}_{rad_Q}\right)$ appears as the radiation force projection in-quadrature with it. Such radiation force active and reactive power components can be determined according to (4.19) and (4.20), resulting in the minimum radiation force coefficients required for achieving maximum instantaneous power absorption.

$$\vec{f}_{rad_P} = \frac{\vec{v}_{WEC,\alpha} \cdot \vec{f}_{rad,\alpha} + \vec{v}_{WEC,\beta} \cdot \vec{f}_{rad,\beta}}{v_{WEC,\alpha}^2 + v_{WEC,\beta}^2} \vec{v}_{WEC} \tag{4.19}$$

$$\vec{f}_{rad_Q} = \vec{f}_{rad} - \vec{f}_{rad_P} \tag{4.20}$$

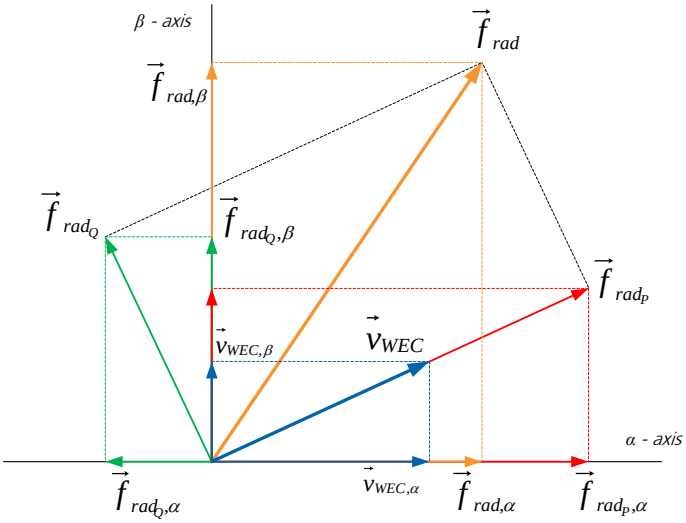

Fig. 4.10 Vector diagram of the proposed wave energy converter controller

Therefore, thanks to the vector control system applied, the PTO satisfies one of the necessary condition for maximizing the power absorption from the resource, as it instantaneously provide a force with equal real part as the radiation force, while cancelling out the possible reactive term introduced by the radiation force transfer function (4.21).

$$F_{PTO} = \left(\Re\left(H_{rad}(s)\right) - \Im\left(H_{rad}(s)\right)\right) \cdot \vec{v}_{WEC} \tag{4.21}$$

For this reason, the estimated reactive component of the radiation force $\left(\vec{f}_{rad_Q}\right)$ appears substracting to the final PTO force $\left(\vec{f}_{PTO}\right)$ in Fig. 4.7, with the purpose of cancelling the imaginary term introduced from the radiation transfer function.

The main advantage of the proposed vectorial approach is that, when obtaining the active and reactive radiation force terms, many power strategies could be used. For the case introduced in (4.19) and (4.20) maximum instantaneous power absorption will be achieved. However, if the interest is found in maximizing the average power extraction, equations (4.22) and (4.23) can be introduced. As will be shown later, the average power control strategy achieves maximum average power absorption levels, very similar to the ones obtained with the instantaneous power theory, while experiencing reduced peak to average ratios. Therefore, the average power theory results in an enhanced control solution when comparing with the instantaneous power strategy, as a reduced overrating would be required from the mechanical and electrical components, due to the reduction in the output power peak to average ratio.

$$\vec{f}_{rad_P} = \frac{\frac{1}{T}\int_t^{t+T}\left(\vec{v}_{WEC,\alpha}\cdot\vec{f}_{rad,\alpha} + \vec{v}_{WEC,\beta}\cdot\vec{f}_{rad,\beta}\right)}{\frac{1}{T}\int_t^{t+T}\left(v_{WEC,\alpha}^2 + v_{WEC,\beta}^2\right)}\vec{v}_{WEC} \tag{4.22}$$

$$\vec{f}_{rad_Q} = \vec{f}_{rad} - \vec{f}_{rad_P} \tag{4.23}$$

Virtual PTO buoyancy coefficient calculator for instantaneous resonance conditions

Aside of providing a resistive force equal to the inherent radiation damping of the wave energy converter, maximum power absorption can only be achieved if the PTO system ensures instantaneous resonance conditions. This is achieved by providing an additional virtual buoyancy term from the PTO (f_Q), which is able to cancel the intrinsic reactive components of the wave energy converter (added mass and buoyancy of the WEC) for any of the dominant estimated frequencies of the FLL. Then, thanks to the adaptive behaviour of the FLL, the PTO force provides a reactive term ensuring system resonance conditions regardless of the frequency of the wave field, as the frequency of the heaving point absorber velocity is continuously estimated by the FLL structure.

Once the wave frequency is obtained, the resonance gain calculator from Fig. 4.7 is the structure in charge of continuously determining the spring term coefficient that the PTO should provide in order to ensure resonance conditions. This resonant gain calculator is determined by accordingly setting the PTO virtual buoyancy coefficient (X_{PTO}), so that the resonator structure composed by the WEC added mass $\left(M + M_A(\infty)\right)$ and buoyancy term (K_s) instantaneously resonates with the frequency of the incoming waves. This resonator structure is introduced in Fig. 4.11. Then, the transfer function of this resonator block is given in (4.24) and its correlation to the resonant frequency is given from equations (4.25) to (4.27).

$$H_{res}(s) = \frac{Y(s)}{X(s)} = \frac{s}{(M + M_A(\infty))s^2 + K_s + X_{PTO}} = \frac{s/(M + M_A(\infty))}{s^2 + (K_s + X_{PTO})/(M + M_A(\infty))} \tag{4.24}$$

$$s^2 + \omega^2 = s^2 + \frac{K_s + X_{PTO}}{\left(M + M_A(\infty)\right)} \Rightarrow \tag{4.25}$$

$$\omega^2 = \frac{K_s + X_{PTO}}{\left(M + M_A(\infty)\right)} \Rightarrow \tag{4.26}$$

$$X_{PTO} = \left(M + M_A(\infty)\right)\omega^2 - K_s \tag{4.27}$$

Where ω is the instantaneous estimated frequency from the FLL structure.

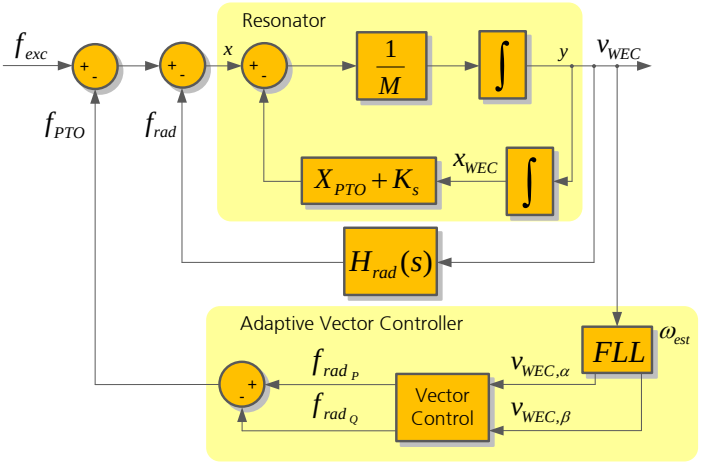

Fig. 4.11 Equivalent adaptive vector control emphasizing the resonator structure

It is worth noting that the main difference between the excitation force and WEC velocity is that a reduced set of frequency components is found in the WEC velocity as a result of the attenuation effect of the WEC buoy and PTO (passive elements from Fig. 4.6). However, the assumption of considering the WEC velocity frequency components for determining the adaptive vectorial tuning parameters is sufficient, as the frequency components with higher energy density in the incoming wave modeling spectrum are the ones present in the WEC velocity. This allows using the buoy velocity as a direct feedback measurement, and not the excitation force. The control strategies based on feedback from the excitation force measurements usually require an accurate characterization of the incoming waves from far positioned measurement buoys, which are prone to introduce uncertainties or incorrect

information depending on the distance to the wave energy converter and on their interactions, if any.

4.4 Hydraulic Power-Take-Off system Modelling and Control

The model of the hydraulic system considered in this section is introduced in Fig. 4.1, from which the hydraulic motor pressure is controlled by regulating the flow over the motor. Then, the instantaneous power provided from the hydraulic cylinder flows over a rectifier bridge valve, achieving in this way a unidirectional flow rate throughout the motor. The main role of the high pressure accumulator is to filter out the highly present output power oscillations, thus contributing towards reducing the peak to average ratio of the power that is finally processed by the hydraulic motor.

In order to achieve the desired system performance, the PTO model and control, introduced in Fig. 4.12, makes use of the reference force from the WEC controller (f_{ref}), the velocity of the buoy (v_{WEC}) and the flow rate of the motor (q_{motor}) as inputs, and provides the corresponding PTO force output (f_{PTO}). The main key factors in achieving a suitable control solution rely on a proper sizing of the accumulator capacity (C) and a proper tuning of the PI controller, which should have a bandwidth in concordance with the capacitor size. The reference of the hydraulic motor pressure is calculated according to the expression from (4.28).

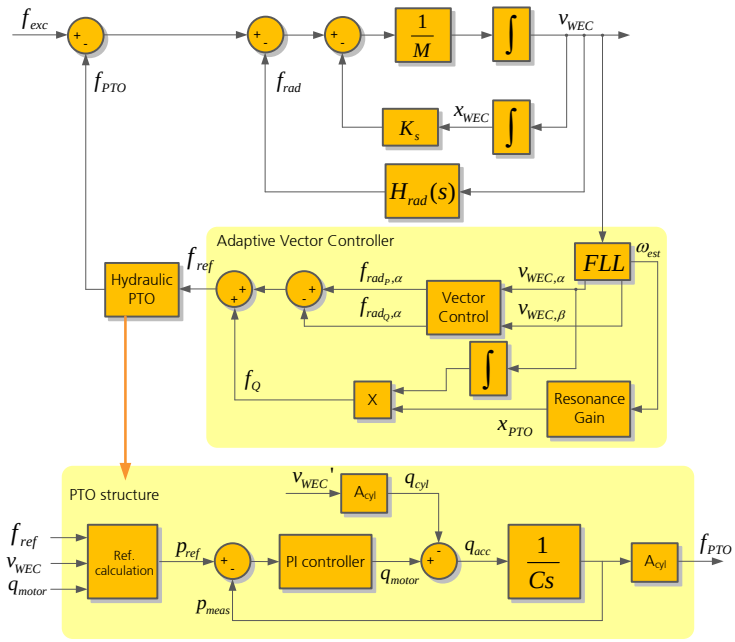

Fig. 4.12 Overall WEC control strategy emphasizing the control system implemented in the PTO

$$p_{ref} = \frac{\left({}^{1}/_{T}\right)\int_{0}^{T} f_{ref} v_{WEC}}{q_{motor}} \tag{4.28}$$

Therefore, the entire wave energy converter model and control can be implemented in simulation along with the model of the hydraulic PTO. The required pressure and flow rate over the motor will be obtained as an output of this simulation, which later it will be transformed to mechanical torque and rotational speed respectively by considering the inherent characteristics of a hydraulic motor of the power range.

The PI controller of the PTO system is tuned according to the pole placement technique, where the zero of the controller appears as the design parameter, as the poles of both the controller and the plant are placed at a fixed position. Regarding the controller performance, it is desired to achieve a very slow control behavior, as in this manner the PI controller will only react to the average reference variation, hence achieving the desired power variation damping from the accumulator. It is worth noting that by adjusting the hydraulic accumulator capacity it is possible to regulate the output peak to average ratio to a desired value. The capacity of the accumulator and the resulting controller tuning parameters are introduced in (4.29) and (4.30),

$$G_{plant} = \frac{1}{Cs} = \frac{1}{0.05 \cdot 10^{-6} s} \overset{tustin}{\Longrightarrow} G_{plant}(z) = \frac{3 \cdot 10^{5} z + 3 \cdot 10^{5}}{z - 1} \tag{4.29}$$

$$C_{PI} = \frac{K_p z + \left(K_i - K_p\right)}{z - 1} = \frac{9.3767 \cdot 10^{-11} z - 9.367 \cdot 10^{-11}}{z - 1} \Rightarrow$$
$$K_p = 2.813 \cdot 10^{-12}, K_i = 0.03 \tag{4.30}$$

The pressure and flow rates of the entire hydraulic system appear represented in Fig. 4.13(a) and Fig. 4.13(b) respectively, with the purpose of testing the system controllability, as well as its capability for reducing the characteristic output power variations. From Fig. 4.13(b) it can be clearly observed how most of the oscillations introduced from the periodic vertical displacement of the cylinder are mitigated by the hydraulic accumulator, obtaining thus a considerable reduction in the peak to average ratio in the hydraulic motor.

Several simulations have been performed in order to analyze the system behavior under a variety of accumulator capacity ranges. As it can be observed in Table 4.1, the selection of the hydraulic accumulator size have a direct impact on the peak to average ratio, as larger accumulator sizes result in lower peak to average ratios and vice versa. Therefore, a suitable sizing of the accumulator capacity can be performed with the goal of achieving a desired output peak to average ratio. Finally, a re-tuning of the PI control parameters should be

considered to presicely adjust the controller dynamics to be in concordance with the selected accumulator size.

$C = 0.05 \cdot 10^{-6}$	$C = 0.03 \cdot 10^{-6}$
$P_{AVG} = 250.77kW$	$P_{AVG} = 263.81kW$
$P_{2AVG} = 1.25$	$P_{2AVG} = 1.72$

Table 4.1 Hydraulic motor average power absorption and peak to average ratios comparison when varying the capacity of the hydraulic accumulator

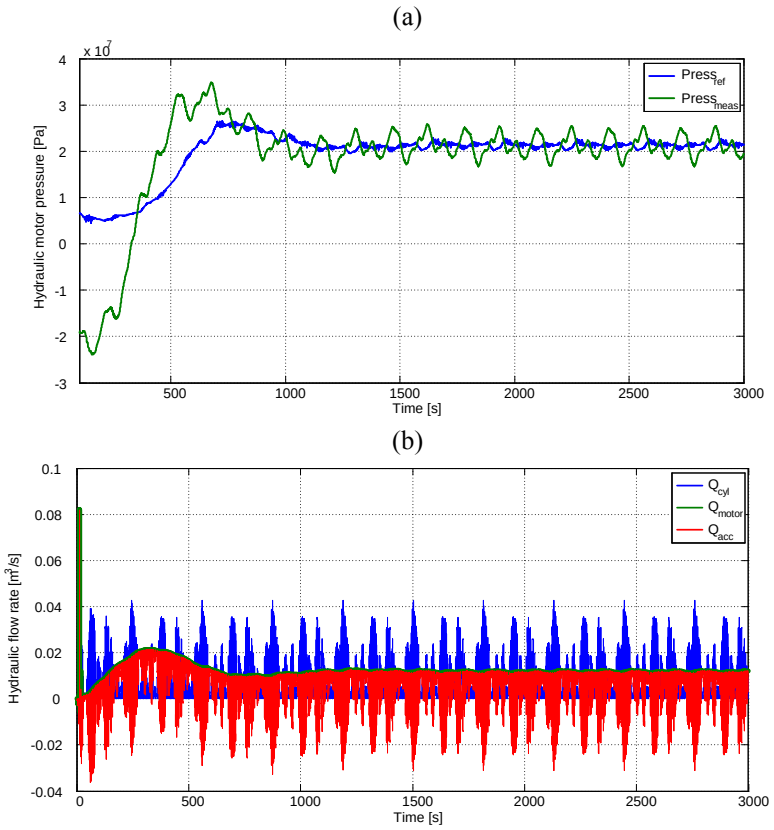

Fig. 4.13 (a) Hydraulic motor pressure, (b) Overall flow rates of the entire hydraulic PTO

4.5 Modelling and control of PMSG and Grid Connected Power Electronic Converters

The implemented PMSG and grid connected control structures can be observed in Fig. 4.14(a) and Fig. 4.14(b) respectively. For the PSMG, the synchronous reference frame field

oriented control (FOC) has been implemented, as it constitutes one of the most well proven and robust modelling and control approach for achieving variable speed operation of generators [125, 126, 127]. In the case of the front-end grid connected converter, a stationary reference frame vector control has been considered for the currents injection to the grid [128, 129].

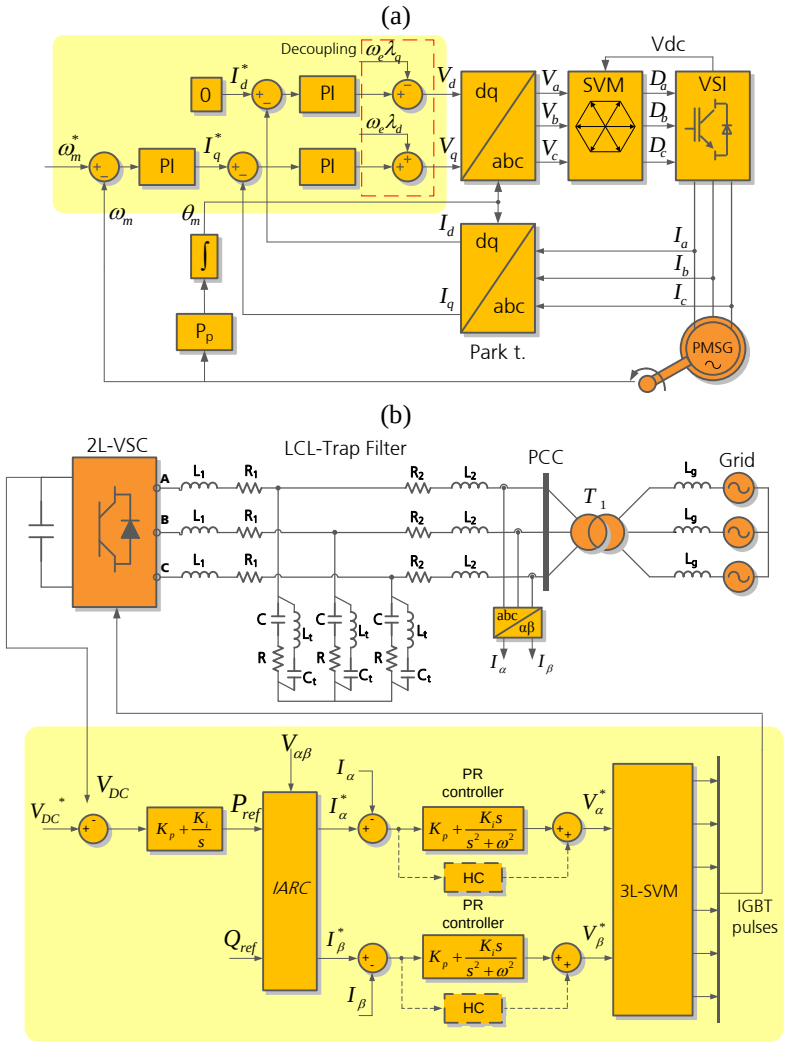

Fig. 4.14 (a) Block diagram of the field oriented vector control applied in the PMSG; (b) Overall grid connected converter control system

The current and speed controllers of the PMSG control system have been described in detail in [130], and the same tuning procedure apply for the considered controllers. The current control loop has been tuned according to the optimum modulus criterium [131],

which is based on cancellation of the pole of the plant with the zero of the controller. For the speed loop, the design criterion was to set a stabilization time around 10 times slower than the inner current loop with a damping factor of 0.7, so both controllers are dynamically decoupled. The tuning parameters of both controllers are given in (4.31)

$$\begin{aligned} K_{p_{current}} = 0.0398; K_{i_{current}} = 7 \cdot 10^{-5} \\ K_{P\_speed} = 5.375, K_{I\_speed} = 0.001 \end{aligned} \tag{4.31}$$

Regarding the grid connected converter model and control, a novel grid filter topology has been implemented, as in [132, 133], resulting in a reduced overall filter cost and size when compared with the conventional LCL filter. The current and DC voltage control of the grid connected front-end inverter has been described in detail in [134], and the same tuning procedure apply for the considered controllers. The current controller has been tuned according to the pole-placement method with the goal of achieving a damping factor of 0.7 and settling time within 20ms as design specifications. The outer DC link controller has been also tuned according to the pole placement method, ensuring a stabilization time and damping factor or $t_s = 0.2$ and $\xi = 0.7$ respetively. The tuning parameters of both controllers are given in (4.32).

$$\begin{aligned} K_{p_{current}} = 0.353184, K_{i_{current}} = 0.345335 \\ K_{P\_DC\_voltage} = 460, K_{I\_DC\_voltage} = 105799.9 \end{aligned} \tag{4.32}$$

4.6 Laboratory implementation of the proposed adaptive vector controller

The proposed adaptive vector controller has been implemented both in the laboratory and in simulations in order to validate its power extraction capabilities. Due to the lack of available resources, the individual performance of a single WEC has been validated in the laboratory, while the overall wave-to-wire model proposed has been implemented only in simulation. The laboratory setup and experiments undergone are embraced under the framework of the public funded project OFFSHORE2GRID from AICIA.

Proposed case study

The proposed adaptive vector controller presented in Fig. 4.7 has been implemented in a 100kW laboratory setup, which reproduces the dynamic behavior of the wave energy converter concept introduced in Fig. 4.1, but only focusing on a single buoy system, as the one introduced in Fig. 4.15(a).

The laboratory setup, which is introduced in Fig. 4.15(b) and Fig. 4.15(c), is built around a 100kW synchronous test bench (DC motor coupled to a PMSG) interfaced by a 100kW back-to-back voltage source converter and connected to a 250kW grid (synchronous test bench acting as a grid emulator). Then the initially sized 250kW wave energy device has been scaled-down to fit the available laboratory equipment rated parameters.

Due to the logistic limitations found in constructing a real WEC prototype, the hydrodynamic and hydraulic system of the WEC have been virtually modelled and implemented in a dSPACE ds1103 real-time system along with the proposed adaptive vector controller. Therefore a virtually modelled hydrodynamic and hydraulic system interacts with the laboratory synchronous test bench in order to evaluate the entire WEC performance.

Regarding the emulated WEC performance in the dSPACE controller, the wave energy resource characteristics are introduced as the input parameters to the WEC hydrodynamics model. Then, the proposed controller monitors the buoy velocity from such hydrodynamic model, and determines the force to be provided by the PTO in order to achieve maximum power extraction. Finally, this force is provided to the hydraulic model, from which the final torque and speed references are generated and provided to the synchronous test bench.

In the synchronous test bench there is a DC machine acting as a motor, providing the required load torque to the generator shaft; and a PMSG acting as a generator, ensuring that the desired mechanical speed is achieved. Both torque and speed controllers are implemented in the motor and PMSG drivers respectively. Therefore, by measuring the shaft speed, the dSPACE controller is able to determine the torque and speed references that should be respectively provided to the motor driver and PMSG controller for achieving maximum power extraction from the waves. The laboratory setup is introduced in Fig. 4.15(c).

(a)

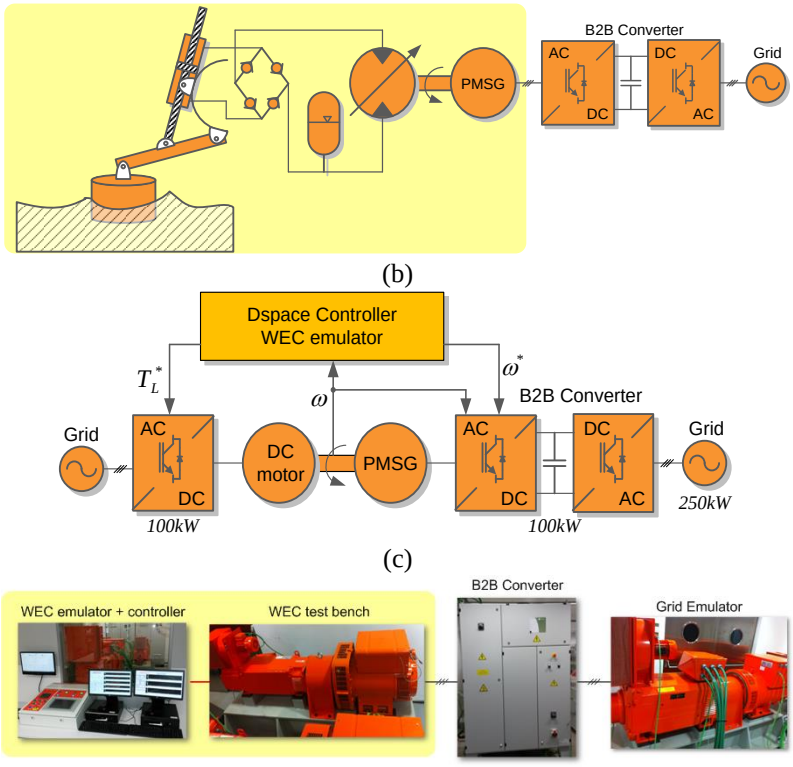

Fig. 4.15 (a) Overall wave energy converter concept considered for the laboratory setup; (b) Experimental setup schematic implemented in the laboratory; (c) Experimental setup

Regarding the control system implemented (Fig. 4.7), it is worth noting that the sampling period of the virtual WEC model is set to 0.5s, which is set slow enough in order to avoid any interference with the inner torque and speed controllers of the DC motor and PMSG drivers respectively. Therefore, the speed and torque references will be updated each 0.5s.

The detailed dSPACE and test bench parameters can be summarized in Table 4.2 in order to set the physical limitations of the laboratory prototype.

The results presenting the adaptive maximum power extraction capabilities of the wave energy converter are provided in this section and correspond to the implementation of the average power theory control from (4.22) and (4.23). In addition, the simulated and experimental tests have been performed considering a wave energy resource with a peak period (T_{wave}) of 7.7s and significant wave height (H_{wave}) of 1.47m.

dSPACE controller	Laboratory setup
$Ts = 0.5s$	$V_{PMSM} = 400V$
$T_1 = 7.7s$	$\omega_{PMSG} = 1500rpm$

$H_{1/3} = 1.47m$	$T_{PMSG} = 553rpm$
$K_{SOGI} = \sqrt{2}$	$V_{DC\_B2B} = 800V$
$\gamma = 0.16$	$V_{AC\_grid} = 400V$

Table 4.2 dSPACE controller and laboratory setup rated parameters

Simulation and experimental results

In this section, the main hydrodynamic and mechanical results are compared in both simulation and laboratory implementations with the purpose of obtaining a meaningful evaluation of the proposed adaptive vector controller when operating at maximum energy absorption conditions.

Regarding the hydrodynamic performance of the WEC under the proposed adaptive vector controller operation, Fig. 4.16(a) and Fig. 4.16(b) present the simulation and experimental comparison between the excitation, radiation and PTO average powers. Where such powers have been obtained from the product between the WEC velocity (v_{WEC}) and the excitation force (f_{exc}), radiation force (f_{rad}) and PTO force (f_{PTO}) respectively. In addition, it is worth noting that the average powers from Fig. 4.16 result from a moving average window of 300 seconds applied to the instantaneous powers.

From Fig. 4.16(a) and Fig. 4.16(b) it can be clearly observed that the proposed adaptive vector controller achieves maximum average power absorption from the resource, as the absorbed average power from the PTO (P_{abs}) equals the average radiation power (P_{rad}), being at the same time half of the average resource power (P_{exc}). This system behaviour was introduced in [120] where the optimum operation conditions were described. According to these, the maximum average power absorption of the resource is limited to its radiation losses.

In addition, Fig. 4.16(c) and Fig. 4.16(d) verify that the proposed controller mainly operates at resonant conditions, as the buoy velocity should appear in phase with the excitation force. In this way, the intrinsic WEC reactive terms such as the added mass, damping, and imaginary radiation components do not add any phase shift, since they are instantaneously cancelled by the PTO virtual buoyancy term, for any of the incoming wave frequency components.

(a) (b)

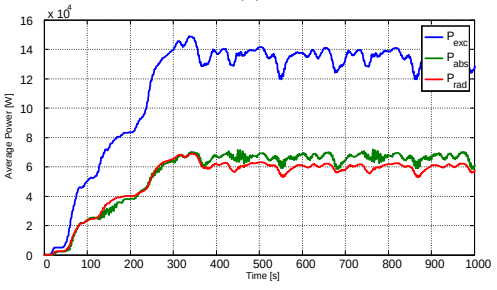

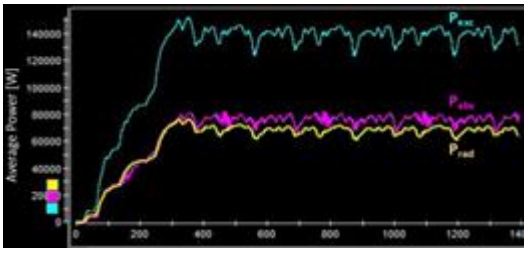

(c) (d)

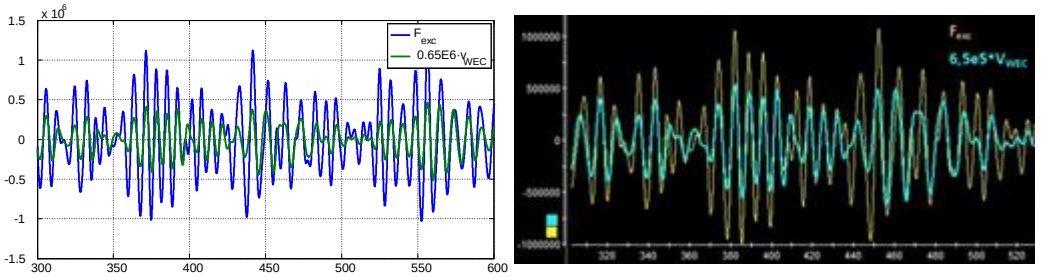

Fig. 4.16 (a) Comparison of average absorption, excitation and radiation powers when the average power based vector controller is applied in simulation; (b) Comparison of average absorption, excitation and radiation powers when the average power based vector controller is applied in laboratory;(c) Comparison of WEC velocity and excitation force in simulation; (d) Comparison of WEC velocity and excitation force in laboratory

Therefore, the observed performance satisfies both of the above mentioned controller conditions, needed for obtaining maximum energy absorption. This is achieved, thanks to the PTO capability of providing a real component force equal to the radiation damping force, while ensuring real-time resonance operating conditions.

As it can be observed from Fig. 4.16, the experimental results obtained are quite similar to the simulation ones, thus a suitable validation of the proposed adaptive vector controller has been achieved, for maximum power extraction under irregular sea states. Due to this matching accuracy, the wave energy converter simulation models developed will be used in a later stage in order to validate the suitable operation of the overall 4-WEC system introduced in Fig. 4.1.

Finally, the mechanical wave energy converter performance has been analyzed, in order to determine if the system complies with the predefined setup specifications. From Fig. 4.17(a) and Fig. 4.17(b), it can be observed that both the PMSG speed and DC motor torque are precisely controlled in real-time, as the measured variables strictly follow the references provided by the proposed adaptive vector controller. Thus the implemented wave energy controller shows a suitable integration with the synchronous test bench setup and its inherent low level motor controllers, as a stable and safe operation has been proved.

From Fig. 4.17, it is also worth noting that some limitations have been added to the speed and torque references with the purpose of keeping the experimental setup under safe operating conditions. Such limits are set for the speed and torque values exceeding 20% of the test-bench rated parameters. In addition, a power saturation has been implemented to ensure that the real-time mechanical power do not overpass the maximum converter rated power (100kW). Then a varying torque reference saturation has been implemented, with a value depending on the instantaneous shaft speed and the maximum converter power.

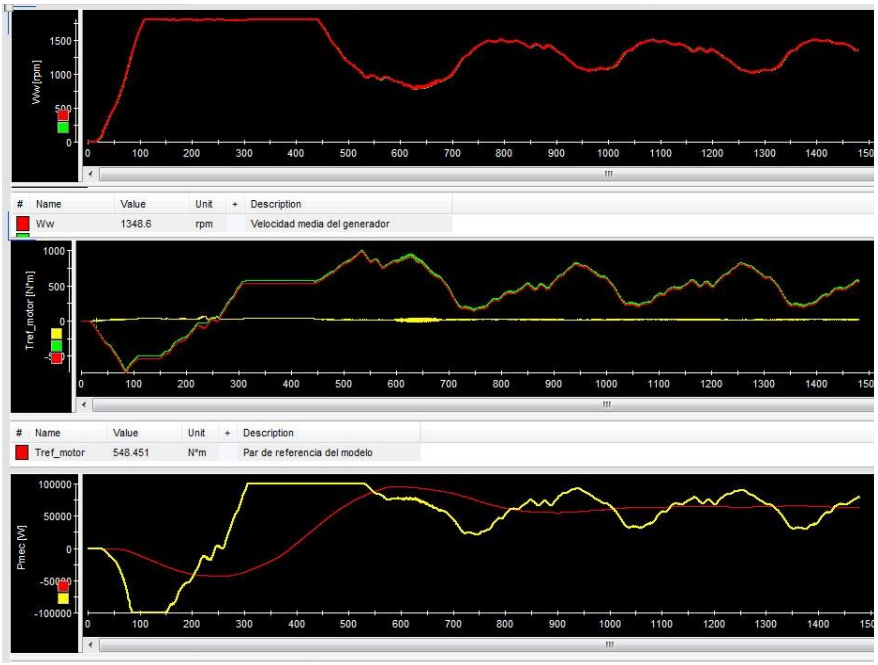

Fig. 4.17 (a)PMSG generator speed reference (green) and measurement (red), (b)DC motor torque reference (red) and measurement (green), (c) Instantaneous (yellow) and average (red) mechanical power

Finally, the instantaneous and average mechanical power applied to the shaft of the synchronous test bench is presented in Fig. 4.17(c). From this figure, it can be observed that the average power is very similar to the one resulting from the hydrodynamic results from Fig. 4.16(a). Finally, it can also be observed that the instantaneous power is below 100kW, which was set as the rated power that the back-to-back power converter can process and supply to the grid.

Results Analysis of proposed Wave Energy Converter Controller

In order to have a meaningful evaluation of the real benefits introduced by the proposed wave energy control strategy, the performance of the instantaneous (4.19)-(4.20) and average (4.22)-(4.23) power theory controllers are compared with the conventional complex conjugate and passive loading control solutions [108, 109]. From Fig. 4.18(a) it can be observed that the proposed instantaneous and average power controllers considerably increase the output power extraction capabilities of the WEC under a set of different wave energy conditions. This average output power increase comes due to the capability of the proposed controller to adaptively resonate with the dominant frequency components of the incoming wave energy resource.

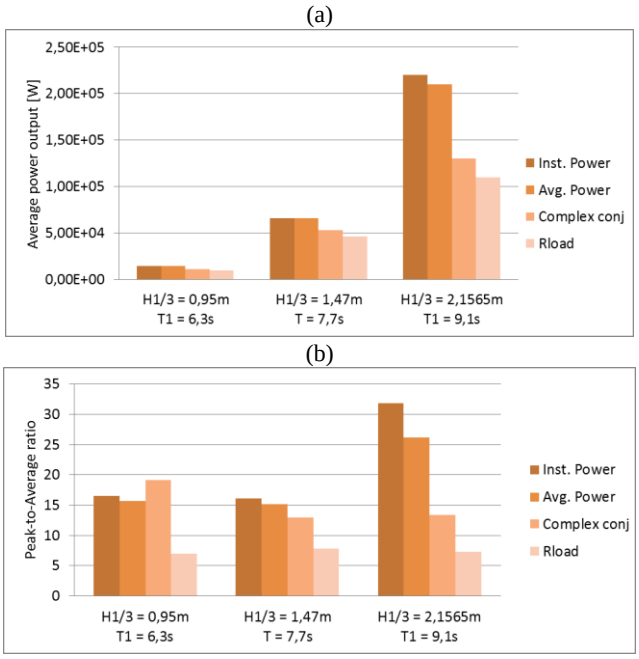

Fig. 4.18 (a) Average power control strategies comparison when considering different sea state conditions; (b) Peak to average control strategies comparison when considering different sea state conditions

Opposing to the reactive control methods, where resonance mainly occur at the dominant sea state level, the proposed adaptive vector controller is able to ensure instantaneous resonance conditions, leading to maximum energy extraction at the wave-to-wave level. In addition, it can be observed that enhanced power extraction capabilities can be achieved for the proposed controllers in the cases where the wave energy resource deviates more from the WEC design sea state conditions (most probable wave period T_{wave} = 7.7s), as the proposed wave energy controller ensures resonance conditions regardless of the dominant wave frequency components.

In addition to the average power extracted from the waves, the maximum instantaneous power or peak to average ratio is of crucial interest, since the possible overrating of mechanical and electrical equipment will depend directly on the maximum power that it should be handled. Regarding the peak to average ratios achieved from the controller strategies analysed here, it can be clearly observed from Fig. 4.18(b) that the average power based strategy provides reduced peak to average rates in comparison with the instantaneous power theory. This reduction in the peak to average ratio is achieved thanks to the capability of maximizing the average power extraction instead of the instantaneous one. Therefore, it can be concluded that the proposed vector controller structure based on the average power extraction appears as the most suitable control strategy among the options analysed, as it

ensures maximum average power extraction levels while contributing in the reduction of its peak to average ratio.

Overall WEC simulation performance extrapolation from the experimental results

The entire wave-to-wire energy conversion system proposed in Fig. 4.1 has been implemented in Matlab Simulink in order to observe the real time performance of the proposed adaptive vector controller, as well as its grid integration. As earlier described, the wave energy converter under test is built-up around 4 wave energy devices, each of them cupled to a 250kW PMSG. The electrical power is processed by a common DC link interconnection, which collects the aggregated instantaneous power from each PMSG and feeds it to a single 1MW front end VSI.

The entire wave-to-wire energy conversion simulation has been developed by replicating the single-device simulation model, validated in the previous section, for each of the 4 wave energy devices. However, different phase angles have been considered in the wave resource modeling, as due to the resource characteristics none of the wave energy devices will be pulsating at the same time.

From the grid interconnection results introduced in Fig. 4.19(a) and Fig. 4.19(b), it can be observed how the DC power aggregation produces the desired smoothing affect over the final output power supplied to the grid. Thanks to the DC interconnection of several WECs, a considerable reduction of the final AC peak to average ratio can be achieved, as shown in Fig. 4.19(b), which arises due to the non-simulaneity of the real-time individual PMSG power generation profiles.

Therefore, the proposed energy conversion chain provides a considerable instantaneous power oscillation reduction due to the inherent storage capability of the PTO and to the electrical interconnection system, which benefits from the aggregation effect of multiple buoys. The proposed electrical interconnection system appears as a suitable solution as well, in case electrical energy storage system would be required, as it could be directly interconnected in the DC link, where the contribution from each of the wave energy converters sum up to reach the final output power.

(a)

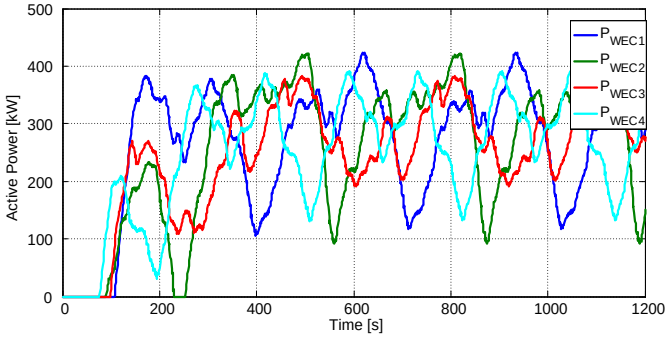

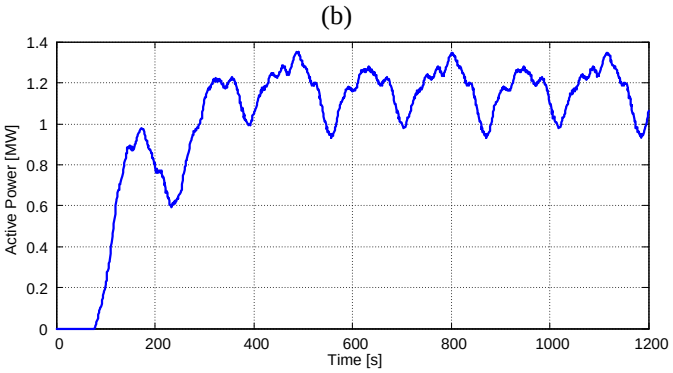

Fig. 4.19 (a) Instantaneous power supply from each of the individual wave energy converters, (b) Instantaneous power supply of the overall wave energy converter system configuration

As a concluding remark, it is worth mentioning that the power generation profiles of the proposed wave energy conversion system (Fig. 4.1), have been suitably validated experimentally and in simulation, for maximum power extraction from the available resource. This is of crucial interest, as the competitive power controller implementation in the selected wave power plant scenario, will make use of such generation profiles to characterize the maximum power operating behavior of WECs.

Chapter 5.

5 Competitive Control of PowerPlants: The Wave Power Plant Scenario

Once the wave energy resource characterization and control have been validated, the present chapter focuses on the real-time implementation of the competitive power controller, along with the detailed operation and maintenance cost models for the selected wave power plant scenario. Furthermore, the power plant performance and final incurred costs will be analyzed through the entire operational lifetime of the plant.

In order to have a meaningful evaluation of the long-term benefits provided by the competitive control strategy, the competitive simulation will be finally compared with the conventional (1/n) power sharing strategy, in which the plant power setpoint is equally shared over the n available resources.

5.1 Introduction

While conventional plants are constituted by a few large controllable synchronous generation units, RES based power plants are usually formed by large amounts of small scale power electronic converters, being poorly controlled and dispersed over a wide geographical location. Up to date, such renewable power plants have been controlled under the “feed-and-forget” philosophy due to the small perturbation impact they had on the power system performance. However, this assumption cannot be considered any more, as with the changing paradigm of future distribution systems, large penetration of RES-based distributed power plants and energy storage systems will raise new efficiency, reliability and security challenges in the manner in which the distribution system has been

operated and controlled up to date. For this reason, there is a clear need in designing highly controllable and manageable distributed power plants, which could provide similar power control and grid service capabilities as conventional power plants. In this regard, distributed power plants could achieve increased benefits from the participation in both energy and ancillary service markets, while considerably improving power system performance due to their characteristic fast power supply dynamics.

In order to achieve such advanced RES-based power plant control functionalities, this chapter presents the detailed implementation and evaluation of the competitive power controller in a wave power plant application. The selection of this particular renewable based power plant is motivated due to the tremendous potential of wave energy, but also for the challenge it constitute to the competitive controller itself, to achieve the desired real-time control capabilities in such a power oscillating generation scenario. Then, the competitive controller is intended to control the real-time production of the wave power plant in order to meet the flat and stable power generation schedules agreed in day-ahead or intra-day markets.

In addition, the real-time power dispatch of the plant plays a critical role for maximizing the economic revenues over its operational lifetime. In this regard, the competitive controller provides the following real-time operation benefits by solely implementing an advanced economic dispatch strategy of generation units:

- Minimization of the internal power plant distribution losses.
- Efficient utilization of available resources of the plant, making use of the generation units with lower marginal costs.
- Minimization of the overall costs derived from the operation and maintenance of the plant

As already mentioned in previous chapters, the competitive power controller implemented in this case is valid for any type of distributed generation systems, such as wind, PV and wave power plants, but also for hybrid power plants or microgrids, where different renewable and conventional generation technologies coexist. The main implementation adjustments among the different application scenarios, relate to the real-time power profile characterization of each generation technology, and to the corresponding plant specific configuration and marginal resource costs.

Finally, due to the still nascent development stage of wave power plants, many of the detailed costs considered in the competitive control implementation have been modeled using the offshore wind energy sector as a reference, as no clear evidences have been found on historical operational data of such power plants. However, the competitive control implemented and the considered costs could be easily replicated to other types of RES based power plants, such as wind or PV applications, whose historical data on incurred costs over the operational lifetime could be more easily found.

5.2 Competitive power control implementation in wave power plants

As a first step prior to the implementation of the competitive controller, it is necessary to develop the design of the power plant configuration and electrical layout, since it may have particular consequences in the competitive control structure implemented hereinafter. In this regard, a wave power plant layout analysis has been performed in Appendix A, where several typical distributed power plant configurations have been compared. As a result, the system under consideration is based on a 10MW star-connected WPP divided in two clusters of 5 WECs each, where each WEC is rated to 1MW output power.

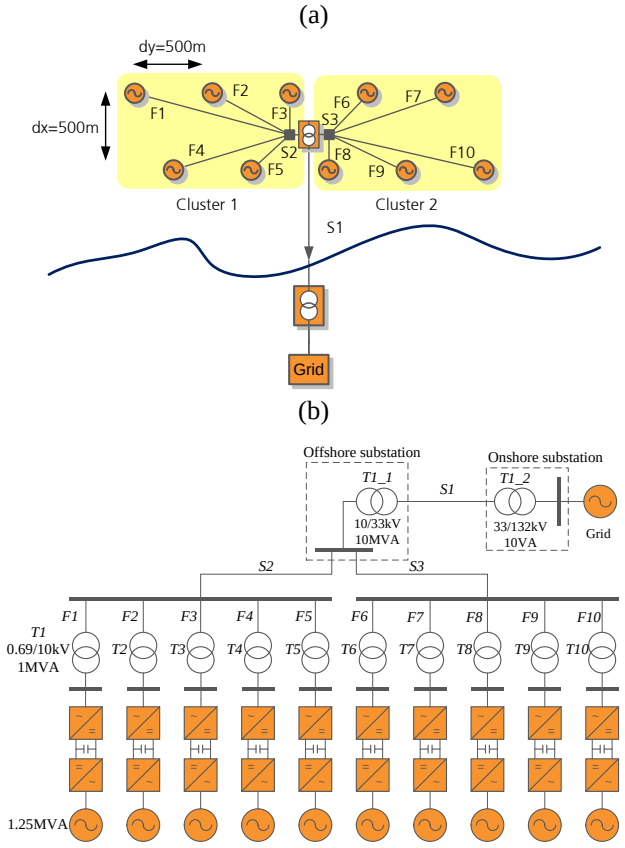

Fig. 5.1 (a) Star-based wave power plant layout, (b) Electrical scheme of the WPP layout divided in two clusters with star structure

The proposed plant layout is introduced in Fig. 5.1 and it was selected since it provides reduced power losses and higher redundancy than conventional radial feeder or string

configuration [135]. Finally, it is worth mentioning that the selected power plant layout is just a particular realization for this specific application, but the competitive controller can be adapted to fit in any plant configuration.

Bearing in mind the principal goal of the competitive power controller, but now being applied to the wave power plant study case, it is possible to ensure real-time control of the plant generation at minimum operation costs through optimal allocation of available resources. Such advanced plant control capabilities can be achieved by transmitting a virtual price signal over the entire hierarchical structure, up to the final-end generation units, which are in charge of deciding its generation involvement based on the price signal received and its own marginal costs.

The hierarchical control structure that has been considered in this case is presented in Fig. 5.2, and has been particularly adapted taking into account the selected wave power plant layout. In this regard, the competitive power sharing is distributed over 4 main hierarchical levels (plant, cluster, station and resource), which refer to the main electrical aggrupations found in the wave power plant configuration.

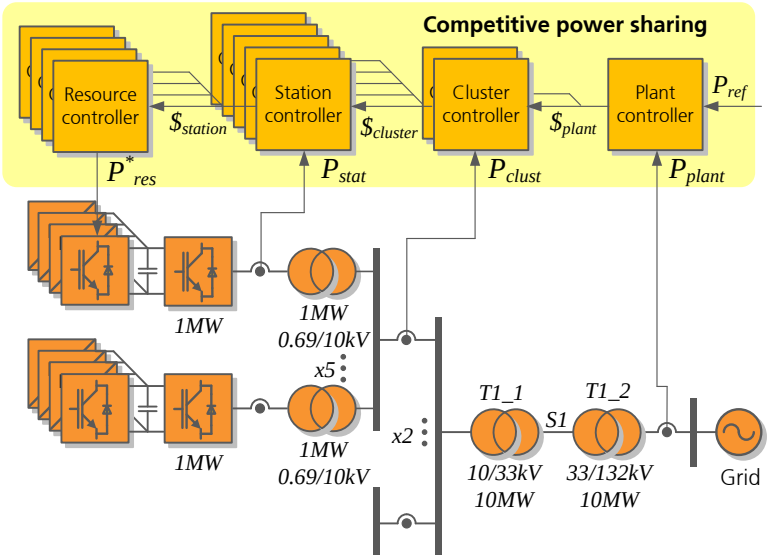

Fig. 5.2 Proposed competitive power sharing control structure

From this figure, it can be observed that the plant controller arises as the front-end controller, in charge of ensuring a real-time control of the power being supplied by the plant. For this purpose, the plant controller generates a real-time virtual price control signal, which results from the control error between the power reference (P_{ref}) and the actual power measurement (P_{plant}) of the plant. Such virtual price signal, which is expressed in price per unit of energy (e.g. in $/MWh), represents the price that the plant controller would be willing

to pay to the cluster controllers, one level below, to satisfy the required production setpoint at the plant interconnection point.

Then, this plant price signal ($\$_{plant}$) is propagated as a common control signal to the next level controllers (cluster controllers), where it is modified considering the production costs related to each individual cluster. Now, the cluster prices ($\$_{clust}$) are representative of the price that each cluster would be willing to pay to each station controller connected to it for satisfying the generation objective at the cluster interconnection point.

Similarly, the cluster price signal ($\$_{clust}$) is provided as a common control signal to the corresponding next level controllers (station controllers), connected to that cluster, where this price signal is modified according to the operation costs of each individual station. Therefore, the generated station price signals ($\$_{stat}$) are representative of the price that each converter controller would be willing to pay to the resource controllers connected to it in order to ensure the desired production objective at the station point of connection.

Finally, each station price signal ($\$_{stat}$) is provided as a common control signal to the corresponding resource controllers connected to that station. In this case, the final price received is compared with its own resource generation costs, giving rise to a power production increase in case the price signal is higher than the costs, and vice versa.

Therefore, the power production references are generated at the resource level according to (5.1) and (5.2), where the price signal originally generated by the plant controller is modified, considering all the intermediate system costs involved in the energy distribution path, to determine the generation increment/decrement rate of the final-end generation resources.

$$P_{res,l.m.n} = \int \left(\$_{plant} - C_{plant} - C_{clust,i} - C_{stat,i.j} - C_{res,i.j.k}\right)\, dt \tag{5.1}$$

$$P^{*}_{res,l.m.n} = \begin{cases} P_{max} & if\ P_{res,l.m.n} > P_{max} \\ P_{res,l.m.n} & if\ 0 > P_{res,l.m.n} > P_{max} \\ 0 & if\ P_{res,l.m.n} < 0 \end{cases} \tag{5.2}$$

where C_{plant} represent the plant-level related costs, $C_{clust,i}$ the cluster i related costs, $C_{stat,j}$ the station j costs, and $C_{res,k}$ the resource k related costs, involved with the energy distribution path of a given generating power resource.

In this manner, the cheaper the costs associated to a given resource, the higher will be its contribution towards the fulfillment of the plan production objective.

As the proposed competitive control strategy is based on receiving a common price control signal among all the controllers of the same hierarchical level, there is a direct competition between them in order to achieve the desired production objective at the minimum cost. Therefore, for a given price signal, the generation units with lower overall marginal costs will start producing earlier than the ones with higher costs, being the latter

progressively introduced as the price signal increases. Similarly, the generation units with the higher costs will be the first ones in stopping when the price signal decreases, remaining operational only those generation units that ensure minimum operation costs. As a result, it can be stated that the proposed competitive controller optimally allocates the generation resources needed to achieve the desired production objective at minimum operation costs. In this regard, it is worth noting that even the price signal considered is a virtual price signal, it can be representative of the real-time marginal costs incurred by the plant for achieving a desired production objective.

In addition, each of the controllers introduced in Fig. 5.2 generate their corresponding price control signal, considering only the price signal received from its immediately higher control level, and the local measurements about its own distribution system performance. This means that the controller does not need to know any detailed information about its associated lower level controllers, considerably reducing, in this manner, the information volume to be exchanged among levels and the computing requirements needed.

Finally, each of the competitive controllers considered in this chapter are referred as logical/control entities, and do not reflect the need of being particularly implemented in different hardware RTUs or PLCs embodiments. In fact, due to the low computing requirements of the competitive controllers, it is possible to aggregate many of them within the same hardware control unit.

In order to have a final picture of the competitive control system implemented, the following subsections provide deep details on the control structures and costs considered in each of the plant, cluster, station and resource controllers introduced in Fig. 5.2. In this regard, it needs to be mentioned that the following costs are the ones established for this particular wave power plant application, but can be further expanded or modified to suitably fit in more generic distributed power system applications.

Plant controller structure

The detailed plant controller of the competitive power control structure is presented in Fig. 5.3. From this figure, it can be observed that a PI controller has been considered in order to generate the root price control signal, as it ensures zero steady state error between the reference and measured power production at the plant PCC.

In the event of any production mismatch between the power plant reference and measurement, the proposed controller will provide a price signal reaction in the desired direction, to motivate a change in the final-end resource generation. Hence, the final plant production can be readjusted towards the desired reference. More specifically, under a power production deficit (e.g. $\Delta P > 0$), the plant controller increases the virtual price signal provided, encouraging more expensive generation units to participate in the overall power supply. Conversely, in the case of a power surplus (e.g. $\Delta P < 0$), the plant controller decreases the virtual price signal provided, resulting on a power reduction of more costly resource generation units.

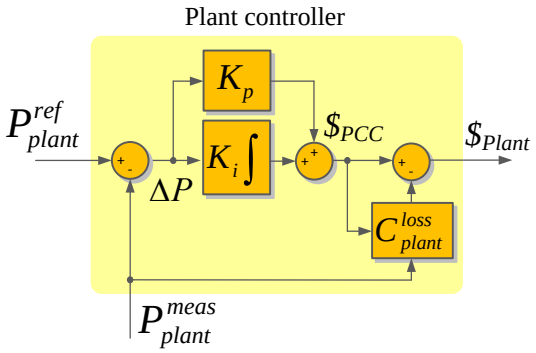

Fig. 5.3 Detailed plant controller of the competitive power control structure

As early mentioned, the PI controller generates the virtual price signal that the plant controller would be willing to pay for the power production at the plant PCC. However, this price signal needs to be accordingly modified, prior being transmitted to the cluster controllers. According to Fig. 5.3, this can be done by introducing the plant specific costs (C_{plant}^{loss}), which are substracted to the PCC price signal ($\$_{PCC}$), in order to obtain the final price signal ($\$_{Plant}$) to be provided to the cluster controllers.

The plant costs that have been considered in this particular case, account for the distribution losses of the common plant related equipment, such as the onshore substation transformer (T_{1_2}), the submarine transmission cable (S_1), and the offshore substation transformer (T_{1_1}), depicted in Fig. 5.1(b). The objective of considering these costs within the plant controller is to transfer them equitably to the lower level controllers (up to the resource controllers), so that the back-end resource controllers will overcome these losses by increasing their power references. Of course, this production increment is not cost-free, as higher price signals will have to be generated at the plant level to cover these costs.

The costs of the plant distribution equipment losses are determined, from (5.3) to (5.6), by multiplying the price signal being paid at the PCC by the per unit equipment losses.

$$C_{plant}^{loss} = \left(P_{T1\_2}^{loss}(P_{PCC}^{meas}) + P_{S1}^{loss}(P_{PCC}^{meas}) + P_{T1\_1}^{loss}(P_{PCC}^{meas})\right) \cdot \$_{PCC} \tag{5.3}$$

$$P_{T1\_2}^{loss}(P_{PCC}^{meas}) = 1 - \eta_{T1\_2}(P_{PCC}^{meas}) \tag{5.4}$$

$$P_{S1}^{loss}(P_{PCC}^{meas}) = 1 - \eta_{S1}(P_{PCC}^{meas}) \tag{5.5}$$

$$P_{T1\_1}^{loss}(P_{PCC}^{meas}) = 1 - \eta_{T1\_1}(P_{PCC}^{meas}) \tag{5.6}$$

A per-unit efficiency function has been assigned to each distribution equipment unit of the plant $\eta_{T1\_2}(P_{PCC}^{meas})$, $\eta_{S1}(P_{PCC}^{meas})$, and $\eta_{T1\_1}(P_{PCC}^{meas})$. Where these efficiencies are

introduced in Fig. 5.4, and have been characterized from several load flow claculations performed in DigSILENT.

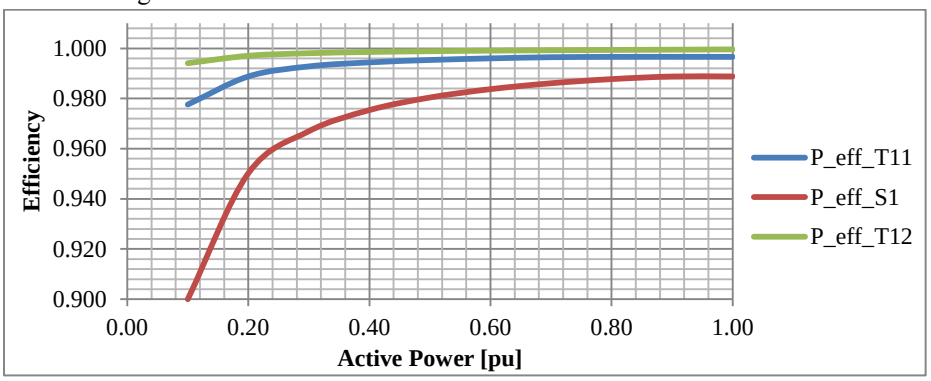

Fig. 5.4 Efficiency curves of the of the plant distribution equipment

Cluster controller structure

From the cluster controllers implemented in the competitive power control structure (Fig. 5.5), it can be observed that the price signal received from the plant controller ($\$_{plant}$), is considered as a common control signal equaly provided to both controllers. Then, this price signal is modified in each cluster controller by considering the costs of distribution power losses (distribution cables, transformers, etc.) and O&M costs, if any, associated to each particular cluster. Therefore, the cluster with lower marginal costs will provide a higher price signal incentive to the station controllers, one level below, for increasing their power production. Where the resulting cluster price signals ($\$_{clust1}$ and $\$_{clust2}$) are representative of the price willing to be paid to the station controllers connected to each cluster, for achieving the desired generation obective at the cluster point of connection.

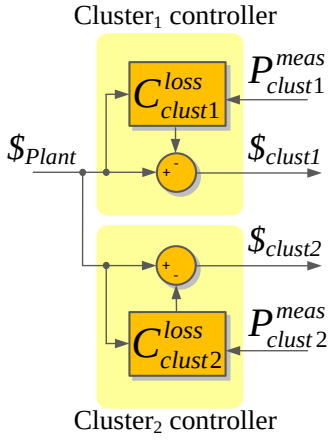

Fig. 5.5 Detailed cluster controllers of the competitive power control structure

In this regard, it is worth noting that each cluster controller is responsible of determining its own associated costs based on their actual production.

The cluster costs that have been considered in this case, account for the costs of distribution losses, associated to the cluster cables *S2* and *S3* depicted in Fig. 5.1(b). These costs have beed introduced due to the implications they maight pose on the competitive control results when using cluster collector cables of different lengths. In such case, the competitive controller would achieve a more efficient power delivery, allocating higher production levels to the cluster with lower costs (i.e. with shorter power cables). However, this is not the case of the proposed wave power plant application, as from the layout symmetry observed in Fig. 5.1(a), both cable collector cables are of the same length. Analogously, as for the plant costs, the costs of the cluster distribution losses are determined, according to (5.7) and (5.8), by multiplying the price signal being paid at the internal plant connection point ($\$_{plant}$) by the per unit equipment losses.

$$C_{clust,1}^{loss} = \left(1 - \eta_{S2}\left(P_{clust,1}^{meas}\right)\right) \cdot \$_{plant} \tag{5.7}$$

$$C_{clust,2}^{loss} = \left(1 - \eta_{S3}\left(P_{clust,2}^{meas}\right)\right) \cdot \$_{plant} \tag{5.8}$$

A per-unit efficiency function has been assigned to each of the cluster cables $\eta_{S2}\left(P_{clust,1}^{meas}\right)$ and $\eta_{S3}\left(P_{clust,2}^{meas}\right)$, where these efficiencies are introduced in Fig. 5.6, and have been characterized from several load flow studies performed in DigSILENT.

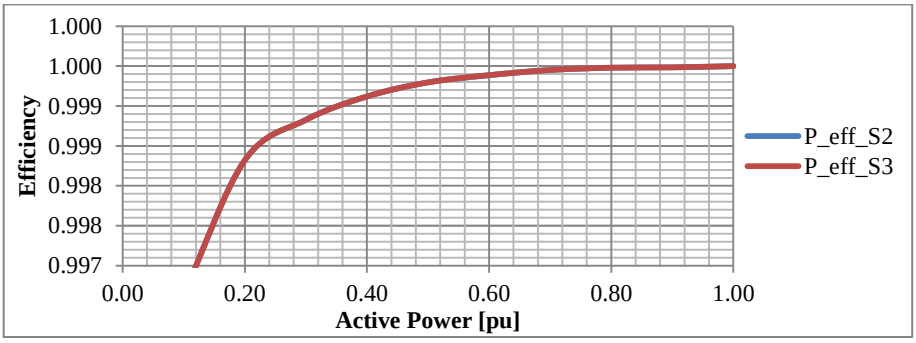

Fig. 5.6 Efficiency curves of the of the cluster distribution cables

Station controller control diagram

Similarly as in the previous layers, the detailed station controller implementation is presented in Fig. 5.7, where the cluster price signal received is provided as a common control signal to all the converter station controllers integrating a given cluster structure. In this case, the price signal received is modified in each station controller, considering the costs of distribution equipment losses, the operation and maintenance costs, and the costs due to sudden efficiency drops (from external factors), associated to the corresponding converter

power stations. All these costs are calculated and updated in real-time within the corresponding station controllers, by solely serving from their actual production measurements.

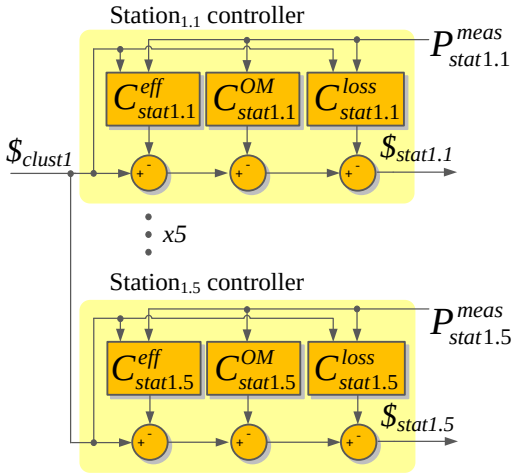

Fig. 5.7 Detailed station controllers of the competitive power control structure

Within the costs considered, the distribution costs are associated to the losses found over the station-specific equipment, such as the F_j flexible cables and the T_j step-up transformers from Fig. 5.1(b). Where *j* denotes a given converter station under consideration. Contrary to what was mentioned about the symmetry of cluster collector cables, the station converters integrated in a given cluster structure are grouped together by using different cables' length. This means that the stations with a closer placement to the collection junction box (i.e. *F3* and *F5* from Fig. 5.1(a)), are expected to have lower distribution losses costs, and thus, higher participation ratios on the final cluster power delivered. In this manner, the competitive controller would achieve a more efficient power delivery at the station level, rewarding the stations with lower distribution costs by increasing their power generation.

Regarding the station step-up transformers, equal per unit efficiency losses are being considered, since the same transformer is provided to each converter station. However, as the instantaneous power production between stations will be different, the costs of transformer losses will also be different.

The costs of the station distribution losses are determined, according to (5.9), (5.10) and (5.11), by multiplying the price signal being paid at the cluster point of connection ($\$_{clust,i}$) by the per unit equipment losses.

$$C^{loss}_{stat,i.j} = \left(P^{loss}_{F,i.j}\left(P^{meas}_{stat,i.j}\right) + P^{loss}_{T,i.j}\left(P^{meas}_{stat,i.j}\right)\right) \cdot \$_{clust,i} \tag{5.9}$$

$$P^{loss}_{F,i.j}\left(P^{meas}_{stat,i.j}\right) = 1 - \eta_{F,i.j}\left(P^{meas}_{stat,i.j}\right) \tag{5.10}$$

$$P_{T,i,j}^{loss}\left(P_{stat,i,j}^{meas}\right) = 1 - \eta_{T,i,j}\left(P_{stat,i,j}^{meas}\right) \quad (5.11)$$

Where the suffixes j and i respectively denote the converter station under consideration and its associated cluster. A per-unit efficiency function has been assigned to each of the station cables $\eta_{F,i,j}\left(P_{stat,i,j}^{meas}\right)$ and transformers $\eta_{T,i,j}\left(P_{stat,i,j}^{meas}\right)$. These efficiencies are introduced in Fig. 5.8 and Fig. 5.9 respectively, and have been characterized from several load flow studies performed in DigSILENT.

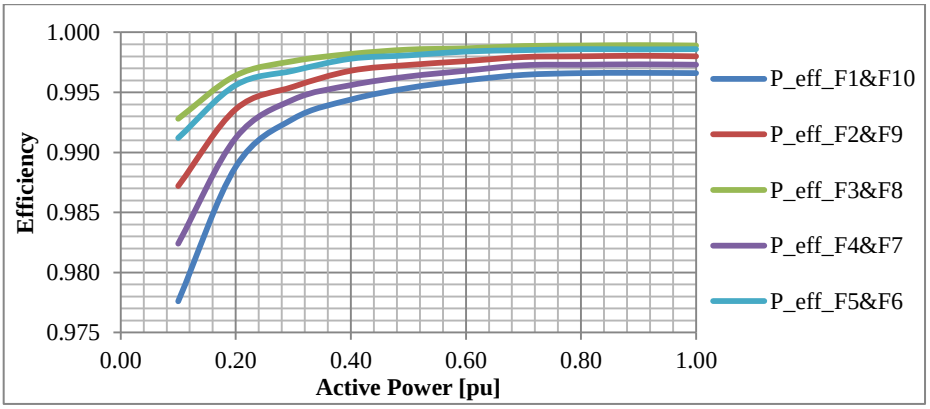

Fig. 5.8 Efficiency curves of the of the station flexible cables

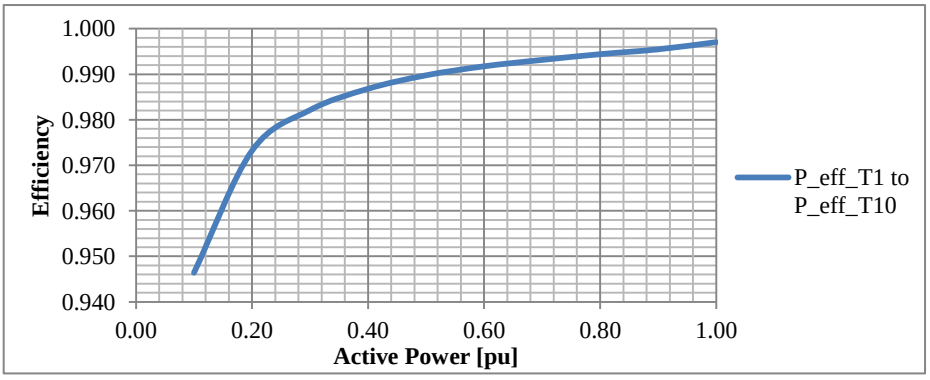

Fig. 5.9 Efficiency curves of the of the station step-up transformers

Besides of the costs of distribution losses, the station operation and maintenance (O&M) costs are also considered under the competitive control algorithm. These costs are calculated in eq. (5.12) by considering the variable O&M costs associated to a given technology from [136]($C_{stat,j}^{var}$), and the costs of corrective maintenance due to sudden unplanned equipment failure. Such unplanned corrective maintenance costs are calculated in real time by dividing the cumulative repairing costs incurred, over the instantaneous energy being delivered.

Therefore, high O&M costs correspond to distribution system equipment failing many times (with costly failure events), or failing at low usability levels.

$$C_{stat,i.j}^{O\&M}(t) = \frac{\sum_{t=0}^{t} C_{stat,i.j}^{fault}(t)}{E_{stat,i.j}(t)} + C_{stat,i.j}^{var} \tag{5.12}$$

Where $C_{stat,i.j}^{fault}(t)$ represent the unplanned equipment failure costs over time, which can be easily determined in a real wave power plant application from the historic failure events and associated costs.

The costs associated to the O&M $\left(C_{stat,i.j}^{O\&M}(t)\right)$ have been considered here, as the failure of different stations occur at different instants, and improved benefits could be achieved from the suitable operation of specific stations.

In addition to the previously introduced costs over the competitive power control structure, the efficiency costs due to external factors can also be accounted as in (5.13)-(5.15). Such sudden efficiency drop in a particular generation unit can result from many malfunctioning reasons of the power extraction mechanism. For example, a power reduction due to the accumulated dust on a PV panel, or due to a hydraulic piston malfunction in the pitch control of a wind turbine, etc.

Such efficiency related costs, named here as performance coefficient (PC), are only enabled when such malfunctioning events are detected at the resource level, from the difference between the power production reference and measurement $\left(P_{res,i.j.k}^{ref} > P_{res,i.j.k}^{meas}\right)$. In order to know that such difference occurs at a particular resource, and is not due to a maximum power point operation saturation, the power of the individual stations need to be compared using (5.13) and (5.14) in higher hierarchical levels

$$P_{avg_{stat}} = \frac{\sum_{j=1}^{m} P_{stat,j}^{meas}}{m} \tag{5.13}$$

$$PC_{stat,j} = \frac{P_{avg\_stat} - P_{stat,j}^{meas}}{P_{avg\_stat}} \tag{5.14}$$

$$C_{stat,j}^{eff} = PC_{stat,j}\$_{clust,i} \tag{5.15}$$

Where m is the number of stations considered for calculating the average station production. This station production $\left(P_{avg\_stat}\right)$ and performance coefficient $\left(PC_{stat,j}\right)$ of a particular station j could be calculated at the plant or cluster controller and transmitted to each of the station controllers, where the associated costs related with the efficiency costs due to external factors $\left(C_{stat,j}^{eff}\right)$ can be determined.

The overall station costs considered, will have a direct impact on the final power being supplied by the resource generation units, as according to their electrical location and particular real-time distribution losses or O&M costs, the price signal ($S_{stat,i,j}$) transmitted to each resource group belonging to a give station will be different. Hence, it encourages or discourages the generation involvement of given power resources, based on the electrical location and real-time O&M conditions of the converter stations.

Finally, it is worth noting that Fig. 5.7 shows the detailed station controller implementation corresponding to the cluster 1. However, the same principle applies for the converter station controllers interconnected to the other cluster.

Resource controller control diagram

Finally, the back-end resource controllers implemented in the competitive control structure appear depicted in Fig. 5.10. As early mentioned, the main objective of this controller is to determine the corresponding resource power reference ($P_{res,i,j,k}$) based on the station price signal ($S_{stat,i,j}$) received. This station price signal is modified, considering the resource equipment losses and efficiency-related costs, which are calculated as in (5.16), for finally determining the price willing to be paid to the primary resource side ($\$_{res,i,j,k}$).

$$C^{loss}_{res,i,j,k} = \left(1 - \eta_{res,i,j,k}\left(P^{meas}_{res,i,j,k}\right)\right) \cdot \$_{stat,i,j} \tag{5.16}$$

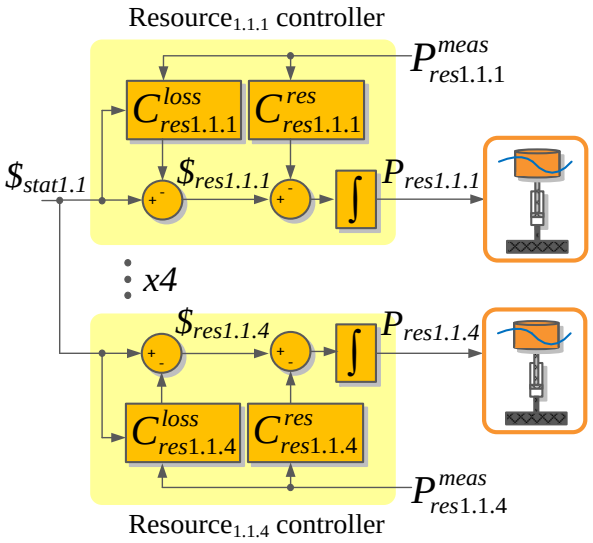

Fig. 5.10 Detailed resource controllers of the competitive power control structure

At the final stage, the output power reference from a given resource controller $\left(P_{res,i,j,k}\right)$ is determined by integrating the error between the resource price signal $\left(\$_{res,i,j,k}\right)$ and its

corresponding primary energy resource cost $\left(C_{res,i.j.k}^{res}\right)$, which mainly relates to the marginal fuel generation costs. In this regard, it is worth mentioning that for the case of renewable energy resources, such as the proposed wave power plant test case scenario, this marginal cost is zero, as the primary energy resource is cost-free.

In this manner, the power production reference increases when the price signal is higher than the overall generation marginal costs, and decreases when the price signal is lower. This output power setpoint will be provided as a production reference to the resource generation unit, in order to increase/decrease its generation involvement, as demanded from the competitive power control system.

Finally, from the particular competitive wave power plant application presented in this chapter, it is worth mentioning that the costs of distribution system losses have a moderate impact over the entire competitive results, due to the symmetry in the clusters and stations of the star-based wave power plant layout considered. In this regard, it has been found that the competitive controller has an emphasized impact in radial distribution systems, as there is a considerable difference in the power losses between the nearest and the farest distributed generation units belonging to a given cluster.

5.2.1 Power plant competitive controller tuning

Once the detailed wave power plant costs have been implemented, it is time for determining the tuning parameters of the plant PI controller in order to achieve the desired real-time plant production dynamics.

Regarding the overall costs considered over the hierarchical competitive control structure, it is worth noting that all the costs updating dynamics have been decoupled from the plant controller dynamics, by a low pass filter with time delay of 25 seconds. This low pass filter has been implemented at the output of each cost calculation block, so the costs updates will be performed smoothly, and will prevent having any undesired unstability effect on the competitive control tunning dynamics. Thanks to this dynamics decoupling, the plant resources instantaneously contribute to the fulfillment of a given step in the production reference, after which they progressively tend to stabilize to its corresponding production references, which are highly influenced by the overall costs considered in the energy distribution chain, from the plant point of interconnection up to the resource.

The considered plant control loop is introduced in Fig. 5.11, where the PI controller generates a price control signal, which is provided to the plant costs modeling block. Thanks to the decoupling between the slower overall costs update and the plant controller dynamics, this plant costs modeling block can be directly neglected. Therefore the plant price control signal directly affects each of the 40 parallel resource controllers conforming the plant.

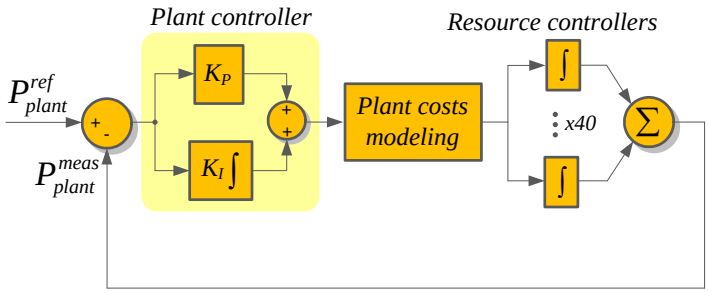

Fig. 5.11 Power plant front end controller loop

In this specific case, the plant controller has been tuned by considering the pole placement method. Where the controller $\big(C(z)\big)$ and plant $\big(G(z)\big)$ transfer functions are introduced in the MATLAB Sisotool as given in (5.17) and (5.18).

$$(z) = \frac{1}{z-1} \tag{5.17}$$

$$G(z) = \frac{40z}{z-1} \tag{5.18}$$

Then, the zero of the controller $\big((K_p + K_i)z - K_p\big)$ has been manually introduced with the objective of placing the closed loop poles at the required position, ensuring a 0.7 damping factor with a step response stabilization time of 60 seconds. The controller parameters ensuring the desired plant controller response are introduced in (5.19) and (5.20), where the tuning closed loop poles and step response is presented in Fig. 5.12.

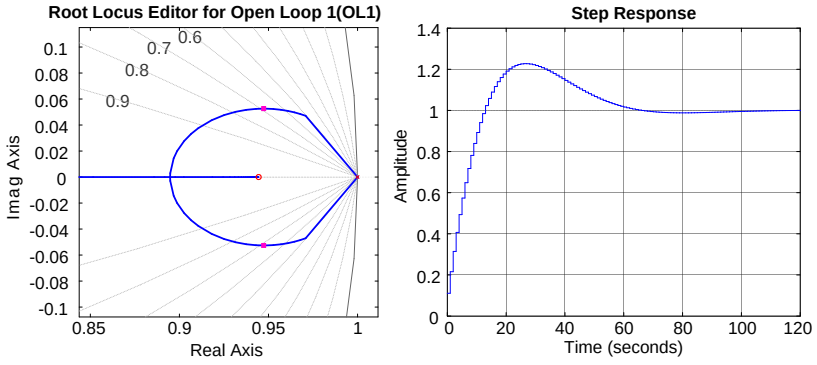

Fig. 5.12 Root-locus and step response of the plant controller in the tuning design

$$C(z) = \frac{0.002773z - 0.002619}{z - 1} \tag{5.19}$$

$$K_p = 0.002619 \; and \; K_i = 0.000154 \tag{5.20}$$

Finally, the overall wave power plant introduced in Fig. 5.1(b) has been implemented in simulation, along with the proposed competitive power control strategy and plant controller parameters. In this regard, it is worth noting that two sets of simulations have been performed to evaluate the behaviour of the competitive controller in this wave energy application.

From one side, a detailed real-time simulation has been developed, to show the real-time individual generation units response towards the fulfillment of the plant production objective. This simulation will also validate the dynamic plant performance capabilities, which should follow the specific requirements set in the controller tuning section.

Besides that, a stationary 20 years simulation has also been performed considering only the hourly average power supply capabilities of the plant. This simulation highlights the individual generation unit performance as the operation costs evolve over the operational lifetime of the plant. Therefore this simulation will demonstrate the suitability of the competitive controller under an economic steady state approach, ensuring minimum operation costs through optimal allocation of available resources.

Such simulation results and main driven conclusions are introduced in the following sections.

5.3 Simulation results of the competitive power controller

As early mentioned, two-sets of simulation have been performed within different time domains and degrees of detail. Initially, the average competitive power model has been simulated in order to describe the power plant performance over its entire operational lifetime. This is required, as the overall plant costs need to be modeled from the start-up date, where they only represent the costs of distribution power losses due to the lack of previous operational experience of the plant. Afterwards, a detailed real-time simulation has been performed over a representative date, in roder to show the full potential of the competitive controller in providing real-time optimum power sharing of available resources.

Regarding the possible sudden failure of station equipment components, a station reliability model has been considered for both simulation sets, as no evidences have been found on historical failure information on the continued operation of realistic commercial wave power plants. In order to determine the different failure events that will be experienced at each station controller over time, a Weibull reliability function has been considered, where

the failure events are generated from a pseudo-random number applied to the failure probability function. This Weibull reliability function has been calculated as in (5.21), and depicted in Fig. 5.13(a), where the Weibull parameters have been selected to achieve a 100% probability failure event after approximately 4 years of operation.

$$y(t) = \left(1 - e^{-\alpha\beta t}\right)\cdot 100$$
$$\alpha = 0.0014 \text{ and } \beta = 0.1 \tag{5.21}$$

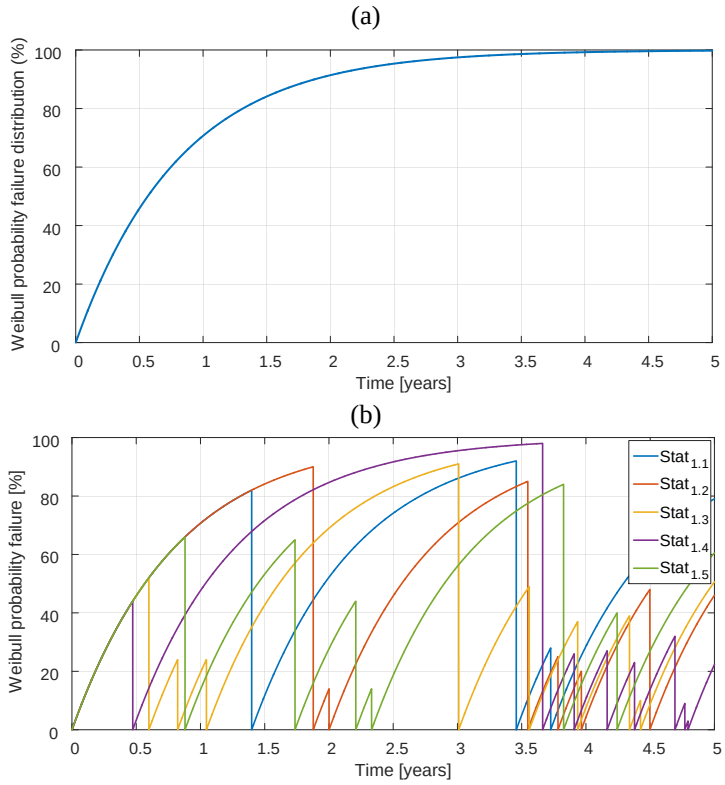

Fig. 5.13 (a) Weibull probability distribution considered for generating the station O&M failure time series, (b) Weibull probability function associated to each wave energy converter station, with corresponding failure events

The Fig. 5.13(b), shows the particular Weibull probability function over time, associated to all the stations belonging to the cluster 1 ($Stat_{1.1}$, $Stat_{1.2}$, $Stat_{1.3}$, $Stat_{1.4}$ and $Stat_{1.5}$) of the wave power plant layout. From this figure it can be observed that the stations are failing at different times over the 5-year period, being the Weibull reliability function reseted after each failure event.

Once the station failure events have been allocated over time, the cost of repairing such failure is determined according to the probability function proposed in (5.22).

$$C_{stat,j}^{fault} = x^3 \cdot (0.5 \cdot 10^6 - 100) + 100 \tag{5.22}$$

Where x is a uniformly generated pseudorandom number. Thanks to the x^3 probability density function introduced in (5.22), it is more likely to incur in cheaper failure costs than in very expensive ones, due to the more frequent replacement of spare parts. Furthermore, the range of failure cost has been delimited between 100$ and 0.5M$. The final O&M costs due to sudden failure events $\left(C_{stat,j}^{fault}\right)$ resulting from this reliability model are introduced in Fig. 5.14, for each of the wave power plant stations considered.

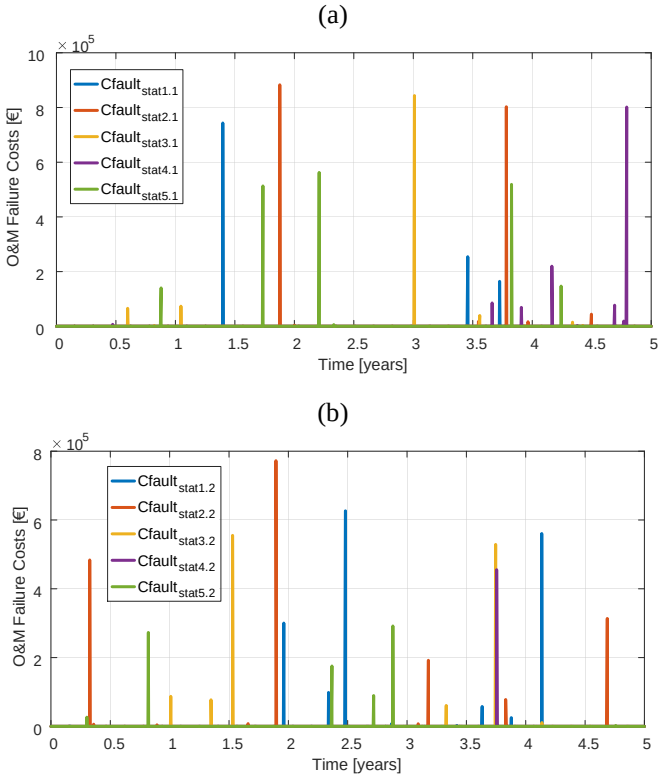

Fig. 5.14 (a) Station 1.1 to 5.1 O&M failure costs resulting from the proposed station reliability model; (b) Station 1.2 to 5.2 O&M failure costs resulting from the proposed station reliability model

As early mentioned, this reliability model is only used in case there is not empirical information available on incurred O&M costs over the plant lifetime. In a realistic wave power plant application, the real costs should be considered at the failure event instant, and would be directly included in the O&M costs calculator of the competitive controller.

Finally, it is worth noting that the competitive controller presented along this chapter will have a limited impact on the optimum power sharing of available resources, in case the power plant under consideration operates at maximum power point. Instaead, if the plant operates according to predefined power generation schedules resulting from energy markets, along with or without reserves capacity, the competitive controller would instantaneously allocate the most efficient generation units, to cope with undesired real-time resource variability effects. In this regard, all the simulations performed have considered a power plant generation schedule equal to the average maximum generation of the plant with a 7% of power reserve capability, as it is requested in several grid interconnection codes [18]. This plant operation performance provides advanced grid support capabilities, as it is able to provide frequency regulation services. Thus, it contributes to maintaining a safe and stable grid operation.

Real-time operation and control of a wave power plant using the competitive power controller

In order to properly analyze the real-time performance of the competitive controller, it is necessary to initially perform the average simulation model over the 20 year operational lifetime of the plant. So the influence of the O&M costs evolution can be considered in the latter real-time simulation model, as such costs are neglectible at operating times close to the start-up date.

The average simulation model has been built in Simulink, by implementing the competitive power control structure, introduced along section 5.2, for the selected wave power plant scenario (Fig. 5.1). In this simulation model, the maximum available resource capacity has been fixed according to the hourly average power profiles, obtained from the historical data of the DanWEc test site facility, and being properly scaled down to fit the power ratings of the resource equipment. Therefore, this hourly average power profiles appear as a common power limit to all the resource generation units involved, as the variability experienced among generation resources will be only visible in the real-time simulation model. Due to the fact, that all the resource generation units will be exhibiting the same maximum power supply capabilities, the resource controller costs have been neglected in the average competitive simulation, as equal power sharing will be experienced among them. This is because the the resource costs of identical generation resources is very similar from one to other, and the power saturation due to maximum power production holds the same for all of them.

Finally, it is worth noting that the average model has been simulated with a 1-minute sample time step basis, which means that the corresponding PI controllers and decoupling cost delays have been retuned in order to meet these new simulation requirements. The justification for this is the time consuming computational cost of simulating 20 years of plant operation. In this regard, the detailed parameters used in the average competitive power

control simulation are introduced in Table 5.1, where the discrete decoupling costs delay transfer function correspond to (5.23).

$$H_{delay}(z) = \frac{A_{filt}z + B_{filt}}{z - C_{filt}} \tag{5.23}$$

Average competitive power simulation parameters
$Ts = 60s$
$K_p^{plant} = 0.09$
$K_i^{plant} = 0{,}018$
$\mathrm{A_{filt}} = 0.01074$
$\mathrm{B_{filt}} = 0.01074$
$\mathrm{C_{filt}} = 0.9785$

Table 5.1 Simulation parameters of the average competitive power control simulation

The plant operation performance over a representative day can be observed in Fig. 5.15. From Fig. 5.15(a) it can be observed that the active power measured at the plant PCC strictly follows the hourly plant production reference scheduled (corresponding to the 93% of the maximum average plant power production according to the DanWEC database). Thus, the closed loop plant controller appears as a suitable control structure to ensure zero steady state error between the power plant reference provided and the actual power being supplied.

Afterwards, Fig. 5.15(b) shows the correlation between the virtual price control signal, generated at the plant level, and the overall costs incurred by each of the individual wave energy stations. It is worth noting, that the virtual price signal provided show appropriate incentive control actions, as the price signal increase in case of power deficit at the PCC and vice versa. Therefore, this price signal arises as the responsible control action for ensuring the accurate power control at the PCC.

Regarding the station costs presented in this figure, it should be emphasized that these station operation costs include all the costs presented in the previous section, but translated to the final WEC stations. In this regard, for example, the plant related costs, are equally shared among the overall stations, while the cluster related costs are translated to the stations located underneath the given cluster. Finally, each station has also considered their individual costs.

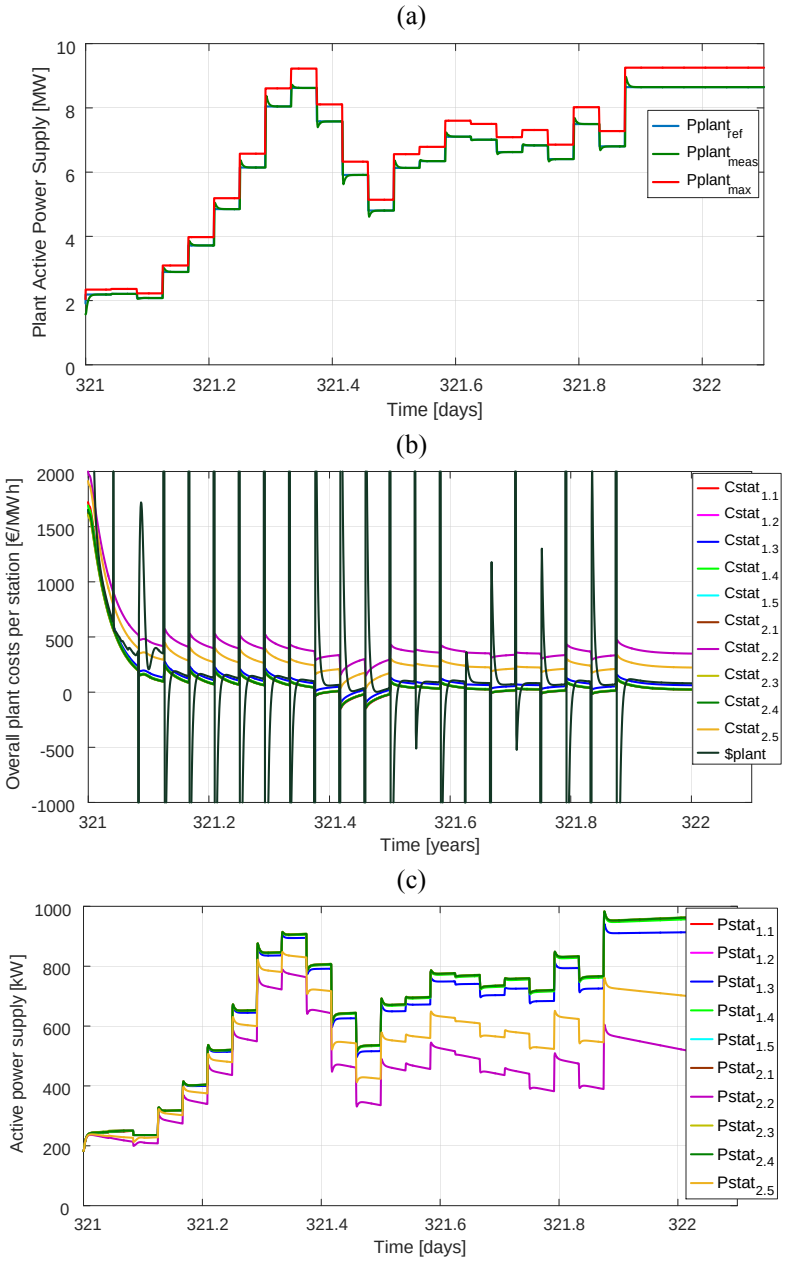

Fig. 5.15 (a)Active power plant reference and measurement supplied by the wave power plant; (b)Price signal comparison with the overall plant costs per station; (c)Active power supply corresponding to each converter station

The individual power production of each converter station appears depicted in Fig. 5.15(c), which results from the integral of the substraction between the plant price signals, and the overall costs associated to a given station. In this manner it can be observed that the results from Fig. 5.15(b) and Fig. 5.15(c) are closely interrelated. Therefore, the converter stations with higher incurred costs than the price control signal (i.e. $stat_{2.2}$ and $stat_{5.2}$), appear with a power decreasing trend in Fig. 5.15(c).

Therefore, the competitive power controller operates as expected, ensuring that the plant production objectives are suitably met at minimum operational costs, by optimally allocating the available generation resources of the plant.

From the weighted impact analysis of incurred costs among converter stations, it is worth stating that the cost component with higher repercussion is the corresponding to the O&M costs of each station. This is because this cost component can be very different among the converter stations, mainly due to the un-even occurrence of unexpected equipment failure, and repairing costs. The evolution of O&M incurred costs over the 20 years operational lifetime of the plant is presented in Fig. 5.16(a), where a zoomed view of the selected representative day is also emphasized (Fig. 5.16(b)). From Fig. 5.16(a), it can be observed that the evolution of the O&M costs follow the dynamics imposed from equation (5.12), for simplicity, here recalled as equation (5.24), making the real-time O&M cost calculation dependent on the energy being supplied.

$$C_{stat,i.j}^{O\&M}(t) = \frac{\sum_{t=0}^{t} C_{stat,i.j}^{fault}(t)}{E_{stat,i.j}(t)} + C_{stat,i.j}^{var} \tag{5.24}$$

In addition, from the zoomed view at the day of interest in Fig. 5.16(b), the stations with higher costs are the $stat_{2.2}$ and $stat_{2.5}$, fact that clearly influences the final power dispatch of available generation resources, as early noted in Fig. 5.15.

(a)

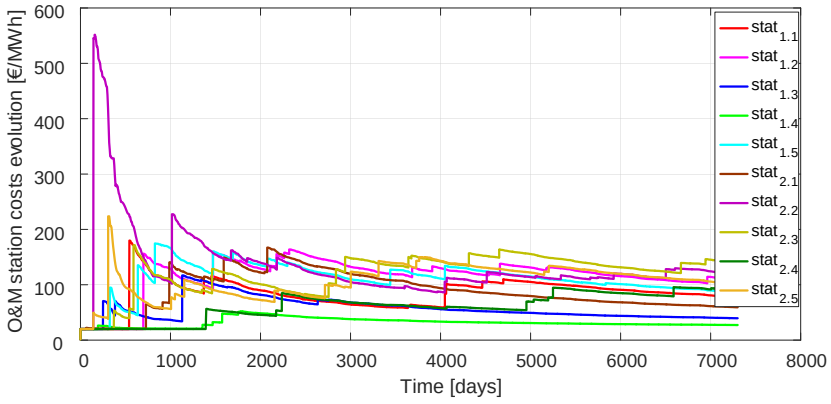

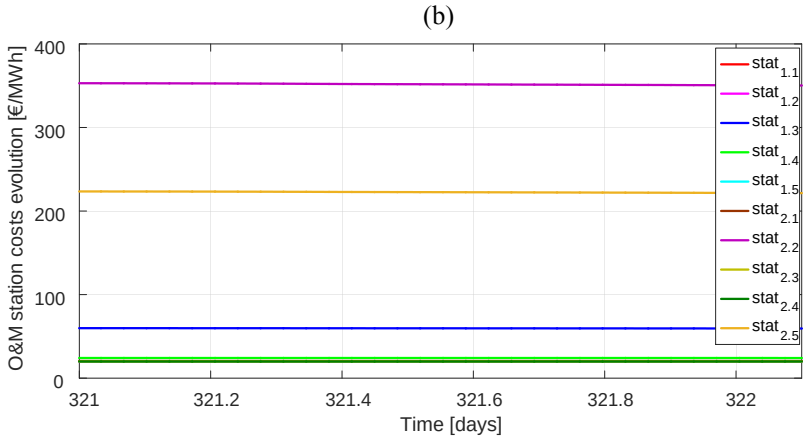

Fig. 5.16 (a)O&M station costs evolution over the operational lifetime of the plant; (b)Zoomed view of the O&M station costs evolution over the selected day of interest

Once the average simulation has been suitably introduced, it is time for focusing on the real-time performance of the competitive power controller. In this case, the real-time wave energy resource characterization has been performed by using the pu variability profile, determined in the simulation and experimental results of the previous chapter, and adding it to the hourly average maximum resource power profile, obtained from the histaorical data of the DanWEc test site facility. In this manner, the maximum real-time resource profile, combines the characteristic oscillating resource variability of the adaptive vector control solution proposed, with the hourly average power production levels of a realistic test site facility. Furthermore, a given variability shifting degree has been considered for each WEC generation resources. Therefore, the instantaneous maximum power extraction from all the WEC will not pulsate simultaneously. An example of the instantaneous maximum resource power profiles, considered along the real-time simulation, are presented in Fig. 5.17, where it can be observed that all of them share the same hourly average power level, but different instantaneous power capabilities.

As similarly specified for the average simulation test case, the power plant generation schedule corresponds to the maximum available resource generation capacity of the plant with a 7% of power reserve capability.

Regarding the simulation parameters used in this real-time simulation, they strictly match with the ones introduced in the power plant competitive controller tuning section (section 5.2.1), and are further introduced in Table 5.2.

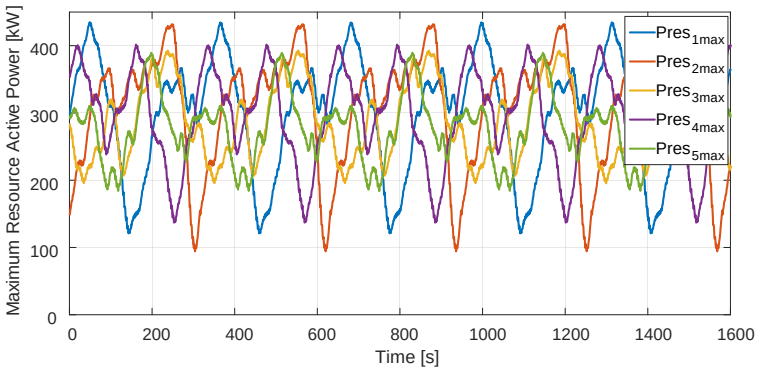

Fig. 5.17 Maximum real-time wave energy resource characterization

Real-time competitive power simulation parameters
$Ts = 1s$
$K_p^{plant} = 0.002619$
$K_p^{plant} = 0.000154$
$\mathrm{A_{filt}} = 0.07692$
$\mathrm{B_{filt}} = 0.07692$
$\mathrm{C_{filt}} = 0.8462$

Table 5.2 Simulation parameters of the real-time competitive power control simulation

Giving continuity to the selected representative date over the entire operational lifetime of the plant, the real-time performance of the competitive power controller implemented within the wave power plant scenario is introduced in Fig. 5.18(a). From this figure, it can be observed that the active power measured at the plant PCC strictly follows the hourly plant production reference scheduled, which corresponds to the 93% of the maximum average plant power production according to the DanWEC database. Despite, the power measurement signal shows a slightly variability effect, introduced by the highly oscillating nature of the resource, which can be considered neglectible due to its reduced amplitude exhibited in Fig. 5.18(b).

In order to determine if the proposed plant controller follow the real-time controller dynamics requested in section 5.2.1, Fig. 5.18(b) provides a zoomed view of Fig. 5.18(a), during a 5-minutes period. In this case, it can be observed that the plant suitably provides the desired real-time dynamic behavior, as it reaches the generation steady state value after approximately 60s. Therefore it can be concluded that the competitive controller provides advanced real-time dynamic capabilities to the plant controller, as it is able to ensure a stable and flat power supply from one of the most oscillating renewable energy resources.

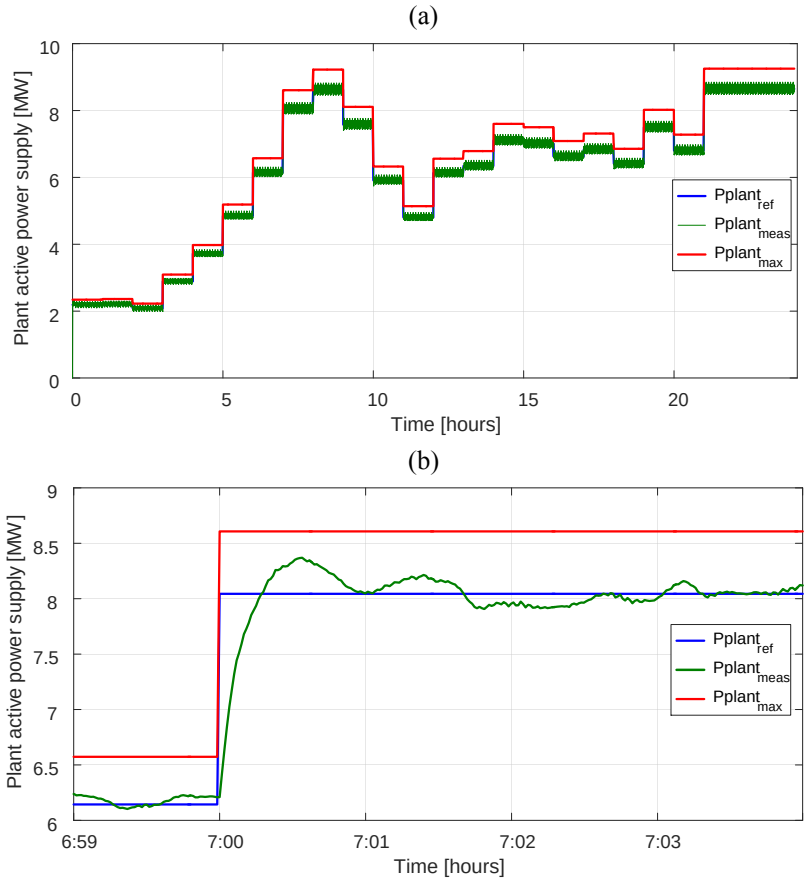

Fig. 5.18 (a)Active power plant reference and measurement supplied by the wave power plant in the real-time simulation model, (b)Zoomed view of Active power plant reference and measurement supplied by the wave power plant in the real-time simulation model

Finally, the real-time contribution from each of the hierarchical control structures is provided in Fig. 5.19, in order to highlight how the final active power supply is met at the plant PCC. For the sake of simplicity, the power supply over 1-hour period has been analyzed. Where Fig. 5.19(a), introduces the active power supply reference and measurement at the plant PCC, Fig. 5.19(b) introduces the active power supply of clusters 1 and 2, Fig. 5.19(c) introduces the power being supplied by the converter stations belonging to cluster 1, Fig. 5.19(d) introduces the power being supplied by the converter stations belonging to cluster 2, and Fig. 5.19(e) introduces the real-time power supply of the resource generation units of the station 1.

(a)

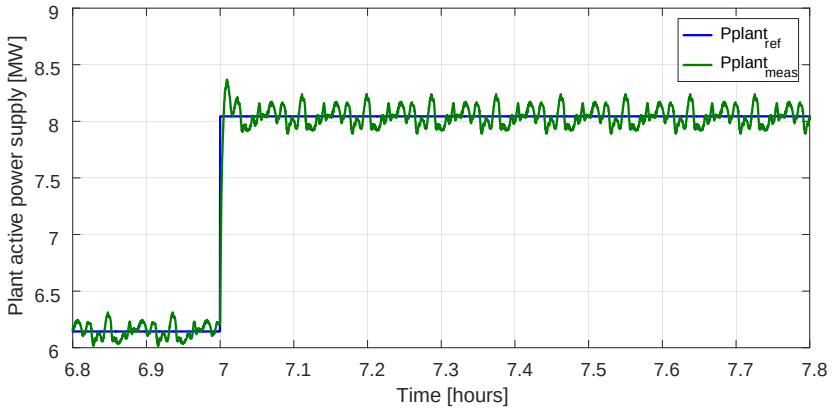
Plant active power supply [MW]
Time [hours]
Pplant_ref
Pplant_meas

(b)

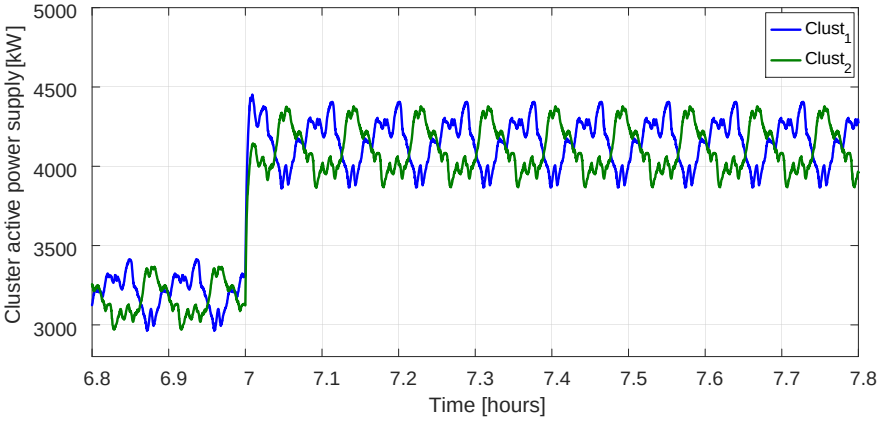
Cluster active power supply [kW]
Time [hours]
Clust_1
Clust_2

(c)

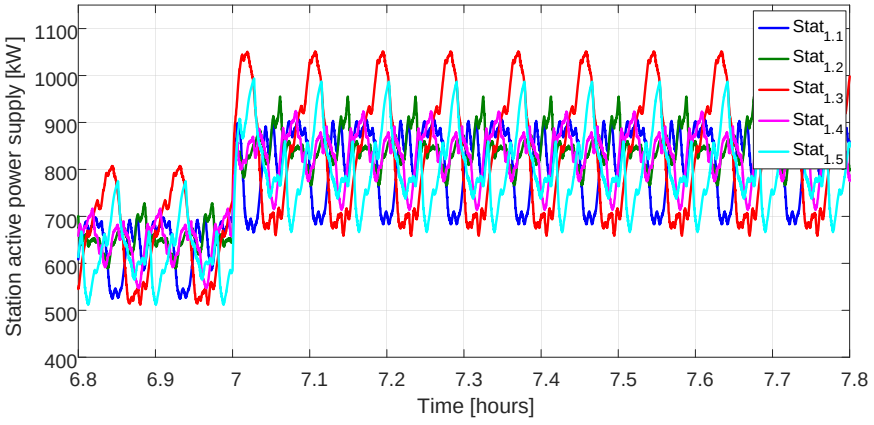
Station active power supply [kW]
Time [hours]
Stat_1.1
Stat_1.2
Stat_1.3
Stat_1.4
Stat_1.5

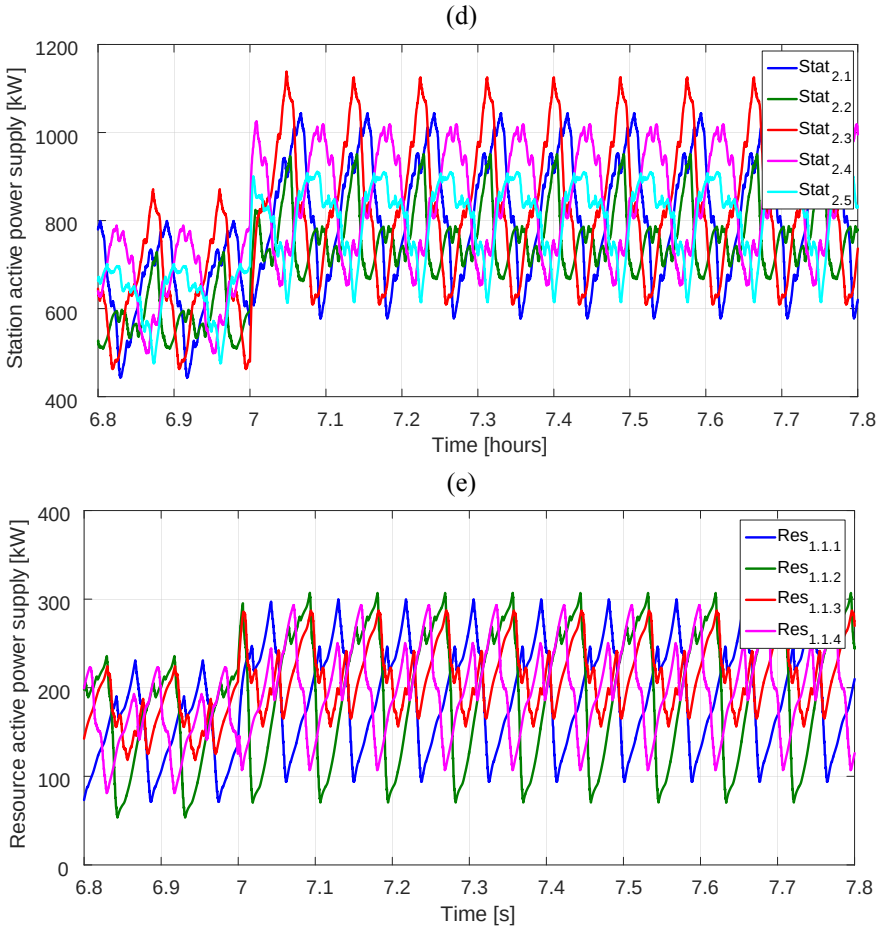

Fig. 5.19 (a) Plant active power supply reference and measurement, (b) Active power supply of clusters 1 and 2, (c) Active power supply of converter stations belonging to cluster 1, (d) Active power supply of converter stations belonging to cluster 2, (e) Active power supply of resources belonging to station 1.

From Fig. 5.19(b) it can be observed that the average power supply from both clusters is very similar, but their real-time profiles appear counteracting the power variations introduced by the other. This is very curious, as this desirable effect contributes towards meeting a flat and stable active power supply at the PCC. The similarities found in the average power levels comes from the slight deviation of incurred cost among power stations.

The instantaneous output power contribution from each of the 1MW power stations has been depicted in Fig. 5.19(c) and Fig. 5.19(d). Although it can not be clearly observed from these figures, the most costly stations from Fig. 5.16(b) arise as the ones with the lowest average power production levels ($stat_{2.2}$ and $stat_{2.5}$). However, they instantaneously

contribute to achieve a quite flat power plant production by adjusting their power supply as economically incentivated by the generated plant price signal. Therefore, the competitive controller ensures optimum real-time allocation of the available generation resources, while achieving the desired production objectives. A better sight of the real-time economic power sharing among converter stations can be observed in Fig: X, where the difference between incurred costs becomes more evident.

Finally, the individual active power supplied by each of the station available resources is provided in Fig. 5.19(e), where the high variability of the generation resources become an evident fact.

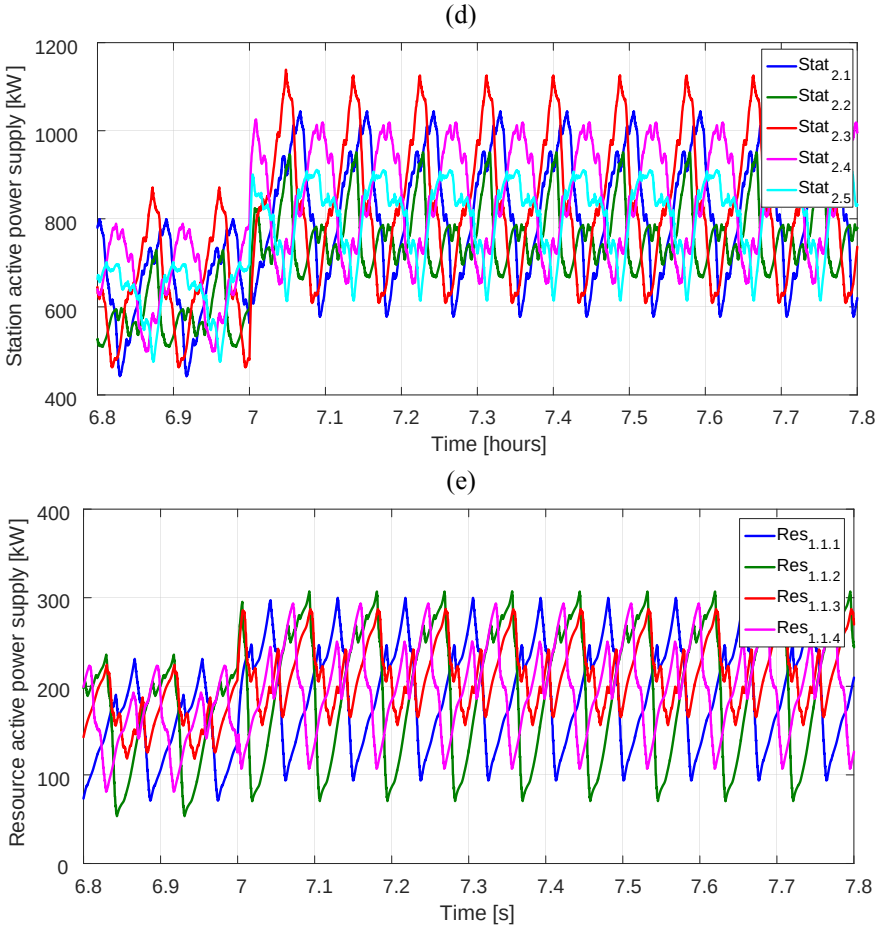

Fig. 5.20 (a) Plant active power supply reference and measurement, (b) Active power supply of clusters 1 and 2, (c) Active power supply of converter stations belonging to cluster 1, (d) Active power supply of converter stations belonging to cluster 2, (e) Active power supply of resources belonging to station 1.

Comparison between competitive and conventional (1/n) control strategies (transients & steady state long term)

In order to have a meaningful evaluation of the long-term benefits provided by the competitive control strategy, the competitive simulation has been compared with the conventional (1/n) power sharing strategy, in which the plant power setpoint is equally shared over the n available resources. Due to the computational burden of performing both simulations, the comparison has been performed for the first 10years of operation of the plant. It is worth noting that the same plant operation conditions have been imposed for both 10-year simulations, in terms of plant production setpoint, maximum resource power, and failure events and related costs. The overall plant production costs have been calculated for both plant operation study cases, and the results over a 10-year period are shown in Fig. 5.21.

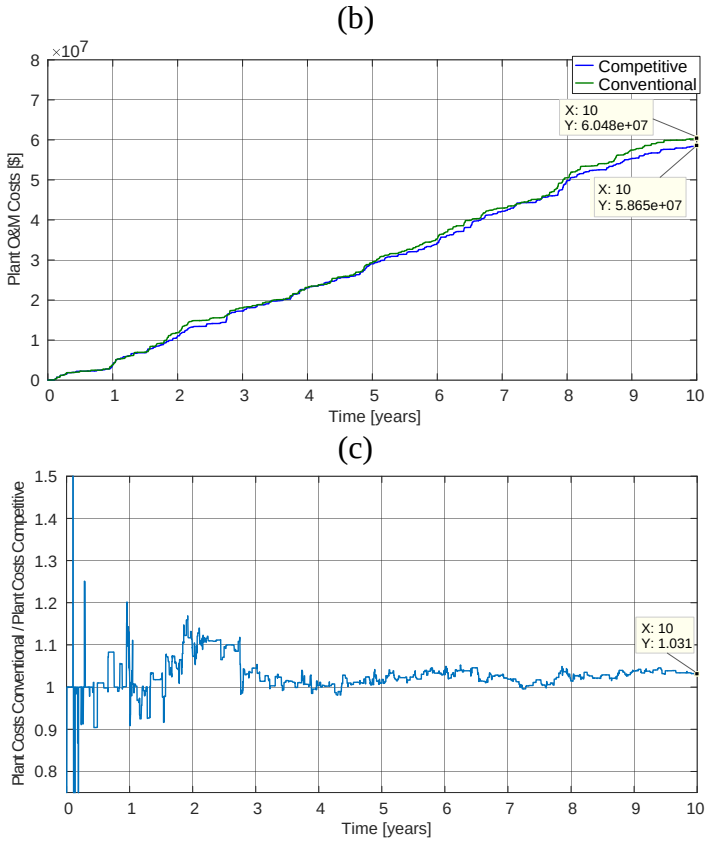

Fig. 5.21 (a)Comparison of the operation and maintenance costs derived from the operation of the simulated plant using the competitive and conventional controlers; (b) Per unit ratio of the conventional over competitive plant operation and maintenance costs

From Fig. 5.21 (a), it can be observed that, despite obtaining similar plant production costs at the beginning of plant operation, the competitive operated plant achieves reduced plant operation costs as the plant operation time increases. This is due to the long term optimum resource allocation performance provided by the competitive controller, since the generation units with the largest aggregated costs have considerably the lowest energy production levels over the plant operation life. Finally, from Fig. 5.21 (b), it is worth noting that the conventional (1/n) power sharing strategy results on a 3.1% increase in the overall plant production costs when compared with the competitive control strategy over a 10-year period. In this regard, such level of improvement is considerably influenced by the reliability model considered. However long term cost reductions can be even improved when considering realistic failure events and associated costs in a real wave power plant application, as the higher the heterogeneity between the station O&M costs experienced, the greater will be the long term costs savings obtained.

Chapter 6.

6 Conclusions and Future Work

6.1 Conclusions

Nowadays, the electrical energy is being generated by large scale conventional power plants (mainly fossil fuel, nuclear or hydro), whose electricity is radially transmitted over long distances, due to the logistic and geographical site-dependence of such generation units. However, the strong dependence of conventional power plants on progressive depletion of fuel resources, their negative impact on environmental pollution, and the lack of system efficiency from large transportation distances, results on a long term unsustainable power generation scenario.

Such problems could be overcome thanks to the increasing trend in generating power at distribution levels, where electricity is typically consumed, by means of non-conventional/renewable based generation units, such as PV, wind, combined heat and power (CHP), etc. These new generation technologies, termed as distributed generation, not only offers a non-pollutant, cheap and efficient source of energy to cover increasing demand, but also enhance the reliability of supply to critical loads and reduce the need for additional grid reinforcements. Aside of the technical benefits provided, DG will integrate new type of loads and end-user actors, such as prosumers, demand responsive loads, or electric vehicles (EV). Where these actors will actively participate in energy and auxiliary service markets, depending on their available or constrained energy needs

However, the main limiting factor to achieve larger shares of renewable based DG on the current power system scenario, comes motivated due to the unpredictable and highly stochastic nature of distributed energy resources. Therefore, under this futuristic distributed power system scenario, there is a clear need for addressing the main operation and control

challenges that these new generation technologies will pose on conventional power systems, and identify the main opportunities that could arise from their suitable system integration.

While conventional plants are constituted by a few large controllable synchronous generation units, RES based power plants are usually formed by large amounts of small scale power electronic converters, being poorly controlled and dispersed over a wide geographical areas. Up to date, such renewable power plants have been controlled under the "feed-and-forget" philosophy due to the small perturbation impact they had on the power system performance. However, this assumption cannot be considered any more, as with the changing paradigm of future distribution systems, massive penetration of RES-based distributed power plants and energy storage systems will raise new efficiency, reliability and security challenges in the manner in which the distribution system has been operated and controlled up to date. For this reason, there is a clear need in designing highly controllable and manageable distributed power plants, which could provide similar power control and grid service capabilities as conventional power plants.

In this context, the research work presented in this Thesis, addresses the main challenges associated with the hierarchical control design and implementation of large scale Distributed Power Plants (DPPs), with the purpose of achieving advanced grid conection performance while reaching maximum economic benefits from its optimum real-time operation. The work carried out along this dissertation results from an industrial PhD project, which has been fully supported by Abengoa.

Therefore, the first steps aligned with the research project purpose, were taken in the direction of getting extensive knowledge on the main RES-based power plant hierarchical control solutions currently on the shelf. This study not only covered the specific case of RES based power plants, but also advanced microgrid and smart grid control solutions. The main hierarchical control structures were initially analyzed, from where it was observed that many of them follow similar approaches in terms of the hierarchical control levels used. In this regard, it has been found that many approaches follow a master/slave architecture, where a centralized controller ensures an acceptable power supply control through the grid point of connection, while providing suitable power dispatch references to the local controllers of generation units. In addition, a revision on energy management systems solutions was performed when being applied in such distributed network structures. In many cases, these EMSs focus on implementing complex optimization algorithms with the objective of minimizing the operation costs of microgrids. However, as most of these approaches require large computation efforts, they do not arise as suitable candidates for performing real-time power dispatch capabilities. Other EMS techniques focused on collaborative control theories, mainly MAS and transactive, where the decision makers are highly distributed in the system. In this regard, a similar outcome was obtained as in the case o centralized structures, as no evidences were found on real-time implementation in microgrid power dispatching applictions.

Once the main RES-based power plant hierarchical solutions were analized, it was possible to propose a novel Hierarchical Distributed Control Structure (HDCS) for increased management of renewable-based active distributed plants. This hierarchical control structure comprises all possible functional levels from the higher long-term economic scheduling layer, to the instantaneous supervisory control of the resource, emphasizing the entire operation and control functionalities needed for increasing the integration of active distributed power plants. The HDCS proposed is based on a 7-levels hierarchy and incorporate several control levels found in distribution networs and power plants. In addition, thanks to the modularity of the proposed solution it can be applied to a wide range of final end-user applications ranging from : (a) large interconnected power systems with multiple power plants and consumption nodes, (b) subtransmission or distribution networks with distributed generators and controllable loads, (c) power plants with multiple generating units or (d) buildings or campuses with controllable loads and power generation units.

In order to achieve real-time control capabilities in active distribution systems, the present chapter introduced a novel power sharing control strategy, based on the competitive operation of multiple active participating agents (distributed generators, demand response and energy storage systems) through the implementation of market rules. This competitive power sharing strategy appears as an alternative to the transactive energy concept, as it proposes a method for optimum real-time balancing of the scheduled generation and demand. Such control capabilities are satisfied by applying a price control signal over the entire grid control architecture, being the final-end participating agent, the responsible entity in charge of deciding its own generation/demand involvement based on its marginal or affordable electricity costs. In addition, it reduces the information volume to be transmitted and processing requirements, as the higher control levels do not need to have knowledge on the detailed distribution system topology and contributing actors.

The main contribution of the proposed competitive controller is based on the real-time economic power balancing of active distribution grids, while being able to provide a reliable and safe operation of the grid through the active participation of distribution system end-users. In this manner, the competitive controller would conglomerate the secondary and tertiary (economic dispatch) conventional grid controllers in a single controller, as the proposed solution has the capability of ensuring real-time balance between generation and demand through the optimum allocation of available resources. Thus, ensuring minimum cost of supply.

This chapter laid down the groundwork of the competitive control concept, along with its main control rules and distributed energy resource performance when being applied in generic active distribution networks. This control philosophy will be later expanded towards the specific control of wave power plants, which is the application of interest of the Thesis.

Finally, a very simplified competitive power control has been implemented in simulation in order to clearly highlight the operation principles and main contributions of the proposed controller. Two study cases have been proposed based on the grid-connected or islanding

operation of a generic active distribution grid. From these simulations results, it can be observed that the power schedules set at the PCC of the active distribution grid can be met in real-time, while ensuring minimum operational costs of the active distributed resources.

However, the worst case scenario validation of the proposed real-time controller was evaluated in a wave power plant application, which came motivated due to the tremendous potential of wave energy, but also for the challenge it constituted to achieve advanced real-time control capabilities in such an oscillating renewable energy resource. Then, the proposed plant controller was intended to control the real-time production of the wave power plant in order to meet the flat and stable power generation schedules agreed in day-ahead or intra-day markets. Furthermore, an increasing concern was found in the wave energy sector, regarding the seamless grid integration of such highly oscillating power plants, due to the near-commercial deployments already achieved of several wave energy converter technologies.

Before implementing the competitive power controller in the selected wave power plant application, it was necessary to develop the realtime characterization of the wave energy resource profile, under maximum energy absorption conditions. For this purpose, chapter 4 proposed a novel adaptive vector controller, which maximizes the energy extraction from the resource regardless of the dominant irregular wave frequency characteristics. This adaptive performance is achieved from a signal monitoring and synchronization system, whose implementation in the wave energy sector has never been considered up to date. In addition, a novel vectorial approach has been introduced for determining the PTO forces acting on the wave energy conversion system, which maximizes the instantaneous or average power extraction from the resource. The proposed novel adaptive vector approach was suitably tested in simulation and experimentally, where it was proven that maximum energy extraction could be achieved regardless of the dominant wave energy resource characteristics. In addition, a comparison was performed against the main traditional passive loading and reactive control strategies, to show a meaningful evaluation of the proposed control concept. From this comparison it was demonstrated that the proposed controller is able to extract higher average power levels, while considerably reducing the peak-to-average ratio for the case of the average power theory implemented.

Finally, the wave energy resource characterization was considered in the competitive wave power plant implementation, giving rise to the maximum power supply capacity from individual resource generation units. From the real time implementation of the competitive power controller in the selected wave power plant application, it is worth noting that the main competitive controllers and associated costs were introduced in detail within the wave power plant architecture. Besides, the plant controller was suitablly tuned to reach the required grid connection performance dynamics. Finally, two sets of simulations were performed in order to evaluate the competitive power plant performance under steady-state and real-time operating conditions. From the steady state simulation, the competitive power controller was simulated over the entire operational lifetime of the plant (20years), starting

from day 0. This simulation served to test the optimum economic power dispatch capabilities of the competitive controller, which should be continuously adapting to changes in costs, derived from the operational experience of each controller. This simulation showed successful results, as the power stations incurring with larger cumulative costs were the ones with lower energy supply. Therefore, the optimum power dispatch of competitive controlled power plants ensure minimum operational costs through the optimum utilization of available resources.

Besides, the real-time simulation was also performed in order to test if the grid interconnection performance dynamics could be suitably met. In this regard, the competitive controller at the plant level strictly ensured the supply of controllable power generation levels (according to scheduled references), while achieving the required dynamic power supply injection performance. Finally, from the real-time simulation results it could be clearly observed that the generation units appear instantaneously contributing with its own generation levels to achieve the desired flat and stable power production setpoint. However, they tend to stabilize in steady state towards its optimaly economical generation point.

As a conclusion, it can be mentioned that the proposed competitive controller results on a suitable alternative to the already existing energy management systems in distributed systems, as it solve the major drawbacks found in ensuring a real time optimum economic control of participating agents. For the specific wave power plant application considered, the competitive control does not only ensures real-time optimum resource allocation for satisfying a given production objective, but also provides optimum long term operation of the system.

As a result, overall plant costs reductions can be achieved under the competitive operation, since the plant scheduled energy is satisfied by making use of the generation units with cheaper cumulative operation costs. This means that the generation units incurring in frequent and costly operation and maintenance duties will be minimally used, only contributing in specific periods where the scheduled power cannot be satisfied by the cheapest ones.

6.2 Future Work

As an extension of the wor carried out in this PhD dissertation one can deeply analyze the impact of the competitive power controller in active distribution networs such as smart grids or similar, in terms of optimal real-time allocation of available resource where massive penetretation of RES based generation, energy storage systems, and demand responsive loads coexist. An additional issue worthy to be analyzed is the role that electric vehicles play in such a competitive power control scenario, and how this promising end-user actors can be massively integrated.

Another field of interest in active distribution networks is to provide intelligent decision actions on the final end-user resources considered, where they could take advantage of large

information datasets on measured variables to perform predictive analyses. Such predictive analyses could be integrated in the form of cost signals, or better pointed out, deciding when to generate or consume in order to get optimum economic revenues from the end-user utilization of electrical energy.

Furthermore, the implementation of the competitive power controller should be analyzed towards a pure electrical power system scenario, considering real-time power system simulation platforms such as DigSilent or PSSE. In this case, the impact on voltage and reuency network variables could be also be considered, while integrating suitable system operation restrictions in the competitive cost structure.

Finally, in the specific case of power plants, the predictive analyses of O&M duties could offer additional room for obtaining even higher economical benefits of the plant operation. In this regard it would be possible to force maintenance actions to be performed when price signals are at its minimum.

Appendix I.

WPP topologies analysis and electrical distribution system design

I.I Introduction

In this appendix, the design of a layout for a wave power plant (WPP) is proposed. This is a topic that has been analyzed before for wind power plants, and some clues can be obtained from them. However, there are significant differences between WPP and wind farms regarding components, facilities or installation that make it necessary to analyze this issue for the WPP case taking into account another factors.

The considered WPP will be composed of 10 WECs rated at 1MW each for a total 10MW power, placed at 20km from the coast at a 200m depth.

I.II Placement

The cabling layout of the WPP will firstly depend on the physical distribution of the WECs. This topic is out of the scope of this work and even it can be stated that some of the aspects are not developed enough yet [137]. However, a general idea is given for justifying the distribution that has been chosen for studying the cable layout.

Once that a general location has been chosen for the whole WPP, according to the potential of the energy to be extracted from the waves, the placement on each WEC along the WPP may depend on factors like:

- Bathymetry. The depth and slope of the seabed can determine how many rows or columns will compose the WPP [138]

- Angle of wave. In the case of an array of WECs if all 5 WECs were in a row which runs parallel to the approaching wavefront they would all react identically and simultaneously (interferences or masking effects are not considered). In order to avoid simultaneous operation, the array layout can be staggered, as shown in Fig. I. I so that some devices will be out of phase with others regardless of the angle of incidence [137]. This means that the 5 WECs may not react simultaneously to the oncoming wavefront, although there may be a combination of wave period and approach angle that allows this to occur.

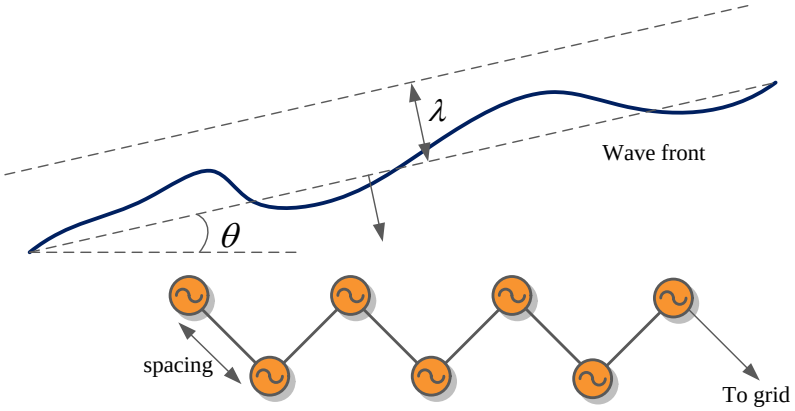

Fig. I. I Array placement in [137]

- Interaction between WECs. This topic is still at an early stage of development. The authors in [139] give an insight on the behavior of WEC arrays, and permits to draw guidelines for designing an array. In Fig. I. II, a matrix of WECs is depicted with two possible configurations, considering waves coming from -x: a) WECs in parallel rows (red points), b) the WECs in a row are staggered (like proposed in [137]). The 1st row of WECs is almost not impacted by the rest of the WEC array (especially because it does not suffer from masking effects). The two last rows of WECs act as reflectors sending waves back to the 1st row, which explains possible positive interactions. The study performed in [139] about the interactions of the WECs concludes:
    - The behavior of square-based arrays depends much more on the WEC type than for the triangle-based arrays case.
    - When the WECs are very efficient, choosing square-based arrays is not appropriate (especially for short separating distances), as strong masking effect occur.
    - Triangle-based arrays, or better, arrays described by two parameters (dx,dy) are the best configuration, as they permit to reach an optimum

between masking effect (destructive interactions) and the WECs sharing each other radiation (constructive interactions).

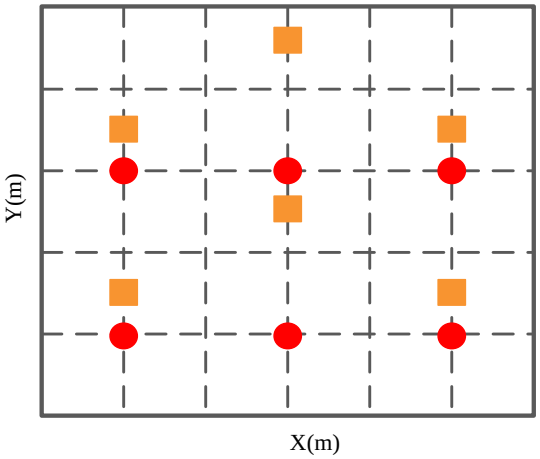

Fig. I. II Array analysis in [139]

In general, the devices will be placed rather in rows than in columns, facing the waves in parallel but staggered (triangle-based) for averaging the power extracted of the waves as a result of the aggregation of WECs.

Although the interactions of WECs should be further studied, the results from [139] indicates also that the triangle-based placement is preferable. Distance between WECs is a significant factor for interferences, therefore, a 500m between WECs has been chosen, in order to reduce possible masking effects between them. This long distance entails also the worst possible case the losses in the cable layout point of view (shorter distance would give rise to a more favorable case).

Considering all these facts, the placement in Fig. I. III is considered. The depth and distances of the WPP greatly depends on the bathymetry of the ocean. After consulting different bathymetry other sources, a 20kM distance and 200m depth have been considered.

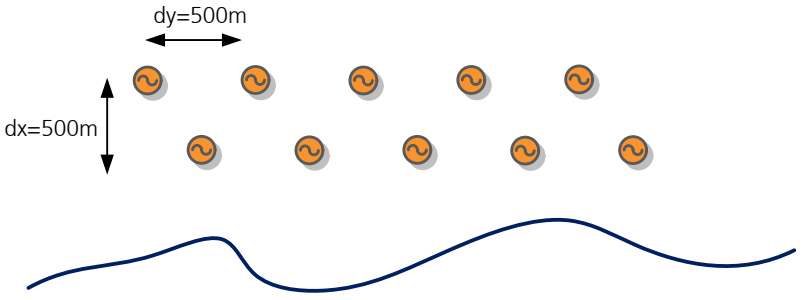

Fig. I. III Placement of the WECs

I.III Main Components

Parts

The main parts in the WPP to be considered are:

- 10 WECs rated at 1MW each.
- Collector system, determining if the WECs are connected by star structures or as arrays, including junction boxes for configuring the topology.
- Off-shore substation for increasing the voltage for the transmission system.
- Transmission cable, from the off-shore substation to the shore.
- On-shore substation, for adapting the transmitted power to the voltage level required by the TSO.

Rating

The rating of the different components in the WPP greatly depends on the available technology.

- A 10kV output voltage of the WECs is chosen, due to the available wet-mate connectors in the state of the technique. Inside the WEC, a transformer boosts the voltage form 400V (given by the front-end power electronic converter) to the specified 10kV.
- The voltage at the transmission level is fixed to 33kV. Although the highest possible value would be desired, this value is suitable for transmitting 10MW by considering available submarine cables [140, 141]. Even considering that specific cables can be designed for this application, next standard voltage level is typically 132kV, maybe too high for the underwater technology to be developed. The chosen value is also on the line of the analysis performed by [142], and on the proposed by O'Sullivan in [107]. Even in [143] 33kV is considered as a good trade-off value. This 33kV voltage would be suitable even for higher power (up to 30MW).
- A 10kV/33KV 10MW off-shore substation is considered. In the case of WPP it is a technology to be developed. In the case of wind farms, according to [144], substations are constructed on offshore platforms, at smaller depths (typically 40m and 100m max). In the case of WPP, the depths are bigger (from 100m to 500m or even higher). Some authors assume floating substations, which are even placed far from the WECs for construction at more shallow waters [107]. In this work, it will be supposed that a 10kV/33kV substation, with the corresponding switchgear, will be placed at the seabed, close to the WECs for minimizing losses. The cost of this substation may be quite high. Due to this reason, it will be considered that only one substation will be used in the 10MW case for boosting the voltage from 10MW to 33MW (for higher power rated WPP, several transformers might be used).

- Another component needed in the case of the WPP is a junction box for joining different nodes in the collector system. This fact entails a significant difference with the wind farms case, because an additional component (whose cost can be high because its placement on the seabed) must be added. As the WECs are floating devices, the connection between them must be carried out in the seabed. The output cable of the WEC is a flexible cable whose weight should not affect to the mass of the WEC, because it would modify its response. Due to this fact, a buoy structure (or a fixed structure fixed to the sea bed) must be added to this downloading cable, close to the WEC, in order to minimize the load induced by the weight of the cable, as seen in **¡Error! No se encuentra el origen de la eferencia.**.

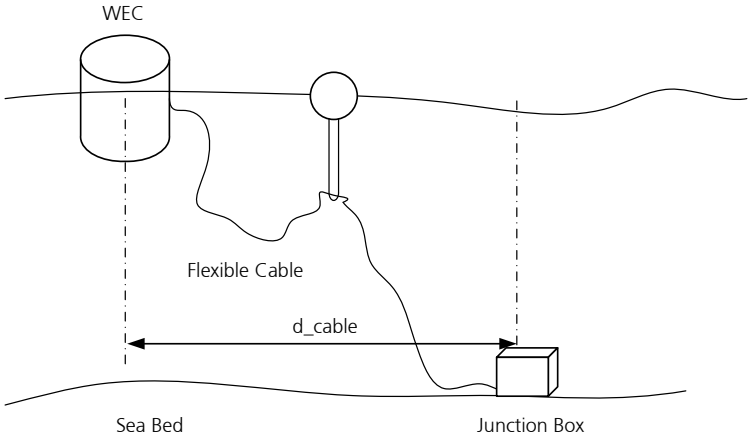

Fig. I. IV Scheme of the flexible downloading cable and its termination in a junction box

I.IV Cable Layout

The selection of a topology for the cabling layout in a power plant composed of several generators (WECs or wind turbines) depends mainly on [143]:

- Cost
- Losses
- Redundancy

Wind farms

In the case of wind, one that the placement of the wind turbines has been chosen, the joint between them is performed in the same structure where the wind turbines are built. As a consequence, different structures like arrays or stars, considering the wind turbines as the place where the nodes are placed. These structures can be mixed, by considering different structures for a determined group of devices (a cluster).

The radial system or daisy chain system can be single or multiple string system. Each string carries power from one or more wind turbine units to a higher rating feeder cable which carries the power to the substation. Higher losses are generally obtained but the cost of the system is lower, because less cabling is used. As a drawback, there is a probability of losing greater number of turbines (than in a star structure) in case of a fault since a greater number of cables carry power from multiple turbine units.

For a star structure, each wind turbine is directly connected to the substation (or connected to a central node in case of several clusters). Higher costs are obtained regarding the cabling, but it also results in lower losses and higher redundancy.

Following with wind farms, in [10], the generators are grouped as arrays, stars and star-clustered structures and both topologies are compared. The costs of generated electricity from the systems are comparable, with highest costs for the star case system and lower for the proposed cluster based system. Because of the lower power losses in the cluster system layout, the annual energy generated by it exceeds the same for the radial configuration. In addition, although the capital costs are higher for the proposed cluster based system compared to the radial system due to higher cable costs and trenching costs, when spread out over the lifetime of the turbines, the annual costs do not vary significantly. This results in slightly lower cost of generated energy in $/KWh for the proposed cluster based system compared to the radial configuration. However, with lower losses, there is greater amount of energy available for transmission.

Wave Power Plants

For the case of wave energy, a deep analysis considering array or ‘fork’ structures is performed in [6]. However, there are some facts in this study that have not been considered, as can be seen in Fig. I. V

- WECs are placed mainly in vertical rows. As explained before, horizontal rows will be mainly considered for WPP. For horizontal rows, the connection to the transmission system can be made at the middle of the string instead of the end, considering two clusters.
- Another fact that has not been taking into account in this cable is that the connection of WECs is performed at the seabed, by means of junction boxes that can be placed at a relative distance from the WEC (the cable will not totally fall in vertical). Therefore an additional flexible cable rated at the power of each WEC must be added. As a consequence, the difference in cabling meters between array and star structures will not be as high as in the case of wind farms (both of them will share a common path which is the flexible cable).

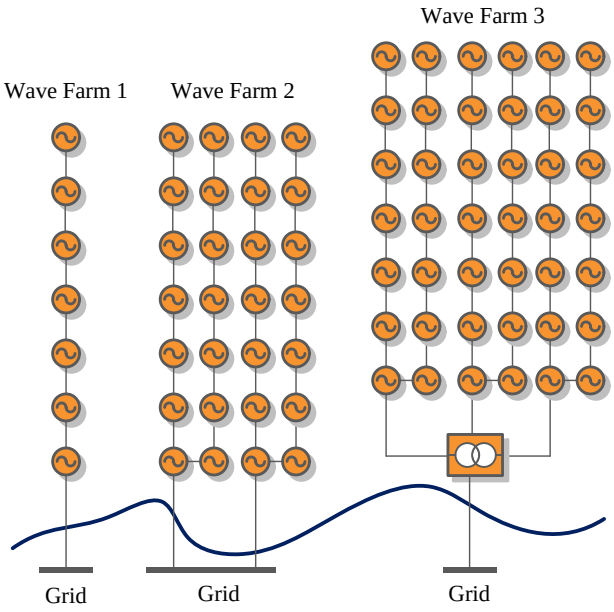

Fig. I. V WPP topology study in [6]

The cluster approach for a WPP is followed in [7], as seen in **¡Error! No se encuentra el rigen de la referencia.**.

In the next sections, a comparison of array and star structures for a WPP (with the placement depicted in Fig. I. III) divided in two clusters, will be performed. This comparison highly depends on the length of the flexible cable.

First, a short flexible cable is considered, so that similar conclusions than for the wind farm case can be extracted.

Later, longer flexible cables (and other particularities of the WPP) are considered so that specific layouts with arrays and star clusters for a WPP will be proposed.

The off-shore substation and transmission cable will be similar for all cases. It will be placed in the middle of the structure for minimizing the cabling distances.

The cabling losses, depending on the rating and the circulating current, have been calculated from the available data from ABB [140] and ZTT [141] cables.

Furthermore, a cost comparison is performed by using the unitized cost for submarine cables (with a 95mm2 cross-section 10kV cable as the reference) from [137], which is summarized in Table I. I.

Installed Cable Unitised Costs				
Cable CSA (mm^2)	**10kV**	**20kV**	**33kV**	**132kV**
35	0.79	0.82	0.85	--
50	0.81	0.85	0.88	--
70	0.85	0.89	0.94	--

95	1.00	1.05	1.11	--
120	1.05	1.11	1.18	--
150	1.10	1.17	1.25	--
185	1.25	1.34	1.43	--
240	1.35	1.46	1.58	--
300	1.65	1.80	1.97	--
400	1.80	1.99	2.21	2.79
500	2.00	2.25	2.53	3.25
630	2.25	2.55	2.89	3.75

Table I. I Unitized cost for submarine cables [137]

The transmission system and transformers that are used in all the cases are similar, so the differences will come from the cabling in clusters and the number of junction boxes that will be needed.

I.V First case: short flexible cable

In this first analysis, the distance between the WEC and the point where flexible cable reaches (d_cable in **¡Error! No se encuentra el origen de la referencia.**) the seabed will be onsidered as 100m.

Array

The array structure for the chosen placement with cables 200m x 100m long (depth x distance) flexible is shown Fig. I. VI.

The off-shore substation has been placed in the middle of the structure for minimizing the cabling distances, and has been represented by a box with a transformer. The junction boxes to be placed in the seabed are marked as black boxes.

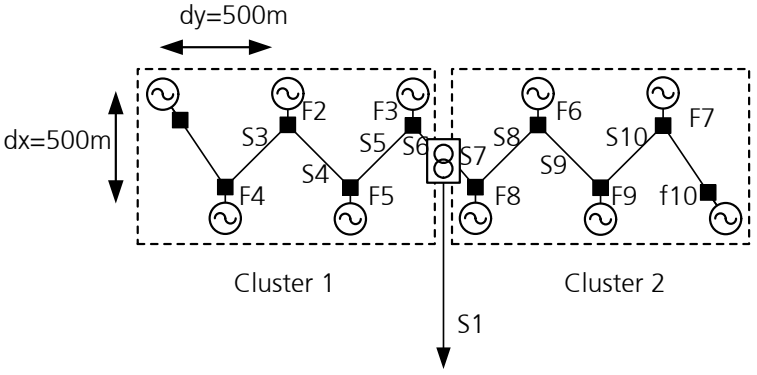

Fig. I. VI WPP layout divided in two clusters with array structure, considering a 100m distance for the downloading of flexible cable

The electrical scheme is shown Fig. I. VII. The off-shore substation and one of the junction boxes placed at sea bed have been marked with a box. Circuit breakers should be

installed inside junction boxes depending on the cost and the desired capability for isolating a possible fault. In this scheme, only one circuit breaker has been included in each junction box.

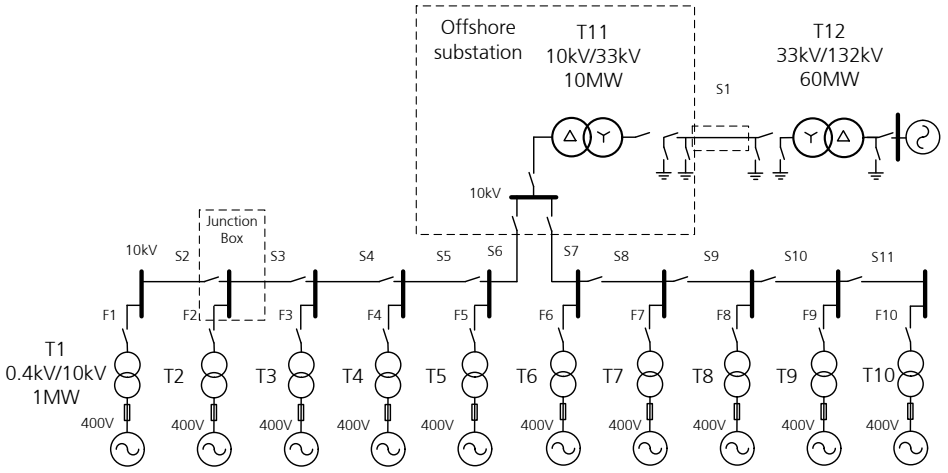

Fig. I. VII. Electrical Scheme of the WPP layout divided in two clusters with array structure

First, it can be observed that the plant is divided in two clusters, because the transmission cable arrives to the off-shore substation placed in the middle of the WPP. By this consideration, the redundancy is higher than considering only one complete array, and the losses are reduced because the power through the cables will be lower than in the case of one array.

The total losses and cost are shown in Table I. II

WPP Power (W)	10000000	
Losses in the Cluster 1 (W)	65764,4	0,65764
Losses in the Cluster 2 (W)	65764,4	0,65764
Losses in the transmission cabling (W)	907254,4	9,07254
Total Cabling Losses (W,%)	1038783	10,3878
Total Transformers Losses (W,%)	244680,2	2,4468
Total Losses (W,%)	1283463	12,8346
Transmission Costs (p.u.)	17,6	
Cluster 1 Cost (p.u, total %)	2,36925	10,6061
Cluster 2 Cost (p.u, total %)	2,36925	10,6061
Total Cabling Cost (p.u.)	22,3385	

Table I. II Total losses and cabling relative cost for array structure with short flexible cables

Star

In this second case, the plant is also divided into two clusters of 5 WECs each, with star structure, as seen in Fig. I. VIII. The electrical scheme is shown in Fig. I. IX. In this case, while the flexible case has the same length than in the array case (assumption made for the sake of comparing, later a more realistic approach will be proposed), and it will be joint to a static cable in the seabed by a junction box (or just by a splice). One junction box for joining the 5 WECs in each WEC is needed while the off-shore substation and transmission cable are similar than in the previous cases.

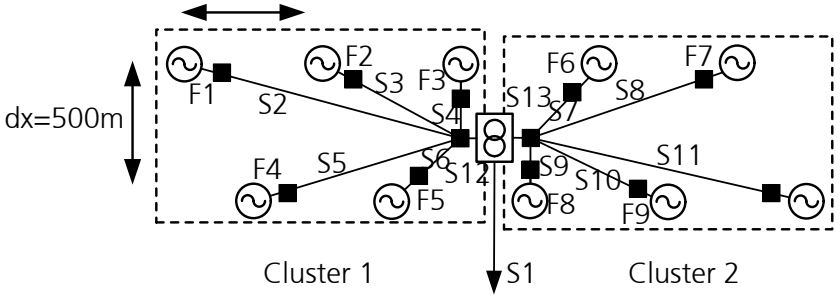

Fig. I. VIII. WPP layout divided in two clusters with radial structure, considering a 100m distance for the downloading of flexible cable

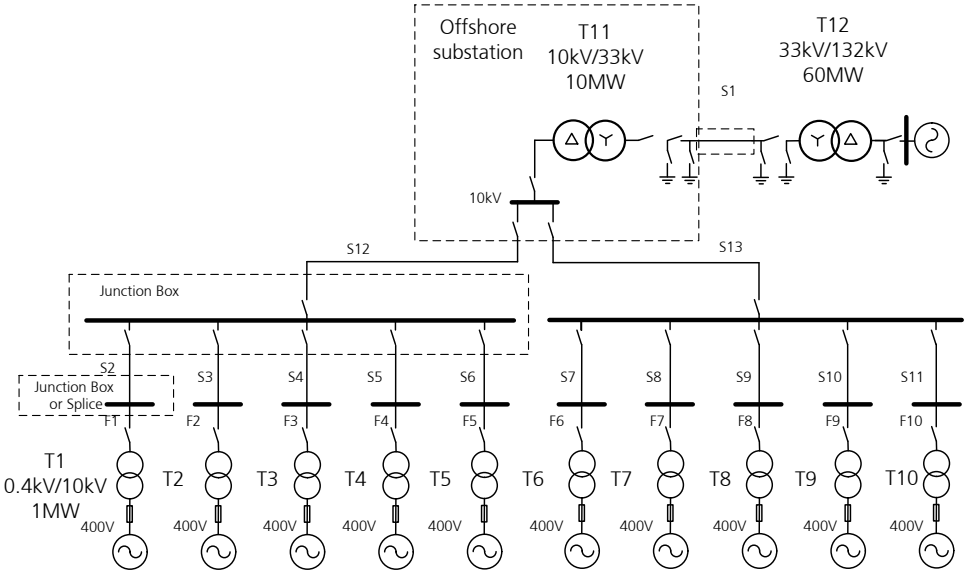

Fig. I. IX. Electrical scheme of the WPP divided in two clusters with radial structure, considering a 100m distance for the downloading of flexible cable

Global results are shown in Table I. III

WPP Power (W)	10000000	
Losses in the Cluster 1 (W)	25511,02	0,25511
Losses in the Cluster 2 (W)	25511,02	0,25511
Losses in the transmission cabling (W)	907254,4	9,07254
Total Cabling Losses (W,%)	958276,4	9,58276
Total Transformers Losses (W,%)	244680,2	2,4468
Total Losses (W,%)	1202957	12,0296
Transmission Costs (p.u.)	17,6	
Cluster 1 Cost (p.u, total %)	3,04748	12,8613
Cluster 2 Cost (p.u, total %)	3,04748	12,8613
Total Cabling Cost (p.u.)	23,69496	

Table I. III. Total losses and cabling relative cost for star-cluster structure with short flexible cables

Comparison

The results for the WPP composed of two clusters with star and array structures are summarized in Table I. IV. As expected, from the results in other papers [135], an array designed entail lower costs (in the cabling), but it exhibits higher losses and worst redundancy.

However, in this difference is not so high as a percentage in this WPP application because both cases share a “common path” which is the one followed by flexible cables.

	Star		**Array**	
WPP Power (W)	10000000		10000000	
Losses in the Cluster 1 (W)	25511,02	0,25511	65764,4	0,65764
Losses in the Cluster 2 (W)	25511,02	0,25511	65764,4	0,65764
Losses in the transmission cabling (W)	907254,4	9,07254	907254,4	9,07254
Total Cabling Losses (W,%)	958276,4	9,58276	1038783	10,3878
Total Transformers Losses (W,%)	244680,2	2,4468	244680,2	2,4468
Total Losses (W,%)	1202957	12,0296	1283463	12,8346
Transmission Costs (p.u.)	17,6		17,6	
Cluster 1 Cost (p.u, total %)	3,04748	12,8613005	2,36925	10,6061284
Cluster 2 Cost (p.u, total %)	3,04748	12,8613005	2,36925	10,6061284
Total Cabling Cost (p.u.)	23,69496		22,3385	

Table I. IV Comparison for a WPP based on two clusters with star and arrays structures respectively considering a short flexible case

I.VI Second case: custom flexible cable

In previous cases, it has been supposed that flexible cases had the same length in all cases, determining the length of the static cables. However, if custom flexible cables are chosen for each case, reductions in the cost (in the case of the star case) or in the lost (array case) can be obtained.

Array

As has been stated before, the inclusion of flexible cables with the individual power of each WEC in the path of the power makes the differences with the star case smaller. As these flexible cables and the junction boxes in seabed are unavoidable for the array case, if the flexible cables length is chosen for minimizing the length of static cables, losses would be reduced for the previous case.

Under this consideration, the layout in the cabling is changed as shown in Fig. I. X, if compared to the one in Fig. I. VI. Two junction boxes have been avoided (individual box from F1 and F10) and even two more could be removed (for WECs 3 and 8, that could be directly connect to the off-shore substation, but it has been preferred to preserve modularity). Two static cables have been avoided and the general length has been reduced.

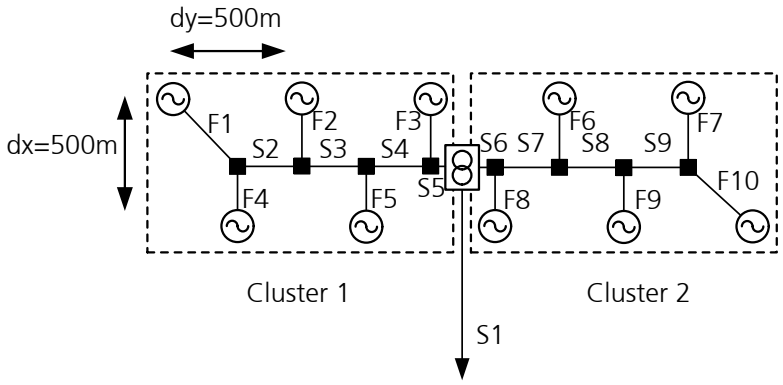

Fig. I. X. WPP layout divided in two clusters with array structure, considering a custom distance for the downloading of flexible cable

The electrical scheme will be quite similar (excepting for the removed junction boxes) as shown in Fig. I. XI.

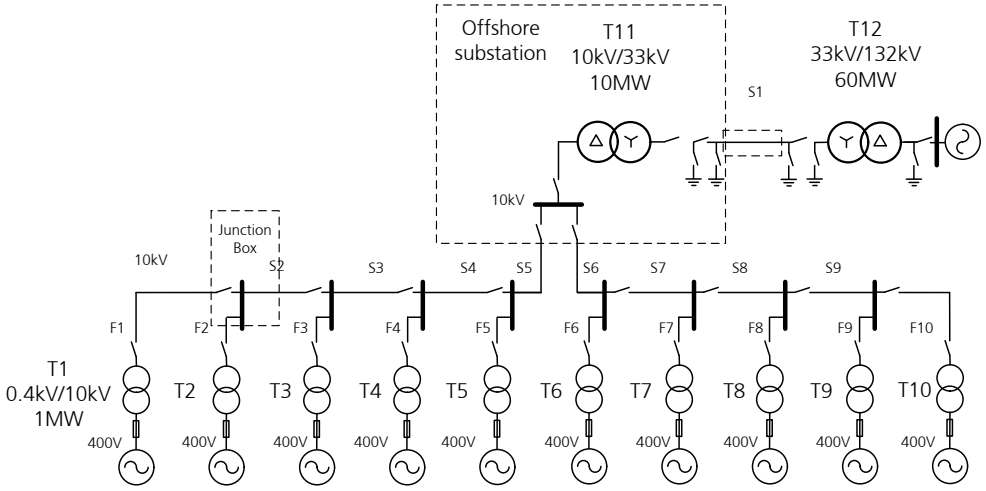

Fig. I. XI. Electrical scheme of the WPP layout divided in two clusters with array structure, considering a custom distance for the downloading of flexible cable.

As a result, the total losses and relative cost (just for the cabling) for this topology are shown in Table I. V

WPP Power (W)	10000000	
Losses in the Cluster 1 (W)	45746,4	0,45746
Losses in the Cluster 2 (W)	45746,4	0,45746
Losses in the transmission cabling (W)	907254,4	9,07254
Total Cabling Losses (W,%)	998747,2	9,98747
Total Transformers Losses (W,%)	244680,2	2,4468
Total Losses (W,%)	1243427	12,4343
Transmission Costs (p.u.)	17,6	
Cluster 1 Cost (p.u, total %)	2,10735	9,66023
Cluster 2 Cost (p.u, total %)	2,10735	9,66023
Total Cabling Cost (p.u.)	21,8147	

Table I. V. Total losses and cabling relative cost for array-cluster structure with customized flexible cables

As a consequence, in the case of an array structure, the length of the flexible cables and the placement of the junction boxes can be chosen for minimizing the losses. As can be checked in Table I. VI, this new array has lower losses and cost than the previous one, and quite close to the star-cluster case.

	String (custom flexible)		Star (short flexible)		String (short flexible)	
WPP Power (W)	10000000		10000000		10000000	
Losses in the Cluster 1 (W)	45746,4	0,457464	25511,02	0,2551102	65764,4	0,657644
Losses in the Cluster 2 (W)	45746,4	0,457464	25511,02	0,2551102	65764,4	0,657644
Losses in the transmission cabling (W)	907254,362	9,07254362	907254,3618	9,07254362	907254,362	9,072543622
Total Cabling Losses (W,%)	998747,162	9,98747162	958276,4018	9,58276402	1038783,16	10,3878316
Total Transformers Losses (W,%)	244680,172	2,44680172	244680,1721	2,44680172	244680,172	2,44680172
Total Losses (W,%)	**1243427,33**	**12,434273 3**	1202956,574	12,0295657	1283463,33	12,8346333
Transmission Costs (p.u.)	17,6		17,6		17,6	
Cluster 1 Cost (p.u, total %)	2,10735	9,66022911	3,04748	12,8613005	2,36925	10,6061284
Cluster 2 Cost (p.u, total %)	2,10735	9,66022911	3,04748	12,8613005	2,36925	10,6061284
Total Cabling Cost (p.u.)	**21,8147**		23,69496		22,3385	

Table I. VIComparison of the array cluster with custom length for flexible cables with previous cases

Star

For the topology with two clusters based on star structure, the use of a custom length cable give rise to a significant reduce in the cost, because the WEC can be directly connected to the cluster node, avoiding the individual junction boxes (or spliced) in the seabed, as shown in Fig. I. XII and in the electrical scheme in Fig. I. XIII.

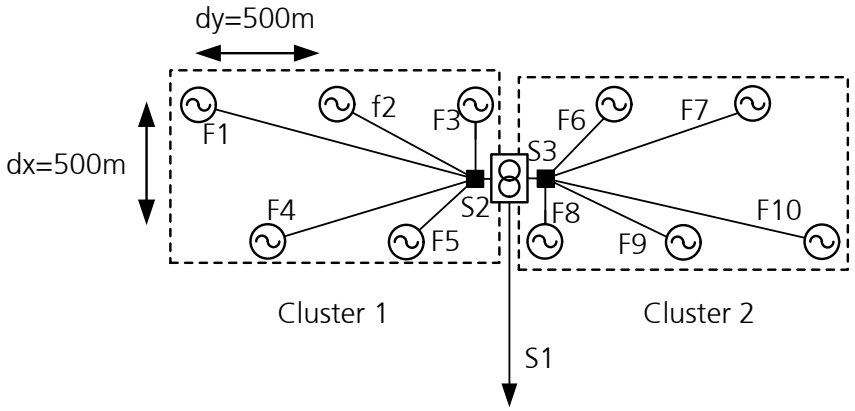

Fig. I. XII. WPP layout divided in two clusters with star structure, considering a custom distance for the downloading of flexible cable

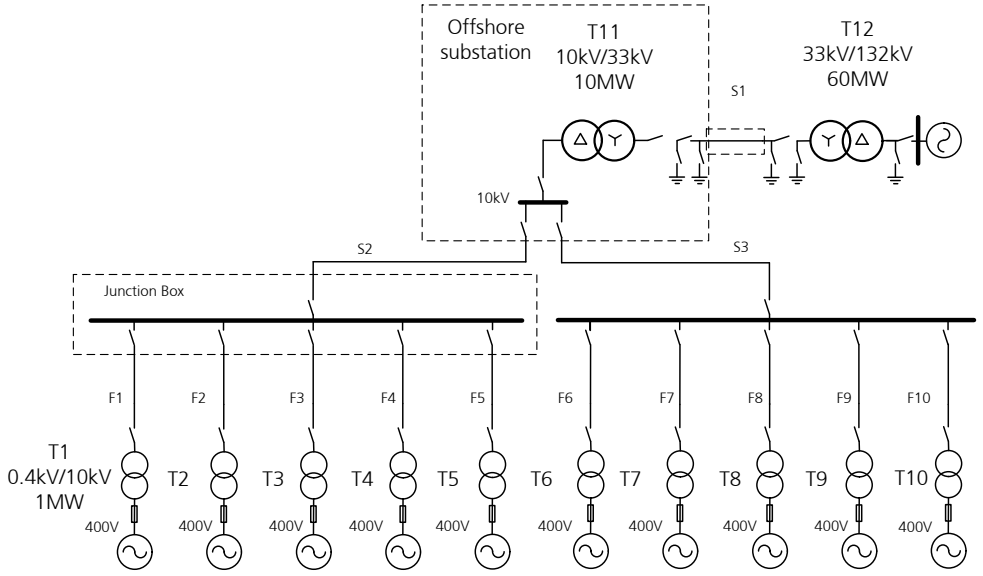

Fig. I. XIII Electrical scheme of the WPP layout divided in two clusters with star structure, considering a custom distance for the downloading of flexible cable

The total length of cables would be similar to the previous star case, so same results than before in Table I. III are obtained.

In this point, limitations come from the used technology.

- Direct connection of several WECs (5 in this case) in clusters by using a single junction box entails a reduction in the cost that will depend on the cost of the individual junction boxes and is difficult to estimate nowadays with the available data.
- However, the connection of several WECs to the same junction box by using a flexible cable can be limited by the deployment of the WECs, considering that the presence of moorings and flexible cables can make it necessary the placement of this junction box in a visible place in between the WEC to be connected. For instance, in our 5 cluster case, the better place for positioning the junction box is shown in Fig. I. XIV
- For this new position, better from the deployment point of view, the losses and the cabling cost is higher because the static cable which carries with a higher amount of power is now longer, as shown in Table I. VII

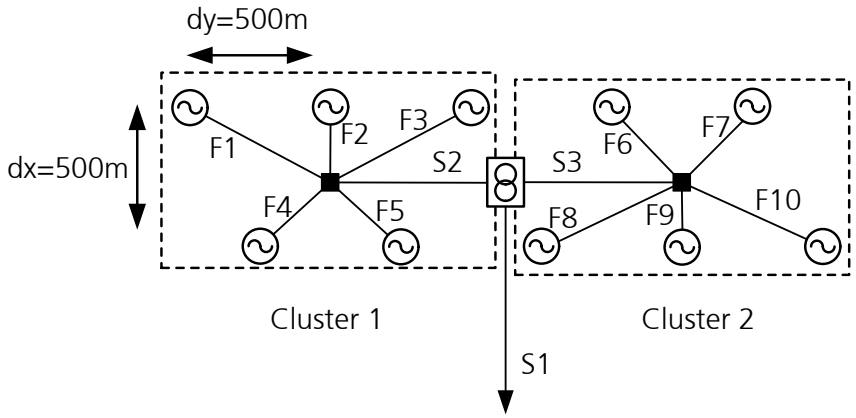

Fig. I. XIV. WPP layout divided in two clusters with star structure, considering a custom distance for the downloading of flexible cable with junction box placed in the center of the star

WPP Power (W)	10000000	
Losses in the Cluster 1 (W)	57536,4	0,57536
Losses in the Cluster 2 (W)	57536,4	0,57536
Losses in the transmission cabling (W)	907254,4	9,07254
Total Cabling Losses (W,%)	1022327	10,2233
Total Transformers Losses (W,%)	244680,2	2,4468
Total Losses (W,%)	1267007	12,6701
Transmission Costs (p.u.)	17,6	
Cluster 1 Cost (p.u, total %)	2,6211	11,4748
Cluster 2 Cost (p.u, total %)	2,6211	11,4748
Total Cabling Cost (p.u.)	22,8422	

Table I. VII. Total losses and cabling relative cost for star-cluster structure with custom flexible cables with junction box placed in the middle of the structure

I.VII Main comparison and structure

The comparisons between all cases that have been considered are summarized in Table I. VIII. The cost of junction boxes is not included.

It can be concluded that the best case, from the losses point of view is the use of a star cluster, with a junction box where 5 WECs are connected simultaneously (Fig. I. XII and Fig. I. XIII) (second column in Table I. VIII). In this way, the use of individual junction boxes

(like in array case) is avoided, reducing the general cost of installation. This structure gives also a high degree of redundancy. **This is the chosen topology in this study.**

Depending on moorings and deployment process, the placement of the junction box for the 5 WECs in the cluster can be shifted towards a more centered position in the cluster. This would give rise to higher losses due to shorter individual flexible cables and a longer static common cluster cable. The best positioning case, but worst for the losses is shown in the first column in Table I. VIII).

The best case for this star would be even to consider one cluster of 10 WECs, and just an offshore substation. However, from the installation point of view and for the sake of scalability, clusters of 5 WECs have been considered.

In the case of using strings for clusters, with custom flexible cables (column), lower cabling costs are obtained, but individual junction boxes should be needed (a total of 8 junction boxes), which could make the total installation more expensive than the star case. Depending on the cost of the technology, the structure considering custom flexible cables that minimizes the static common cable (

Fig. I. X and Fig. I. XI) could be suitable for obtaining an easy deployment with a good trade-off value of losses. However, higher redundancy would be still achieved by the star case.

Even if the initial supposition of the placement of the WECs in a triangle-based approach is not followed, the cluster concept is still valid and similar results would be obtained.

It can be concluded that specific characteristics of WPP, especially considering installation issues, makes the selection of the topology different than in the case of wind turbines.

	Star (custom flexible cable, worst losses case)		Star (Custom flexible best losses case)		String (custom flexible cable)		String (fixed flexible cable)	
WPP Power (W)	10000000		10000000		10000000		10000000	
Losses in the Cluster 1 (W)	57536,4	0,57	25511,02	0,25	45746,4	0,45	65764,4	0,65
Losses in the Cluster 2 (W)	57536,4	0,57	25511,02	0,25	45746,4	0,45	65764,4	0,65
Losses in the transmission cabling (W)	907254,3	9,07	907254,3	9,07	907254,3	9,07	907254,3	9,07
Total Cabling Losses (W,%)	1022327,1	10,22	958276,4	9,58	998747,1	9,98	1038783,1	10,38
Total Transformers Losses (W,%)	244680,1	2,44	244680,1	2,44	244680,1	2,44	244680,1	2,44
Total Losses (W,%)	1267007,3	12,6	**1202956,5**	**12,02**	1243427,3	12,4	1283463,3	12,83
Transmission Costs (p.u.)	17,6		17,6		17,6		17,6	
Cluster 1 Cost (p.u, total %)	2,6211	11,47	3,04748	12,86	2,10735	9,66	2,36925	10,60
Cluster 2 Cost (p.u, total %)	2,6211	11,47	3,04748	12,86	2,10735	9,66	2,36925	10,60
Total Cabling Cost (p.u.)	**22,8422**		23,69496		**21,8147**		22,3385	
Junction boxes	**2 (for the 2 clusters)**		**2 (for the 2 clusters)**		8 junction boxes		10 junction boxes	

Table I. VIII. Comparison of results for all cases

References

[1] U.S. Energy Information Administration, "International Energy Outlook 2017," 2017.

[2] IEA - International Energy Agency, "World Energy Outlook 2016 Part B: Special Focus on Renewable Energy," 2016.

[3] J. Svensson, Active Distributed Power Systems. Functional structures for Real-Time Operation of Sustainable Energy Systems, Lund: Lund University, 2006.

[4] I. J. Perez-Arriaga, Regulation of the Power Sector, Springer, 2013.

[5] A. Gómez-Expósito, A. Conejo and C. Cañizares, Electric Energy Systems. Analysis and Operation, Boca Raton: CRC Press, 2009.

[6] P. Kundur, Power System Stability and Control, New York: McGraw-Hill, 1994.

[7] State of New York Public Service Commission, "Proceeding on Motion of the Commission in Regard to Reforming the Energy Vision - Order adopting Regulatory Policy Framework and Implementation Plan," February 2015.

[8] N. D. o. P. Service, "Reforming the Energy Vision - DPS Staff Report and Proposal," 2014.

[9] S. Chowdury, S. Chowdury and P. Crossley, Microgrids and Active Distribution Networks, Stevenage: The Institution of Engineering and Technology, 2009.

[10] J. Martínez-Garcia and M. Babazadeh, "Control of large scale wind power plants,"

IEEE Power and Energy Society General Meeting, 2012.

[11] B. Badrzadeh, M. Bradt, N. Castillo, R. Janakiraman, R. Kennedy, S. Klein, T. Smith and L. Vargas, "Wind power plant SCADA and controls," *IEEE Power and Energy Society General Meeting*, 2011.

[12] P. Rodriguez, I. Candela and A. Luna, "Control of PV generation systems using the synchronous power controller," *IEEE Energy Conversion Congress and Exposition*, pp. 993-998, 2013.

[13] UCTE, "Technical paper - Definition of a set of requirements to generating units," 2008.

[14] A. Hansen, P. Sørensen, F. Iov and F. Blaabjerg, "Centralised power control of wind farm with doubly fed induction generators," *Renewable Energy*, vol. 31, pp. 935-951, 2006.

[15] J. Svensson and P. Karlsson, "Wind farm control software structures," *3rd International Workshop on Transmission Networks for Offshore Wind Farms, Stockholm*, 2002.

[16] Mita-Teknik, "Wind Park Control Brochure," 14 12 2017. [Online]. Available: http://www.mita-teknik.com/media/2225/mt_park-control_brochure_pdf-version_web_en_r1_0.pdf.

[17] M. Cardinal, "Monitoring, control, and automation of large wind plants," *2008 IEEE/PES Transmission and Distribution Conference and Exposition, Chicago, IL*, pp. 1-6, 2008.

[18] A. Gesino, B. Lange and K. Rohrig, "Large scale integration of offshore wind power through Wind Farm Clusters," *Renewable Energy World Conference & Expo Europe*, 2010.

[19] M. Wolff, R. Mackensen, G. Füller, B. Lange, K. Rohrig, F. Fischer, L. Hofmann, S. Heier and B. Valov, "Advanced Operating Control for Wind Farm Clusters," *Sixth International Workshop on Large-Scale Integration of Wind Power and Transmission Systems for Offshore Wind Farms, Delf*, 2006.

[20] Z. Lu, X. Ye, Y. Qiao and Y. Min, "Initial exploration of wind farm cluster hierarchical coordinated dispatch based on virtual power generator concept," *CSEE Journal of Power and Energy Systems*, vol. 1, no. 2, pp. 62-67, June 2015.

[21] H. Gaztañaga, J. Landaluze, I. Etxeberria-Otadui, A. Padrós, I. Berazaluce and D. Cuesta, "Enhanced experimental PV plant grid-integration with a MW Lithium-Ion energy storage system," *2013 IEEE Energy Conversion Congress and Exposition, Denver, CO*, 2013.

[22] J. Agorreta, M. Borrega, J. Lopez and L. Marroyo, "Modeling and control of N-paralleled grid-connected inverters with LCL filter coupled due to grid impedance

in PV plants," *IEEE Transactions on Power Electronics,* vol. 26, no. 3, pp. 770-785, 2011.

[23] E. Alves, M. Yano and M. Hofmann, "Integration of control, protection and supervisory systems in hydro power plants - State of the art and trends," *IEEE/PES Transmission and Distribution Conference and Exposition: Latin America,* 2010.

[24] C. Cabrera, J. Molina and J. Benoit, "Business benefits of implementing a new hydro-electric plant control system," *IEEE/PES Transmission and Distribution Conference and Exposition: Latin America,* 2008.

[25] CEN-CENELEC-ETSI Smart Grid Coordination Group, "Smart Grid Reference Architecture," 2012.

[26] IEC TR 62357-1, "Power systems management and associated information exchange - Part 1: Reference architecture," IEC, 2016.

[27] IEC 62264-3,4, "Enterprise-control system integration," IEC, 2016.

[28] T. Vandoorn, B. Zwaenepoel, J. De Kooning, B. Meersman and L. Vandevelde, "Smart microgrids and virtual power plants in a hierarchical control structure," *2011 2nd IEEE PES International Conference and Exhibition on Innovative Smart Grid Technologies,* pp. 1-7, Manchester, 2011.

[29] O. Palizban, .. Kauhaniemi and J. Guerrero, "Microgrids in active network management—Part I: Hierarchical control, energy storage, virtual power plants, and market participation," *Renewable and Sustainable Energy Reviews,* vol. 36, pp. 428-439, 2014.

[30] O. Palizban, K. Kauhaniemi and J. Guerrero, "Microgrids in active network management – part II: System operation, power quality and protection," *Renewable and Sustainable Energy Reviews,* vol. 36, pp. 440-451, 2014.

[31] C. Ionita, "Advanced Active Power and Frequency Control of Wind Power Plants," Aalborg University, 2017.

[32] X. Guan and G. Van der Molen, "Distributed control of large-scale offshore wind farms(aeolus)-deliverable 3.1: Control strategy review and specification," AEOLUS Technical report, 2009.

[33] R. de Almeida, E. Castronuovo and J. Lopes, "Optimum generation control in wind parks when carrying out system operator requests," *IEEE Transactions on Power Systems,* vol. 21, no. 2, pp. 718-725, 2006.

[34] Z. Bie, J. An, H. Xie and X. He, "A New Method for Active Power Dispatch in Wind Farms," *Energy Procedia,* vol. 61, pp. 747-750, 2014.

[35] C. Moyano and J. Peças-Lopes, "An optimization approach for wind turbine commitment and dispatch in a wind park," *Electric Power Systems Research,* vol.

79, no. 1, pp. 71-79, 2009.

[36] D. Madjidian, "Low-Rank Distributed Control with Application to Wind Energy," PhD Thesis. Lund University, 2014.

[37] V. Spudić, "Coordinated Optimal Control of WInd Farm Active Power," PhD Thesis. University of Zagreb, 2012.

[38] X. Zhang, W. Cai and Z. Gan, "Optimal dispatching strategies of active power for DFIG wind farm based on GA algorithm," *2016 Chinese Control and Decision Conference (CCDC)*, pp. 6094-6099, 2016.

[39] F. Ebrahimi, A. Khayatiyan and E. Farjah, "A novel optimizing power control strategy for centralized wind farm control system," *Renewable Energy*, vol. 86, pp. 399-408, 2016.

[40] D. E. Olivares, A. Mehrizi-Sani, A. Etemadi, C. Cañizares, R. Iravani, M. Kazerani, A. Hajimiragha, O. Gomis-Bellmunt, M. Saeedifard, R. Palma-Behnke, G. Jiménez-Estévez and N. Hatziargyriou, "Trends in Microgrid Control," *IEEE Transactions on Smart Grid*, vol. 5, no. 4, pp. 1905-1919, 2014.

[41] C. Cecati, C. Citro and P. Siano, "Combined Operations of Renewable Energy Systems and Responsive Demand in a Smart Grid," *IEEE Transactions on Sustainable Energy*, vol. 2, no. 4, pp. 468-476, 2011.

[42] A. Chaouachi, R. Kamel, R. Andoulsi and K. Nagasaka, "Multiobjective Intelligent Energy Management for a Microgrid," *IEEE Transactions on Industrial Electronics*, vol. 60, no. 4, pp. 1688-1699, 2013.

[43] R. Palma-Behnke, C. Benavides, F. Lanas, B. Severino, L. Reyes, J. Llanos and D. Sáez, "A Microgrid Energy Management System Based on the Rolling Horizon Strategy," *IEEE Transactions on Smart Grid*, vol. 4, no. 2, pp. 996-1006, 2013.

[44] A. Khodaei, "Microgrid Optimal Scheduling With Multi-Period Islanding Constraints," *IEEE Transactions on Power Systems*, vol. 24, no. 3, pp. 1383-1392, 2014.

[45] W. Shi, X. Xie, C. Chu and R. Gadh, "Distributed Optimal Energy Management in Microgrids," *IEEE Transactions on Smart Grid*, vol. 6, no. 3, pp. 1137-1146, 2015.

[46] A. Luna, N. Diaz, F. Andrade, M. Graells, J. Guerrero and J. Vasquez, "Economic Power Dispatch of Distributed Generators in a Grid-Connected Microgrid," *9th International Conference on Power Electronics and ECCE Asia (ICPE-ECCE Asia)*, 2015.

[47] R. Rigo-Mariani, B. Sareni, X. Roboam and C. Turpin, "Optimal power dispatching strategies in smart-microgrids with storage," *Renewable and Sustainable Energy Reviews*, vol. 40, pp. 649-658, 2014.

[48] W. Shi, N. Li, C. Chu and R. Gadh, "Real-Time Energy Management in Microgrids," *IEEE Transactions on Smart Grid,* vol. 8, no. 1, pp. 228-238, 2017.

[49] C. Hernandez-Aramburo, T. Green and N. Mugniot, "Fuel consumption minimization of a microgrid," *IEEE Transactions on Industry Applications,* vol. 41, no. 3, pp. 673-681, 2005.

[50] Y. Zhang, N. Gatsis and G. Giannakis, "Robust Energy Management for Microgrids With High-Penetration Renewables," *IEEE Transactions on Sustainable Energy,* vol. 4, no. 4, pp. 944-953, 2013.

[51] W. Su, J. Wang and J. Roh, "Stochastic Energy Scheduling in Microgrids With Intermittent Renewable Energy Resources," *IEEE Transactions on Smart Grid,* vol. 5, no. 4, pp. 1876-1883, 2014.

[52] Z. Wang, B. Chen, J. Wang, M. Begovic and C. Chen, "Coordinated Energy Management of Networked Microgrids in Distribution Systems," *IEEE Transactions on Smart Grid,* vol. 6, no. 1, pp. 45-53, 2015.

[53] A. Khodaei, "Resiliency-Oriented Microgrid Optimal Scheduling," *IEEE Transactions on Smart Grid,* vol. 5, no. 4, pp. 1584-1591, 2014.

[54] F. Farzan, M. Jafari, R. Masiello and L. Lu, "Toward Optimal Day-Ahead Scheduling and Operation Control of Microgrids Under Uncertainty," *IEEE Transactions on Smart Grid,* vol. 6, no. 2, pp. 499-507, 2015.

[55] Y. Xiang, J. Liu and Y. Liu, "Robust Energy Management of Microgrid With Uncertain Renewable Generation and Load," *IEEE Transactions on Smart Grid,* vol. 7, no. 2, pp. 1034-1043, 2016.

[56] S. Salinas, M. Li, P. Li and Y. Fu, "Dynamic Energy Management for the Smart Grid With Distributed Energy Resources," *IEEE Transactions on Smart Grid,* vol. 4, no. 4, pp. 2139-2151, 2013.

[57] Y. Huang, S. Mao and R. Nelms, "Adaptive Electricity Scheduling in Microgrids," *IEEE Transactions on Smart Grid,* vol. 5, no. 1, pp. 270-281, 2014.

[58] S. Sun, M. Dong and B. Liang, "Joint supply, demand, and energy storage management towards microgrid cost minimization," *2014 IEEE International Conference on Smart Grid Communications (SmartGridComm), Venice,* pp. 109-114, 2014.

[59] S. Conti, R. Nicolosi and S. Rizzo, "Optimal dispatching of distributed generators in an MV autonomous micro-grid to minimize operating costs and emissions," *2010 IEEE International Symposium on Industrial Electronics, Bari,* pp. 2542-2547, 2010.

[60] N. Hatziargyriou, G. Contaxis, M. Matos, J. Lopes, G. Kariniotakis, D. Mayer, J. Halliday, G. Dutton, P. Dokopoulos, A. Bakirtzis, J. Stefanakis, A. Gigantidou, P.

O'Donnell, D. McCoy, M. Fernandes, J. Cotrim and A. Figueira, "Energy management and control of island power systems with increased penetration from renewable sources," *2002 IEEE Power Engineering Society Winter Meeting*, pp. 335-339, 2002.

[61] C. Colson, M. Nehrir and S. Pourmousavi, "Towards real-time microgrid power management using computational intelligence methods," *IEEE PES General Meeting, Minneapolis, MN,*, pp. 1-8, 2010.

[62] C. Colson, M. Nehrir and C. Wang, "Ant colony optimization for microgrid multi-objective power management," *2009 IEEE/PES Power Systems Conference and Exposition, Seattle, WA*, pp. 1-7, 2009.

[63] C. Schwaegerl, L. Tao, P. Mancarella and G. Strbac, "A multi-objective optimization approach for assessment of technical, commercial and environmental performance of Microgrids," *European Transactions on Electrical Power*, vol. 21, no. 2, pp. 1269-1288, 2011.

[64] E. Alvarez, A. Lopez, J. Gómez-Aleixandre and N. de-Abajo, "On-line minimization of running costs, greenhouse gas emissions and the impact of distributed generation using microgrids on the electrical system," *2009 IEEE PES/IAS Conference on Sustainable Alternative Energy (SAE), Valencia*, pp. 1-10, 2009.

[65] H. Kanchev, D. Lu, B. Francois and V. Lazarov, "Smart monitoring of a microgrid including gas turbines and a dispatched PV-based active generator for energy management and emissions reduction," *2010 IEEE PES Innovative Smart Grid Technologies Conference Europe (ISGT Europe), Gothenburg*, pp. 1-8, 2010.

[66] .. Katiraei, R. Iravani, N. Hatziargyriou and A. Dimeas, "Microgrids management," *IEEE Power and Energy Magazine*, vol. 6, no. 3, pp. 54-65, 2008.

[67] C. Colson and M. Nehrir, "Comprehensive Real-Time Microgrid Power Management and Control With Distributed Agents," *IEEE Transactions on Smart Grid*, vol. 4, no. 1, pp. 617-627, 2013.

[68] A. Dimeas and N. Hatziargyriou, "Operation of a Multiagent System for Microgrid Control," *IEEE Transactions on Power Systems*, vol. 20, no. 3, pp. 1447-1455 , 2005.

[69] T. Logenthiran, D. Srinivasan and D. Wong, "Multi-agent coordination for DER in MicroGrid," *2008 IEEE International Conference on Sustainable Energy Technologies, Singapore*, 2008.

[70] J. Oyarzabal, J. Jimeno, J. Ruela, A. Engler and C. Hardt, "Agent based micro grid management system," *2005 International Conference on Future Power Systems, Amsterdam*, 2005.

[71] K. De Brabandere, K. Vanthournout, J. Driesen, G. Deconinck and R. Belmans, "Control of Microgrids," *2007 IEEE Power Engineering Society General Meeting, Tampa, FL,* 2007.

[72] W. Zheng and J. Cai, "A multi-agent system for distributed energy resources control in microgrid," *2010 5th International Conference on Critical Infrastructure (CRIS), Beijing,* pp. 1-5, 2010.

[73] D. Hammerstrom, S. Widergren and C. Irwin, "Evaluating Transactive Systems: Historical and Current U.S. DOE Research and Development Activities," *IEEE Electrification Magazine,* vol. 4, no. 4, pp. 30-36, 2016.

[74] F. Rahimi, A. Ipakchi and F. Fletcher, "The Changing Electrical Landscape: End-to-End Power System Operation Under the Transactive Energy Paradigm," *IEEE Power and Energy Magazine,* vol. 14, no. 3, pp. 52-62, 2016.

[75] The GridWise Architecture Council, "GridWise Transactive Energy Framework," 2015.

[76] D. Hammerstrom, T. Oliver, R. Melton and R. Ambrosio, "Standardization of a Hierarchical Transactive Control System," *GridInterop '09 Conference,* 2009.

[77] D. Jin, X. Zhang and S. Ghosh, "Simulation models for evaluation of network design and hierarchical transactive control mechanisms in Smart Grids," *2012 IEEE PES Innovative Smart Grid Technologies (ISGT), Washington, DC,* pp. 1-8, 2012.

[78] P. Huang, J. Kalagnanam, R. Natarajan, D. Hammerstrom, R. Melton, M. Sharma and R. Ambrosio, "Analytics and Transactive Control Design for the Pacific Northwest Smart Grid Demonstration Project," *2010 First IEEE International Conference on Smart Grid Communications, Gaithersburg, MD,* pp. 449-454, 2010.

[79] D. Chassin and L. Kiesling, "Decentralized Coordination through Digital Technology, Dynamic Pricing, and Customer-Driven Control: The GridWise Testbed Demonstration Project," *The Electricity Journal,* vol. 21, no. 8, pp. 51-59, 2008.

[80] D. Hammerstrom, "Pacific Northwest GridWise Testbed Demonstration Projects - Part I. Olympic Peninsula Project," Pacific Northwest National Laboratory, 2007.

[81] K. Subbarao, J. Fuller, K. Kalsi, R. Pratt, S. Widergren and D. Chassin, "Transactive Control and Coordination of Distributed Assets for Ancillary Services," Pacific Northwest National Laboratory, 2013.

[82] P. Kundur, Power System Stability and Control, New York: McGraw-Hill, 1994.

[83] A. Gomez-Exposito, A. J. Conejo and C. Cañizares, Electric Energy Systems: Analysis and Operation, CRC Press, 2008.

[84] J. Svensson, Active Distributed Power Systems Functional Structures for Real-Time Operation of Sustainable Energy Systems, Lund: Department of Industrial Electrical Engineering and Automation, Lund Institute of Technology, 2006.

[85] S. Chowdury, S. Chowdury and P. Crossley, Microgrids and Active Distribution Networks, Institution of Engineering and Technology (IET), 2009.

[86] The GridWise Architecture Council, "GridWise Transactive Energy Framework Version 1.0," The GridWise Architecture Council, January 2015.

[87] D. Hammerstrom, T. Oliver, R. Melton and R. Ambrosio, "Standardization of a Hierarchical Transactive Control System," in *GridInterop Conference*, 2009.

[88] P. Huang, J. Kalagnanam, R. Natarajan, M. Sharma, R. Ambrosio, D. Hammerstrom and R. Melton, "Analytics and Transactive Control Design for the Pacific Northwest Smart Grid Demonstration Project," in *First IEEE International Conference on Smart Grid Communications (SmartGridComm)* , 2010.

[89] D. P. Chassin and L. Kiesling, "Descentralized Coordination through Digital technology, Dynamic Pricing, and Customer-Driven Control: The GridWiseTestbed Demonstration Project," *The Electricity Journal,* vol. 21, no. 8, pp. 51-59, 2008.

[90] D. M. Sajjadi, P. Mandal, T. L. B. Tseng and M. Velez-Reyes, "Transactive Energy Market in Distribution Systems: A case Study of Energy Trading between Transactive Nodes," in *2016 North American Power Symposium (NAPS)*, Denver, CO, USA, 2016.

[91] L. Kristov, P. D. Martini and J. D. Taft, "A Tale of Two Visions: Designing a Descentralized Transactive Electric System," *IEEE Power and Energy Magazine,* vol. 14, no. 3, pp. 63-69, May-June 2016.

[92] A. M. Cantarellas, D. Remon and P. Rodriguez, "Control Structure and Method for a Distributed Electric Power System, and Distributed Electric Power System". Spain Patent P201531918, 2016.

[93] P. Interconnection, "Locational Marginal Pricing Map," [Online]. Available: http://www.pjm.com/library/maps/lmp-map.aspx. [Accessed 17 04 2017].

[94] C. ISO, "Market price maps," [Online]. Available: http://www.caiso.com/pages/pricemaps.aspx. [Accessed 17 04 2017].

[95] J. Yu, "Locational marginal pricing in ERCOT market," in *IEEE Power Engineering Society General Meeting*, Quebec, 2006.

[96] California ISO, "Locational Marginal Pricing (LMP): Basics of Nodal Price Calculation," 12 08 2005. [Online]. Available: http://www.caiso.com/docs/2004/02/13/200402131607358643.pdf. [Accessed 17 04 2017].

[97] I. Perez-Arriaga, Ed., Regulation of the Power Sector, Springer, 2013.

[98] IEA - International Energy Agency, "World Energy Outlook," 2011.

[99] IEA - International Energy Agency, "Renewable Energy medium term market report," 2012.

[100] T. Ahmed and A. F. Zobaa, "Offshore power conditioning system connecting arrays of wave energy converters to the electric power grid," in *8th International Conference on Advances in Power System Control, Operation and Management (APSCOM 2009)*, 2009.

[101] L. Margheritini, A. M. Hansen and P. Frigaard, "A method for EIA scoping of wave energy converters—based on classification of the used technology," *Environmental Impact Assessment Review*, vol. 32, no. 1, pp. 33-44, 2012.

[102] J. Cruz, Ocean Wave Energy: Current Status and Perspectives, Bristol - UK: Springer, 2008.

[103] T. Ahmed, K. Nishida and M. Nakaoka, "The commercial advancement of 16 MW offshore wave power generation technologies in the southwest of the UK," in *8th International Conference on Power Electronics - ECCE Asia*, Jeju, 2011.

[104] A. F. d. O. Falcão, "Wave energy utilization: A review of the technologies," *Renewable and Sustainable Energy Reviews*, vol. 14, no. 3, pp. 899-918, 2010.

[105] B. Drew, A. R. Plummer and M. N. Sahinkaya, "A review of wave energy converter technology," *Proceedings of the Institution of Mechanical Engineers, Part A: Journal of Power and Energy*, 2009.

[106] B. Czech and P. Bauer, "Wave Energy Converter Concepts : Design Challenges and Classification," *Industrial Electronics Magazine*, vol. 6, no. 2, pp. 4-16, 2012.

[107] D. L. O'Sullivan, G. Dalton and A. W. Lewis, "Regulatory, technical and financial challenges in the grid connection of wave energy devices," *IET Renewable Power Generation*, vol. 4, no. 6, pp. 555-567, November 2010.

[108] E. Tedeschi, M. Carraro, M. Molinas and P. Mattavelli, "Effect of Control Strategies and Power Take-Off Efficiency on the Power Capture From Sea Waves," *IEEE Transactions on Energy Conversion*, vol. 26, no. 4, pp. 1088-1098, Dec. 2011.

[109] J. Hals, J. Falnes and T. Moan, "A Comparison of Selected Strategies for Adaptive Control of Wave Energy Converters," *Journal of Offshore Mechanics and Arctic Engineering*, vol. 133, no. 3, 2011.

[110] S. Nielsen, Q. Zhou, M. Kramer, B. Basu and Z. Zhang, "Optimal control of nonlinear wave energy point converters," *Ocean Engineering*, vol. 72, pp. 176-187,

2013.

[111] J. Hals, J. Falnes and T. Moan, "Constrained Optimal Control of a Heaving Buoy Wave-Energy Converter," *Journal of Offshore Mechanics and Arctic Engineering,* vol. 133, no. 1, 2010.

[112] J. S. d. Costa, P. Beirao and D. Valerio, "Internal Model Control applied to the Archimedes Wave Swing," in *International Conference on Systems and Computer Science*, 2007.

[113] F. Fusco and J. V. Ringwood, "A Simple and Effective Real-Time Controller for Wave Energy Converters," *IEEE Transactions on Sustainable Energy*, vol. 4, no. 1, pp. 21-30, Jan. 2013.

[114] M. Molinas, O. Skjervheim, P. Andreasen, T. Undeland, J. Hals, T. Moan y B. Sorby, «Power electronics as grid interface for actively controlled wave energy converters,» de *2007 International Conference on Clean Electrical Power*, Capri, 2007.

[115] D. O'Sullivan and G. Dalton, "Challenges in the Grid Connection of Wave Energy Devices," in *European Conference in Wave and Tidal Energy (EWTEC)*, 2009.

[116] T. Ackermann, Wind Power in Power Systems, John Wiley & Sons, 2005.

[117] J. Hals, Modelling an phase control of wave-energy converters, PhD Thesis, NTNU - Norwegian University of Science and Technology, 2010.

[118] A. Price, New Perspectives on Wave Energy Converter Control, PhD dissertation, University of Edingurgh, 2009.

[119] R. Taghipour, T. Perez y T. Moan, «Hybridfrequency-time domainmodelsfordynamic response analysis of Marine Structures,» *Ocean Engineering*, vol. 35, nº 7, May 2008.

[120] J. Falnes, Ocean waves and oscillating systems: Linear interaction including wave-energy extraction, Cambridge University Press, 2004.

[121] E. Tedeschi y M. Molinas, «Wave-to-wave buoys control for improved power extraction under electro-mechanical constraints,» de *IEEE International Conference on Sustainable Energy Technologies (ICSET)*, Kandy, 2010.

[122] R. Teodorescu, M. Liserre y P. Rodriguez, Grid Converters for Photovoltaic and Wind Power Systems, Wiley-IEEE Press, January 2011.

[123] P. Rodríguez, A. Luna, R. S. Muñoz-Aguilar, I. Etxeberria-Otadui, R. Teodorescu y F. Blaabjerg, «A Stationary Reference Frame Grid Synchronization System for Three-Phase Grid-Connected Power Converters Under Adverse Grid Conditions,» *IEEE Transactions on Power Electronics,* vol. 27, nº 1, pp. 99-112, Jan. 2012.

[124] P. Rodriguez, A. Luna, I. Etxeberria, J. R. Hermoso y R. Teodorescu, «Multiple second order generalized integrators for harmonic synchronization of power converters,» de *2009 IEEE Energy Conversion Congress and Exposition (ECCE)*, San Jose, CA,, 2009.

[125] B. Bose, Modern Power Electronics and AC Drives, Penitence Hall, 2002.

[126] R. Krishnan, Electric Motor Drives – Modelling, Analysis and Control, Penitence Hall, 2001.

[127] M. Singh, V. Khadkikar y A. Chandra, «Grid synchronisation with harmonics and reactive power compensation capability of a permanent magnet synchronous generator-based variable speed wind energy conversion system,» *IET Power Electronics*, vol. 4, nº 1, pp. 122-130, 2011.

[128] F. Blaabjerg, R. Teodorescu, M. Liserre y A. V. Timbus, «Overview of Control and Grid Synchronization for Distributed Power Generation Systems,» *IEEE Transactions on Industrial Electronics*, vol. 53, nº 5, pp. 1398-1409, Oct. 2006.

[129] A. Vidal, F. Freijedo, A. Yepes, J. Malvar, Ó. López y J. Doval-Gandoy, «Transient response evaluation of stationary-frame resonant current controllers for grid-connected applications,» *IET Power Electronics*, vol. 7, nº 7, pp. 1714-1724, July 2014.

[130] A. Cantarellas, D. Remon, W. Zhang y P. Rodriguez, «Adaptive vector control based wave-to-wire model of wave energy converters,» *IET Power Electronics*, vol. 10, nº 10, pp. 1111-1119, 2017.

[131] M. Vítečková y A. Víteček, «Modulus optimum for digital controllers,» *Acta Montanistica Slovaca*, vol. 8, nº 4, p. 214 – 216, 2003.

[132] A. Cantarellas, E. Rakhshani, D. Remon y P. Rodriguez, «Design of the LCL+trap filter for the two-level VSC installed in a large-scale wave power plant,» de *IEEE Energy Conversion Congress and Exposition (ECCE)*, Denver, CO, 2013.

[133] M. Sanatkar-Chayjani y M. Monfared, «Design of LCL and LLCL filters for single-phase grid connected converters,» *IET Power Electronics*, vol. 9, nº 9, pp. 1971-1978, 2016.

[134] A. Cantarellas, E. Rakhshani, D. Remon y P. Rodriguez, «Grid connection control of VSC-based high power converters for wave energy applications,» de *IECON 2013 - 39th Annual Conference of the IEEE Industrial Electronics Society*, Vienna, 2013.

[135] S. Dutta y T. J. Overbye, «A clustering based wind farm collector system cable layout design,» de *2011 IEEE Power and Energy Conference at Illinois*, Champaign, IL, 2011.

[136] NREL, "Transparent cost database open energy information," [Online]. Available: http://en.openei.org/wiki/Transparent_Cost_Database.

[137] F. Sharkey, E. Bannon, M. Conlon and K. Gauhgan, "Dynamic Electrical Ratings and the Economics of Capacity Factor for Wave Energy Converter Arrays," *the European Wave and Tidal Energy Conference,* 2011.

[138] S. M. R. SEA. , "Environmental Report Section C SEA Assessment: Chapter C1 Bathymetry," http://www.seaenergyscotland.net/public_docs/ER_C1_Bathymetry_Final.pdf, 2012.

[139] B. Borgarino, A. Babarit and P. Ferrant, "Impact of wave interactions effects on energy absorption in large arrays of wave energy converters," *Ocean Engineering,* vol. 41, pp. 79-88, 2012.

[140] ABB, "Cables for Offshore Wind Farms".

[141] ZTT, "Submarine Cable catalogue".

[142] F. Sharkey, M. Conlon and K. Gauhgan, "Investigation of Wave Farm Electrical Network Configurations," *World Renewable Energy Congress 2011, Linköping, Sweden,* 2011.

[143] Y. Jin, J. O'Reilly and J. Fletcher, "Redundancy analysis of offshore wind farm collection and transmission systems," *International Conference on Sustainable Power Generation and Supply SUPERGEN '09,* pp. 1-7, 2009.

[144] M. Zubiaga, G. Abad, J. Barrena, S. Aurtenetxea and A. Cárcar, Energy Transmission and Grid Integration of AC Offshore Wind Farms, 2012.